Katarzyna Dominika Służalska

Biosynthesis and release of phospholipids by fibroblast-like synoviocytes from human osteoarthritic knee joint

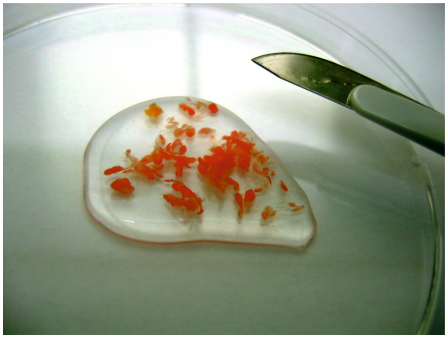

INAUGURAL DISSERTATION
submitted to the Faculty of Medicine
in partial fulfilment of the requirements
for the PhD degree
of the Faculties of Veterinary Medicine and Medicine
of the Justus Liebig University Giessen, Germany

édition scientifique
VVB LAUFERSWEILER VERLAG

1. Auflage 2017

1st Edition 2017

Printed in Germany

édition linguistique
VVB LAUFERSWEILER VERLAG

STAUFENBERGRING 15, D-35396 GIESSEN
Tel: 0641-5599888 Fax: 0641-5599890
email: redaktion@doktorverlag.de

www.doktorverlag.de

Biosynthesis and release of phospholipids by fibroblast-like synoviocytes from human osteoarthritic knee joint

Inaugural Dissertation

submitted to the

Faculty of Medicine

in partial fulfilment of the requirements

for the PhD-Degree

of the Faculties of Veterinary Medicine and Medicine

of the Justus Liebig University Giessen

by

Katarzyna Dominika Służalska

of

Busko-Zdrój, Poland

Giessen 2017

From the Laboratory of Experimental Orthopaedics

Head: Prof. Dr. rer. nat. Jürgen Steinmeyer

Department of Orthopaedic Surgery

Director/ Chairman: Prof. Dr. med. Markus Rickert

of the Faculty of Medicine of the Justus Liebig University Giessen

First Supervisor and Committee Member: Prof. Dr. rer. nat. Jürgen Steinmeyer

Second Supervisor and Committee Member: Prof. Dr. med. vet. Heinz-Jürgen Thiel

Committee Members: Prof. Dr. Klaus T. Preissner

Prof. Dr. rer. nat. Sabine Grösch

Date of Doctoral Defence: 21st of September 2017

I. TABLE OF CONTENTS

II. LIST OF FIGURES

III. LIST OF TABLES

IV. LIST OF ABBREVIATIONS

AB serum	Antibody-free serum
ACTB	Beta-actin
ADAMTS	A disintegrin and metalloproteinase with thrombospondin motifs
ANOVA	Analysis of variance
APC	Allophycocyanin
Apo	Apolipoprotein
B2M	Beta-2-micrpglobulin
BCA	Bicinchoninic acid
BMI	Body mass index
BMP	Bone morphogenetic protein
CCL5	Chemokine (C-C motif) ligand 5
CCT	CTP:phosphocholine cytidylyltransferase
CD	Cluster of differentiation
cDNA	Complementary deoxyribonucleic acid
CDP-choline	Cytidine-diphosphocholine
CDP-DAG	Cytidine-diphosphodiacylglycerol
CDP-ethanolamine	Cytidine-diphosphoethanolamine
CDS	CDP-diacylglycerol synthase
Cer	Ceramide
Cer1P	Cearmide-1-phosphate
CHT1	High-affinity choline transporter 1
CK	Choline kinase
COX	Cyclooxygenase
CPT	Cholinephosphotransferase
CRP	C reactive protein
Ct	Threshold cycle
CTL1	Choline transporter-like protein 1
CTP	Cytidine triphosphate

DAG	Diacylglycerol
Dex	Dexamethasone
dhSph	Dihydrosphingosine
DMEM	Dulbecco's modified Eagle's medium
DMSO	Dimethyl sulfoxide
dpm	Disintegration per minute
DPPC	Dipalmityol-phosphatidylcholine
ECT	CTP:phosphoethanolamine cytidylyltransferase
EDTA	Ethylenediaminetetraacetic acid
EK	Ethanolamine kinase
EPT	Ethanolaminephosphotransferase
ERK	Extracellular signal–regulated kinases
ESI-MS/MS	Electrospray ionization tandem mass spectrometry
FA	Fatty acid
FACS	Fluorescence-activated cell sorting
FBS	Fetal bovine serum
FGF	Fibroblast growth factor
FLS	Fibroblast-like synoviocytes
GAPDH	Glyceraldehyde 3-phosphate dehydrogenase
HA	Hyaluronic acid
HC-3	Hemicholinium-3
HEPES	4-(2-hydroxyethyl)-1-piperazineethanesulfonic acid
HPLC	High-performance liquid chromatography
IGF-1	Insulin-like growth factor-1
IL	Interleukin
JNK	c-Jun N-terminal kinases
KdhSph	3-keto-dihydrosphingosine
LPC	Lysophosphatidylcholine
LPCAT	Lysophosphatidylcholine acyltransferase
LPDS	Lipoprotein deficient serum

LPE	Lysophosphatidylethanolamine
LSC	Liquid scintillation counting
MMP	Matrix metalloproteinase
mRNA	Messenger ribonucleic acid
MS	Mass spectrometry
m/z	Mass to charge ratio
NAM	β-Nicotinamide mononucleotide
ND	Not determined
NF-κB	Nuclear factor kappa-light-chain-enhancer of activated B cells
NK cells	Natural killer cells
NO	Nitric oxide
NS	Not significant
OA	Osteoarthritis
p38 MAPK	p38 mitogen-activated protein kinases
PA	Phosphatidic acid
PBS	Dulbecco's phosphate buffered saline
PC	Phosphatidylcholine
PC O	Ether-phosphatidylcholine
PC P	Phosphatidylcholine-based plasmalogen
PE	Phosphatidylethanolamine
PE	Phycoerythrin
PEMT	Phosphatidylethanolamine N-methyltransferase
PE P	Phosphatidylethanolamine-based plasmalogen
PG	Phosphatidylglycerol
PGE2	Prostaglandin E2
PI3K	Phosphatidylinositol-3-kinases
PI	Phosphatidylinositol
PL	Phospholipid
PPAR	Peroxisome proliferator-activated receptors
PRG4	Proteoglycan 4

PS	Phosphatidylserine
PSD	Phosphatidylserine decarboxylase
PSS	Phosphatidylserine synthase
RA	Rheumatoid arthritis
ROS	Reactive oxygen species
RT	Room temperature
RT	Reverse transcriptase
RT-PCR	Reverse transcription polymerase chain reaction
S1P	Spingosine-1-phosphate
SD	Standard deviation
SDS	Sodium dodecyl sulfate
SF	Synovial fluid
SIRT	Sirtuin
SM	Sphingomyelin
SMS	Sphingomyelin synthase
Sph	Sphingosine
SZP	Superficial zone protein
TAE buffer	Tris-acetate-EDTA buffer
TGF	Transforming growth factor
TLC	Thin layer chromatography
TNFα	Tumor necrosis factor alpha
VEGF	Vascular endothelial growth factor

V. SUMMARY

In human joints phospholipids (PLs) are produced and released by fibroblast-like synoviocytes (FLS). However, the regulatory mechanism of these processes remains poorly understood. Elevated levels of cytokines and growth factors as well as of PLs were found in synovial fluid (SF) during osteoarthritis (OA). Therefore, we hypothesized that PL metabolism in FLS is regulated by various agents being present in OA SF. This study aimed to develop two *in vitro* models to study the biosynthesis and release of PLs in order to evaluate the effects of cytokines, growth factors and drugs on PL metabolism.

To measure the biosynthesis of PLs, FLS were cultured in DMEM containing 5% lipoprotein deficient serum in the presence of stable isotope-labelled precursors of PLs and various agents. To study the release of PLs, FLS were cultured in DMEM containing 10% FBS in the presence of radiolabelled precursors of PLs. Cells were starved and the release of radiolabelled PLs was determined in DMEM containing 2% FBS in the presence of agents to be tested. Lipids were extracted from cellular lysates and media, and then quantified using electrospray ionization tandem mass spectrometry in the biosynthesis model or liquid scintillation counting in the release model.

The results of our lipidomic study provide for the first time a detailed overview of PLs being synthesized and released from human FLS. We were able to demonstrate that IL-1β induced the biosynthesis of phosphatidylethanolamine (PE) and PE-based plasmalogens (PE P), whereas TNFα induced only the biosynthesis of PE. Also, BMPs induced the biosynthesis of several PE and PE P species. *In vivo* PE P could protect against cartilage destruction mediated by ROS, whereas elevated PE could induce apoptosis of hypertrophic FLS and osteophytes. Furthermore, growth factors such as TGF-β1, IGF-1, and BMP-2 upregulated the biosynthesis of phosphatidylcholine (PC) which *in vivo* could be responsible for joint lubrication as well as mediation of the signal transduction. Additionally, dexamethasone was found to decrease the biosynthesis of PE. Moreover, we demonstrated that the release of radiolabelled PLs is a time-dependent process. However, tested agents did not influence the release of PLs using our *in vitro* model. Thus, the mechanism controlling PL release needs to be further investigated.

In conclusion, our results indicate that cytokines and growth factors regulate PL biosynthesis and may contribute to the altered PL composition in OA SF. Moreover, our data suggest that FLS undergo PL alterations to adapt to the new diseased environment. Understanding intra- and extracellular functions of elevated PLs within human articular joints is a new challenge for lipidomic studies.

VI. ZUSAMMENFASSUNG

In menschlichen Gelenken werden Phospholipide (PLs) durch Fibroblasten-ähnliche Synoviozyten (FLS) produziert und freigesetzt. Der regulatorische Mechanismus dieser Prozesse bleibt jedoch schlecht verstanden. Erhöhte Konzentrationen von Zytokinen und Wachstumsfaktoren sowie PLs wurden in Synovialflüssigkeit (SF) bei Osteoarthritis (OA) gefunden. Daher haben wir vermutet, dass der PL-Metabolismus in FLS durch verschiedene Substanzen reguliert wird, die in der pathologischen SF vorhanden sind. Diese Studie zielte darauf ab, zwei *in vitro*-Modelle zu entwickeln, um die Biosynthese und Freisetzung von PLs zu untersuchen, um die Auswirkungen von Zytokinen, Wachstumsfaktoren und Medikamenten auf PL-Metabolismus zu bewerten.

Um die Biosynthese von PLs zu messen, wurden FLS in DMEM, das 5% Lipoprotein-defizientes Serum enthielt, in Gegenwart von stabilen isotopenmarkierten Vorläufern von PLs und mit verschiedenen Substanzen kultiviert. Um die Freisetzung von PLs zu untersuchen, wurden FLS in DMEM mit 10% FBS, in Gegenwart von radioaktiv markierten Vorläufern von PLs kultiviert. Die Zellen wurden ausgehungert und die Freisetzung von radioaktiv markierten PLs wurde in DMEM mit 2% FBS, in Gegenwart von zu testenden Substanzen bestimmt. Die Lipide wurden aus zellulären Lysaten und Medien extrahiert und dann unter Verwendung von Elektrospray-Ionisations-Tandem-Massenspektrometrie im Biosynthese-Modell oder einer Flüssigkeitsszintillationszählung im Freisetzungsmodell quantifiziert.

Die Ergebnisse unserer lipidomischen Studie liefern erstmals einen detaillierten Überblick über PLs, die synthetisiert und aus humanem FLS freigesetzt werden. Wir konnten nachweisen, dass IL-1β die Biosynthese von Phosphatidylethanolamin (PE) und PE-basierten Plasmalogenen (PE P) induzierte, während TNFα nur die Biosynthese von PE induzierte. Auch BMPs induzierten die Biosynthese von mehreren PE- und PE P-Spezies. *In vivo* könnte PE P gegen die durch ROS vermittelte Knorpelzerstörung schützen, während erhöhte PE eine Apoptose von hypertrophischen FLS und Osteophyten induzieren könnte. Darüber hinaus haben Wachstumsfaktoren wie TGF-β1, IGF-1 und BMP-2 die Biosynthese von Phosphatidylcholin (PC), die *in vivo* für die Gelenkschmierung sowie die Vermittlung der Signaltransduktion verantwortlich sein könnten, hochreguliert. Zusätzlich konnte gezeigt werden, dass Dexamethason die Biosynthese von PE verringert. Darüber hinaus haben wir gezeigt, dass die Freisetzung von radioaktiv markierten PLs ein zeitabhängiges Verfahren ist. Allerdings beeinflussten die getesteten Wirkstoffe die Freisetzung von PLs nicht in unserem *in vitro* Modell. Somit muss der Mechanismus, der die PL-Freigabe steuert, weiter untersucht werden.

Abschließend zeigen unsere Ergebnisse, dass Zytokine und Wachstumsfaktoren die PL-Biosynthese regulieren und zu der veränderten PL-Zusammensetzung in OA SF beitragen können. Darüber hinaus deuten unsere Daten darauf hin, dass FLS PL Änderungen vornehmen, um sich an die neue, beeinflusste Umgebung anzupassen. Das Verständnis der intra- und extrazellulären Funktionen von erhöhten PLs innerhalb menschlicher Gelenkverbindungen ist eine neue Herausforderung für lipidomische Studien.

1. INTRODUCTION

1.1. Osteoarthritis

Osteoarthritis (OA) is the most common form of joint disorder worldwide, and it occurs mostly in developed countries (1-3). This degenerative joint disease affects millions of people and according to World Health Organisation the prevalence of OA is expected to increase. OA is associated with significant morbidity, physical disability, and increased health care expenses in elderly individuals. Interestingly, the prevalence of rheumatoid arthritis (RA) is lower, but until now public attention focused mostly on RA issue (2). OA affects joint tissues before middle age, however it can not be diagnosed until it becomes symptomatic years later. The mechanisms responsible for OA progression are complex, multifactorial and poorly understood. Unfortunately, so far mostly symptomatic treatment is available which gives patients pain relief but does not stop progression of the disease. Finally, the affected joint needs to be replaced by an endoprosthetic surgery (4, 5). Therefore, understanding the pathophysiology of OA is an important scientific goal.

1.1.1. Disease

The clinical symptoms of OA are pain and functional impairment that includes joint stiffness and dysfunction which lead to limited daily life activities. In 80% of OA patients movement is limited to some degree (2). The major morphological characteristic of OA is cartilage breakdown with only episodic synovitis. Moreover, changes occur in the bone, synovium and muscle (2). Radiographic signs of the disease include joint space narrowing, synovial thickening, bone resorption, and the presence of osteophytes (6). OA may also damage ligaments, menisci and muscles (7). OA can occur in any joint, but is most common in large joint such as knee, hip, hand and ankle (3). The risk factors of OA include age, overweight, gender, excessive mechanical loading, joint injury and genetic predisposition (1, 3, 8). Secondary OA can result from injury or might be caused by specific job-related activities (1).

1.1.2. Tissue involved in OA

OA is generally the result of an imbalance between applied mechanical stress and the biochemical ability of the articular cartilage to resist this stress (4). However, the disease affects the whole joint as an organ, not only the articular cartilage (2). All articular tissues and the crosstalk between them contribute to OA progression. In normal joints, articular cartilage acts as a smooth structure gliding between bones. The cartilage consists of chondrocytes and extracellular matrix including proteoglycans, from which aggrecan is the most abundant, as well as collagen fibres (9). During OA multiple biological agents, including pro-inflammatory cytokines and chemokines, as well as proteolytic enzymes and biomechanical stress induce and propagate cartilage lesions, so that the cartilage surface becomes rougher. Aggrecanases such as ADAMTS-4 and -5 are responsible for aggrecan degradation, while collagens and aggrecan fragments are cleaved by matrix metalloproteinases (MMPs) (10). Already low pre-inflamed OA joints produce cyclooxygenases (COX) enzyme products for instance prostaglandin E2 (PGE2) which can lead to enhanced production of MMPs as well as inhibition of proteoglycan synthesis (9). With disease progression chondrocytes undergo cell death or phenotypical changes, and express enzymes responsible for matrix degradation. When the disease is advanced, cartilage undergoes endochondral ossification, accompanied by invading blood vessels within the osteochondral area.

As the cartilage breaks down, changes occur in the underlying bone. The subchondral bone thickens and becomes irregular. In later stages of disease, severe bone remodelling processes take place, in particular bone sclerosis and necrosis, as well as osteophyte formation and their vascularization (2). The underlying mechanism of this process is not fully understood, but increased load on the subarticular bone as well as action of cytokines and growth factors seem to be responsible.

An imbalance of cytokines and growth factors promotes thickening and fibrosis of the capsule, so that movement of the joint becomes restricted. Finally, the synovium develops inflammation as a result of cartilage breakdown products also called detritus (11). Activated synoviocytes can proliferate and lead to synovial hyperplasia. Several studies have shown that enhanced synovitis can further accelerate cartilage damage. Moreover, a reduced viscosity of OA synovial fluid was observed. During disease the weakness of ligaments, tendons, and muscles also occur (2, 7).

1.1.3. Role of cytokines and growth factors in OA

OA was traditionally described as non-inflammatory disease in contrast to RA. However, since decades it is known that inflammation contributes to the symptoms and progression of OA (12, 13). In 2002 Attur *et al.* already reported that cartilage behaves like inflamed tissue based on inflammatory molecules being expressed (13). It is believed that the overproduction of cytokines and growth factors by the inflamed synovium and activated chondrocytes is a key phenomenon during OA pathophysiology (14).

The pro-inflammatory cytokines affect the majority of cells present in synovial joint via intracellular signal transduction pathways. They stimulate production of cytokines, enzymes, and other inflammatory compounds. Among this group the most important are IL-1β, TNFα, IL-6, IL-15, IL-17, and IL-18 (15). Patients with OA display elevated levels of these cytokines in synovial fluid and serum (16-19). IL-1β and TNFα stimulate their own production and induce expression of IL-6, IL-8, and CCL5 in fibroblast-like synoviocytes (FLS), chondrocytes, macrophages, and osteoblasts (12, 15). They also block chondrocytes to produce extracellular matrix components such as collagen type II and aggrecan, but stimulate these cells to produce catabolic enzymes like MMP-1, -3, -13, and ADAMTS (15, 20). Moreover, they induce production of NO, COX-2, and thus PGE2. During OA progression, IL-1β stimulates the synthesis of reactive oxygen species (ROS), which leads to cartilage damage (21, 22). It is worth to mention that NO and ROS which are present in OA cartilage can induce apoptosis and senescence of chondrocytes (23). Remarkably, the expression of IL-R1 receptor and TNF-R2 is also increased in FLS and chondrocytes from patients with OA (15).

IL-6 is produced in chondrocytes, osteoblast, FLS, macrophages, and adipocytes in response to IL-1β and TNFα. IL-6 is a cytokine which strongly enhances inflammatory response, although some of its effects might be anti-inflammatory. IL-6 is considered to be a key cytokine responsible for promoting osteoclast formation and thus subchondral bone resorption (24).

IL-15 was found to stimulate the differentiation and proliferation of T cells and NK cells. Also, it has been noted that IL-15 can induce secretion of MMPs (15). IL-17 is produced by T cells and mast cells that infiltrate synovium. FLS and chondrocytes are mostly affected by this cytokine. It has been shown that IL-17 inhibits proteoglycan synthesis and promotes MMPs production. Moreover, IL-17 stimulates secretion of VEGF by chondrocytes

and FLS, and thus favours vascularisation of the joint tissue (25, 26). In addition, chondrocytes, osteoblast, FLS, and macrophages produce IL-18 which acts similar to other cytokines by the stimulation of MMPs synthesis and inhibition of proteoglycan and aggrecan production (15).

Also anti-inflammatory cytokines are involved in the pathogenesis of OA such as IL-4, IL-10, and IL-13 (12, 15, 27). T cells infiltrating the synovium produce IL-4. The increased IL-4 concentration was observed in synovial fluid of OA patients. IL-4 was reported to inhibit the degradation of proteoglycans, decrease the secretion of pro-inflammatory cytokines as well as other mediators of inflammation such as NO and PGE2, and expression of COX-2 enzyme (28-30). IL-10 produced by chondrocytes is involved in stimulating the synthesis of type II collagen and aggrecan. IL-10 also induces the expression of BMP-2 and BMP-6, and reduces the effect TNFα (15). It has been reported that IL-13 inhibits production and secretion of the inflammatory cytokines such as IL-1β and TNFα from FLS of OA patients (29, 31).

Current research focus also on the anabolic growth factors in rheumatic disorders (32). It has been found that TGF-β superfamily members participate in the development of OA (33-35). TGF-β isoforms are expressed in cartilage, bone and synovium. However, TGFβ signalling play quite different role in these tissues. TGF-β stimulates chondrocytes to proliferate and inhibits their hypertrophy and maturation, promotes osteoblast maturation, and induces synovial tissue fibrosis (35). Recently, elevated TGF-β levels have been found in sera of OA patients (36). Also, TGF-β levels were increased in human OA osteoblasts when compared to normal (37). TGF-β1 has been reported to stimulate synoviocytes proliferation and fibrosis in murine knee joint (38). Furthermore, blocking of TGF-β with antibodies resulted in a decreased thickness of calcified cartilage, reduced proteoglycan loss, and slowed degeneration of cartilage in ACLT-induced OA murine model (39).

Several studies highlighted the contribution of BMPs to the pathogenesis of OA (40, 41). The level of BMP-2 was found to be higher in OA cartilage compared to normal (42). Overexpression of BMP-2 in murine knee joint stimulated proteoglycan synthesis and also increased degradation of aggrecan (43). BMP-7 levels in plasma and synovial fluid have been correlated with OA severity (44). Moreover, BMP-7 stimulates the synthesis of extracellular matrix proteins by chondrocytes and blocks the expression of matrix metalloproteinases involved in cartilage destruction (45, 46).

The role of IGF-1 has been also intensively studied. Changes in IGF-1 levels in rheumatic disorders remain controversial (47). Similar to other growth factors, IGF-1 induces anabolic effects and decreases catabolic responses in articular cartilage. Also IGF-1 was found to have protective effects on synovium resulting in decreased thickening and decreased evidence of inflammation (34, 48). Moreover, the combination of IGF-1 and BMP-7 treatment resulted in improved cartilage repair than agents alone (49). The members of FGF family also participate in OA changes within joint. FGF-2 was found to decrease aggrecanases activity in chondrocytes and induce synovial proliferation. FGF-18 increased chondrocyte proliferation as well as induced synovial thickening (34).

Since OA is a complex disease, cytokines and growth factors are just one part of the OA pathogenesis including progression. Many other factors such as lipids, epigenetics, adipokines, hormones, autophagy, aging, and exercises are in the scope of current research (32, 47, 50, 51).

1.2. Synovial joint

Synovial joints are the most common type of joints in human body, which allow wear-resistant movement between opposing surfaces (52). In these joints, articular surfaces are covered with avascular, non-nervous and elastic cartilage. Between the articular surfaces there is a joint cavity filled with synovial fluid (SF). The cavity can be partially or completely subdivided by meniscus. The joint is surrounded by an articular capsule lined by synovial membrane (4).

1.2.1. Synovial fluid

SF is essentially an ultarfiltrate of plasma with the addition of constitutes that are synthesized locally by the synovial tissue cells and then secreted into SF. Therefore, it is a clear, straw-coloured, viscous, and relatively acellular liquid. The main functions of SF are lubrication of surfaces, nutrition and the removal of metabolic waste products, load bearing, and shock absorption in the joint (52). SF contains molecules which play a key role in boundary lubrication such as lubricin, hyaluronic acid (HA), and surface-active phospholipids (PLs). The concentrations of mentioned lubricants depend on the health status of joint, and

they are altered in SF of patients with OA and RA (53, 54). SF also contains morphogens, growth factors, and cytokines which mediate communication between cells in the joint (52).

1.2.2. Synovial membrane

The synovium encapsulates the joint. Its main functions are to provide structural support, lubricate the surfaces, provide nutrients to cartilage as well as remove metabolites and degradation products from the synovial space (55). The synovium is a delicate membrane ~ 50 μm lining composed of two types of cell named type A and type B synoviocytes. The synovial membrane is a loose association of cells embedded in an extracellular matrix interspersed with collagen, proteoglycans, hyaluronan, and other matrix proteins (56). This kind of organization allows diffusion of the nutrients in serum to the avascular cartilage. In diseases such as OA and RA synovium thickening, hyperplasia, and inflammation occurs (11). In joint injury and disease, alterations in the synovial membrane result in pathological SF (52).

1.2.2.1. Macrophage-like synoviocytes

Type A synoviocytes, also called macrophage-like, derive from bone marrow and display hematopoietic origin. They migrate to the synovium and become resident cells. Macrophage-like synoviocytes express CD16, CD45, CD14, CD68, and CD11b. Type A cells are terminally differentiated with little capacity to proliferate. The presence of vacuoles suggests their phagocytic activity (55).

1.2.2.2. Fibroblast-like synoviocytes

Type B synovial cells, also named fibroblast-like synoviocytes (FLS) are mesenchymal cells that display many characteristics of fibroblast. They express type IV and V collagen, vimentin, CD90 (Thy-1), CD55, CD106, and cadherin-11 (55). Moreover, FLS have an ability to synthesize and secrete hyaluronan and lubricin (57, 58). They also contribute to local production of cytokines, mediators of inflammation, and proteolytic enzymes that degrade extracellular matrix (55). It has been reported that lamellar bodies,

which are responsible for phospholipid synthesis, are present within the rough endoplasmic reticulum of FLS (59).

1.3. Lubrication of articular joints

Lubrication reduces friction of the surfaces which slide past each other to low levels. In the absence of lubricants, the articular surfaces are smooth but possess strong surface energy. It is believed that low coefficient of friction in the boundary lubrication of articular cartilage is conditioned by surface layers of specialized molecules in SF adhered to the cartilage surface such as HA, lubricin, and surface-active PLs (60).

Understanding the nature and mechanism of boundary lubrication was intensively studied. In the past, two main theories concerning boundary lubrication have been proposed. First theory assumed that hydrophobic proteoglycans or glycoproteins contribute to water binding on the surface of cartilage thereby providing low friction liquid film. The second theory postulated that PL layer lubricate the surface of the articular cartilage (60). According to current knowledge, all three mentioned components seem to act together. Lubricin in the outer superficial zone and at the articular cartilage surface interacts with and immobilized hyaluronan at the cartilage surface, which in turn complexes with PLs to provide lubrication at the exposed PL groups via the hydration lubrication mechanism (Figure 1). Bilayers of PLs, especially phosphatidylcholine (PC), exposing their head groups in aqueous medium provide extremely efficient lubricating elements (61).

The integrity of the whole lubricant net plays a role in maintaining the good lubricating properties. Pathological condition of the joint such as OA begins with damage of cartilage leading to a disruption of lubrication, which in turn causes further damage of the cartilage.

1.3.1. Hyaluronan

Hyaluronan also called hyaluronic acid (HA) is a high-molecular-weight polymer of disaccharides, composed of D-glucuronic acid and D-N-acetylglucosamine. The concentration of hyaluronan in SF is around 3 mg/ml (54). HA forms long chains that considerably influence the viscosity of SF (60). High viscosity enhances hydrodynamic lubrication. HA

concentration in SF in pathological diseases such OA is decreased (54). Nevertheless, the friction coefficient measured directly reveals that HA is rather a poor boundary lubricant (61). However, HA has been often used as an intra-articular injected supplement to alleviate OA symptoms (61).

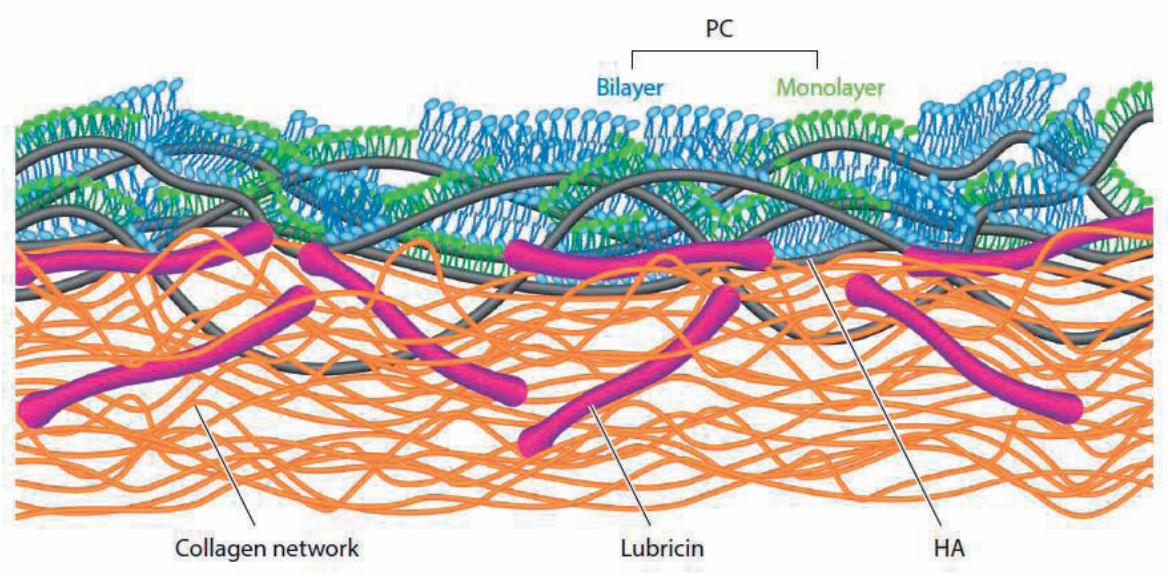

Figure 1. Schematic representation of the cartilage boundary lubricant layer. [Picture obtained with permission from: S. Jahn et al. Annu. Rev. Biomed. Eng. 2016].

1.3.2. Lubricin

Lubricin also known as superficial zone protein (SZP) or PRG4 is a glycoprotein found in SF with a concentration of around 350 µg/ml (54). The central part of the molecule is similar to mucin in structure, which provides a considerable water-holding capacity with a negative charge. The end domains of lubricin are globular with a positive charge. The peripheral parts of the molecule are attached to the negatively charged cartilage matrix, while the mucin-like region with water sheets is looped towards the surface (60). Highly hydrophilic mucin-like region at the cartilage surface contribute to water binding to the surface thereby contributing to a low friction liquid film. Direct measurements of friction between lubricin layers reveal that lubricin is not an especially efficient boundary lubricant (61). Nevertheless, the levels of lubricin in OA SF were found to be decreased (54).

1.3.3. Phospholipids

Surface-active phospholipids (PLs) have been proposed to adsorb to the articular surface, providing its hydrophobic character (62-64). PLs are highly present in the SF, especially PC (53, 54). The PL structure consists of hydrophilic head groups and hydrophobic fatty acid chains. The positively charged head groups can adsorb to the negatively charged extracellular cartilage matrix composed of HA and proteoglycans (60). Also, other monolayers of surfactants can be adsorbed to the hydrophobic surfaces of fatty acid chains. Experiments proved that multilayers of PLs result in a lower friction coefficient (61). Our previous analysis showed that the concentrations of specific PLs in OA SF are elevated (53).

1.4. Phospholipids – structure, occurrence and biosynthesis

PLs are the class of lipids that contain two fatty acid molecules esterified at the *sn*-1 and *sn*-2 positions of glycerol, and which contain a head group linked by a phosphate residue at the *sn*-3 position. The head group forms a hydrophilic region and determines the type of phospholipids. The fatty acid chains are hydrophobic.

In animal tissues, the PL composition is rather constant with PC as the most abundant class (65). However, the levels of PLs may vary between organs, tissues, and cell types as well as pathological conditions. PLs have many functions in eukaryotic cells. For instance they are constituents of cell membranes and lipoproteins, they are also signalling molecules, lung surfactants, joint lubricants, some of them have anti- or pro- inflammatory properties, they are also intermediate metabolites, and some of them are antioxidants (66). Moreover, many studies have connected PLs with diseases such as osteoarthritis and respiratory disorders, heart failure, Alzheimer's disease, Down syndrome, fatty liver disease, metabolic disease, or cancer (53, 54, 67-69). For this reason PLs have become an important research target.

PL synthesis is highly dependent on the availability of fatty acids (FA) and phosphatidic acid (PA). The source of FA is serum and their uptake is mediated by FA binding proteins. PA is synthesized from glucose or glycogen within the mitochondria, endoplasmic reticulum, and peroxisomes. The conversion of PA into diacylglycerol (DAG) is essential for the PL synthesis.

1.4.1. Choline-based phospholipids

Choline must be obtained from dietary sources in mammals. Around 95% of choline is used to synthesize phosphatidylcholine (PC). The rest is used for sphingomyelin (SM), phosphatidylcholine-based plasmalogens (PC P), and lysophosphatidylcholine (LPC) production. Choline is also oxidized to betaine in the mitochondria of kidney and liver and converted to acetylcholine in the nervous system (70, 71).

Choline and choline metabolites can be regenerated by breakdown of phospholipids containing choline. For instance PC can be hydrolysed by phospholipase D to produce choline and PA, as well as by phospholipase A to produce free FAs and glycerol-phosphocholine (70).

1.4.1.1. Phosphatidylcholine

Phosphatidylcholine (PC) is a class of PLs containing choline as a head group. PC is the most abundant PL class within eukaryotic cells, accounting 50% of total PLs. In particular, PC is present in the outer leaflet of the plasma membranes. It is also the principal PL circulating in the plasma. It is believed that PC is the main surface-active component produced by alveolar cells as well as within SF. It is also the precursor for other lipids, and their intermediate metabolites are involved in signal transduction pathways (70, 72). PC also plays a role in bile secretion and lipoprotein formation, and thus contributes to the maintenance of liver homeostasis (73). The median concentration of PC in healthy human SF is around 135 nmol/ml of SF, while in early OA SF 372 nmol/ml, and in late OA SF 737 nmol/ml PC was quantified (53).

All mammalian cells make PC via CDP-choline pathway, also known as the Kennedy pathway (70, 71, 74). This pathway consists of three enzymatic steps (Figure 2). First, extracellular choline is imported into cell through choline transporters and phosphorylated to phosphocholine (P-choline) by cytosolic enzyme choline kinases (CK). Then, the CTP:phosphocholine cytidylyltransferase (CCT) uses cytidine triphosphate (CTP) to convert generated products from previous step into cytidine-diphosphocholine (CPD-choline). The final step of the synthesis is catalysed by cholinephosphotransferase (CPT) by the transfer of phosphocholine from CDP-choline to DAG with production of PC. Several studies have shown that the first enzymatic reaction catalysed by CK is not a rate-limiting step of PC

biosynthesis, but still changes in CK activity were found to influence the rate of PC synthesis. Under most conditions, production of CDP-choline is the rate-limiting reaction for the biosynthesis of PC.

In an alternative pathway for PC biosynthesis (Figure 2), phosphatidylethanolamine (PE) is converted to PC by three methylation reactions catalysed by PE N-methyltransferase (PEMT). Around 30% of PC produced in hepatocytes comes mostly from this reaction (75). PC can be also formed via acylation of LPC by lysophosphatidylcholine acyltransferase (LPCAT). Remodelling of PC includes hydrolysis and re-acylation which introduce polyunsaturated FAs.

1.4.1.2. Lysophosphatidylcholine

Lysophosphatidylcholine (LPC) consists of one fatty acid chain and one choline head group attached to the glycerol backbone. It is a major plasma lipid. LPC possess both surfactant- and detergent-like properties. LPC has also pro-inflammatory properties. Moreover, it has been recognized to be an important cell signalling molecule (76). The median concentration of LPC in healthy human SF is around 16 nmol/ml which increases up to 55 nmol/ml during early OA respectively 82 nmol/ml during late OA (53).

LPC derives from PC of lipoproteins or from cell membrane-derived PC as a result of phospholipase A2 activity (Figure 2). The reverse reaction also occurs and is catalysed by lysophosphatidylcholine acyltransferase (LPCAT) (72).

1.4.2. Ethanolamine-based phospholipids

Animals cannot synthesize ethanolamine and must therefore obtain it from food. Conversion of serine to ethanolamine may occur in mammalian cells, also some amount of ethanolamine can be generated from sphingolipids (70). Ethanolamine is used for phosphatidylethanolamine (PE), lysophosphatidylethanolamine (LPE), and PE-based plasmalogens production.

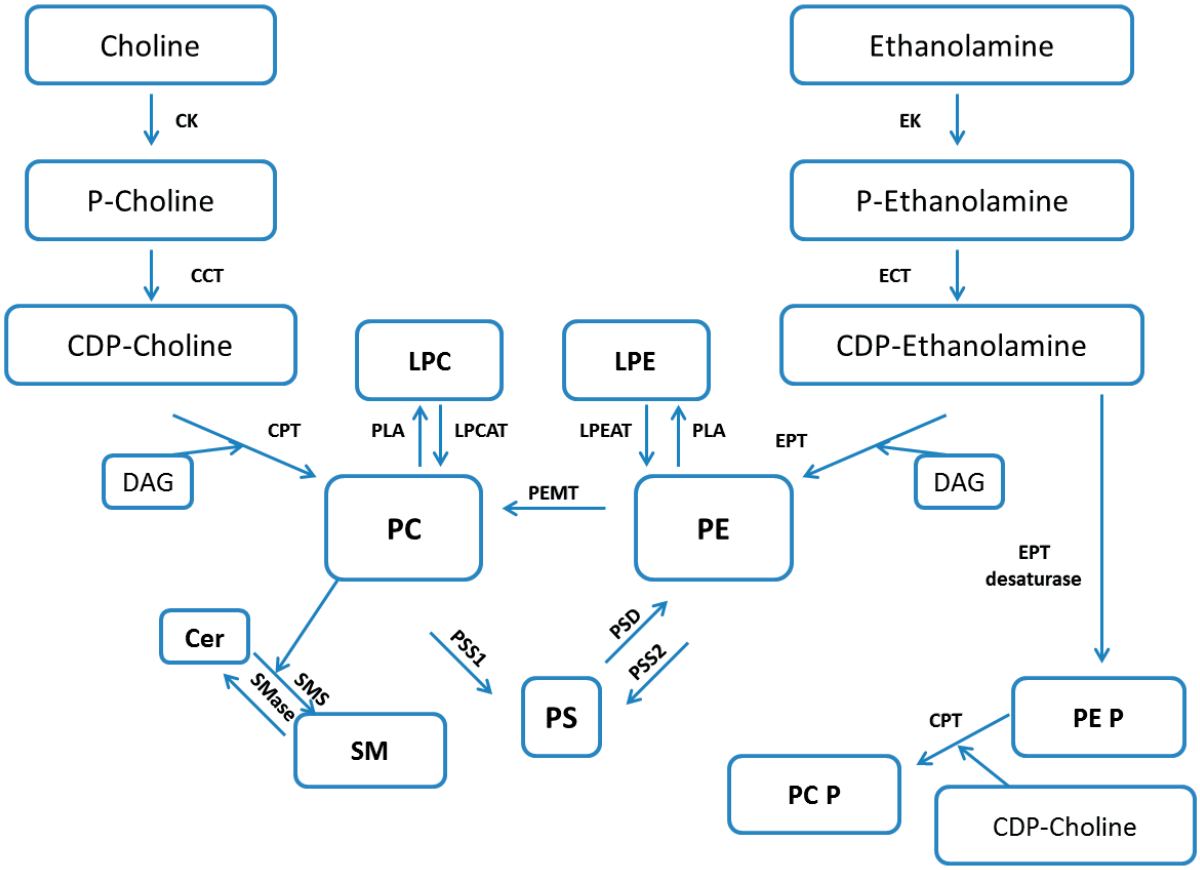

Figure 2. Schematic representation of the main PL classes biosynthesis.
CCT = CTP:phosphocholine cytidylyltransferase; CDP-Choline = cytidine-diphosphocholine; CDP-Ethanolamine = cytidine-diphosphoethanolamine; Cer = ceramide; CK = choline kinase; CPT = cholinephosphotransferase; DAG = diacylglycerol; ECT = CTP:phosphoethanolamine cytidylyltransferase; EK = ethanolamine kinase; EPT = ethanolaminephosphotransferase; LPC = lysophosphatidylcholine; LPCAT = lysophosphatidylcholine acyltransferase; LPEAT = lysophosphatidylethanolamine acyltransferase; LPE = lysophosphatidylethanolamine; PC = phosphatidylcholine; P-Choline = phosphocholine; PC P = phosphatidylcholine-based plasmalogen; PE = phosphatidylethanolamine; P-ethanolamine = phosphoethanolamine; PEMT = phosphatidylethanolamine N-methyltransferase; PE P = phosphatidylethanolamine-based plasmalogen; PLA = phospholipase A; PS = phosphatidylserine; PSD = phosphatidylserine decarboxylase; PSS = phosphatidylserine synthase; SM = sphingomyelin; SMase = sphingomyelinase; SMS = sphingomyelin synthase.

1.4.2.1. Phosphatidylethanolamine

Phosphatidylethanolamine (PE) contains ethanolamine as a head group. PE is the second most abundant PL class in eukaryotic cells. Mostly, it is concentrated in the inner leaflet of the plasma membrane. It is involved in membrane fusion and dynamics. It seems to be required for actin filament disassembly at the final stage of cytokinesis. Finally, PE is the precursor of many biologically active molecules, which modulate pain perception, inflammation, autophagy, and apoptosis (70, 72, 77). PE is also involved in glucose

metabolism and oxidative phosphorylation in murine hepatocytes (73, 75). The median concentration of PE in healthy human SF is around 2 nmol/ml of SF, and increases up to 4 nmol/ml during early OA and 6 nmol/ml during late OA (53).

PE is made in mammalian cells by two main biosynthetic pathways (Figure 2) (70, 74, 78). First, PE is formed via a separate branch of the Kennedy pathway, also called CDP-ethanolamine pathway, and occurs in endoplasmic reticulum membranes. Similar to PC synthesis, ethanolamine is first imported into cells and phosphorylated to phosphoethanolamine (P-ethanolamine) by ethanolamine kinase (EK). Then, the CTP:phosphoethanolamine cytidylyltransferase (ECT) uses CTP to convert generated products from previous step into cytidine-diphosphoethanolamine (CDP-ethanolamine). The final step of the synthesis is catalysed by ethanolaminephosphotransferases (EPT) by the transfer of ethanolamine from CDP-ethanolamine to DAG with the production of PE. Investigation of the rate-limiting reaction of the PE synthesis generated conflicting results. Under most conditions, the step catalysed by ECT is essential in PE biosynthesis (70, 79). However, another study reported that overexpression of EK in mammalian cells resulted in acceleration of the rate of [3H]-ethanolamine incorporation into PE (80).

The other pathway utilizes phosphatidylserine decarboxylase (PSD), an enzyme that is restricted to mitochondrial inner membranes and decarboxylates phosphatidylserine (PS) to PE. Moreover, PE can be also formed via acylation of lysophosphatidylethanolamine (LPE) and calcium-dependent head group exchange with existing PLs (73). The remodelling processes including hydrolysis and re-acylation often lead to the final FA composition.

1.4.2.2. Phosphatidylethanolamine-based plasmalogen

Phosphatidylethanolamine-based plasmalogens (PE P) are characterized by a vinyl-ether linkage at the *sn*-1 position and ester linkage at the *sn*-2 position. Plasmalogens make up approximately 18% of the PL mass in humans, but their content in individual tissues or cell types vary. Besides the maintenance of membrane dynamics and FA composition, plasmalogens participate in intracellular signalling. Importantly, they can act as antioxidants and protect against ROS (67). The median concentration of PE-based plasmalogen in healthy human SF is around 6 nmol/ml of SF, and increases up to 10 nmol/ml during early OA and 17 nmol/ml during late OA (53).

The biosynthesis of PE-based plasmalogens begins with the esterification of the hydroxyl group of dihydroxyacetone phosphate with a molecule of long chain acyl CoA catalysed by dihydroxyacetone phosphate acyltransferase (67). The activity of this enzyme is rate-limiting for plasmalogen biosynthesis. The enzyme named alkyl-dihydroxyacetone phosphate synthase then catalyses the replacement of the *sn*-1 fatty acid with a long chain fatty alcohol, which results in the formation of the ether bond. In the third step of the plasmalogen biosynthesis, an enzyme called acyl/alkyl-dihydroxyacetone phosphate reductase generates ether linkage at the *sn*-2 position. The next three reactions are catalysed by enzyme systems of acyltransferases to form an ester linkage at the *sn*-2 position. Phosphatidate phosphohydrolase then removes the phosphate group from the molecule, and the ethanolaminephosphotransferase (EPT) catalyses the attachment of the phosphoethanolamine (P-ethanolamine) head group to the molecule. Finally, plasmanylethanolamine desaturase catalyses the formation of a double bound between C1 and C2 also named vinyl-ether linkage, which is characteristic for plasmalogens.

Further, cholinephosphotransferase can catalyse simple exchange of ethanolamine head group to choline forming PC-based plasmalogen (PC P; Figure 2). However, this mechanism is not fully understood.

1.4.3. Phosphatidylserine

Phosphatidylserine (PS) contains serine as a head group. It is located on the inner monolayer surface of the plasma membrane. PS is involved in blood coagulation processes and regulation of apoptosis. Moreover, PS is an essential cofactor that binds to protein kinase C, a key enzyme in signal transduction (72, 78). The median concentration of PS in human SF is at low level, accounting 0.4 nmol/ml for heathy SF, 0.07 nmol/ml for early OA SF, and 0.3 nmol/ml for late OA SF (53).

PS is synthesized in mammalian cells by two distinct PS synthases, PS synthase-1 (PSS-1) and PS synthase-2 (PSS-2) in endoplasmic reticulum as well as mitochondria-associated membranes (Figure 2). These synthases catalyse a base-exchange reaction in which serine replaces the choline or ethanolamine head group of PC (by PSS-1) or PE (by PSS-2) (78). PS also undergoes the process of remodelling.

1.4.4. Phosphatidylinositol

Phosphatidylinositol (PI) is characterized by the presence of inositol as a head group. PI is especially abundant in brain tissue, but is present in all cell types. It is a membrane constituent and main source of signalling molecules (72). PI is involved in organization of cytoskeleton, vesicles trafficking, as well as autophagosome formation (81). So far PI was not detected within human SF, so its concentration must be at low level, below the detection limit.

PI is synthesized via the formation of CDP-diacylglycerol (CDP-DAG) from PA and cytidine triphosphate (CTP) catalysed by endoplasmic reticulum-associated CDP-diacylglycerol synthase (CDS). The second step utilizes *myo*-inositol and CDP-DAG in reaction catalysed by PI synthase or CDP-diacylgylcerol:inositol-3-phosphatidyltransferase (72). Moreover, PI undergoes the remodelling process.

1.4.5. Phosphatidylglycerol

Phosphatidylglycerol (PG) is a PL with a glycerol as a head group. PG plays an important role in regulating innate immunity and viral infection. It is also the second most abundant lung surfactant (72). The median concentration of PG in healthy human SF is low, accounting 0.1-5.0 pmol/ml of SF and it increases 3.5-fold during OA (82).

PG is synthesized from CDP-DAG produced from PA, and then converted by glycerophosphate phosphatidyltransferease to phosphatidylglycerolphosphate followed by its dephosphorylation to PG catalysed by phosphatidylglycerophosphatase (72). The final FA composition of PG is attained by the process of remodelling.

1.4.6 Sphingolipids

Sphingolipids are characterized by the presence of sphingoid based backbone being *O*-linked to the head group. This family includes sphingomyelin (SM), ceramide (Cer), sphingosine (Sph), Sph-1-phosphate (S1P), and Cer-1-phosphate (C1P) (68). These bioactive molecules were found to play a role in regulation of signal transduction pathways, direction of protein sorting, and mediation of cell-to-cell interaction.

Cer can be synthesized through *de novo* pathway or by hydrolysis of SM. The *de novo* synthesis begins with the condensation of serine and palmitoyl-CoA by serine palmityol transferase to form 3-keto-dihydrosphingosine (KdhSph). KdhSph is subsequently reduced to dihydrosphingosine (dhSph), which is N-acetylated by Cer synthases to produce dhCer or Cer. Cer was found to be involved in cell growth, differentiation, necrosis, proliferation, and apoptosis. It may also regulate protein kinase C and raf-1 (68, 83). The median Cer concentration in healthy human SF is around 1.4 nmol/ml of SF, and increases up to 2.8 nmol/ml during early OA and 5.5 nmol/ml during late OA (82).

SM is the most abundant sphingolipid. SM is synthesized from two precursors - Cer and PC that are made in endoplasmic reticulum and transported to the Golgi (68, 72). The majority of SM is made by SM synthase-1 (SMS-1) in the Golgi apparatus but some of them are also made by SM Synthase-2 (SMS-2) in plasma membranes. SM is a component of cellular membranes and lipid rafts. It has been also reported to play important roles in cellular signalling, cell growth, proliferation, differentiation, and survival (84). The median concentration of SM in healthy human SF is around 39 nmol/ml of SF, and increases up to 92 nmol/ml during early OA and 172 nmol/ml during late OA (82).

Furthermore, Cer can be phosphorylated to C1P. It can be also metabolized by ceramidases to form Sph, which can be further available for phosphorylation by Sph kinases to form S1P (68). C1P plays a role in inflammation and vesicular trafficking (85). Sph was reported to be associated with cell cycle arrest, apoptosis, regulation of cytoskeleton, and endocytosis (68). S1P regulates cell proliferation, growth, survival, migration, inflammation, and angiogenesis (86). Several studies have shown that S1P can counteract the effect of IL-1β in chondrocytes (87, 88). Moreover, Cer and Sph were reported to act as tumor-suppressor lipids (68). The concentrations of Sph, S1P, and C1P are at low levels in human SF and therefore are often below the detection limit of 6 pmol/ml of SF (82).

In conclusion, PLs are one of the components of SF being responsible for lubrication of articular joints. Previous studies reported that concentrations of PLs in SF are related to the health status of the joint. During OA, the levels of PC, LPC, PE-based plasmalogens, PS, SM, and Cer were significantly elevated. FLS are thought to be cells of synovial membrane which produce and release PLs into SF. Nevertheless, there is still not much known how the biosynthesis and release of PLs is controlled. Apart lubricating properties, PLs are involved in many other biological process. Taken together, certain PLs in SF were altered during OA. However, the cause of these changes still remains unknown. Also, the concentrations of

cytokines and growth factors in OA SF were found to be increased, which might suggest their role in the regulation of PL metabolism. Therefore, evaluation of the effects of these agents on PL biosynthesis and release could enhance our knowledge, providing novel targets to treat OA.

2. AIM OF THE STUDY

Surface-active phospholipids (PLs) together with hyaluronan and lubricin were reported to provide boundary lubrication within human articular joints. Considering altered levels of PLs in synovial fluid during OA when compared to normal (53, 54, 82), we hypothesized that (a) PLs are partly derived from FLS, and that (b) biosynthesis and release of PLs during OA is regulated by cytokines and growth factors.

The overall goal of this study was to investigate the effect of cytokines, growth factors as well as pharmacological agents on the biosynthesis of PLs and their release into cell culture media.

The specific aims of this study were:

1. Development of an *in vitro* model of FLS to study *de novo* biosynthesis of PL species using stable isotopes and ESI-MS/MS.

2. Development of an *in vitro* model of FLS to study the release of PLs using radioactive isotopes.

3. Evaluation of the effects of cytokines, growth factors and dexamethasone on the biosynthesis and release of PLs from FLS.

4. Determination of the mechanisms of action of agents found to influence PL biosynthesis and release.

3. MATERIALS AND METHODS

3.1. Materials

3.1.1. Technical equipment

Name	Company
Autoclave, model 3850 EL	Tuttnauer Europe B.V., Breda, Netherlands
Balance, model 770-12	Kern & Sohn GmbH, Balingen-Frommern, Germany
Balance, model EG2200-2NM	Kern & Sohn GmbH, Balingen-Frommern, Germany
Biological Safety Cabinet, Microflow®	Thermo Scientific Inc., Rockford, USA
Cell culture CO_2 incubator, HeraCell™ 150i	Thermo Scientific Inc., Rockford, USA
Countess®II Automated Cell Counter	Invitrogen, Thermo Fisher Scientific GmbH, Waltham, MA, USA
Drying oven, model 700	Memmert GmbH & Co. KG, Schwabach, Germany
Electrophoresis chamber horizontal, Wide Min-SUB® Cell GT	Bio-Rad Laboratories GmbH, Munich, Germany
BD FACS Canto™ II flow cytometer	Becton Dickinson GmbH, Hilderberg, Germany
Freezer -20°C, model KGE 34422	Bosch GmbH, Gerlingen-Schillerhoehe, Germany
Freezer -86°C, model HFU 486 Top	Thermo Electron GmbH, Langenselbold, Germany
Gel iX Imager INTAS®	Intas Science Imaging Instruments GmbH, Goettingen, Germany
Horizontal shaker, Polymax 1040	Heidolph Instruments GmbH & Co. KG, Schwabach, Germany
Laboshake, RO 500	C. Gerhardt GmbH & Co. KG, Koenigswinter, Germany
Light microscope, Axiovert® 40 CFL	Carl Zeiss, Goettingen, Germany

Magnetic stirrer, model MR 3002	Heidolph Instruments GmbH & Co. KG, Schwabach, Germany
Mass Spectrometer, Quattro Ultima Triple™ Quadrupole	Micromass, Manchester, United Kingdom
Microcentrifuge, model 5415D	Eppendorf AG, Hamburg, Germany
Microplate absorbance reader, Sunrise™	Tecan Group Ltd., Maennedorf, Switzerland
Microplate luminescence reader, Infinite® 200 PRO	Tecan Group Ltd., Maennedorf, Switzerland
Microplate shaker, model LD-45	Kisker Biotech GmbH & Co. KG, Steinfurt, Germany
Microwave, model VFD60M105IIE	LG Electronics, Englewood, NY, USA
Multichannel pipette 12-channels	Eppendorf AG, Hamburg, Germany
Multi-Purpose Scintillation Counter, LS 6500	Beckman Coulter Inc., Fullerton, CA, USA
PCR-Mastercycler®, Personal	Eppendorf AG, Hamburg, Germany
pH-meter digital, handylab 1	Schott Glaswerke, Mainz, Germany
Pipetboy, Easypet®	Eppendorf AG, Hamburg, Germany
Pipette, single channel: 0.5-10 µl, 10-100 µl, 100-10000 µl	Eppendorf AG, Hamburg, Germany
Pipetting Robot Genesis, RSP 150	Tecan Group Ltd., Maennedorf, Switzerland
Power Supply, PowerPac™ HC	Bio-Rad Laboratories GmbH, Munich, Germany
Pump, model 16612	Sartorius, Goettingen, Germany
Real Time PCR System, 7500 Fast	Applied Biosystems, Thermo Fisher Scientific GmbH, Waltham, MA, USA
Refrigerator +4 °C, model KGU66920	Bosch GmbH, Gerlingen-Schillerhoehe, Germany
Sonopuls, model UW 2010	Bandelin electronic GmbH & Co. KG, Berlin, Germany
Spectrophotometer, NanoDrop™ 1000	Thermo Fisher Scientific GmbH, Waltham, MA, USA
Thermomixer, Comfort	Eppendorf AG, Hamburg, Germany

Universal centrifuge, model 320R	Hettich GmbH & Co. KG, Tuttlingen, Germany
Vacuum concentrator, Christ RVC	Wolf Laboratories Limited, York, UK
Vortex mixer, Vortex-Genie®2	Scientific Industries Inc., Bohemia, NY, USA
Water bath, AQUAline AL5	DJB Labcare Ltd., Buckinghamshire, UK

3.1.2. Consumables

Name	**Company**
Bottle Top Filter, 0.22 µm	EMD Millipore, Merck Chemicals GmbH, Darmstadt, Germany
Cell culture Petri dish, 94 mm x 16 mm	Greiner bio-one GmbH, Frickenhausen, Germany
Cell culture T-75 flask	Greiner bio-one GmbH, Frickenhausen, Germany
Cell culture multiwell plates, 6 well, 96 well	Greiner bio-one GmbH, Frickenhausen, Germany
Cell scraper, 25 cm	Greiner bio-one GmbH, Frickenhausen, Germany
Cell strainer, 70 µm, sterile	Becton Dickinson GmbH, Heidelberg, Germany
Centrifuge tubes, 18 mm, screw cap	Brand GmbH & Co. KG, Wertheim, Germany
Centrifuge tubes, Pyrex®, screw cap	Corning B.V., Amsterdam, Netherlands
Conical tubes, 15 ml	Becton Dickinson GmbH, Heidelberg, Germany
Conical tubes, 50 ml	Greiner bio-one GmbH, Frickenhausen, Germany
Countess™ cell counting chamber slides	Invitrogen, Thermo Fisher Scientific GmbH, Waltham, MA, USA
CryoPure tubes, 1.8 ml	Sarstedt AG & Co., Nuembrecht, Germany
Filter Tips: 10 µl, 100 µl, 1000 µl	Nerbe plus GmbH, Winsen, Germany
Freezing container	Carl Roth GmbH & Co. KG, Karlsruhe, Germany
Glass bottles: 250 ml, 500 ml	Simax Inc., Sázava, Czech Republic

Hollow needles, 18G	Becton Dickinson GmbH, Heidelberg, Germany
Hollow needles, 22G	Terumo GmbH, Hamburg, Germany
Measuring cylinders: 100 ml, 500 ml	Duran group GmbH, Wertheim, Germany
MicroAmp™ Fast 96-well plate	Applied Biosystems, Thermo Fisher Scientific GmbH, Waltham, MA, USA
Microplate, 96 well	Greiner bio-one GmbH, Frickenhausen, Germany
Pasteur Pipettes, glass, 230 mm	VWR International GmbH, Darmstadt, Germany
PCR tubes: 0.2 ml	Nerbe plus GmbH, Winsen, Germany
Pincette, 12.5 cm, sterile	Seidel Medizin GmbH, Buchendorf, Germany
Pipette tip: 10 µl, 200 µl, 300 µl, 1000 µl	Sarstedt AG & Co., Nuembrecht, Germany
Plastic tubes, 5 ml	Sarstedt AG & Co., Nuembrecht, Germany
Plastic tubes, 5ml for flow cytometry	Sarstedt AG & Co., Nuembrecht, Germany
Polyethylene vials, 20 ml	PerkinElmer, Thermo Fisher Scientific GmbH, Waltham, MA, USA
Reaction tubes: 1.5 ml, 2 ml	Sarstedt AG & Co., Nuembrecht, Germany
Seal sheets, adhesive	Thermo Fisher, Thermo Fisher Scientific GmbH, Waltham, MA, USA
Serological pipettes: 5 ml, 10 ml, 25 ml	Greiner bio-one GmbH, Frickenhausen, Germany
Sterile scalpel Nr. 21	Feather Safety Razor Co. Ltd., Osaka, Japan
Sterile syringe: 2 ml, 5 ml, 10ml	B. Braun Melsungen AG, Melsungen, Germany
Super Polyethylene vials, 6ml	Packard Bioscience S.V., Groningen, Netherlands
Syringe filters, 0.22 µm, 0.45 µm	Merck Millipore GmbH, Darmstadt, Germany
Syringe filters, 0.2 µm	PALL GmbH, Dreieich, Germany

3.1.3. Reagents

Name	Company
Acetic acid, ReagentPlus®, ≥99%	Sigma-Aldrich GmbH, Steinheim, Germany (#A6283)
Agarose, analytical grade	Promega Corporation, Madison, WI, USA (#3121)
Antibody-free serum, (AB serum)	provided by Prof. Dr. H. Hackstein, Giessen, Germany
Aqua B. Braun	B. Braun Melsungen AG, Melsungen, Germany (#75/12604052/0503)
APC anti-human CD90 (thy1), Clone 5E10	BioLegend, London, UK (#328113)
APC Mouse IgG1, κ isotype Ctrl (FC), Clone MOPC-21	BioLegend, London, UK (#400121)
Apolipoprotein A-I, human plasma, HDL (Apo A-I)	EMD Millipore, Merck Chemicals GmbH, Darmstadt, Germany (#178452)
β-Nicotinamide mononucleotide (NAM)	Sigma-Aldrich GmbH, Steinheim, Germany (#N3501)
Blue/Orange 6x Loading Dye	Promega Corporation, Maddison, WI, USA (#G190A)
Carbachol	Sigma-Aldrich GmbH, Strasbourg, France (#Y0000113)
Chloroform, HiPerSolv, for HPLC	VWR International GmbH, Darmstadt, Germany (#UN1888)
Choline chloride, [methyl-^{3}H]-	PerkinElmer, Thermo Fisher Scientific GmbH, Waltham, MA, USA (#NET109001MC)
Choline chloride, trimethyl-D9, 98%	Cambridge Isotope Laboratories, Andover, MA, USA (#DLM-549-1)
Choline Kinase-α inhibitor (CK37)	EMD Millipore, Merck Chemicals GmbH, Darmstadt, Germany (#229103)
Citric Acid, ≥99.5%	Carl Roth GmbH, Karlsruhe, Germany (#6490.3)
D-(+)-Trehalose dehydrate	Sigma-Aldrich GmbH, Steinheim, Germany (#T0167)
Dexamethasone, BioReagent, ≥ 97%	Sigma-Aldrich GmbH, Steinheim, Germany (#D4902)

Dimethyl sulphoxide (DMSO), sterile	Sigma-Aldrich GmbH, Steinheim, Germany (#2650)
Dispase II	PAN Biotech GmbH, Aidenbach, Germany (#P10-032100)
DMEM medium	PAN Biotech GmbH, Aidenbach, Germany (#P04-01550)
DMEM w/o phenol red, w/o L-serine and w/o choline chloride	PAN Biotech GmbH, Aidenbach, Germany (#P04-01550S2)
DNA Ladder, 100 bp	Promega Corporation, Madison, WI, USA (#G210A)
Dulbecco's phosphate buffered saline (1x PBS)	PAN Biotech GmbH, Aidenbach, Germany (#P04-36500)
Epinephrine hydrochloride	Sigma-Aldrich GmbH, Steinheim, Germany (E4642)
Ethanol absolute, ≥ 99.8%	Sigma-Aldrich GmbH, Steinheim, Germany (#32205)
Ethanolamine, D4, 98%	Cambridge Isotope Laboratories, Andover, MA, USA (#DLM-552-1)
Ethanolamine hydrochloride, [1, 2-^{14}C]-	Hartmann Analytic, Braunschweig, Germany (#MC407H)
Ethidium bromide, 1%	Carl Roth GmbH, Karlsruhe, Germany (#2218.1)
Ethylendinitrilo-N, N, N', N', - tetra-acetic-acid (EDTA)	Sigma-Aldrich GmbH, Steinheim, Germany (#E5513)
Emulsifier-Safe™	PerkinElmer, Waltham, MA, USA (#6013389)
ERK inhibitor SCH772984	Selleckchem, Munich, Germany (#S7101)
Fetal bovine serum (FBS)	Sigma-Aldrich GmbH, Steinheim, Germany (#F7524)
Folic acid	Sigma-Aldrich GmbH, Steinheim, Germany (#F8785)
Gelatin EIA grade reagent	Bio Rad Laboratories GmbH, Arnsberg, Germany (#170-6537)
Glucocorticoid receptor antagonist RU 486, Mifeprostone	Selleckchem, Munich, Germany (#S2606)
Hemicholinium-3	Sigma-Aldrich GmbH, Steinheim, Germany (#H108-100MG)

2-(4-2-hydroxyethyl)-piperazinyl-1-ethansulfonate (HEPES), 1M	Gibco, Thermo Fisher Scientific GmbH, Waltham, MA, USA (#15630080)
JNK inhibitor SP600125	Selleckchem, Munich, Germany (#S1460)
Lipoprotein deficient serum (LPDS)	provided by Dr. A. Sigruener, Regensburg, Germany
L-Serine	Sigma-Aldrich GmbH, Steinheim, Germany (#S4311)
Methanol, for HPLC, ≥ 99.9%	Sigma-Aldrich GmbH, Steinheim, Germany (#34860)
NF-kB inhibitor QNZ	Selleckchem, Munich, Germany (#S4902)
Nuclease-Free Water	Promega Corporation, Madison, WI, USA (#P119C)
Quinacrine dihydrochloride	Sigma-Aldrich GmbH, Steinheim, Germany (#Q3251)
P38 inhibitor SB203580	Selleckchem, Munich, Germany (#S1076)
PE anti-human CD45, clone 2D1	BioLegend, London, UK (#368509)
PE Mouse IgG1, κ isotype Ctrl (FC), clone MOPC-21	BioLegend, London, UK (#400113)
Penicillin-Streptomycin (100x), Penicillin 1000 U/ml, Streptomycin 10 mg/ml	PAN Biotech GmbH, Aidenbach, Germany (#P06-07100)
PeqGOLD TriFast™	Peqlab Biotechnologie GmbH, Erlangen, Germany (#12-6834-00)
PI3K inhibitor LY294002	Selleckchem, Munich, Germany (#S1105)
Pilocarpine hydrochloride	Sigma-Aldrich GmbH, Strasbourg, France (#P1650000)
2-Propanol, Rotisolv®, ≥ 99.9%	Carl Roth GmbH, Karlsruhe, Germany (#T910.1)
Recombinant human Apolipoprotein E4 (Apo E4)	Peprotech GmbH, Hamburg, Germany (350-04)
Recombinant human BMP-2	Peprotech GmbH, Hamburg, Germany (#120-02)
Recombinant human BMP-4	Peprotech GmbH, Hamburg, Germany (#120-05ET)
Recombinant human BMP-7	Peprotech GmbH, Hamburg, Germany (#120-03)

Recombinant human IGF-1	Peprotech GmbH, Hamburg, Germany (# 100-11)
Recombinant human IL-1β	R&D Systems GmbH, Wiesbaden, Germany (# 201-LB-005)
Recombinant human IL-6	Life Technologies, Eugene, OR, USA (#10395-HNAE)
Recombinant human TGF-β1	Peprotech GmbH, Hamburg, Germany (#100-21)
Recombinant human TNF-α	Peprotech GmbH, Hamburg, Germany (#300-01A)
Sirtinol, 10mM/1ml in DMSO	Selleckchem, Munich, Germany (#S2804)
Sirtuin-Inhibitor EX 527, Selisistat	Selleckchem, Munich, Germany (#S1541)
Sodium chloride, 0.9% solution	B. Braun Melsungen AG, Melsungen, Germany (#2350748)
Sodium dodecyl sulfate (SDS)	Carl Roth GmbH, Karlsruhe, Germany (#2326.1)
Staurosporine	Calbiochem, Merck Millipore, Darmstadt, Germany (#569397)
Sytox® Blue Dead Cell Stain	Life Technologies, Eugene, OR, USA (#S34857)
Terbutaline hemisulfate salt	Sigma-Aldrich GmbH, Steinheim, Germany (#T2528)
TGF-β type I receptor activin receptor-like kinase inhibitor SB431542	Selleckchem, Munich, Germany (#S1067)
Tris, pufferan ® ≥ 99%	Carl Roth GmbH, Karlsruhe, Germany (#5429.3)
Trypan blue stain 0.4%	Life Technologies, Eugene, OR, USA (#T10282)
Trypsin/EDTA 0.5% in PBS (10x)	PAN Biotech GmbH, Aidenbach, Germany (#P10-02410)

3.1.4. Reagent kits

Name	**Company**
Caspase-Glo® 3/7 Assay	Promega Corporation, Madison, WI, USA (#G8091)
Cell Titer 96®Non-Radioactive Cell Proliferation Assay	Promega Corporation, Madison, WI, USA (#G4001)

QuantiTect® Primer Assay, B2M: Hs_B2M_1SG	Qiagen, Hilden, Germany (# QT00088935)
QuantiTect® Primer Assay, βactin: Hs_ACTB_2_SG	Qiagen, Hilden, Germany (#QT01680476)
QuantiTect® Primer Assay, GAPDH: Hs_GAPDH_2_SG	Qiagen, Hilden, Germany (#QT01192646)
QuantiTect® Reverse Transcription Kit	Qiagen, Hilden, Germany (#205313)
QuantiFast® SYBR® Green PCR Kit	Qiagen, Hilden, Germany (#204057)
PCR Mycoplasma Test Kit I/C	PromoKine, PromoCell GmbH, Heidelberg, Germany (#PK-CA91-1024)
Pierce™ BCA Protein Assay Kit	Thermo Fisher Scientific GmbH, Waltham, MA, USA (#23227)

3.1.5. Buffers and solutions

0.2% SDS solution

0.2 g of SDS was dissolved in 100 ml of aqua B. Braun and stored at RT up to 6 months.

1.4% agarose gel with ethidium bromide

1.68 g of agarose was dissolved in 120 ml of 1x TAE buffer. Then 8µl of ethidium bromide was added.

50x TAE buffer

Component	**Total volume 1000 ml**	**Final concentration**
Tris	242 g	2 M
Acetic acid	57.1 ml	1 M
EDTA,0.5 M	100 ml	0.05 M
Aqua B. Braun	900 ml	

The pH was adjusted to 8.3. Solution was stored at RT up to 3 years.

1x TAE buffer

50x TAE buffer was diluted 1:50 in aqua B. Braun.

1x Trypsin/EDTA

10x Trypsin/EDTA solution was diluted 1:10 in 1x PBS and then sterile filtered through a 0.22 µm filter. Aliquots were stored at -20°C up to 24 months.

Apolipoprotein A-I stock solution

250 µl of 2 mg/ml Apolipoprotein A-I was diluted with 250 µl of trehalose solution under sterile conditions, mixed by shaking, aliquoted and stored at -20°C up to 3 months.

Apolipoprotein E4 stock solution

500 µg of Apo E4 was reconstituted in 0.5 ml of trehalose solution under sterile conditions, mixed by shaking, aliquoted and stored at -20°C up to 3 months.

β-Nicotinamide mononucleotide (NAM) 50 mM stock solution

250 mg of NAM was dissolved in 1.5 ml of trehalose solution, vortexed, allowed to dissolve 30 min, vortexed, filtered through a 0.45 µm filter and aliquoted. Aliquots were stored at -20°C up to 6 months.

BMP-2, -4 and -7 and TNFα stock solutions

10 µg of each BMP and 10 µg of TNFα were dissolved in 2 ml trehalose solution under sterile conditions, mixed by shaking, aliquoted and stored at -20°C up to 12 months.

Carbachol, epinephrine, hemicholinium-3, quinacrine, pilocarpine and terbutaline stock solutions

Carbachol (1.8269 mg, 1 mM), epinephrine (2.1967 mg, 1 mM), hemicholinium-3 (5.7435 mg, 1mM), quinacrine (4.728 mg, 1 mM), pilocarpine (5 mg, 1 mM) and terbutaline (2.7432 mg, 1 mM) were dissolved in 10 ml of aqua B. Braun, vortexed, allowed to dissolve 30 min, vortexed, filtered through a 0.45 µm filter, aliquoted and stored at -20°C up to 12 months.

Cell culture "Complete DMEM medium"

Component	**Total volume 500 ml**	**Final concentration**
FBS (heat-inactivated)	50 ml	10% (v/v)
HEPES buffer , 1M	5 ml	10 mM
Penicillin/Streptomycin	5 ml	10 U/ml penicillin 0.1 mg/ml streptomycin

DMEM medium	440 ml

Media were stored at 4°C up to 2 weeks.

Cell culture "LPDS medium"

Component	**Total volume 500 ml**	**Final concentration**
LPDS	25 ml	5% (v/v)
HEPES buffer , 1M	5 ml	10 mM
Penicillin/Streptomycin	5 ml	10 U/ml penicillin 0.1 mg/ml streptomycin
Folic acid	2 mg	4 mg/l
L-serine	21 mg	42 mg/l
DMEM medium	440 ml	

w/o phenol red, w/o L-serine and w/o choline chloride

Media were stored at 4°C up to 2 weeks.

Cell culture "LPDS medium w/o L-serine"

Component	**Total volume 500 ml**	**Final concentration**
LPDS	25 ml	5% (v/v)
HEPES buffer , 1M	5 ml	10 mM
Penicillin/Streptomycin	5 ml	10 U/ml penicillin 0.1 mg/ml streptomycin
Folic acid	2 mg	4 mg/l
DMEM medium	440 ml	

w/o phenol red, w/o L-serine and w/o choline chloride

Media were stored at 4°C up to 2 weeks.

Cell culture "radioactive labelling medium"

Component	**Total volume 500 ml**	**Final concentration**
FBS (heat-inactivated)	50 ml	10% (v/v)
HEPES buffer , 1M	5 ml	10 mM
Penicillin/Streptomycin	5 ml	10 U/ml penicillin 0.1 mg/ml streptomycin

DMEM medium	440 ml

w/o phenol red, w/o L-serine and w/o choline chloride

Media were stored at 4°C up to 2 weeks.

Cell culture "2% starvation medium"

Component	**Total volume 500 ml**	**Final concentration**
FBS (heat-inactivated)	10 ml	2% (v/v)
HEPES buffer , 1M	5 ml	10 mM
Penicillin/Streptomycin	5 ml	10 U/ml penicillin 0.1 mg/ml streptomycin
DMEM medium	480 ml	

Media were stored at 4°C up to 2 weeks.

Cell culture "5% starvation medium"

Component	**Total volume 500 ml**	**Final concentration**
FBS (heat-inactivated)	25 ml	5% (v/v)
HEPES buffer , 1M	5 ml	10 mM
Penicillin/Streptomycin	5 ml	10 U/ml penicillin 0.1 mg/ml streptomycin
DMEM medium	465 ml	

Media were stored at 4°C up to 2 weeks.

Choline Kinase-α inhibitor (CK37) 1 mM stock solution

5 mg of CK37 inhibitor was dissolved in 13.5 ml of DMSO, vortexed, allowed to dissolve 30 min, vortexed, filtered through a 0.45 µm filter, aliquoted and stored at -20°C up to 3 months.

Citric acid 10 mM solution

1.9213 g of citric acid was dissolved in 990 ml of aqua B. Braun, then filled up to 1 l. pH was adjusted to 3.0. Solution was sterile filtered through a 0.22 µm filter and stored at RT up to 6 months.

[D4]-ethanolamine stock solution

10 µl of [D4]-ethanolamine was dissolved in 990 µl of LPDS medium, filtered through a 0.45 µm filter, aliquoted and stored at 4°C up to 1 week.

[D9]-choline chloride stock solution

10 mg of [D9]-choline chloride was dissolved in 1ml of LPDS medium, filtered through a 0.45 µm filter, aliquoted and stored at 4°C up to 1 week.

Dexamethasone stock solutions

Dexamethasone (3.9246 mg, 1 mM and 7.8492 mg, 2 mM) was dissolved in 10 ml of 95% ethanol, vortexed, allowed to dissolve 30 min, vortexed, filtered through a 0.45 µm filter, aliquoted and stored at -20°C up to 24 months.

EDTA 0.5 M solution

186.1 g of EDTA was dissolved in 1000 ml of aqua B. Braun. The pH was adjusted to 8.0. Solution was stored at 4°C up to 4 months.

ERK inhibitor SCH772984 0.5 mM stock solution

5 mg of SCH772984 inhibitor was dissolved in 17 ml of DMSO, vortexed, allowed to dissolve 30 min, vortexed, filtered through a 0.45 µm filter, aliquoted and stored at -20°C up to 6 months.

Gelatin-PBS solution

20 mg of gelatin was dissolved in 20 ml of 1x PBS under slight heating (max. 50°C), then cooled down and sterile filtered through a 0.45 µm filter. Aliquots were stored at -20°C up to 6 months.

Glucocorticoid receptor antagonist RU 486 0.5 mM stock solution

5 mg of SCH772984 inhibitor was dissolved in 23.278 ml of DMSO, vortexed, allowed to dissolve 30 min, vortexed, filtered through a 0.45 µm filter, aliquoted and stored at -20°C up to 6 months.

Heat-inactivation of FBS

The heating process inactivates proteins of the complement cascade. This process is recommended in immunological studies and the culture of embryonic stem cells, insect cells and smooth muscle cells. 500 ml of completely thawed FBS was incubated in water bath at 56ºC. When fluid temperature reached 56ºC, FBS was heat-inactivated for 30 min. Aliquots were stored at -20°C up to given expiration date.

IGF-1 stock solution

100 µg of IGF-1 was dissolved in 20 ml trehalose solution under sterile conditions, mixed by shaking, aliquoted and stored at -20°C up to 12 months.

IL-1β stock solution

5 µg of IL-1β was dissolved in 10 ml of gelatin-PBS solution under sterile conditions, mixed by shaking, aliquoted and stored at -20°C up to 3 months.

IL-6 stock solution

5 µg of Il-6 was dissolved in 10 ml of trehalose solution under sterile conditions, mixed by shaking, aliquoted and stored at -20°C up to 12 months.

JNK inhibitor SP600125 5 mM stock solution

5 mg of SP600125 inhibitor was dissolved in 4.541 ml of DMSO, vortexed, allowed to dissolve 30 min, vortexed, filtered through a 0.45 µm filter, aliquoted and stored at -20°C up to 6 months.

NF-kB inhibitor QNZ 5 mM stock solution

5 mg of QNZ inhibitor was dissolved in 2.649 ml of DMSO, vortexed, allowed to dissolve 30 min, vortexed, filtered through a 0.45 µm filter, aliquoted and stored at -20°C up to 6 months.

P38 inhibitor SB203580 5 mM stock solution

5 mg of SB203580 inhibitor was dissolved in 2.806 ml of DMSO, vortexed, allowed to dissolve 30 min, vortexed, filtered through a 0.45 µm filter, aliquoted and stored at -20°C up to 6 months.

PI3K inhibitor LY294002 5 mM stock solution

5 mg of LY294002 inhibitor was dissolved in 3.254 ml of DMSO, vortexed, allowed to dissolve 30 min, vortexed, filtered through a 0.45 µm filter, aliquoted and stored at -20°C up to 6 months.

Sirtuin-Inhibitor EX 527 stock solutions

5 mg of EX 527 inhibitor (40 mM) was dissolved in 0.5 ml DMSO, vortexed, allowed to dissolve 30 min, vortexed and aliquoted. To prepare 25 mM solution, 0.25 ml of 40 mM EX 527 stock solution was diluted with 0.15 ml of DMSO, vortexed, filtered through a 0.45 µm filter and aliquoted. To prepare 0.5 mM solution, 10 µl of 40 mM EX 527 stock solution was diluted with 0.790 ml of DMSO, vortexed, filtered through a 0.45 µm filter and aliquoted. Aliquots were stored at -20°C up to 6 months.

Staurosporine 1mM solution

100 µg of staurosporine was dissolved in 0.22 ml DMSO, vortexed, allowed to dissolve 30 min, vortexed, aliquoted and stored at -80°C up to 6 months.

TGF-β receptor inhibitor SB431542 5 mM stock solution

5 mg of SB431542 inhibitor was dissolved in 2.602 ml of DMSO, vortexed, allowed to dissolve 30 min, vortexed, filtered through a 0.45 µm filter, aliquoted and stored at -20°C up to 6 months.

TGF-β1 stock solution

2 µg of TGF-β1 was dissolved in 20 µl 10 mM citric acid (pH 3.0) under sterile conditions, then 3.980 ml trehalose solution was added, solution was mixed by shaking, aliquoted and stored at -20°C up to 12 months.

Trehalose solution

2.5 g of trehalose was dissolved in 50 ml of aqua B. Braun, then sterile filtered using a 0.22 µm filter. Aliquots were stored at -20°C up to 12 months.

3.1.6. Human FLS

The study was approved by the Ethical review Committee of Faculty of Medicine (Justus Liebig University, Giessen, Germany). All patients provided written consent to donor samples for research. FLS were obtained from patients undergoing total knee replacement surgery and fulfilling the following inclusion criteria: diagnosed OA, both genders, age 50-85 years, BMI between 20 and 35, all CRP values. FLS were excluded due to (a) a joint disease other than OA such as RA, infection, gout, trauma, (b) knee joint surgery within the last 6 months, (c) severe diseases including HIV, tumor near to joint, severe liver and kidney diseases, drug abuse and (d) intake of immunosuppressive drugs, corticosteroids or HA within last 6 months. In case of preliminary experiments patients fulfilled inclusion/exclusion with few exceptions in terms of BMI. Inclusion/exclusion criteria were strongly followed during screening and main experiments. Table 1 and 2 present characterization of patients used for the experiments.

	Main Experiment – Screening- (see 3.4.1.)	Main Experiment - Mechanism - (see 3.4.2.)
N	6	5
Age (years) mean ± SD	73.5±7.1	80.2±6.2
Gender ♂	2	3
♀	4	2
BMI mean ± SD	29.1±3.5	28.6±2.4
CD90+ (%)	87.4±7.6	96.4±3.5
Diagnosis	OA	OA
Other diseases	Cardiovascular diseases (5x) Hypertension (4x) Hyperlipidemia (2x) Hypothyroidism (1x) Obesity (1x) Chronic obstructive pulmonary disease (1x)	Cardiovascular diseases (3x) Hypertension (5x) Hyperlipidemia (2x) Hypothyroidism (1x) Obesity (2x) Diabetes mellitus (2x) Kidney disease (2x) Constipation (1x)

Table 1. Characterization of the patients used for the biosynthesis experiments.

	Main Experiment – Screening- (see 3.4.3.)	Main Experiment - Mechanism - (see 3.4.4.)
N	5	6
Age (years) mean ± SD	75.2±9.0	81.8±5.5
Gender ♂	2	4
♀	3	2
BMI mean ± SD	28.4±3.0	29.4±3.0
CD90+ (%)	77.4±18.4	97.4±1.5
Diagnosis	OA	OA
Other diseases	Cardiovascular diseases (1x) Hypertension (3x) Hyperlipidemia (1x) Diabetes mellitus (1x) Obesity (1x) Gastritis (1x) Gallstone (1x)	Cardiovascular diseases (3x) Hypertension (6x) Hyperlipidemia (2x) Hypokalemia (3x) Diabetes mellitus (2x) Obesity (1x) Hypothyroidism (2x) Kidney diseases (2x)

Table 2. Characterization of the patients used for the release experiments.

3.1.7. Analysis Software

Name	Company
7500 Fast System Software	Applied Biosystems, Thermo Fisher Scientific, GmbH, Waltham, MA, USA
Excel Macros	provided by Dr. G. Liebisch, Regensburg, Germany
FACSDiva software, version 6.1.3	Becton Dickinson GmbH, Hilderberg, Germany
Graph Pad Prism 5.2	Graphpad Software Inc., La Jolla, CA, USA
i-control™, microplate reader software	Tecan Group Ltd., Maennedorf, Switzerland
Intas® GDS	Intas Science Imaging Instruments GmbH, Goettingen, Germany
Magellan™, microplate reader software	Tecan Group Ltd., Maennedorf, Switzerland
Microsoft Office Excel 2007	Microsoft, Redmond, WA, USA
NanoDrop™ 1000 Operating Software, version 3.8.1	Thermo Fisher Scientific GmbH, Waltham, MA, USA

3.2. Methods

3.2.1. FLS isolation

FLS isolation is based on a mechanical and enzymatic disaggregation using a bacterial protease dispase II. This proteolytic enzyme cleaves fibronectin, collagen IV, and to a lesser extent collagen I, thereby destroying cell-cell adhesion.

FLS isolation was performed under sterile conditions according to a method previously described (89). In brief, synovial tissue was rinsed with cold, sterile 1x PBS and separated using a scalpel from blood vessels, fatty cells and connective tissue (Figure 3). Required synovial tissue was chopped into less than 1 mm^3 pieces. Those small pieces were digested for 1 hour at RT in 1x PBS containing 1% dispase II. The cell suspension was filtered through a 70 µm cell strainer, centrifuged at 300 x g for 10 min, resuspended in 15 ml of complete DMEM medium, and plated into cell culture T-75 flasks. FLS were maintained in a humidified incubator at 37°C and 10% CO_2.

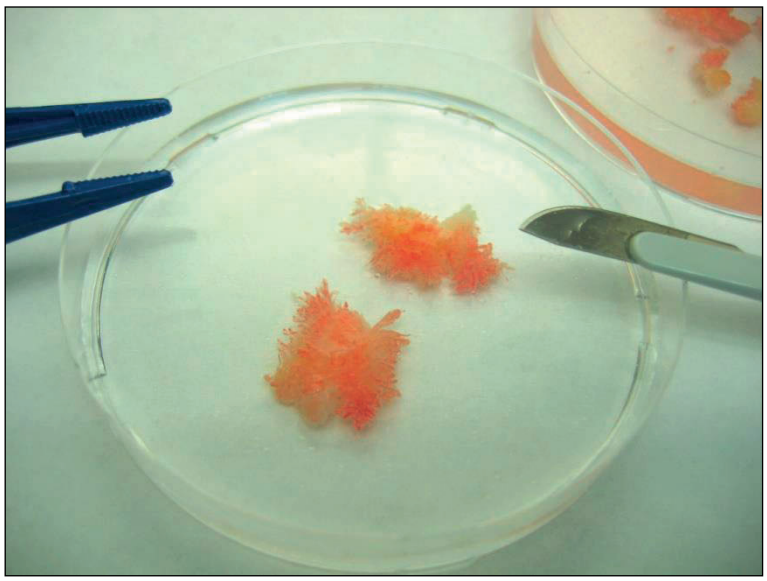

Figure 3. Synovial membrane during isolation.

3.2.2. FLS culture

FLS were cultured in complete DMEM medium in a humidified atmosphere at 37°C and 10% CO_2. Media were changed three times a week, on Mondays, Wednesdays and Fridays. Confluent FLS were washed with 1x PBS and trypsinized with 1x Trypsin/EDTA. Reaction of trypsin was stopped with complete DMEM medium. Cells were centrifuged at

300 x g for 10 min and then passaged into new T-75 flasks. In case of freezing FLS were trypsinized and frozen in FBS containing 10% of DMSO using a freezing container filled up with isopropanol to achieve -1°C/min rate of cooling, and stored at -86°C. When needed, FLS were thawed, centrifuged 300 x g for 10 min and resuspended in complete DMEM medium. All experiments were carried out with FLS from passage 4 to 5 to ensure stable phenotype and genotype of FLS (89).

3.2.3. Mycoplasma detection

Mycoplasma contamination in cell culture is a problem that can cause non-reproducible, questionable results in research. The presence of contaminative mycoplasma species can be easily and sensitively detected using a PCR-based test which displays the bands of amplified DNA fragments after gel electrophoresis.

To ensure that FLS culture is myoplasma-free, PCR Mycoplasma Test Kit I/C was used according to the instructions provided by the manufacturer. Briefly, 10 µl of amplification products were mixed with 2 µl of Blue/Orange 6x Loading Dye and separated on ethidium bromide stained 1.4% agarose gel in 1x TAE buffer. The DNA bands were visualized and documented by the Gel iX Imager. All experiments were carried out with mycoplasma negative FLS.

3.2.4. FACS analysis

Flow cytometry measures optical and fluorescence characteristics of single cells. Antibodies conjugated to fluorescent dyes can bind to specific cellular antigens. When labelled cells are passed by a light source, the fluorescent molecules are excited to a higher energy state. Upon returning to their resting states, the fluorochromes emit light energy at higher wavelengths. During analysis fluorescent character of each cell is measured.

To ensure purity of isolated FLS, cells were characterized by positive staining for fibroblast-specific antigen CD90 and negative stained for macrophage-specific antigen CD45 using fluorescence-activated cell sorting (FACS). Antigens were detected as follows (Table 3):

Antigen	Antibody	Fluorescent dye	Excitation	Emission
CD45	Anti-human CD45	Phycoerythrin (PE)	496 nm	578 nm
CD90	Anti-human CD90	Allophycocyanin (APC)	650 nm	660 nm

Table 3. Detection of cell-surface antigens of FLS.

To prepare FLS for analysis, cells were trypsinized or thawed, centrifuged at 300 x g for 10 min in RT and resuspended in 200 µl of 1x PBS at a concentration of 100,000 cells per 100 µl of 1x PBS. The cell suspension was divided into CD90/CD40 sample and isotype control, 100 µl each. Non-specific interactions were blocked with 10 µl of antibody free serum (AB serum) which is a serum of AB type blood. Surface antigens were stained for 45 min at RT as follows (Table 4):

Sample	Antibody	Volume
CD90/CD45 sample	PE anti-human CD45	2.5 µl (undiluted)
	APC anti-human CD90	2.5 µl (undiluted)
Isotype control	PE Mouse IgG1, κ Isotype Ctrl	0.5 µl (undiluted)
	APC Mouse IgG1, κ Isotype Ctrl	0.5 µl (undiluted)

Table 4. List of antibodies used for detection of cell-surface antigens of FLS.

Then samples were washed with 1 ml of 1x PBS, vortexed and centrifuged at 1200 rpm for 10 min at 4°C. 950 µl of 1x PBS was removed, then samples were transferred into FACS tubes, vortexed and stained with 1 µl of Sytox® Dye dead cell stain. Afterwards samples were analysed in BD FACS Canto II flow cytometer (Figure 4). CD90 positive cells were presented as a percentage of total cells.

In case of preliminary and screening experiments frozen FLS were used for FACS analysis, which caused problems with staining. Thus, for the main experiments fresh FLS of passage 5 at 100% confluency were analysed and at least 90% were CD90 positive (Figure 4).

3.2.5. Cell counting and viability assay

Trypan blue solution is routinely used as a cell stain to assess cell viability using the dye exclusion test. It is based on the principle that live cells possess intact cell membranes that exclude dyes such as trypan blue, whereas dead cells do not.

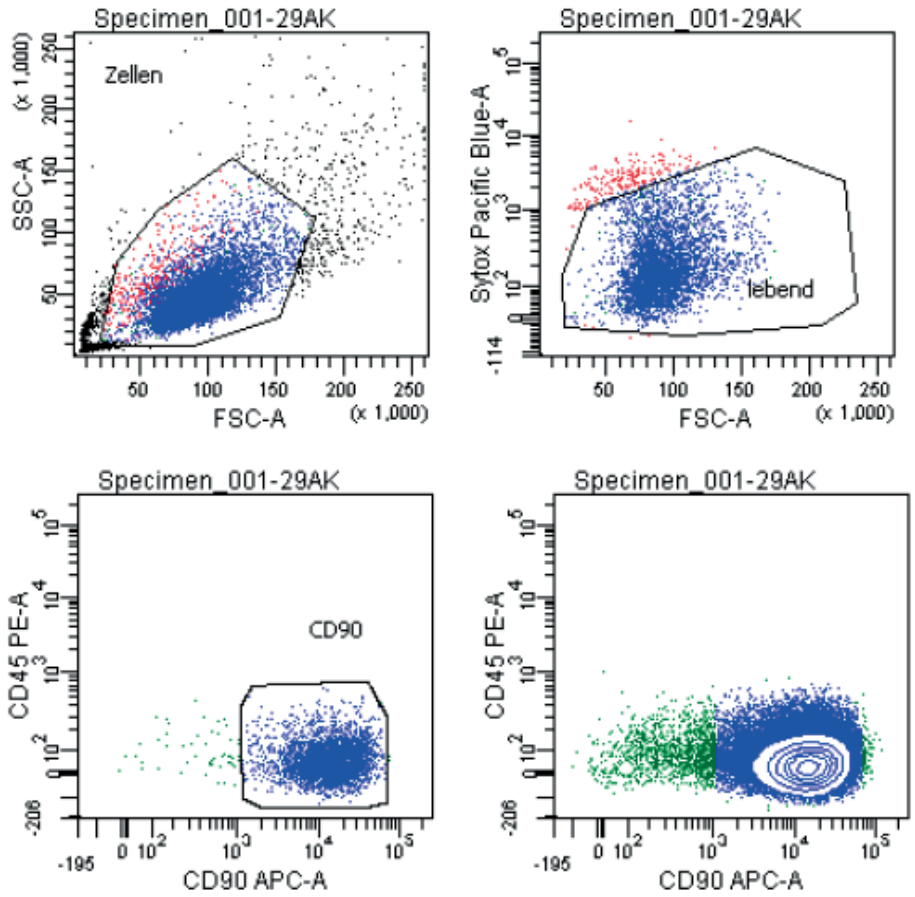

Figure 4. Characterization of FLS. Representative FACS analysis. Upper panel presents gates for total cells and living cells. Lower panel shows CD90 positive FLS.

In order to determine cell number and viability, FLS were trypsinized and centrifuged at 300 x g for 10 min and then resuspended in 1 ml or 0.5 ml of complete DMEM medium. 10 µl of sample was mixed with 10 µl of 0.4% trypan blue solution and pipetted into a disposable Countess™ chamber slide. Measurement was performed in Countess™ II Automated Cell Counter which uses trypan blue staining combined with an autofocus optical system and sophisticated image analysis algorithm to obtain accurate cell and viability counts.

3.2.6. Mitochondrial activity assay

The MTT assay is a colorimetric assay for assessing cell metabolic activity. Living cells possess mitochondrial reductases which are capable to reduce the yellow tetrazolium dye MTT 3-(4,5-dimethylthiazol-2-yl)-2,5-diphenyltetrazolium bromide to insoluble formazan, which has a purple colour. After solubilisation of formazan, the absorbance of coloured

solution can be quantified at 560 nm. Cells with a low metabolism produce very little formazan, whereas highly active cells exhibit huge MTT reduction.

To describe the mitochondrial activity of FLS in our both *in vitro* models, the MTT assay was performed using Cell Titer 96®Non-Radioactive cell Proliferation assay according to manufacturer protocol. Briefly, FLS from 3 patients were seeded into 6 well plates at density 80,000 cells per well and were cultured according to the method used in the biosynthesis (see chapter 3.3.1.) or release model (see chapter 3.3.2.) including various labelling respectively release steps. The labelling steps in the biosynthesis model lasted 8, 16 and 24 hours. The release steps in the release model lasted 12, 24 and 36 hours.

Absorbance of each sample was measured at 560 nm in the Sunrise ™ microplate absorbance reader. Data were normalized to 100,000 viable cells, averaged, and compared with the control condition (complete DMEM medium).

3.2.7. Apoptosis assay

Activation of apoptotic caspases e.g. caspase-3, and -7 results in activation of a cascade of signalling events permitting the controlled demolition of cellular components. The Caspase-Glo® 3/7 Assay is a luminescent assay that measures caspase-3 and -7 activities in cultures of adherent cells. The assay provides a proluminescent caspase-3/7 substrate, which contains the tetrapeptide sequence DEVD. This substrate is cleaved by caspase-3/7 to release aminoluciferin, a substrate of luciferase used in the production of light.

Due to decreased mitochondrial activity of FLS in our biosynthesis model, apoptosis was evaluated using the Caspase-Glo® 3/7 Assay according to the instructions provided by the manufacturer. In brief, FLS from 3 patients were seeded into 96 well plates at density 15,000 cells per well and cultured according to the method used in the biosynthesis model (see chapter 3.3.1.) and the duration of labelling steps lasting 8, 16 and 24 hours.

1 μM of staurosporine was used as a positive control for the activation of apoptosis. Luminescence was measured in Infinite® 200 PRO microplate luminescence reader. Data were averaged and compared with those of the control condition (complete DMEM medium) as well as with those of the positive control (1 μM of staurosporine).

3.2.8. Analysis of reference genes

Reference genes, also called housekeeping genes are involved in basic cell maintenance, and are therefore expected to maintain constant expression levels in all cells and conditions.

To check whether the expression of housekeeping genes in our both *in vitro* models of FLS are stable, RNA was isolated from FLS and used to synthesize cDNA, which was further analysed by quantitative real-time PCR. Briefly, FLS from 3 patients were seeded into 6 well plates at a density of 80,000 cells per well and cultured according to the method used in the biosynthesis (see chapter 3.3.1.) or release model (see chapter 3.3.2.) including various labelling (8, 16, 24 hours) respectively release (12, 24, 36 hours) steps.

RNase-free equipment was used during handling with RNA and cDNA. Also work was performed under RNase-free conditions.

3.2.8.1. RNA isolation

Isolation of RNA with peqGOLD TriFast™ is based on the acid guanidinium thiocyanate-phenol-chloroform extraction (90). This method relies on phase separation by centrifugation of a mixture of the aqueous sample and a solution containing phenol and chloroform, resulting in an upper aqueous phase containing RNA, the interphase containing DNA, and a lower organic phase in which the proteins are present.

Total RNA was isolated from FLS according to the manufacturer's instruction. Concentration and purity of obtained RNA was determined spectrophotometrically at 260 nm and 280 nm wavelengths using NanoDrop™ 1000. The 260/280 ratio was calculated. Only samples containing pure RNA with 260/280 ratio between 1.8 and 2.0 were used for further analysis.

3.2.8.2. Reverse transcription

Reverse transcription is the synthesis of single-stranded complementary DNA (cDNA) using single-stranded RNA as a template, mediated by the enzyme reverse transcriptase (RT). The cDNA can be used as a template for amplification by PCR.

To perform reverse transcription QuantiTect® Reverse Transcription Kit was used according to manufacturer protocol. The obtained cDNA was used for real-time PCR.

3.2.8.3. Quantitative real-time PCR

SYBR Green is a commonly used fluorescent dye that binds double-stranded DNA molecules by intercalating between the DNA bases. It is used in quantitative PCR because the fluorescence can be measured at the end of each amplification cycle to determine, relatively or absolutely, how much DNA was amplified.

In order to investigate the expression of housekeeping genes, QuantiFast® SYBR® Green PCR Kit was used according to manufacturer protocol. Briefly, cDNA samples obtained from reverse transcription were diluted 1:4 with RNase-free water and 2 µl of each sample was mixed with SYBR Green Master Mix and primers. For amplification of specific products of the genes of interest established by Qiagen the following QuantiTect® Primer Assays were used (Table 5):

Gene	Name	Specific product
Beta-2-microglobulin	B2M: Hs_B2M_1SG	NM_004048 (987 bp)
Beta-actin	βactin: Hs_ACTB_2_SG	NM_001101 (1852 bp)
Glyceraldehyde 3-phosphate dehydrogenase	GAPDH Hs_GAPDH_2_SG	NM_002046 (1421 bp)

Table 5. List of real-time PCR primers obtained from Qiagen.

PCR amplification of specific transcripts was carried out in Real Time PCR System 7500 Fast. The threshold cycles (Ct) were determined for all samples and used for calculation of the ratios of levels of expression of the reference genes of FLS cultured in 5% LPDS versus 10% FBS as well as 2% FBS versus 10% FBS and 5% FBS versus 10% FBS.

3.2.9. Protein quantification

The bicinchoninic acid assay (BCA assay) is a biochemical assay to determine the total protein concentration in a solution (91). The first step of reaction is the chelation of copper with protein in an alkaline environment. In the second step bicinchoninic acid (BCA) reacts with the reduced cuprous cation that was formed in step one resulting in an intense purple-coloured reaction. The BCA/copper complex is water-soluble and exhibits a strong linear absorbance at 562 nm with increasing protein concentrations.

To determine protein concentrations within 0.1% SDS cell lysates, Pierce™ BCA Protein Assay Kit with bovine albumin as a standard was used according to manufacturer protocol. The standard curve was prepared and used for the determination of the protein concentration of each unknown sample.

3.2.10. Lipid extraction

The extraction of lipids in a solution relies on a phase separation by centrifugation (92). Originally, the tissue homogenate is mixed with chloroform and methanol in such proportions that a miscible system is formed with the water in the tissue. Dilution with chloroform and water separates the homogenate into two layers, the lower chloroform layer contains all lipids and the upper methanolic layer contains all non-lipids. A purified lipid extract is obtained by isolating the chloroform layer.

3.2.10.1. Lipid extraction of stable isotope-labelled samples

Extraction of PLs from stable isotope-labelled cell lysates was performed according to the method of Bligh and Dyer in the presence of non-naturally occurring lipid species which served as internal standards. The following lipid species were added as internal standards: PC 14:0/14:0, PC 22:0/22:0, PE 14:0/14:0, PE 20:0/20:0, PS 14:0/14:0, PS 20:0/20:0, PG 14:0/14:0, PG 20:0/20:0, LPC 13:0, LPC 19:0, Cer 14:0, Cer 17:0, D_7-FC, CE 17:0, and CE 22:0. Mixture of 300 µl of cellular extract and 500 µl of water was used as starting material. PLs were isolated by adding 3 ml of methanol/chloroform (2:1, v/v) followed by 1 hour incubation at RT. Separation of phases was performed by adding 1 ml of chloroform and 1 ml of water. Subsequently, samples were centrifuged at 4000 rpm for 10 min at RT. 1.2 ml of the

chloroform phases containing PLs was collected using a Pipetting Robot Genesis and dried in a vacuum centrifuge for 1 hour. For further ESI-MS/MS analysis, dried samples were dissolved in 1 ml methanol/chloroform solution (3:1, v/v) containing 7.5 mM ammonium acetate.

3.2.10.2. Lipid extraction of radioactive isotope-labelled samples

Extraction of PLs from radioactive isotope-labelled cell lysates and experimental media was performed according to the method of Bligh and Dyer. The volumes of reagents were added to samples as follow (Table 6):

Sample	Methanol/chloroform	Chloroform	Water
Cell lysate: 500 µl	1.875 ml	0.625 ml	0.625 ml
Medium: 100 µl	0.375 ml	0.125 ml	0.125 ml

Table 6. The volumes of reagents added to radiolabelled samples during lipid extraction according to Bligh and Dyer.

First, samples were incubated with methanol/chloroform solution (2:1, v/v) and incubated for 1 hour at RT. Separation of phases was performed by the addition of chloroform and water. Subsequently, samples were centrifuged at 4000 rpm for 10 min at RT. The chloroform phase was collected: 1 ml in case of media or 200 µl in case of cell lysate extract and further analysed by liquid scintillation counting.

3.2.11. Mass spectrometry ESI-MS/MS

Mass spectrometry analysis is based on the mass and charge differences of the molecules. With this powerful method both unlabelled and labelled lipid species can be analysed at the same time. During electrospray ionization tandem mass spectrometry (ESI-MS/MS) a spray of solvent and solute expands from a narrow orifice held at a high electrical potential resulting in charged droplets which subsequently explodes, forming smaller droplets, which are directed to the mass analyser optics. MS/MS spectrometer has two mass analysers linked in tandem, separated by a collision cell. The first analyser measures the mass of ionized molecules. In the collision cell ionized molecules undergo fragmentation. The second

analyser measures the ion fragments generated in the previous step. Molecules of smaller mass reach the detector first.

Lipid species of stable isotope-labelled samples were quantified by ESI-MS/MS using the mass spectrometer Quattro Ultima™ Triple Quadruple and analytical setup and strategy described by PD Dr. rer. nat. G. Liebisch of the Institute for Clinical Chemistry and Laboratory Medicine, University Hospital of Regensburg, Germany. In brief, precursor ion scan of mass/charge (*m/z*) 184 specific was used for phosphatidylcholine (PC), sphingomyelin (SM), and lysophosphatidylcholine (LPC) detection (93). [D9]-choline-labelled lipids were analysed by precursor ion scan of 193. Neutral loss scans of 141 and 185 were used for detection of phosphatidylethanolamine (PE) and phosphatidylserine (PS), respectively (94). [D4]-ethanolamine-labelled lipids were analysed by neutral loss scan of 145. PE-based plasmalogen (PE P) was analysed according to method described by Zemski *et al.* (95). Briefly, fragment ions of *m/z* 364, 380 and 382 were used for detection PE P-16:0, PE P-18:1, and PE P-18:0, respectively. Ammonium adductions of phosphatidylglycerol (PG) and phosphatidylinositol (PI) were determined by neutral loss scans of 189 and 277, respectively (96). Ceramides (Cer) were measured using a product ion of *m/z* 264 (97). Internal standards added to samples during lipid extraction were used to quantity corresponding lipid classes. Besides this, PC internal standards were used also for SM determination and PE internal standards were used for PE P determination. Correction of isotopic overlap of lipid species was performed by self-programmed Excel Macros for all lipids (93).

The quantitative values of all PL species were normalized to determined protein content and are expressed as nmol/mg protein. Only PL species with a level higher than 1% of the corresponding PL class were considered. Moreover, only values which were three times higher than the internal standard blank were taken to account. Lipid species were annotated according to the "Shorthand notation of lipid structures that are derived from mass spectrometry" (98). For each PL class and species the percentage of labelled PL was calculated using the following equation:

$$\%\ \text{labelled PL} = \frac{\text{labelled PL}\left(\frac{\text{nmol}}{\text{mg protein}}\right)}{\text{labelled PL}\left(\frac{\text{nmol}}{\text{mg protein}}\right) + \text{unlabelled PL}\left(\frac{\text{nmol}}{\text{mg protein}}\right)} \text{ x } 100$$

Data for individual PL species were related to corresponding control equal 1.0, averaged and presented as x-fold change of % labelled PL compared to control.

3.2.12. Liquid scintillation counting

Liquid scintillation counting (LSC) is the standard laboratory method to quantify the radioactivity of low energy radioactive isotopes, mostly β-emitting and α-emitting isotopes. The LSC detection method requires specific cocktails to absorb the energy emitted by radioisotopes. Liquid scintillator cocktails contain two basic components, the solvent and the scintillator. The solvent carries out the bulk of the energy absorption, while scintillator converts the absorbed energy into light. The intensity of the light is proportional to the β particle's initial energy. Blue light flashes hit the photo cathode and then amplitude of the electrical pulse is converted into digital value.

Lipids of radioactive isotope-labelled samples were quantified using LSC. Briefly, the chloroform phases taken from lipid extraction were mixed with Emulsifier-Safe™ cocktail: 1 ml of medium extract with 15 ml of cocktail and 200 µl from cell lysate extract with 4 ml of cocktail. Samples were shaken overnight on the rocker and measured in [^{3}H]- and [^{14}C]-channels in the Multi-Purpose Scintillation Counter LS 6500. The quantitative values of all lipids were normalized to the cellular protein content and are expressed as dpm/mg cellular protein. The percentages of released [^{3}H]-choline- and [^{14}C]-ethanolamine-labelled PLs were calculated using the following equation:

$$\%\ \text{released PLs} = \frac{\text{total media counts}\left(\frac{\text{dpm}}{\text{mg protein}}\right)}{\text{total media counts}\left(\frac{\text{dpm}}{\text{mg protein}}\right) + \text{total cellular counts}\left(\frac{\text{dpm}}{\text{mg protein}}\right)} \text{ x } 100$$

3.2.13. Statistical analysis of data

All data are expressed as mean ± SD. We have assumed normally distribution of data. Grubb's test was chosen to eliminate significant outliers from the data.

For establishing experimental models different tests were used. Statistical comparison of the effect of single and double labelling and the effect of different concentrations of isotopes were tested by 2-way ANOVA. The paired t-tests were applied to analyse the effect of increasing concentrations of radioactive isotopes on radiolabelled PLs. Correlation between the time of labelling and PL labelling as well as time of release and PL release were calculated using the Spearman's rank correlation. The impacts of the addition of L-serine to the cell culture on the labelling of PL as well as on the caspase 3/7 activity were tested using

the paired t-test. Significant differences between experimental (LPDS medium, 2 and 5% starvation medium) and control conditions (complete DMEM medium) in terms of cell viability, MTT and expression of housekeeping genes values related to control conditions were calculated and then evaluated by 1-way ANOVA.

The effects of various treatments on PL biosynthesis (% labelled PL, x-fold change of % labelled PL compared to control, and % released PLs) were determined by the t-tests. Bonferroni correction for multiple testing was applied for screening the effect of various cytokines on the biosynthesis and release of PLs.

P-values < 0.05 (*), < 0.01 (**) and < 0.001 (***) were considered statistically significant. Significance is shown in the respective figures.

The statistical analysis was performed using Graph Pad Prism 5.2.

3.3. Preliminary experiments

3.3.1. An *in vitro* model to study the biosynthesis of PLs

To investigate the biosynthesis of PLs, the stable isotopes [D9]-choline and [D4]-ethanolamine were used. Choline and ethanolamine are precursors which are incorporated into PLs during *de novo* synthesis. ESI-MS/MS measures both, labelled and unlabelled PL species, so that newly synthesized PLs can be distinguished.

Experiments were performed in medium containing 5% lipoprotein deficient serum (LPDS). Using LPDS medium avoided binding of lipids to lipoproteins. Moreover, this medium introduced less external PLs to cells then complete DMEM, containing 10% FBS, so that cells are stimulated to synthesize lipids. Addition of folic acid to culture media accelerated cell metabolism. To enhance uptake of the stable isotope [D9]-choline, DMEM medium w/o phenol red, w/o L-serine and w/o choline chloride was used. Depletion of phenol red ensured no interference such as quenching of the phenol during ESI-MS/MS analysis. Starvation period helped to synchronize FLS.

The final biosynthesis model was designed as presented in Figure 5.

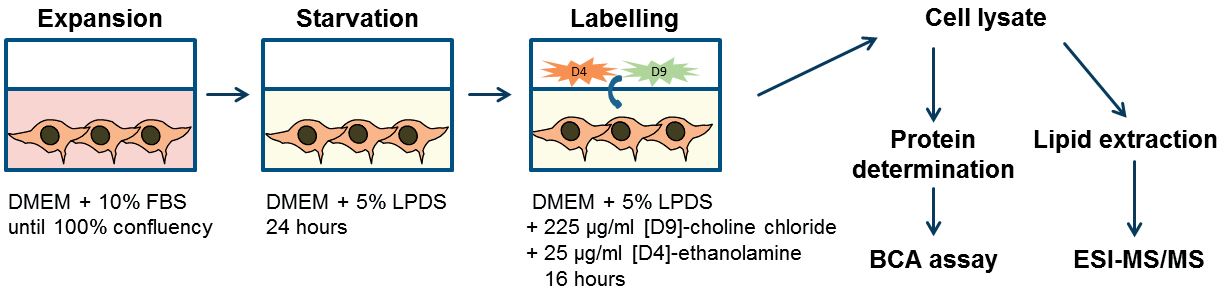

Figure 5. Schematic representation of the biosynthesis model.

FLS were seeded into 6-well-plates at a density of 80,000 cells per well. FLS were cultured using complete DMEM medium in humidified 10% CO_2 atmosphere at 37°C. At a confluence of 100%, cells were prewashed with phenol red-free DMEM and then 2 ml per well of LPDS medium w/o L-serine was added. Cells were starved for 24 hours. Media were changed to the LPDS medium w/o L-serine and 225 µg/ml of [D9]-choline and 25 µg/ml of [D4]-ethanolamine were added. Experiments were terminated after 16 hours. Cells were washed twice with 1x PBS and lysed by the addition of 0.5 ml of 0.2% SDS. Lysed wells were washed with 0.5 ml of aqua B. Braun, combined extracts were ultrasonicated for 6 sec, 3 x 10% pulse, with 40-50% power. Protein concentration within lysates was evaluated using BCA assay. Lipids were extracted according to Bligh and Dyer, and analysed by ESI-MS/MS.

3.3.2. Optimization of an *in vitro* model to study the biosynthesis of PLs

Before the final biosynthesis model was established, several parameters needed to be optimized.

3.3.2.1. PL background of the experimental media

To investigate the PL background of experimental media, 2 ml of complete DMEM medium, 2 ml of LPDS medium w/o L-serine and 2 ml of LPDS medium (containing L-serine) were incubated in humidified 10% CO_2 atmosphere at 37°C for 24 hours, then frozen. Lipids were extracted according to Bligh and Dyer, and then samples were evaluated by ESI-MS/MS.

3.3.2.2. Effect of single versus double labelling on the incorporation of precursors into PLs

To investigate the effect of single and double labelling on the incorporation of isotope-labelled precursor into two main PL classes PC and PE, FLS from 3 patients were seeded into culture dishes at a density of 480,000 cells per dish. FLS were cultured in LPDS medium w/o L-serine until 80% confluency and labelled with 100 µl/ml of [D9]-choline and/or 100 µl/ml of [D4]-ethanolamine for a duration of 24, 48 and 72 hours.

3.3.2.3. Identification of cell number needed to study the biosynthesis of PLs

To find optimal cell number to study the biosynthesis of PLs, FLS from 3 patients were seeded into culture dishes at a density of 480,000 cells per dish, 6 wells in 6-well-plate at a density of 80,000 cells per well, and 4 wells in 6-well-plate at a density of 80,000 cells per well. FLS were cultured in LPDS medium w/o L-serine until 80% confluency. Cells were labelled with 100 µl of [D9]-choline and 100 µl/ml of [D4]-ethanolamine for a duration of 24 hours.

3.3.2.4. Concentration-dependent effect on the incorporation of stable isotope-labelled precursors into PLs

The physiological concentration of choline in human blood is 9 times higher than ethanolamine. Thus we checked the concentrations of isotopes in this proportion. To investigate whether increasing concentrations of isotopes resulted in enhanced labelled PLs, FLS from 3 patients were seeded into culture dishes at a density of 480,000 cells per dish and cultured in LPDS medium w/o L-serine until 80% confluency. FLS were labelled with:

- 225 µl/ml of [D9]-choline and 25 µl/ml of [D4]-ethanolamine
- 450 µl/ml of [D9]-choline and 50 µl/ml of [D4]-ethanolamine
- 900 µl/ml of [D9]-choline and 100 µl/ml of [D4]-ethanolamine, or
- 1800 µl/ml of [D9]-choline and 200 µl/ml of [D4]-ethanolamine

for a duration of 24, 48 and 72 hours.

3.3.2.5. Effect of cell confluency on the biosynthesis of PLs

To investigate the impact of cell confluency on the biosynthesis of PLs, FLS from 3 patients were seeded in culture dishes until 80% confluency. Cells were labelled with 200 µg/ml of [D9]-choline and 200 µl/ml of [D4]-ethanolamine for a duration of 4, 8, 12 and 24 hours.

3.3.2.6. Effect of the time of labelling on the incorporation of stable isotope-labelled precursors into PLs

To investigate whether increasing the time of labelling enhances the amount of incorporated precursors into PLs, FLS from 3 patients were seeded into 4 wells in 6-well-plates at a density of 80,000 cells per well. FLS were cultured in LPDS medium w/o L-serine until 100% confluency, and were labelled with 225 µl/ml of [D9]-choline and 25 µl/ml of [D4]-ethanolamine for a duration of 8, 16 and 36 hours.

3.3.2.7. Effect of L-serine on the incorporation of stable isotope-labelled precursors into PLs

In our main experiments, we used LPDS medium containing L-serine to ensure access of all amino acids to enzymes and proteins. To investigate whether the presence of L-serine in culture medium has an impact on the incorporation of precursors into PLs, FLS from 6 patients were seeded into 3 wells of 6-well-plates at a density of 80,000 cells per well. FLS were cultured in LPDS medium w/o L-serine or LPDS medium (containing 42 mg/l of L-serine) until 100% confluency, and were then labelled with 225 µl/ml of [D9]-choline and 25 µl/ml of [D4]-ethanolamine for a duration of 16 hours.

3.3.3. An *in vitro* model to study the release of PLs

To investigate the release of PLs, the radioactive isotopes [^{3}H]-choline and [^{14}C]-ethanolamine were used. The release of radiolabelled PLs into the cell culture media from FLS was measured using LSC. Data from both, cellular extracts and media allowed us to

calculate the rate of PL release. Release of choline-based PLs in [^{3}H]-labelled fraction and ethanolamine-based PLs in [^{14}C]-labelled fraction were quantified.

The FLS of our *in vitro* model were labelled with radioactive isotopes, and then washed until no radioactivity was detected in culture medium. To enhance uptake of [^{3}H]-choline, choline- and serine-depleted DMEM was used. Experiments were carried out in media with decreasing serum content to synchronize cells. Adaptation steps reduced cell stress caused by starvation. Experiments were performed in media containing 2% of FBS, to stimulate cells to release PLs into media and to reduce import of external lipids. Phenol red used in DMEM did not interfere with LSC measurements.

The final release model was designed as presented in Figure 6.

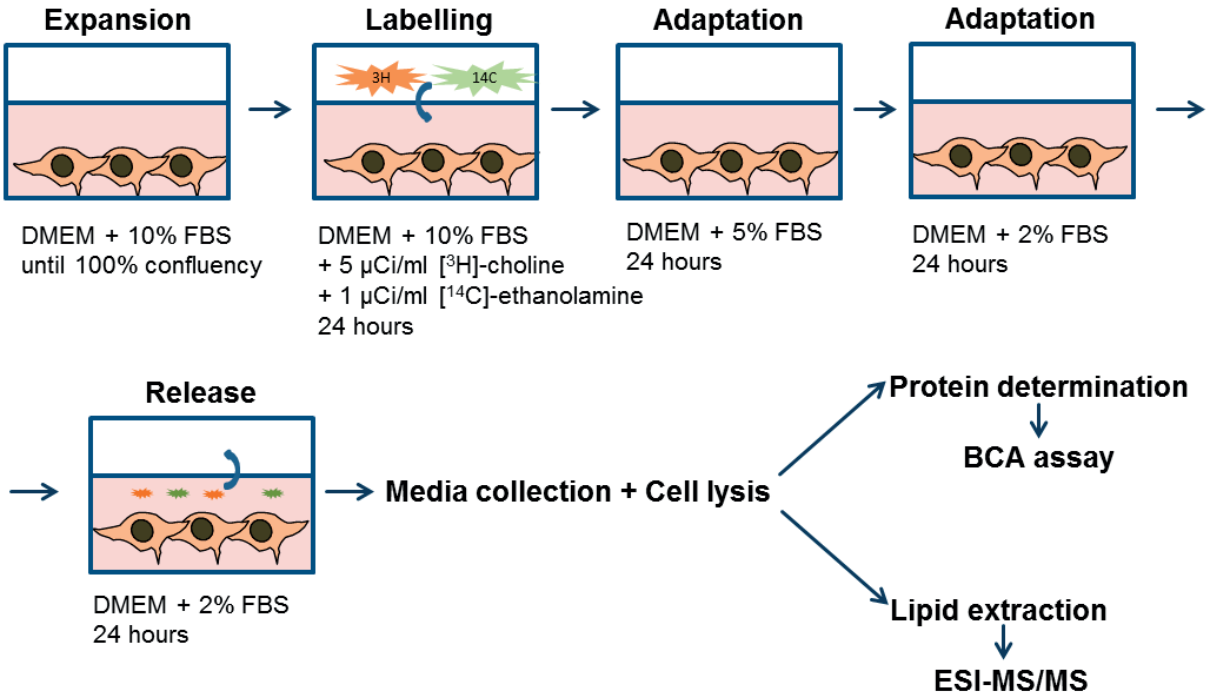

Figure 6. Schematic representation of the release model.

FLS were seeded into 6-well-plates at a density of 80,000 cells per well. FLS were cultured using complete DMEM medium in humidified 10% CO_2 atmosphere at 37°C. At 100% confluency media were changed to 2 ml of labelling medium, and 5 µCi/ml of [^{3}H]-choline and 1 µCi/ml of [^{14}C]-ethanolamine were added. Radiolabelling lasted 24 hours. 0.1 ml of media was measured in scintillation counter, and then cells were washed 5 times with 2 ml of 5% starvation medium until dpm values were below 5,000 counts. 0.1 ml of the last wash was also measured in scintillation counter to ensure that all unincorporated isotopes are not

present in the medium. 2 ml of 5% starvation medium was added to cells for a duration of 24 hours. After that 0.1 ml of media was measured in scintillation counter. Media were changed to 2% starvation medium for next 24 hours. 0.1 ml of media was measured in scintillation counter, and media were changed to new 2% starvation medium.

After 24 hours in the presence or absence of agents media were collected, volume of samples were determined, and media were centrifuged 400 x g for 10 min, filtered through the 0.2 μm pore size filter. 2 ml of media were split into 0.1ml, which was measured in scintillation counter, and 1.9 ml, which was stored at 4°C and used for lipids extraction. Cells were washed at least twice with 2 ml of 1x PBS until dpm values were below 1,000. Cells were subsequently lysed by the addition of 0.2 ml 0.2% SDS, scraped and harvested. Wells were washed with 0.2 ml of aqua B. Braun, combined extracts were ultrasonicated for 6 sec, 3 x 10% pulse, with 40-50% power. 0.4 ml of extracts were split as follow 75 μl was used for the determination of protein concentration using BCA assay, 25 μl was measured in scintillation counter, and 0.3 ml was snap-frozen in liquid nitrogen, then stored in -86°C and later used for lipids extraction. Radioactivity within lipids samples extracted according to Bligh and Dyer were measured by LSC.

3.3.4. Optimization of our *in vitro* model to study PL release

Before the final release model was established, several parameters needed to be optimized.

3.3.4.1. PL background of the experimental media

To investigate the PL background of experimental media, 2 ml of complete DMEM medium and 2 ml of 2% starvation medium were incubated in humidified 10% CO_2 atmosphere at 37°C for 24 hours, then frozen. Lipids were extracted according to Bligh and Dyer, and then samples were evaluated by ESI-MS/MS.

3.3.4.2 Concentration-dependent effect on the incorporation of radiolabelled precursors into PLs

To investigate whether increasing concentrations of radioisotopes resulted in enhanced labelled PLs, FLS from 3 patients were seeded into 1 well of 6-well-plates and cultured until 100% confluency. FLS were labelled with:

- 1 μCi/ml of [^{3}H]-choline and 1 μCi/ml of [^{14}C]-ethanolamine
- 5 μCi/ml of [^{3}H]-choline and 5 μCi/ml of [^{14}C]-ethanolamine
- 10 μCi/ml of [^{3}H]-choline and 10 μCi/ml of [^{14}C]-ethanolamine

in the labelling medium for a duration of 48 hours. Cells were then adapted in 5% starvation medium for 24 hours, followed by adaptation in 2% starvation medium for the next 24 hours. The entire release experiment lasting 24 hours was performed in 2% starvation medium.

3.3.4.3. Effect of the time of labelling on the incorporation of radiolabelled precursors into PLs

To investigate whether increasing time of labelling enhances the amount of incorporated precursors into PLs, FLS from 3 patients were seeded into 6-well-plates, cultured until 100% confluency, and were labelled with 5 μCi/ml of [^{3}H]-choline and 1 μCi/ml of [^{14}C]-ethanolamine for a duration of 6, 12, 24, 36 and 48 hours. Cells were then adapted in 5% starvation medium for 24 hours, followed by adaptation in 2% starvation medium for the next 24 hours. The entire release experiment lasting 24 hours was performed in 5% or 2% starvation media.

3.3.4.4. Effect of the time of release on the delivery of PLs from FLS into media

To investigate the correlation between time of release and amount of PLs being releases, FLS from 3 patients were seeded into 6-well-plates. FLS were cultured until 100% confluency, and were labelled with 5 μCi/ml of [^{3}H]-choline and 1 μCi/ml of [^{14}C]-ethanolamine for a duration of 12 or 24 hours. Cells were then adapted in 5% starvation medium for 24 hours, followed by adaptation in 2% starvation medium for the next 24 hours. The entire release experiments lasting 12, 24 and 36 hours were performed in 10%, 5% or 2% starvation media.

3.4. Main experiments

3.4.1. Screening the effects of agents on the biosynthesis of PLs

To screen the effects of cytokines, growth factors, pharmacological agents and specific inhibitors on the biosynthesis of PLs, FLS from 6 patients were cultured according to our established biosynthesis model (see chapter 3.3.1. and 4.3.). During labelling step cells were stimulated as follow:

- 10 ng/ml of IL-1β
- 100 ng/ml of TNFα
- 10 ng/ml of IL-6
- 5 μM of quinacrine (phospholipase A2 inhibitor)
- 10 μM/ 5 μM/ 1 μM of CK37 (choline kinase inhibitor)
- 10 ng/ml of TGF-β1
- 100 ng/ml of IGF-1
- 10 μM of dexamethasone
- 10 μM of terbutaline
- 10 μM of epinephrine
- 10 μM of carbachol
- 10 μM of pilocarpine
- 50 μM of hemicholinium-3
- 10 μM/1 μM of sirtinol (sirtuin inhibitor)

3.4.2. The mechanism of action of selected agents on the biosynthesis of PLs

Data from our screening experiment lead us to focus on the effects of IL-1β, TGF-β1, IGF-1 and dexamethasone. Especially, we wanted to investigate whether inhibition of specific signalling pathways or receptors abolish the effects of these agents on the biosynthesis of PLs. Due to the strong effect of growth factors on the biosynthesis of PLs, the impact of various BMPs was also investigated. Moreover, the effect of a more potent sirtuin inhibitor EX 537 was investigated. FLS from 5 patients were cultured according to our established biosynthesis model (see chapter 3.3.1. and 4.3.) with the modification that the LPDS medium contained 42

mg/l L-serine, to provide access of all amino acids to enzymes and proteins. During the labelling step cells were treated as follow:

- 10 ng/ml of IL-1β
- 10 ng/ml of IL-1β + 10 μM of QNZ (NF-κB inhibiotr)
- 10 ng/ml of IL-1β + 10 μM of SB203580 (p38 inhibitor)
- 10 ng/ml of IL-1β + 10 μM of SP600125 (JNK inhibitor)
- 10 ng/ml of TGF-β1
- 10 ng/ml of TGF-β1 + 10 μM of SB431542 (TGF-β receptor I kinase inhibitor)

- 100 ng/ml of IGF-1
- 100 ng/ml of IGF-1 + 10 μM of LY294002 (PI3K inhibitor)
- 100 ng/ml of IGF-1 + 1 μM of SCH772984 (ERK inhibitor)

- 100 ng/ml of BMP-2
- 100 ng/ml of BMP-4
- 100 ng/ml of BMP-7

- 10 μM of dexamethasone
- 10 μM of dexamethasone + 1 μM of RU 486 (glucocorticoid receptor inhibitor)

- 1 μM of EX 527 (SIRT1 inhibitor)
- 50 μM of EX 527 + 10 mM NAM (all sirtuins inhibitor)

Cells were first pretreated for 30 min with inhibitors and then stimulated with cytokines, growth factors or drugs.

3.4.3. Screening of the effects of agents on the release of PLs

To screen the effect of cytokines, growth factors, pharmacological agents and specific inhibitors on the release of PLs, FLS from 5 patients were cultured according to our established release model (see chapter 3.3.3. and 4.4.). During the entire release period of 24 hours, cells were treated as follow:

- 10 ng/ml of IL-1β

- 100 ng/ml of TNFα
- 10 ng/ml of IL-6
- 5 μM of quinacrine (phospholipase A2 inhibitor)
- 10 ng/ml of TGF-β1
- 100 ng/ml of IGF-1
- 10 μM of dexamethasone
- 10 μM of terbutaline
- 10 μM of epinephrine
- 10 μM of carbachol
- 10 μM of pilocarpine
- 50 μM of hemicholinium-3
- 1 μM of sirtinol (sirtuin inhibitor)

3.4.4. The mechanism of action of selected agents on the release of PLs

Data from our screening experiment lead us to focus on the effect of IL-1β. However, due to the altered cell morphology during treatment with IL-1β, the release model was modified. The concentration of FBS in culture media was increased and the period of adaptation was decreased. After labelling with radioactive isotopes, cells were incubated in 5% starvation medium or complete DMEM medium for 24 hours, and then the release experiment was performed in the same fresh media. Subsequently, media were collected after 24 hours. FLS from 3-6 patients were used. This experiment investigated the effect of different concentrations of IL-1β and inhibition of specific signalling pathways on the release of PLs. The impact of the sirtuin inhibitor EX 537 and different apolipoproteins on the release of PLs was also determined.

During the entire release period of 24 hours, cells were treated as follow:

<u>5% starvation medium</u>

- 5 ng/ml of IL-1β
- 5 ng/ml of IL-1β + 10 μM of SB203580 (p38 inhibitor)
- 1 μM of EX 527 (SIRT1 inhibitor)
- 10 μg/ml of Apo A-I
- 10 μg/ml of Apo E4

Complete DMEM medium

- 2 ng/ml of IL-1β
- 5 ng/ml of IL-1β
- 10 ng/ml of IL-1β
- 5 ng/ml of IL-1β + 10 μM of QNZ (NF-κB inhibiotr)
- 5 ng/ml of IL-1β + 10 μM of SB203580 (p38 inhibitor)

Cells were first pretreated for 30 min with inhibitors and then stimulated with IL-1β.

4. RESULTS

4.1. Optimization of an *in vitro* model to study the biosynthesis of PLs

In order to study the biosynthesis of PLs by FLS, an *in vitro* model was developed using the stable isotopes [D9]-choline and [D4]-ethanolamine. Before the final biosynthesis model was established, several aspects were optimized.

4.1.1. PL background of the experimental media

Since serum contains a high lipid content, we searched for an alternative introducing less external lipids to cells. Therefore, we compared the PL background of the experimental media "complete DMEM medium" (containing 10% FBS) with "LPDS medium" w/o or with L-serine (containing 5% LPDS). The concentrations of PLs present in experimental media were measured by ESI-MS/MS. The level of PLs were markedly higher in medium containing 10% FBS than 5% LPDS (Figure 7, Appendix Table 1). For example, the concentrations of PC and PE were in the range of 14.6±0.3 nmol/ml medium and 0.40±0.0 nmol/ml medium for 10% FBS medium and 1.11±0.0 nmol/ml medium and 0.08±0.0 nmol/ml medium for 5% LPDS medium, respectively. Moreover, "LPDS media" w/o and with L-serine gave similar results, except the PS and PI levels. Our result indicates that media containing LPDS import much less PLs and appear to be suitable for the analysis of PL biosynthesis.

4.1.2. Effect of single versus double labelling on the incorporation of precursors into PLs

In order to investigate whether the presence of two stable isotope-labelled precursors modulate the incorporation of any of them into PLs, 80% confluent FLS from 3 patients were labelled with [D9]-choline and/or [D4]-ethanolamine for a duration of 24-72 hours. The presence of [D4]-ethanolamine did not change the percentage of [D9]-choline incorporation into PC (Figure 8A). However, [D9]-choline slightly decreased the percentage of [D4]-ethanolamine incorporated into PE (Figure 8B). Nevertheless, the labelling of PE was more efficient then PC, and displayed high values lying in the range of 38-64% of labelled PC or PE from total (labelled and unlabelled) PC or PE, respectively. Thus, the two precursors were

used simultaneously in further experiments. Moreover, Figure 8 A, B shows that the incorporation of precursors into PLs increases with time (2-way ANOVA; $P < 0.0001$).

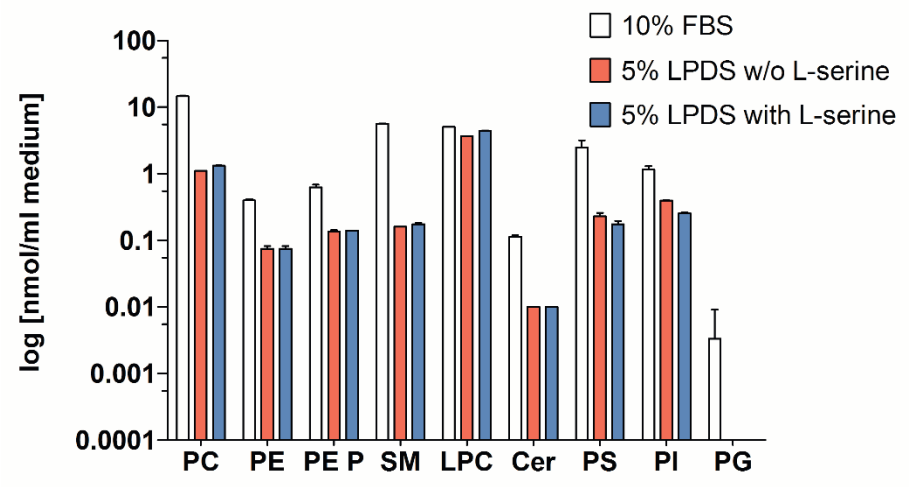

Figure 7. PL background of the experimental media in the biosynthesis model. Lipids were extracted from complete DMEM medium containing 10% FBS, 5% LPDS medium w/o or with L-serine, quantified by ESI-MS/MS and expressed as nmol PL/ml medium. Data are presented as means ± SDs (n = 3). PC = phosphatidylcholine; PE = phosphatidylethanolamine; PE P = phosphatidylethanolamine-based plasmalogens; SM = sphingomyelin; LPC = lysophosphatidylcholine; Cer = ceramide; PS = phosphatidylserine; PI = phosphatidylinositol; PG = phosphatidylglycerol.

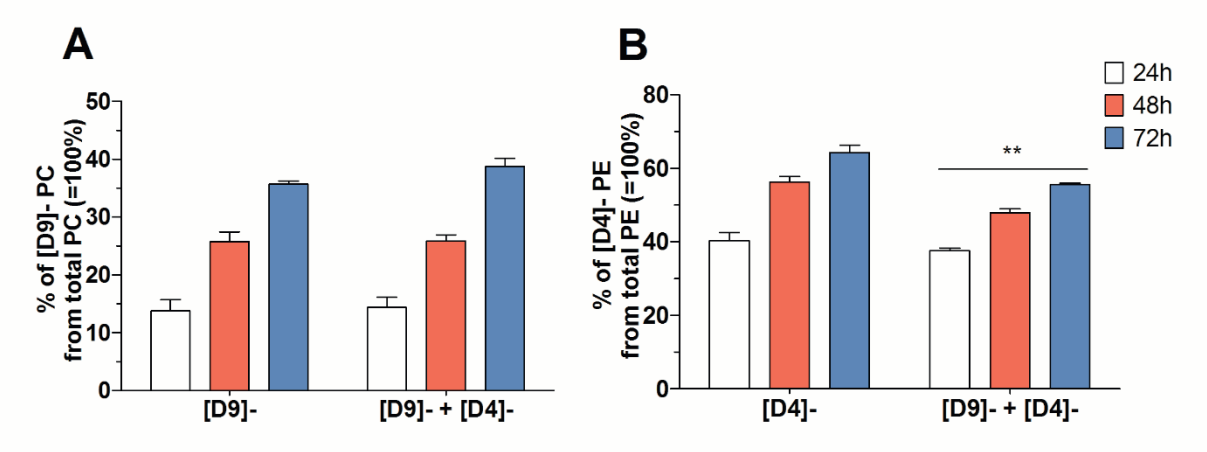

Figure 8. Effect of single versus double labelling on the incorporation of precursors into PC (A) and PE (B). FLS were labelled with 100 µg/ml [D9]-choline and/or 100 µg/ml [D4]-ethanolamine for a duration of 24, 48 and 72 hours. Lipids were extracted and quantified by ESI-MS/MS. Data are expressed as means ± SDs (n = 3). The significance was tested using 2-way ANOVA. ** = $P \leq 0.01$. PC = phosphatidylcholine; PE = phosphatidylethanolamine.

4.1.3. Identification of cell number needed to study the biosynthesis of PLs

In order to obtain high and well measurable values, the number of FLS needed for our experiments was determined. FLS from 3 patients were seeded into culture dishes (1,000,000 cells), 6 wells (480,000 cells), or 4 wells (320,000 cells) of 6-well-plates. FLS were cultured until 80% confluency, and then labelled with [D9]-choline and [D4]-ethanolamine for a duration of 24 hours. Increasing the number of FLS significantly increased the concentrations of newly synthesized PC and PE per mg cellular protein (Figure 9A). However, the percentage of newly synthesized PC remained constant, whereas the percentage of newly synthesized PE decreased with higher cell numbers (Figure 9B). Based on these data, we concluded that cells seeded even into 3 wells will be enough to measure PL biosynthesis.

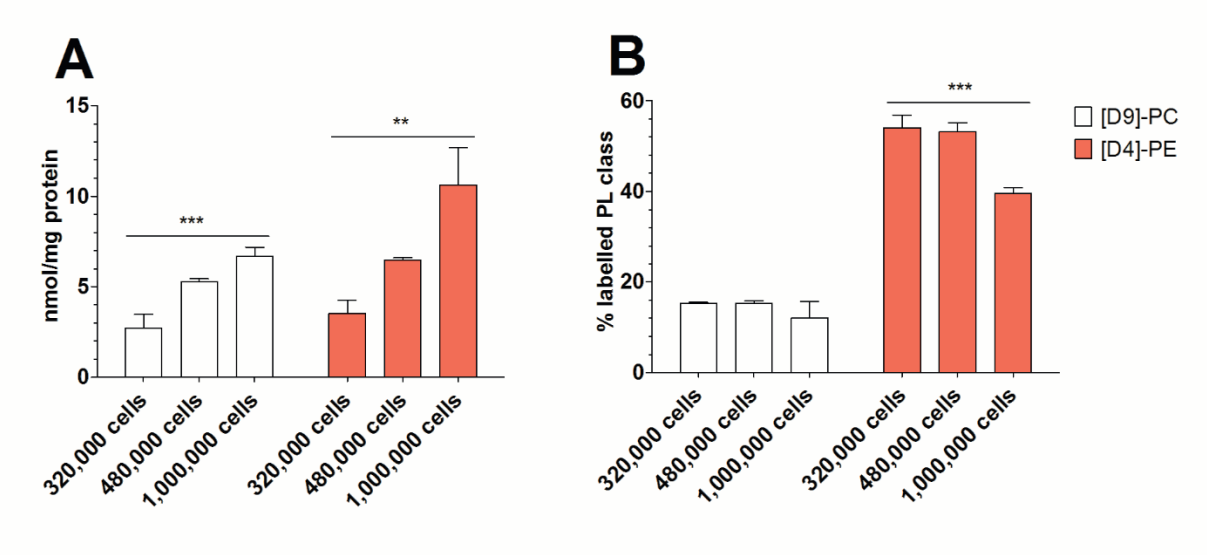

Figure 9. Identification of cell number needed to study the biosynthesis of PLs. (**A**) The concentrations of total PL per mg cellular protein, and (**B**) the percentages of labelled PLs from total corresponding labelled and unlabeled class are shown. FLS were seeded into culture dishes (1,000,000 cells), 6 wells (480,000 cells) or 4 wells (320,000 cells) of 6-well-plates. FLS were cultured until 80% confluency, and then labelled with 100 µg/ml [D9]-choline and 100 µg/ml [D4]-ethanolamine for a duration of 24 hours. Lipids were extracted and quantified by ESI-MS/MS. Data are expressed as means ± SDs (n = 3). The significance was tested using 1-way ANOVA. ** = $P \leq 0.01$; *** = $P \leq 0.001$. PC = phosphatidylcholine; PE = phosphatidylethanolamine.

4.1.4. Concentration-dependent effect on the incorporation of stable isotope-labelled precursors into PLs

We have investigated the impact of the concentration of precursors on their incorporation into PLs. 80% confluent FLS from 3 patients were labelled with 225-1800 µg/ml [D9]-choline and 25-200 µg/ml [D4]-ethanolamine for a duration of 24, 48 and 72

hours. The isotopes were used at a physiological ratio of choline to ethanolamine as found in human blood to be equal 9:1. Analysis showed that increasing the concentration of precursors resulted in an enhanced incorporation of precursors into PC (2-way ANOVA; $P = 0.0036$; Figure 10A) and PE (2-way ANOVA; $P < 0.001$; Figure 10B). Nevertheless, using high concentrations of precursors may disturb the balance of phospholipid precursors. To avoid that and to obtain well measurable levels of labelled PLs, 225 µg/ml [D9]-choline and 25 µg/ml ethanolamine were used in further experiments. Here again we could observe that the incorporation of stable isotope-labelled precursors into PLs correlated with the time of labelling (2-way ANOVA; $P < 0.0001$; Figure 10A, B).

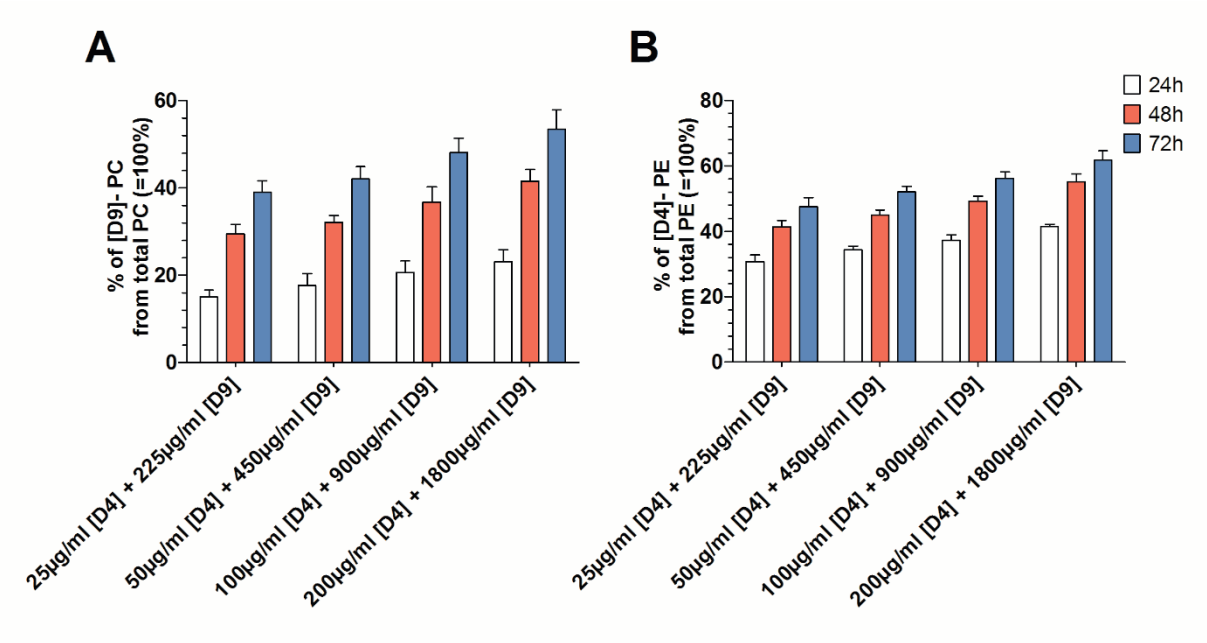

Figure 10. Concentration-dependent effect on the incorporation of stable isotope-labelled precursors into PLs. The percentages of labelled PC (**A**) and PE (**B**) as dependent on concentration of precursors. FLS were labelled with 225-1800 µg/ml [D9]-choline and 25-200 µg/ml [D4]-ethanolamine for a duration of 24, 48 and 72 hours. Lipids were extracted and quantified by ESI-MS/MS. Data are expressed as means ± SDs (n = 3). The significance was tested using 2-way ANOVA. PC = phosphatidylcholine; PE = phosphatidylethanolamine.

4.1.5. Effect of the time of labelling and cell confluency on the incorporation of stable isotope-labelled precursors into PLs

Since dividing cells generate cell membranes which are highly enriched with PLs, the impact of cell confluency on the PL biosynthesis was studied. Moreover, we investigated again whether increasing the time of labelling enhances the amount of incorporated precursors into PLs. 100% or 80% confluent FLS from 3 patients were labelled with 225 or 200 µg/ml

[D9]-choline and 25 or 200 µg/ml [D4]-ethanolamine from 4 to 36 hours. Incorporation of [D9]-choline into PC, SM and LPC was correlated with time (r = 1; Figure 11A). Incorporation of [D4]-ethanolamine into PE and PE-based plasmalogens was also correlated with time (r = 1, Figure 11B). To compromise between sufficiently labelled PLs, degradation of synthesized PLs and re-uptake of precursors, a 16 hours period of labelling was used in further experiments. Importantly, we observed that 80% confluent cells incorporated more precursors into PLs reflecting increased synthesis of cell membranes.

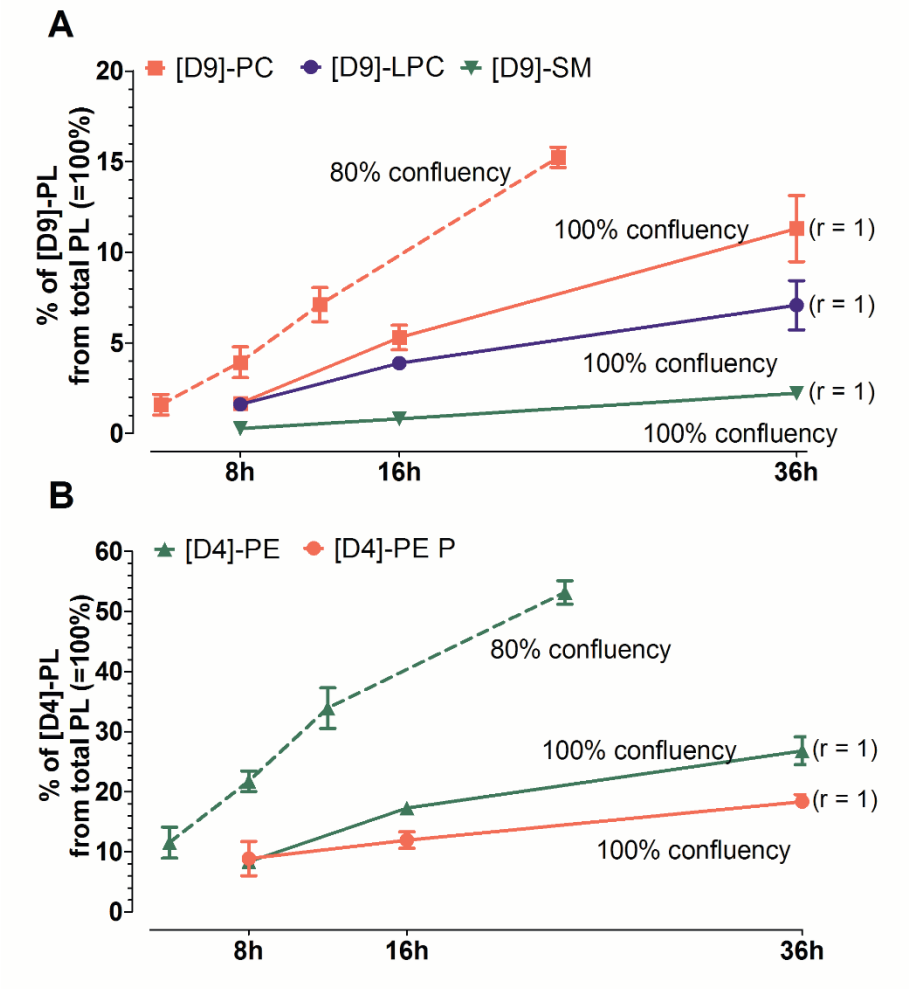

Figure 11. Effect of the time of labelling and cell confluency on the incorporation of stable isotope-labelled precursors into PLs. Effect of time of labelling on [D9]-choline (**A**) and [D4]-ethanolamine (**B**) incorporation into PL. 100% confluent FLS were labelled with 225 µg/ml [D9]-choline and 25 µg/ml [D4]-ethanolamine for 8-36 hours. 80% confluent FLS were labeled with 200 µg/ml [D9]-choline and 200 µg/ml [D4]-ethanolamine for 2-24 hours. Lipids were extracted and quantified by ESI-MS/MS. Data are expressed as means ± SDs (n = 3). Spearman's coefficients were calculated to evaluate correlations. PC = phosphatidylcholine; PE = phosphatidylethanolamine; PE P = phosphatidylethanolamine-based plasmalogens; SM = sphingomyelin; LPC = lysophosphatidylcholine.

4.1.6. Effect of L-serine on the incorporation of stable isotope-labelled precursors into PLs

To investigate whether the presence of L-serine in culture medium has an impact on the incorporation of precursors into PLs, FLS from 6 patients were labelled with 225 µg/ml [D9]-choline chloride and 25 µg/ml [D4]-ethanolamine for 16 hours in LPDS medium without or with L-serine. The paired t-test analysis revealed that presence of L-serine has no impact on the newly synthesized PC or PE, neither on the nmol/mg protein values nor percentages of labelled PL classes (data not shown). These data are in agreement with our finding reported previously (see chapter 4.1.1.).

4.2. Optimization of an *in vitro* model to study PL release

In order to study the release of PLs from FLS into culture media, an *in vitro* model was developed using the radioactive isotopes [^{3}H]-choline and [^{14}C]-ethanolamine. Before the final release model was established, several parameters needed to be optimized.

4.2.1. PL background of the experimental media

To stimulate FLS to release PLs into media, we used media containing a lower amount of PLs. Therefore, we looked at the PL background of the experimental media "complete DMEM medium" (containing 10% FBS) and "2% starvation medium" (containing 2% FBS). Figure 12 shows that the concentrations of PLs were markedly higher in medium containing 10% then 2% FBS. For instance, the levels of PC and PE were in the range of 14.6±0.3 nmol/ml medium and 0.40±0.0 nmol/ml medium for 10% FBS and 2.56±0.1 nmol/ml medium and 0.25±0.0 nmol/ml medium for 2% FBS, respectively (Appendix Table 1). This result indicates that medium containing 2% FBS is suitable for the analysis of PL release.

4.2.2. Concentration-dependent effect on the incorporation of radiolabelled precursors into PLs

In order to ensure high incorporation of radioactive precursors into PLs of FLS, we determined their optimal concentrations. 100% confluent FLS from 3 patients were labelled

with 1-10 µCi/ml [^{3}H]-choline and [^{14}C]-ethanolamine for a duration of 48 hours in medium containing 10% FBS. Further, cells were incubated in medium containing 2% FBS according to the method used in the release model (see chapter 3.3.3.). Increasing the concentration of [^{3}H]-choline significantly increased the incorporation of radioactive precursor into PLs of FLS, whereas increasing the concentration of [^{14}C]-ethanolamine from 1 to 5 µCi/ml had no impact (P = 0.41; Figure 13). The concentration 10 µCi/ml of [^{14}C]-ethanolamine was toxic for cells. Thus, the concentrations of 5 µCi/ml of [^{3}H]-choline and 1 µCi/ml of [^{14}C]-ethanolamine were used in further experiments.

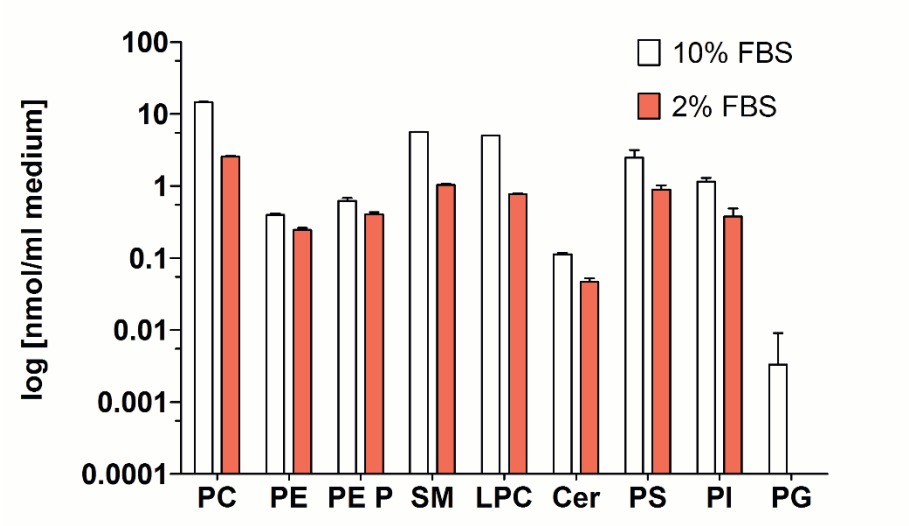

Figure 12. PL background of the experimental media in the release model. Lipids were extracted from "complete DMEM medium" and "2% starvation medium", quantified by ESI-MS/MS and expressed as nmol/ml medium. Data are presented as means ± SDs (n =3). PC = phosphatidylcholine; PE = phosphatidylethanolamine; PE P = phosphatidylethanolamine-based plasmalogens; SM = sphingomyelin; LPC = lysophosphatidylcholine; Cer = ceramide; PS = phosphatidylserine; PI = phosphatidylinositol; PG = phosphatidylglycerol.

4.2.3. Effect of the time of labelling on the incorporation of radiolabelled precursors into PLs

The effect of the time of labelling on the incorporation of radioactive isotopes into FLS in various cell culture media was investigated. 100% confluent FLS from 3 patients were labelled with 5 µCi/ml [^{3}H]-choline and 1 µCi/ml [^{14}C]-ethanolamine for 6-48 hours in medium containing 10% FBS. Further, cells were incubated in medium containing 5 or 2% FBS according to the method used in the release model (see chapter 3.3.3.). Analyses revealed that labelling of PLs with 5 µCi/ml [^{3}H]-choline and 1 µCi/ml [^{14}C]-ethanolamine and

investigation of the release in DMEM containing 5% FBS was correlated with time (r = 1). Labelling of PLs with 5 µCi/ml [^{3}H]-choline and investigation of release in DMEM containing 2% FBS also increased with time (r = 0.9). However, labelling of PLs with 1 µCi/ml [^{14}C]-ethanolamine and investigation of release in DMEM containing 2% FBS from 24 to 48 hours was not correlated with time (r = -1) (Figure 14). In order to sufficiently label PLs with less degradation, a 24 hours period of labelling was used in further experiments.

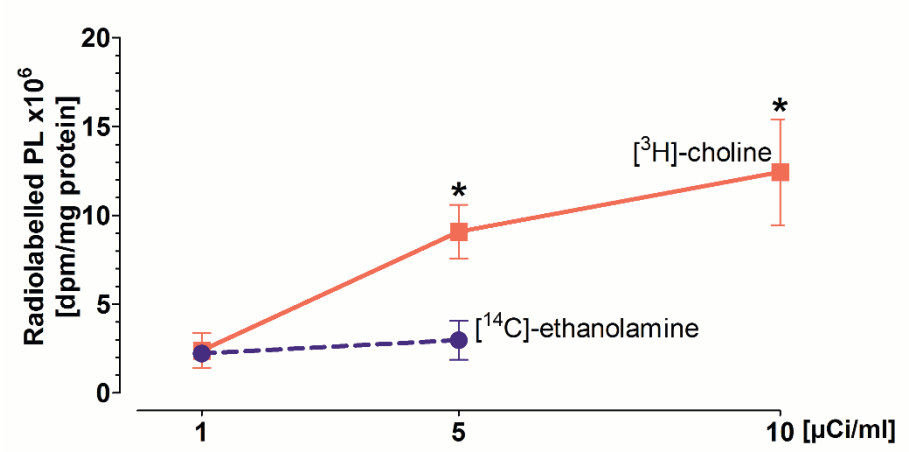

Figure 13. Concentration-dependent effect on the incorporation of radiolabelled precursors into PLs. FLS were labelled with 1, 5, and 10 µCi/ml [^{3}H]-choline as well as 1 or 5 µCi/ml [^{14}C]-ethanolamine for duration of 48 hours. Lipids were extracted and quantified by LSC. Data are expressed as means ± SDs (n = 3). Significant differences of the concentrations of radiolabelled precursors compared to 1 [µCi/ml] as determined by paired t-test: * = $P < 0.05$.

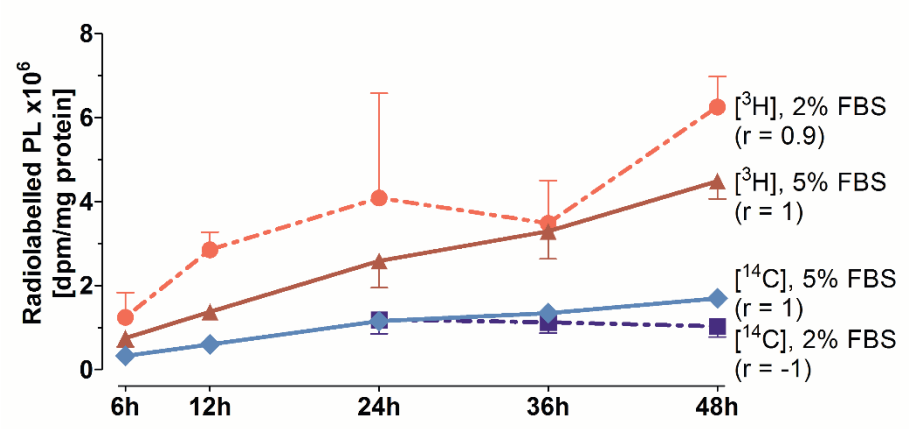

Figure 14. Effect of the time of labelling on the incorporation of radiolabelled precursors into PLs. FLS were labelled with 5 µCi/ml [^{3}H]-choline and 1 µCi/ml [^{14}C]-ethanolamine for 6-48 hours. Lipids were extracted and quantified by LSC. Data are expressed as means ± SDs (n = 3). Spearman's coefficients were calculated to evaluate correlations.

4.2.4. Effect of the time of release on the delivery of PLs from FLS into media

The time course of radiolabelled PLs being released from FLS into media was evaluated. 100% confluent FLS from 3 patients were labelled with 5 µCi/ml [^{3}H]-choline and 1 µCi/ml [^{14}C]-ethanolamine for 12 and/or 24 hours. The release of PLs was measured after 12, 24 and 36 hours. The release of [^{3}H]-choline-labelled (Figure 15A) and [^{14}C]-ethanolamine-labelled PL (Figure 15B) into DMEM containing 2% FBS correlated with time (r = 1). To minimize reuptake of labelled PLs, the release during 24 hour period was determined in further experiments.

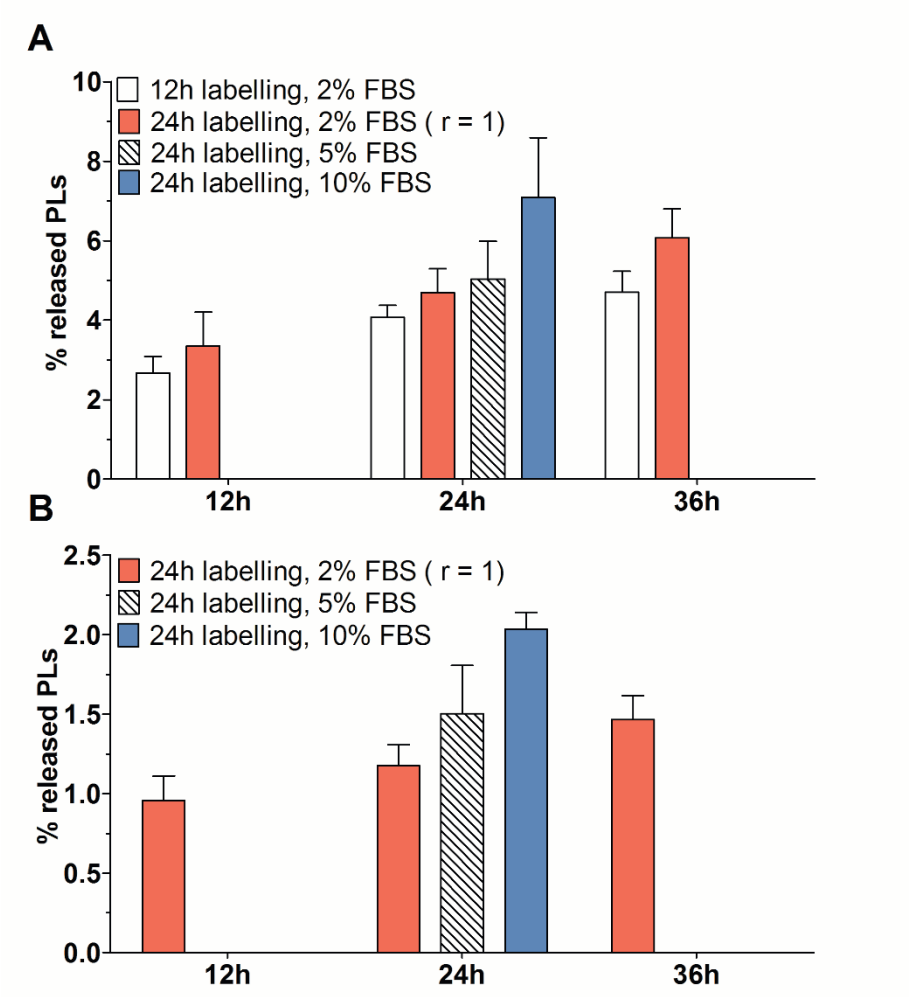

Figure 15. Effect of the time of release on the efflux of PLs from FLS into media. The percentage of released [^{3}H]-choline-labelled PLs (**A**) and [^{14}C]-ethanolamine-labelled PLs (**B**) from total radiolabeled PLs detected in media and FLS were calculated. FLS were labelled with 5 µCi/ml [^{3}H]-choline and 1 µCi/ml [^{14}C]-ethanolamine for 12 and/or 24 hours. The release of PL was investigated during 12-36 hours in media containing various amounts of FBS. Lipids were extracted and quantified by LSC. Data are presented as means ± SDs (n = 3). Spearman's coefficients were calculated to evaluate correlations.

4.3. Final description of the biosynthesis model being used

The following *in vitro* model to study PL biosynthesis was established: FLS were seeded at a density of 80,000 cells per well into 3 wells of 6-well-plate, cultured until 100% confluency, labelled with 225 µg/ml [D9]-choline and 25 µg/ml [D4]-ethanolamine for 16 hours in the presence or absence of agents to be tested. Afterwards, cells were washed twice with 1x PBS and lysed with 0.5 ml of 0.2% SDS. Lysed wells were washed with 0.5 ml of aqua B. Braun, and combined extracts were ultrasonicated for 6 sec, 3 x 10% pulse, with 40-50% power. Protein concentration within lysates was evaluated using BCA assay. Lipids were extracted according to Bligh and Dyer, and analysed by ESI-MS/MS.

4.3.1. Lipid composition of human FLS

To determine the concentrations of PL classes in FLS, lipids were isolated from cells from 6 patients and evaluated using ESI-MS/MS. Nine PL classes were determined: PC, PE, PE-based plasmalogens, SM, LPC, Cer, PS, PI, and PG. The most abundant lipid class was PC, accounting 32.9±0.8% of all phospholipids (79.1±3.4 nmol/mg protein), followed by PE-based plasmalogens (18.1±1.0%; 43.5±3.4 nmol/mg protein), PS (15.5%; 37.2 nmol/mg protein), SM (10.5±1.4%; 25.2±2.4 nmol/mg protein), PE and PI (9.3±1.1%; 22.3±2.9 nmol/mg protein and 9.3±0.7%; 22.3±2.0 nmol/mg protein, respectively). Cer, LPC, and PG were detected at low concentrations (0.16-9.5 nmol/mg protein) and constituted 0.1-3.9% of the analysed phospholipid classes (Figure 16A, B).

4.3.2. Composition of newly synthesized PL classes and species in human FLS

To determine *de novo* biosynthesis of PLs, FLS from 5 patients were labelled with 225 µg/ml [D9]-choline and 25 µg/ml [D4]-ethanolamine for 16 hours. Lipids were extracted and evaluated using ESI-MS/MS.

Using stable isotope-labelled precursors of PLs we were able to detect newly synthesized PC, SM LPC, PE, and PE-based plasmalogens. Due to the added precursors, we measured *de novo* synthesis via the Kennedy pathway only for PC and PE. Other classes were labelled indirectly because of the links between PL synthesis pathways. The concentration of newly synthesized PC was 4.6±1.6 nmol/mg protein, which constituted 5.9±2.1% of total PC.

The concentration of newly synthesized PE was 3.0±0.6 nmol/mg protein, which formed 13.9±1.8% of total PE. The concentration of newly synthesized PE-based plasmalogens was 2.4±0.3 nmol/mg protein, which composed 5.5±0.5% of total PE P. Finally, the concentration of newly synthesized SM was 0.10±0.03 nmol/mg protein, which formed 0.40±0.12% of total SM, while the concentration of newly synthesized LPC was 0.02±0.0 nmol/mg protein, which made 2.1±0.5% of total LPC (Figure 17A, B).

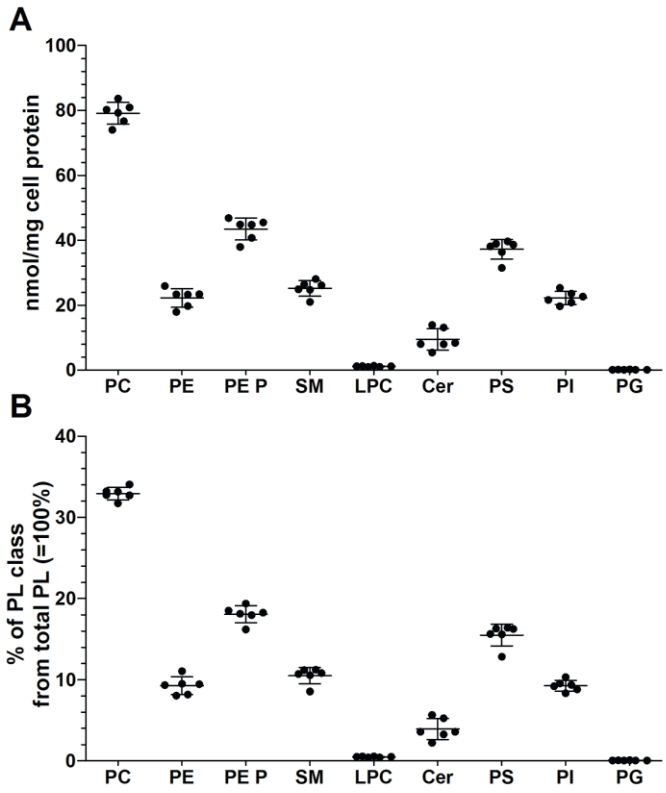

Figure 16. Lipids composition of human FLS. Concentrations (**A**) and percentages of total PL classes (labelled plus unlabelled PLs) from total analyzed PLs representing 100% (**B**) after 16 hours of culture. Lipids were extracted and quantified by ESI-MS/MS. Data are presented as means ± SDs (n = 6). PC = phosphatidylcholine; PE = phosphatidylethanolamine; PE P = phosphatidylethanolamine-based plasmalogens; SM = sphingomyelin; LPC = lysophosphatidylcholine; Cer = ceramide; PS = phosphatidylserine; PI = phosphatidylinositol; PG = phosphatidylglycerol.

Nineteen newly synthesized PC species and ten newly synthesized ether PC (PC O) species were identified within FLS (Table 7). The major PC species was PC 34:1. The concentrations of newly synthesized PC species varied between 33±8 pmol/mg protein (PC 34:3) and 780±208 pmol/mg protein (PC 34:1). The concentrations of newly synthesized PC O were low and varied between 5 and 65 pmol/mg protein. Furthermore, newly synthesized

PC existed mainly in unsaturated form (87.4±0.7%) and their lengths of FA chains according to carbon atoms were mostly ≤ 36 (72.7±5.6%).

Moreover, ten newly synthesized SM species were detected (Table 8). The major SM species was SM 34:1 at the concentrations of 50±18 pmol/mg protein. The concentrations of other species were low. Newly synthesized SM existed mainly in unsaturated form (96.6%).

Additionally, only three newly synthesized LPC species were above the limit of detection: LPC 16:0, LPC 18:0 and LPC 18:1 (Table 9). All of them were present at low concentrations of around 8 pmol/mg protein.

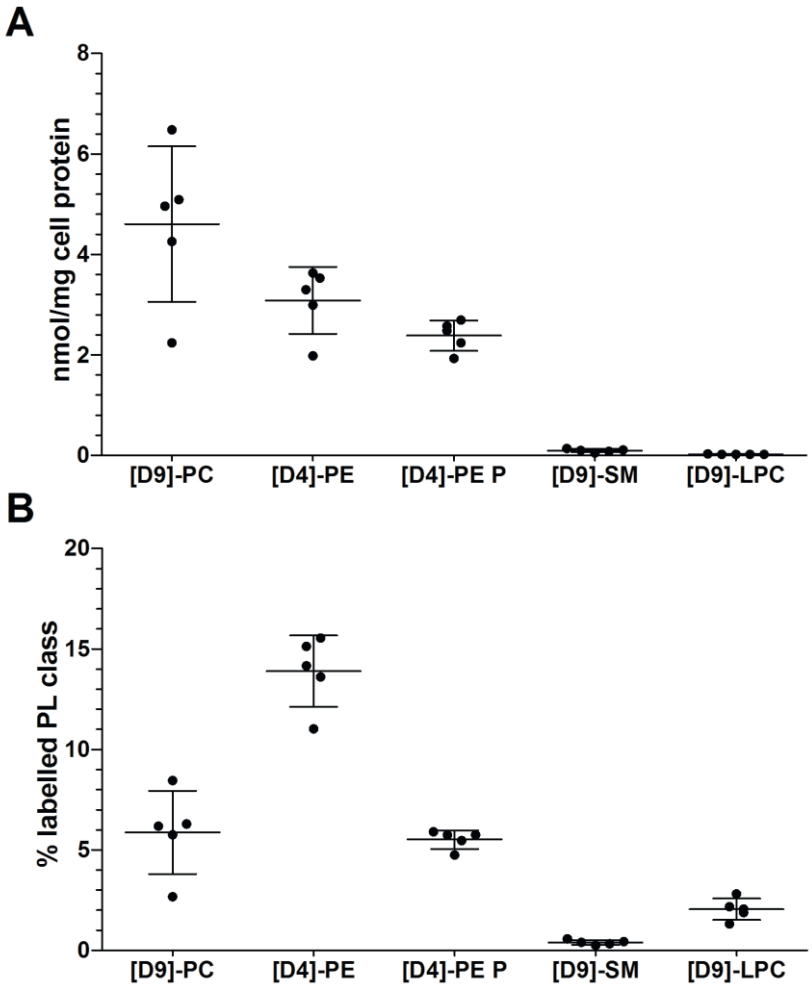

Figure 17. Newly synthesized PL classes of human FLS. Concentrations (**A**) and percentages of newly synthesized PL classes (**B**). FLS were labelled with 225 µg/ml [D9]-choline and 25 µg/ml [D4]-ethanolamine for 16 hours. Lipids were extracted and quantified by ESI-MS/MS. Data are presented as means ± SDs (n = 5). PC = phosphatidylcholine; PE = phosphatidylethanolamine; PE P = phosphatidylethanolamine-based plasmalogens; SM = sphingomyelin; LPC = lysophosphatidylcholine.

Besides, thirteen newly synthesized PE species were determined (Table 10). The major PE species was PE 38:4. The concentrations of newly synthesized PE species varied between 31±13 pmol/mg protein (PE 34:2) and 765±176 pmol/mg protein (PE 38:4). Moreover, newly synthesized PE existed only in unsaturated form. The lengths of FA chains according to carbon atoms were mostly > 36 (84.4±4.5%).

Specie	pmol/mg protein	% labelled
[D9]-PC 30:0	41±11	3.8±1.1
[D9]-PC 32:0	408±142	5.2±1.4
[D9]-PC 34:0	58±29	5.3±1.9
[D9]-PC 32:1	131±29	4.7±1.4
[D9]-PC 34:1	780±208	5.3±1.9
[D9]-PC 36:1	330±115	5.5±2.5
[D9]-PC 34:2	305±84	7.8±2.5
[D9]-PC 36:2	322±96	5.9±2.3
[D9]-PC 34:3	33±8	9.4±2.6
[D9]-PC 36:3	184±59	6.9±2.5
[D9]-PC 38:3	131±58	7.7±3.5
[D9]-PC 36:4	352±156	6.2±1.8
[D9]-PC 38:4	624±322	6.6±2.5
[D9]-PC 40:4	72±41	12.7±6.4
[D9]-PC 36:5	44±17	7.1±2.0
[D9]-PC 38:5	280±119	7.0±2.0
[D9]-PC 40:5	99±54	10.6±5.0
[D9]-PC 38:6	61±23	6.1±1.6
[D9]-PC 40:6	50±25	7.4±2.8
[D9]-PC O 30:0	5±2	3.8±1.3
[D9]-PC O 32:0	41±14	3.5±1.1
[D9]-PC O 34:0	31±9	4.3±1.2
[D9]-PC O 32:1	13±4	3.0±1.0
[D9]-PC O 34:1	65±18	3.9±1.3
[D9]-PC O 36:1	38±11	3.7±1.4
[D9]-PC O 34:2	20±5	4.8±1.6
[D9]-PC O 36:2	24±6	4.7±1.9
[D9]-PC O 36:4	17±7	3.5±1.2
[D9]-PC O 36:5	49±19	5.5±1.0

Table 7. Concentrations and percentages of newly synthesized PC species. The quantitative values obtained for each stable isotope-labelled PL species were normalized to cellular protein content and are expressed as pmol/mg protein. For each PL specie the percentage of stable isotope-labelled PL from total labelled and unlabelled PL was calculated. Data are presented as means ± SDs (n = 5). PC = phosphatidylcholine; PC O = ether PC.

Additionally, nineteen newly synthesized PE-based plasmalogens species were detected within FLS (Table 11). The major species was PE P 18:1/20:4. The concentrations of newly synthesized PE P species varied between 30±5 pmol/mg protein (PE P 18:0/18:1) and 556±87 pmol/mg protein (PE P 18:1/20:4). The lengths of FA chains according to carbon atoms were mostly > 36 (78.0±2.4%).

Specie	pmol/mg protein	% labelled
[D9]-SM 34:0	3±1	0.4±0.2
[D9]-SM 32:1	5±1	1.2±0.4
[D9]-SM 33:1	4±1	0.7±0.1
[D9]-SM 34:1	50±18	0.3±0.1
[D9]-SM 36:1	5±3	0.3±0.2
[D9]-SM 42:1	8±3	0.3±0.1
[D9]-SM 34:2	4±1	1.2±0.4
[D9]-SM 35:2	8±2	1.0±0.2
[D9]-SM 36:2	3±1	1.6±0.3
[D9]-SM 42:2	10±6	0.4±0.2

Table 8. Concentrations and percentages of newly synthesized SM species. The quantitative values obtained for each stable isotope-labelled PL species were normalized to cellular protein content and are expressed as pmol/mg protein. For each PL specie the percentage of stable isotope-labelled PL from total labelled and unlabelled PL was calculated. Data are presented as means ± SDs (n = 5). SM = sphingomyelin.

Specie	pmol/mg protein	% labelled
[D9]-LPC 16:0	8±2	1.4±0.3
[D9]-LPC 18:0	8±3	3.8±1.8
[D9]-LPC 18:1	8±1	2.0±0.4

Table 9. Concentrations and percentages of newly synthesized LPC species. The quantitative values obtained for each stable isotope-labelled PL species were normalized to cellular protein content and are expressed as pmol/mg protein. For each PL specie the percentage of stable isotope-labelled PL from total labelled and unlabelled PL was calculated. Data are presented as means ± SDs (n = 5). LPC = lysophosphatidylcholine.

4.3.3. FLS viability and mitochondrial activity

In our *in vitro* model to study PL biosynthesis, FLS were starved for 24 hours and then labelled with stable isotope-labelled precursors in medium containing 5% LPDS. To ensure the metabolic stability of FLS in our culture condition of the biosynthesis model, viability and mitochondrial activity of cells were evaluated. FLS displayed stable mitochondrial activity and viability over time in medium containing 5% LPDS (Figure 18A, B). Nevertheless, mitochondrial activity was significantly decreased when compared to control containing 10% FBS ($P = 0.007$).

Specie	pmol/mg protein	% labelled
[D4]-PE 34:1	132±54	11.9±1.8
[D4]-PE 36:1	154±73	10.0±1.9
[D4]-PE 34:2	31±13	13.9±2.4
[D4]-PE 36:2	100±39	11.4±2.3
[D4]-PE 36:3	36±11	16.4±3.2
[D4]-PE 38:3	206±38	15.1±2.4
[D4]-PE 36:4	41±11	13.1±2.6
[D4]-PE 38:4	765±176	9.2±1.4
[D4]-PE 40:4	338±65	18.8±3.0
[D4]-PE 38:5	258±65	11.9±1.9
[D4]-PE 40:5	323±78	18.9±3.4
[D4]-PE 38:6	187±57	24.9±4.2
[D4]-PE 40:6	383±84	23.5±3.4

Table 10. Concentrations and percentages of newly synthesized PE species. The quantitative values obtained for each stable isotope-labelled PL species were normalized to cellular protein content and are expressed as pmol/mg protein. For each PL specie the percentage of stable isotope-labelled PL from total labelled and unlabelled PL was calculated. Data are presented as means ± SDs (n = 5). PE = phosphatidylethanolamine**.**

Specie	pmol/mg protein	% labelled
[D4]-PE P 16:0/18:1	44±17	2.8±0.3
[D4]-PE P 16:0/20:4	308±75	3.4±0.3
[D4]-PE P 16:0/22:4	139±31	7.5±1.0
[D4]-PE P 16:0/22:5	119±29	7.2±1.2
[D4]-PE P 16:0/22:6	90±22	5.7±0.9
[D4]-PE P 18:1/16:0	51±9	6.4±1.4
[D4]-PE P 18:1/18:1	55±14	7.9±0.5
[D4]-PE P 18:1/20:4	556±87	10.6±1.1
[D4]-PE P 18:1/20:5	59±15	15.0±1.5
[D4]-PE P 18:1/22:4	91±8	15.4±2.8
[D4]-PE P 18:1/22:5	79±19	14.8±2.5
[D4]-PE P 18:1/22:6	95±4	12.5±2.4
[D4]-PE P 18:0/16:0	41±4	11.5±2.4
[D4]-PE P 18:0/18:1	30±5	3.7±1.5
[D4]-PE P 18:0/20:4	367±70	3.1±0.5
[D4]-PE P 18:0/20:5	51±5	5.8±0.8
[D4]-PE P 18:0/22:4	67±5	5.0±0.6
[D4]-PE P 18:0/22:5	76±17	5.5±1.1
[D4]-PE P 18:0/22:6	66±17	4.0±0.8

Table 11. Concentrations and percentages of newly synthesized PE P species. The quantitative values obtained for each stable isotope-labelled PL species were normalized to cellular protein content and are expressed as pmol/mg protein. For each PL specie the percentage of stable isotope-labelled PL from total labelled and unlabelled PL was calculated. Data are presented as means ± SDs (n = 5). PE P = phosphatidylethanolamine-based plasmalogens**.**

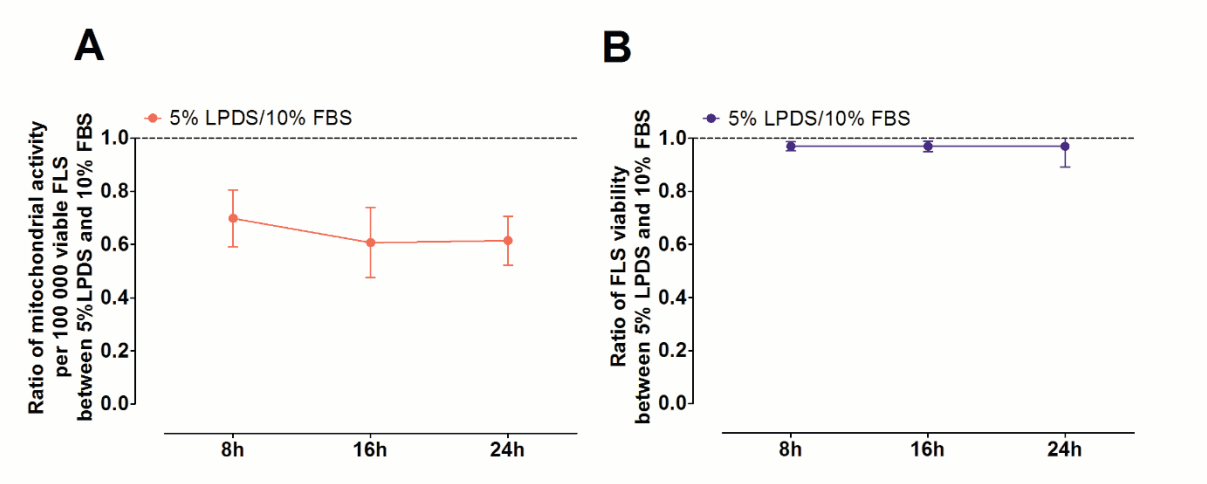

Figure 18. Viability and mitochondrial activity of the biosynthesis model of FLS. FLS were cultured according to the method used in the biosynthesis model. After 8, 16, and 24 hours mitochondrial activity assay or viability assay were performed. Obtained data for FLS cultured in 5% LPDS were related to control FLS cultured in 10% FBS medium (=1). Data are presented as means ± SDs (n = 3). The significance was tested using 1-way ANOVA.

4.3.4. Apoptosis of FLS

Due to significantly decreased mitochondrial activity of FLS in the biosynthesis model, we have evaluated their apoptosis using caspase 3/7 assay. The mean caspase 3/7 activity of FLS cultured in medium containing 5% LPDS was significantly higher ($P = 0.03$) than in FLS cultured in "complete DMEM medium" containing 10% FBS. However, it was also 10 times lower than FLS treated with 1 µM staurosporine which was used as a positive control to induce apoptosis (Figure 19). Our data suggest that FLS displayed basic level of caspase 3/7 activity in medium containing 5% LPDS, and are not apoptotic.

4.3.5. Expression of reference genes of FLS

To check whether the expression of reference genes in our biosynthesis model of FLS is stable, quantitative real-time PCR was performed. Measured Ct data were related to control condition – "complete DMEM medium" (containing 10% FBS). FLS displayed stable expression of ACTB, B2M and GAPDH over time in medium containing 5% LPDS (Figure 20A-C, Appendix Table 2).

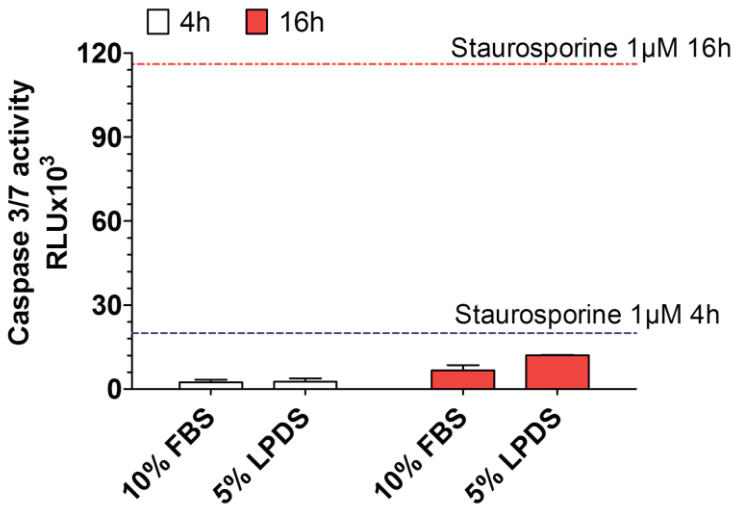

Figure 19. Apoptosis of FLS in the biosynthesis model. FLS were cultured according to the method used in the biosynthesis model. After 4 or 16 hours caspase 3/7 assay was performed. 1 µM of staurosporine was used as a positive control for induction of apoptosis. Data are presented as means ± SDs (n = 3). The significance was tested using t-test.

4.4. Final description of the release model being used

The following *in vitro* model to study PL release was established: 80,000 FLS were seeded into 1 well of 6-well-plates, cultured until 100% confluency, labelled with 5 µCi/ml [^{3}H]-choline and 1 µCi/ml [^{14}C]-ethanolamine for 24 hours. Then FLS were adapted in "5% starvation medium" for 24 hours, next in "2% starvation medium" for 24 hours, and the release lasting 24 hours was determined in "2% starvation medium" in the presence or absence of agents to be tested. Cells were washed twice with 1x PBS to remove radiolabelled precursors of PLs and lysed with 0.2 ml of 0.2% SDS. Lysed wells were washed with 0.2 ml of aqua B. Braun, and combined extracts were ultarsonificated for 6 sec, 3 x 10% pulse, with 40-50% power. Protein concentration within lysates was evaluated using BCA assay. Lipids were extracted from media as well as cell lysates according to Bligh and Dyer, and analysed by LSC. Bligh and Dyer extraction was a further method to remove radiolabelled precursors of PLs. The percentage of PLs released into media was calculated from total lipid extracts of media plus cell lysates (= 100%).

4.4.1. PL release

Using radioactive isotope-labelled precursors we were able to detect two fractions of released PLs: [^{3}H]-choline-labelled PLs and [^{14}C]-ethanolamine-labelled PLs. Figure 21

shows that 5.0±0.8% of [^{3}H]-choline-labelled PLs from total cell lysates plus media as well as 1.8±0.3% of [^{14}C]-ethanolamine-labelled PLs from total cell lysates plus media were released into cell culture media.

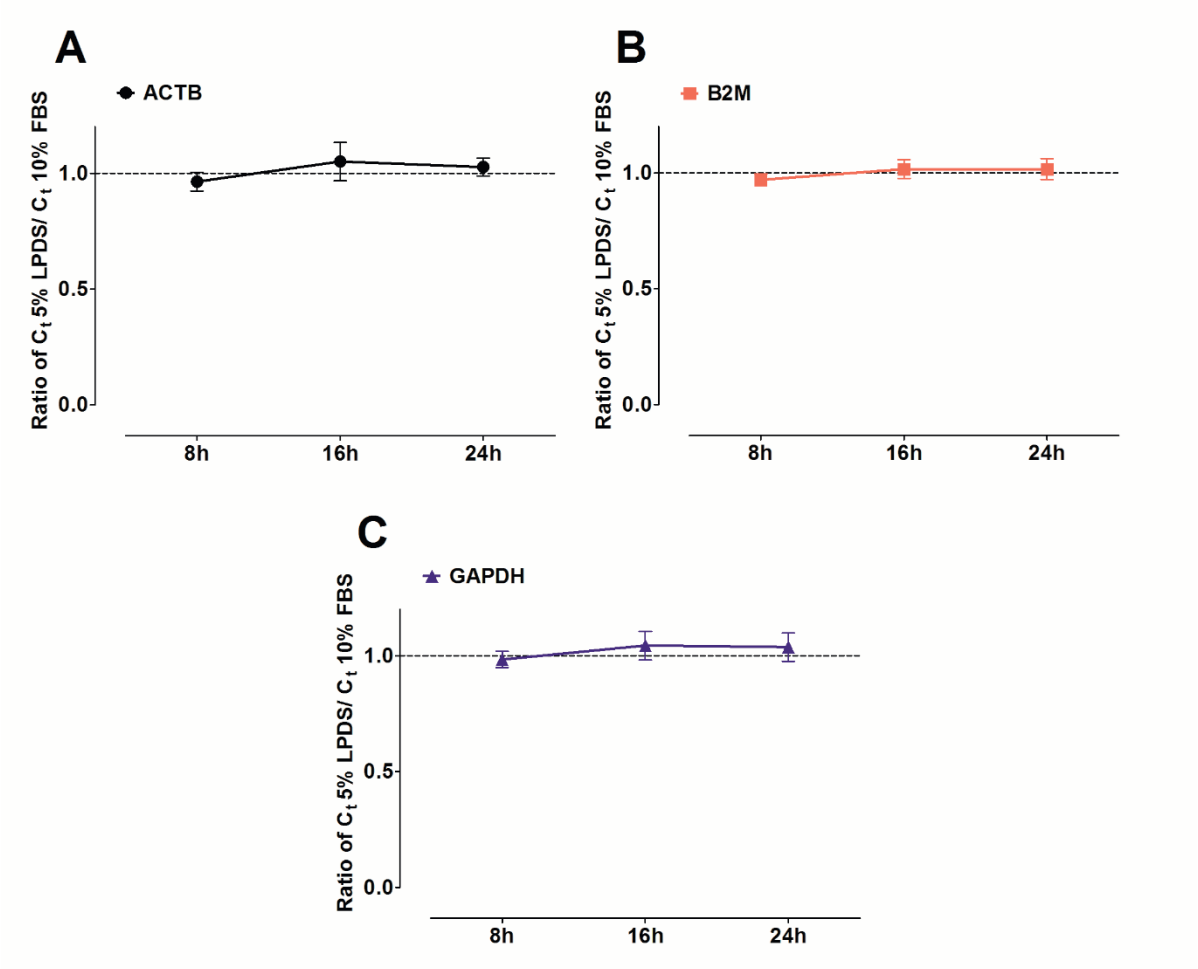

Figure 20. Expression of reference genes from the biosynthesis model of FLS. FLS were cultured according to the method used in the biosynthesis model. After 8, 16, and 24 hours RNA isolation was performed. Expression of ACTB, B2M and GAPDH was determined by quantitative real time PCR. Obtained data for FLS cultured in 5% LPDS were related to control FLS cultured in 10% FBS medium (=1). Data are presented as means ± SDs (n = 3). The significance was tested using 1-way ANOVA.

4.4.2. FLS viability and mitochondrial activity

In our *in vitro* model to study release of PLs, FLS were labelled with radiolabelled precursors, and then incubated up to 3 days in DMEM with decreasing amount of FBS. To confirm metabolic stability of cell culture conditions, viability and mitochondrial activity of cells were evaluated. Culture media (containing 5% and 2% FBS) as being used in our experiments were tested. Measured mitochondrial activity at 560 nm were normalized to

100,000 living cells, averaged and related to control condition – "complete DMEM medium" (containing 10% FBS). Calculated viability was also related to control condition. FLS displayed stable mitochondrial activity and viability over time in media containing both, 2% and 5% FBS (Figure 22A, B).

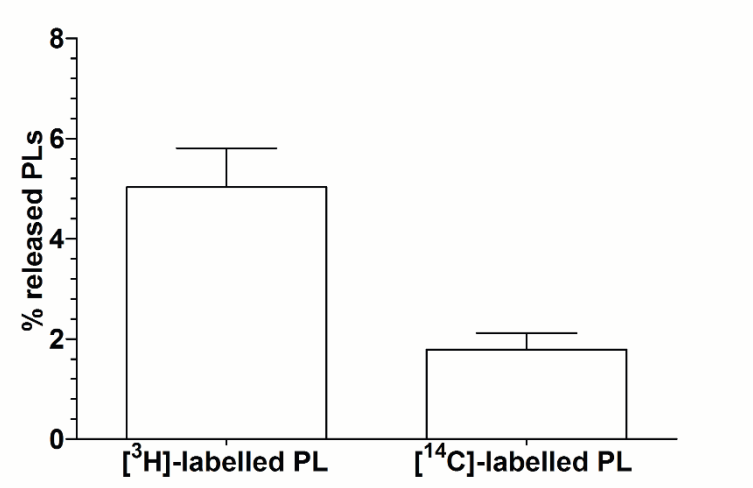

Figure 21. The release of PLs from FLS. FLS were labelled with 5 µCi/ml [^{3}H]-choline and 1 µCi/ml [^{14}C]-ethanolamine for 24 hours. The release of PLs was investigated after 24 hours in media containing 2% FBS. Lipids were extracted and quantified by LSC. Data are presented as means ± SDs (n = 5).

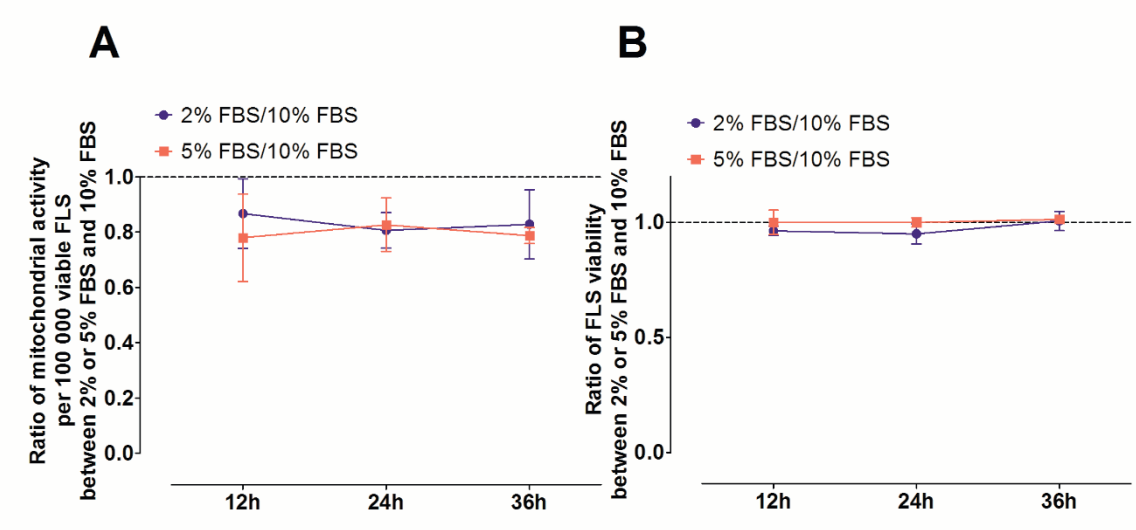

Figure 22. Viability and mitochondrial activity of the release model of FLS. FLS were cultured according to the method applied in the release model. After 12, 24, and 36 hours mitochondrial activity assay or viability assay were performed. Obtained data for FLS cultured in 2 or 5% FBS were related to control FLS cultured in 10% FBS medium (=1). Data are presented as means ± SDs (n =3). The significance was tested using 1-way ANOVA.

4.4.3. Expression of reference genes of FLS

To check whether the expression of reference genes of FLS in our release model is stable, quantitative real-time PCR was performed. We have tested culture media (containing 5% and 2% of FBS) as being used for our experiments. The measured Ct data were related to control condition – "complete DMEM medium" (containing 10% FBS). ACTB, B2M and GAPDH were stable expressed over time in media containing both, 2% and 5% FBS (Figure 23A-F, Appendix Table 2).

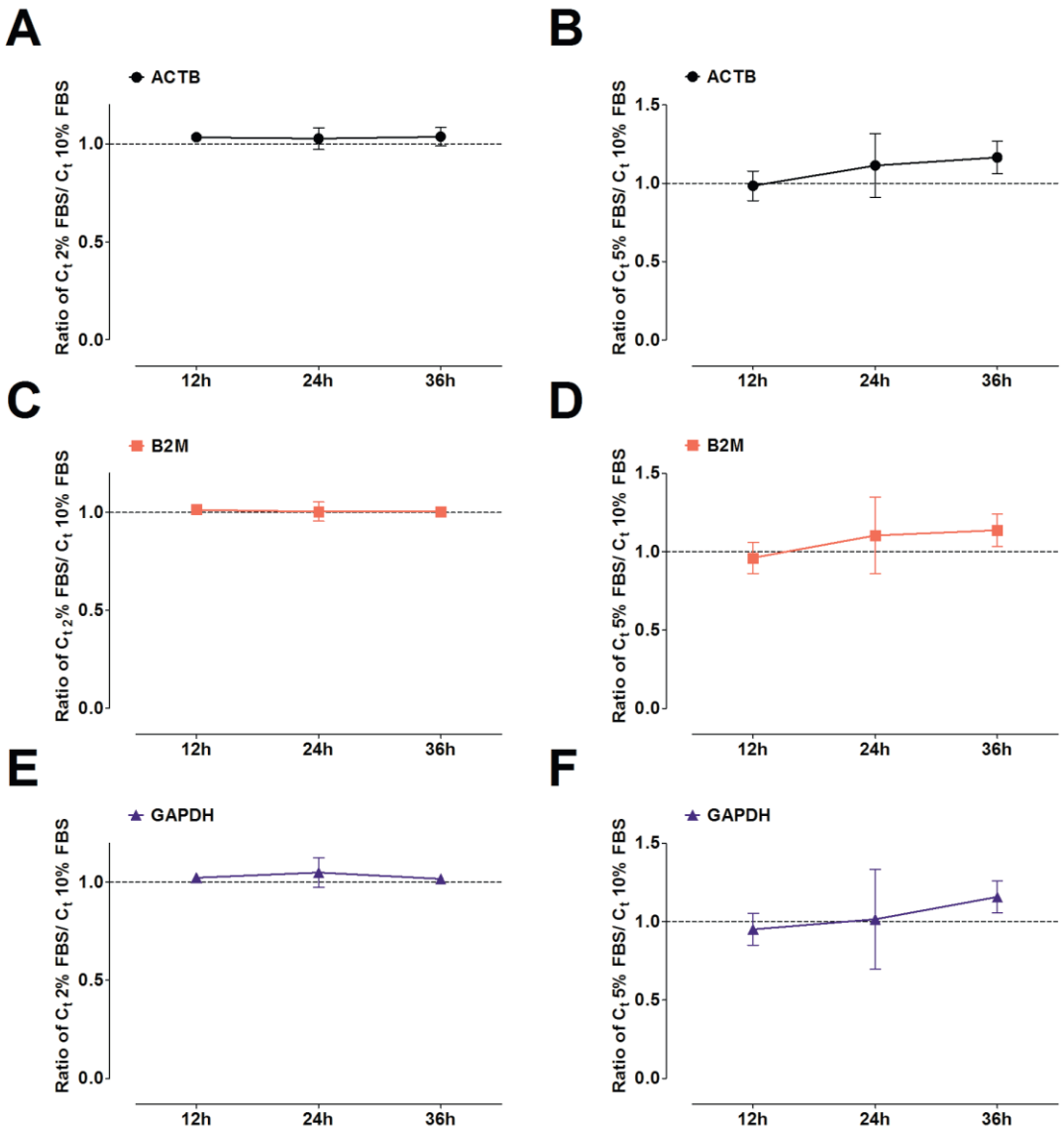

Figure 23. Expression of reference genes from the release model of FLS. FLS were cultured according to the method used in the release model. After 12, 24, and 36 hours RNA isolation was performed. mRNA expression of ACTB, B2M and GAPDH was determined by quantitative real-time PCR. Obtained data for FLS cultured in 2 or 5% FBS were related to control FLS cultured in 10% FBS medium (=1). Data are presented as means ± SDs (n = 3). The significance was tested using 1-way ANOVA.

4.5. The effect of agents on *de novo* synthesis of PLs by FLS

We have used our established biosynthesis model to investigate the effect of various agents on the PL biosynthesis.

4.5.1. Screening of the action of agents on the biosynthesis of PLs

Since there is not much known how the biosynthesis of PLs is regulated, we have decided to screen the effect of cytokines, growth factors, drugs and specific inhibitors (Table 12, Appendix Table 3). The morphology of FLS cultured in medium containing 5% LPDS was not affected by any of agents.

We focused on IL-1β, TNFα and IL-6 which are known to be involved in the pathogenesis of OA (12, 15). IL-1β significantly increased 1.29-fold the biosynthesis of PE (31.1±2.2%) when compared to untreated controls (24.0±2.8%). Also the level of PE-based plasmalogens was elevated 1.32-fold (11.6±1.5%) when compared to untreated controls (8.8±1.9%). However, IL-1β did not have any impact on the biosynthesis of PC, SM and LPC. TNFα significantly increased only the biosynthesis of PE by 1.3-fold (31.4±2.0%) when compared to untreated controls (24.0±2.8%), whereas IL-6 did not modulate the biosynthesis of any PL class.

Members of TGF-β superfamily were found to play a role in the progression of OA (35, 40). Thus, we investigated the effect of TGF-β1, BMP-2, BMP-4, and BMP-7. TGF-β1 enhanced the synthesis of the PC class, but this did not reach statistical significance during our screening experiment, probably due to the applied Bonferroni correction. BMP-2 increased the synthesis of PC (5.0±1.0%) by 1.13-fold as well as of SM (0.34±0.03%) by 1.15-fold when compared to untreated controls (4.5±0.9% and 0.30±0.02%, respectively). SM derives from PC, so the ratios of newly synthesized SM to newly synthesized PC were calculated. Our analysis revealed that this ratio did not change upon BMP-2 treatment which indicates a non-specific effect on the biosynthesis of SM. Besides, BMP-7 increased by 1.10-fold synthesis of PE-based plasmalogens (5.8±0.6%) when compared to untreated control (5.3±0.5%), whereas BMP-4 had no impact on the PL biosynthesis. Nevertheless, BMPs significantly increased the biosynthesis of some PC, PE and PE-based plasmalogen species (Appendix Table 12-14).

We also investigated the effect of IGF-1, which was found to have a protective effect on synovium (34). IGF-1 significantly increased the biosynthesis of PC (16.5±3.2%) by 1.29-fold, of PE (26.9±1.7%) by 1.12-fold, as well as of SM (1.6±0.3%) by 1.70-fold, and of LPC (5.2±1.7%) by 1.20-fold when compared to untreated controls. Since PC is a precursor of SM and LPC biosynthesis, the ratios of newly synthesized SM or LPC to newly synthesized PC were calculated. Analysis revealed some slightly increased ratio of SM/PC for IGF-1 treatment (0.10±0.02) when compared to untreated control (0.08±0.02). LPC/PC ratio did not change upon IGF-1 treatment which indicates that the effect of IGF-1 on the LPC biosynthesis was not agent specific.

Dexamethasone induces production of pulmonary surfactants (99). Also, intra-articular injections of glucocorticoids during OA were also suggested to induce PL biosynthesis (100). In our experiment dexamethasone significantly reduced synthesis of PC (11.4±3.5%) by 0.84-fold, of PE (21.3±2.3%) by 0.82-fold, of PE-based plasmalogens (8.2±1.2%) by 0.87-fold and of SM (0.64±0.22%) by 0.64-fold when compared to untreated controls (13.6±4.9%, 26.7±2.7%, 9.4±1.3% and 1.0±0.3%, respectively). Since SM derives from PC, the ratios of newly synthesized SM to its precursor newly synthesized PC were calculated. The analysis revealed some slightly decreased ratio for dexamethasone treatment (0.06±0.02) when compared to untreated control (0.08±0.02).

Because B2-adrenergic receptor antagonist and muscarinic receptor antagonists promotes pulmonary surfactants secretion (101), their effect on the PL biosynthesis was investigated. Adrenergic receptor antagonist – terbutaline and epinephrine as well as muscarinic receptor antagonist – carbachol and pilocarpine were tested. However, none of these agents influenced the PL biosynthesis, except terbutaline which increased the biosynthesis of LPC (5.0±1.3%) by 1.26-fold when compared to untreated control (3.9±1.2%). Since LPC derives from PC, the ratios of newly synthesized LPC to newly synthesized PC were calculated. Our findings revealed that ratios did not change upon terbutaline treatment which indicates a non-specific effect on LPC biosynthesis.

We also investigated whether inhibition of phospholipase A2 with quinacrine prevents the hydrolysis of PC and PE (102). Our data shows that quinacrine significantly inhibited PL hydrolysis, since the synthesis of PC (16.0±4.5%) was increased by 1.36-fold, and that of PE (26.8±2.2%) by 1.18-fold, of SM (1.2±0.3%) by 1.40-fold, and of LPC (9.0±4.00%) by 2.28-fold when compared to untreated controls (11.8±3.2%, 23.4±2.8%, 0.88±0.21%, and 3.9±1.2%, respectively). Since PC is a precursor of SM and LPC biosynthesis, the ratios of

newly synthesized SM or LPC to newly synthesized PC were calculated. Analysis revealed that SM/PC ratio remained unchanged upon quiancrine treatment which suggests a non-specific effect on the SM biosynthesis. However, LPC/PC ratio was increased (0.55±0.10) when compared to untreated control (0.33±0.02) which indicates an agent specific effect on the LPC biosynthesis.

Moreover, inhibition of choline kinase with specific inhibitor CK 37 displayed no effect on the PL biosynthesis. Only a high concentration of CK 37 (10 μM) increased the rate of synthesis of PC (16.0±4.2%) by 1.15-fold, of SM (1.3±0.3%) by 1.23-fold, and of PE-based plasmalogens (11.9±1.6%) by 1.11-fold when compared to untreated controls (14.0±3.2%, 1.1±0.3% and 10.7±1.9%, respectively). Here again, the ratio of newly synthesized SM to newly synthesized PC did not change which indicates a non-specific effect of CK 37 on the SM biosynthesis.

Sirtuins are known to be also associated with pathogenesis of OA (50, 103). Therefore, we investigated the effect of two different sirtuin inhibitors: Sirtinol and EX 527. Using 1 μM sirtinol, which blocks SIRT1 and SIRT2, slightly increased the biosynthesis of PE (25.4±2.8%) by 1.07-fold and of LPC (5.25±1.9%) by 1.30-fold when compared to untreated controls (23.7±2.7% and 4.0±1.3%). At a higher concentration of 10 μM Sirtinol increased the biosynthesis of PC (14.3±3.8%) by 1.14-fold, of PE (28.1±2.5%) by 1.18-fold, of PE-based plasmalogens (11.2±2.77%) by 1.29-fold, and of LPC (5.58±1.62%) by 1.38-fold when compared to untreated controls (12.6±3.6%, 23.7±2.7, 8.7±1.77%, and 4.0±1.3%, respectively). Since LPC derives from PC, the ratios of newly synthesized LPC to newly synthesized PC were calculated. Our analysis revealed that LPC/PC ratio was changed upon sirtinol treatment at the concentration of 1 μM, but not 10 μM, which indicates that only sirtinol at the concentration of 1 μM significantly affected LPC biosynthesis. Inhibition of SIRT1 with 1 μM of EX 527 had no impact on the PL biosynthesis, whereas inhibition of all sirtuins with 50 μM of EX 527 together with 10 μM of NAM decreased the biosynthesis of PC (4.5±1.3%) by 0.86-fold when compared to untreated control (5.3±1.1%).

Since the PC biosynthesis starts with the uptake of choline which is mediated by choline transporters, we have investigated the effect of the choline transporter inhibitor hemicholinium-3 on PL biosynthesis. Hemicholinium-3 did not affect the synthesis of PL based on choline, but unexpectedly increased the biosynthesis of PE (25.6±2.0%) by 1.13-fold and of PE-based plasmalogens (0.97±0.27%) by 1.22-fold when compared to untreated controls (23.4±3.0% and 0.82±0.17%, respectively).

Treatment	[D9]-PC		[D4]-PE		[D4]-PE P	
n = 6	% labelled	*P* values	% labelled	*P* values	% labelled	*P* values
control + 40 µl 5% trehalose	**12.8±3.93**	-	**24.0±2.84**	-	**8.80±1.93**	-
IL-1β (10 ng/ml)	12.7±4.80	NS	31.1±2.18	**	11.6±1.54	***
TNFα (100 ng/ml)	15.6±4.97	NS	31.4±1.99	***	9.87±1.73	NS
IL-6 (10 ng/ml)	12.8±5.13	NS	23.5±2.03	NS	8.35±1.22	NS
TGF-β1 (10 ng/ml)	16.5±4.10	NS	26.4±2.50	NS	9.38±1.94	NS
IGF-1 (100 ng/ml)	16.5±3.17	**	26.9±1.73	**	9.90±2.23	NS
control + 20 µl 95% ethanol	**13.6±4.89**	-	**25.8±2.71**	-	**9.37±1.31**	-
Dexamethasone (10 µM)	11.4±3.47	*	21.3±2.31	**	8.15±1.21	*
control + 20 µl H_2O	**11.8±3.18**	-	**22.6±2.87**	-	**8.02±1.87**	-
Terbutaline (10 µM)	12.5±4.05	NS	23.8±1.75	NS	8.37±1.10	NS
Epinephrine (10 µM)	12.8±4.86	NS	24.2±2.29	NS	8.78±1.32	NS
Carbachol (10 µM)	12.5±4.81	NS	24.1±2.75	NS	8.50±1.91	NS
Pilocarpine (10 µM)	12.8±5.42	NS	24.5±2.73	NS	8.54±1.71	NS
Quinacrine (5 µM)	16.0±4.46	**	26.8±2.16	**	8.08±1.53	NS
control + 20 µl DMSO	**14.0±3.17**	-	**26.3±2.83**	-	**10.7±1.93**	-
CK37 (10 µM)	16.0±4.21	*	25.8±2.15	NS	11.9±1.60	**
CK 37 (5 µM)	14.1±3.96	NS	24.2±1.32	NS	9.56±1.29	NS
control + 2 µl DMSO	**12.6±3.60**	-	**23.7±2.71**	-	**8.68±1.73**	-
CK37 (1 µM)	12.4±3.67	NS	22.5±2.03	NS	8.44±1.79	NS
Sirtinol (1 µM)	13.6±4.61	NS	25.4±2.77	NS	9.37±2.25	NS
Sirtinol (10 µM)	14.3±3.77	**	28.1±2.50	**	11.2±2.77	**
control + 100 µl H_2O	**11.5±3.07**	-	**22.5±3.04**	-	**7.98±1.67**	-
Hemicholinium-3 (50 µM)	13.4±4.69	NS	25.6±1.96	**	9.72±1.70	**
Treatment	**[D9]-PC**		**[D4]-PE**		**[D4]-PE P**	
n = 5	**% labelled**	***P* values**	**% labelled**	***P* values**	**% labelled**	***P* values**
control + 40 µl 5% trehalose + 4 µl DMSO	**5.3±1.07**	-	**12.8±1.92**	-	**6.56±0.91**	-
EX 527 (1 µM)	5.6±0.91	NS	13.8±1.67	NS	6.43±0.66	NS
EX 527 (50 µM) + NAM (10 mM)	4.5±1.34	*	12.7±0.74	NS	6.37±0.37	NS
control + 40 µl 5% trehalose	**4.5±0.93**	-	**9.83±1.88**	-	**5.25±0.53**	-
BMP-2 (100 ng/ml)	5.0±1.02	*	11.0±2.48	NS	5.78±0.89	NS
BMP-4 (100 ng/ml)	4.9±1.17	NS	10.6±1.80	NS	5.44±0.54	NS
BMP-7 (100 ng/ml)	5.3±0.94	NS	11.5±1.93	NS	5.78±0.56	**

Table 12. The effects of agents on the percentage of newly synthesized PL classes.

Treatment	[D9]-SM		[D9]-LPC	
n = 6	% labelled	*P* values	% labelled	*P* values
control + 40 µl 5% trehalose	**0.93±0.22**	-	**4.32±1.65**	-
IL-1β (10 ng/ml)	0.98±0.22	NS	4.88±2.65	NS
TNFα (100 ng/ml)	1.12±0.12	NS	5.55±2.32	NS
IL-6 (10 ng/ml)	0.88±0.25	NS	3.95±1.70	NS
TGF-β1 (10 ng/ml)	1.28±0.41	NS	5.45±1.39	NS
IGF-1 (100 ng/ml)	1.58±0.26	***	5.20±1.70	**
control + 20 µl 95% ethanol	**1.00±0.25**	-	**4.47±1.61**	-
Dexamethasone (10 µM)	0.64±0.22	**	4.33±1.07	NS
control + 20 µl H_2O	**0.88±0.21**	-	**3.93±1.19**	-
Terbutaline (10 µM)	0.83±0.20	NS	4.97±1.25	**
Epinephrine (10 µM)	0.88±0.24	NS	5.40±1.59	NS
Carbachol (10 µM)	0.90±0.28	NS	4.65±1.67	NS
Pilocarpine (10 µM)	0.90±0.29	NS	5.30±1.99	NS
Quinacrine (5 µM)	1.23±0.33	**	8.95±3.96	**
control + 20 µl DMSO	**1.08±0.26**	-	**4.17±0.59**	-
CK37 (10 µM)	1.33±0.32	*	5.37±1.05	NS
CK 37 (5 µM)	1.12±0.27	NS	4.88±1.76	NS
control + 2 µl DMSO	**0.93±0.19**	-	**4.03±1.26**	-
CK37 (1 µM)	0.92±0.27	NS	4.16±1.23	NS
Sirtinol (1 µM)	1.03±0.28	NS	5.25±1.86	*
Sirtinol (10 µM)	1.14±0.26	NS	5.58±1.62	**
control + 100 µl H_2O	**0.82±0.17**	-	**3.87±0.62**	-
Hemicholinium-3 (50 µM)	0.97±0.27	NS	4.93±1.02	*
Treatment	**[D9]-SM**		**[D9]-LPC**	
n = 5	**% labelled**	***P* values**	**% labelled**	***P* values**
control + 40 µl 5% trehalose + 4 µl DMSO	**0.42±0.02**	-	**1.75±0.27**	-
EX 527 (1 µM)	0.43±0.05	NS	1.92±0.21	NS
EX 527 (50 µM) + NAM (10 mM)	0.38±0.07	NS	2.24±0.46	NS
control + 40 µl 5% trehalose	**0.30±0.02**	-	**1.65±0.20**	-
BMP-2 (100 ng/ml)	0.34±0.03	**	1.56±0.18	NS
BMP-4 (100 ng/ml)	0.33±0.03	NS	1.87±0.48	NS
BMP-7 (100 ng/ml)	0.36±0.06	NS	1.78±0.26	NS

Continuation of Table 12. The effects of agents on the percentage of newly synthesized PL classes. The quantitative values obtained for each stable isotope-labelled PL class were normalized to cellular protein content and are expressed as nmol/mg protein. For each PL class the percentage of stable isotope-labelled PL from total labelled and unlabelled PL was calculated. Data are presented as means ± SDs (n = 5-6). The significance was tested using t-tests and further Bonferroni correction for multiple testing was applied. * = $P < 0.05$; ** = $P \leq 0.01$; *** = $P \leq 0.001$. PC = phosphatidylcholine; PE = phosphatidylethanolamine; PE P = phosphatidylethanolamine-based plasmalogens; SM = sphingomyelin; LPC = lysophosphatidylcholine; NS = not significant.

4.5.2. Specific effects of IL-1β

Because IL-1β strongly influenced PL biosynthesis our further analysis focused on the possible mechanism of action. FLS from 5 patients were labelled with precursors, pretreated for 30 min with specific signalling pathways inhibitors QNZ for NF-κB, SB203580 for p38 MAPK and SP600125 for JNK, and were then treated with IL-1β. In this experiment, "LPDS medium" was enriched with L-serine to ensure access of all amino acid to enzymes. None of these treatments affected the morphology of FLS cultured in medium containing 5% LPDS.

IL-1β again significantly increased 1.37-fold the biosynthesis of PE (16.8±1.3%; 3.84±0.36 nmol/mg protein) when compared to untreated control (12.3±1.3%; 2.66±0.34 nmol/mg protein) as well as of PE-based plasmalogens (7.8±0.7%; 3.29±0.36 nmol/mg protein) by 1.25-fold when compared to untreated control (6.3±0.5%; 2.62±0.30 nmol/mg protein) (Figure 24A, B, Appendix Table 4). Also, the biosynthesis of SM (0.4±0.1%; 0.10±0.02 nmol/mg protein) was increased by 1.28-fold when compared to untreated control (0.3±0.1%; 0.08±0.02 nmol/mg protein). Inhibition of the intracellular signalling pathways of NF-κB with QNZ inhibitor, JNK with SP600125 inhibitor, and p38 MAPK with SB203580 abolished the stimulatory effect of IL-1β on the biosynthesis of PE and PE-based plasmalogens. However, inhibition of p38 MAPK enhanced IL-1β-induced biosynthesis of PC by 1.7-fold, SM by 2.0-fold, and LPC by 1.3-fold when compared to sole IL-1β treatment. Since PC is the biosynthetic precursor of SM and LPC, the ratios of these newly synthesized classes to their newly synthesized precursor PC were calculated. Our analysis revealed no altered ratios upon treatments suggesting no specific but precursor-dependent stimulatory effect on SM biosynthesis.

ESI-MS/MS allowed us a detailed analysis of individual PL species being newly synthesized. To determine changes in the synthesis rate of PL species, the x-folds of change of % labelled PL related to untreated control, which equals 1.0, were calculated. Nineteen newly synthesized PC and ten PC O species were identified in human FLS. The concentrations of newly synthesized PC species varied between 35±10 pmol/mg protein (PC 40:6) and 677±151 pmol/mg protein (PC 34:1) for untreated control and between 30±9 pmol/mg protein (PC 40:6) and 757±168 pmol/mg protein (PC 34:1) for treatment with IL-1β (Appendix Table 5). IL-1β significantly enhanced the synthesis of only four PC species compared to control: PC 32:0 by 1.13-fold, PC 34:0 by 1.41-fold, PC 32:1 by 1.20-fold, and PC 36:1 by 1.26-fold. However, the biosynthesis of PC 40:6 was decreased by 0.89-fold.

Inhibition of NF-κB with QNZ abolished the effect of IL-1β on the synthesis of three PC species, whereas inhibition of JNK with SP600125 did not modulate the IL-1β effect.

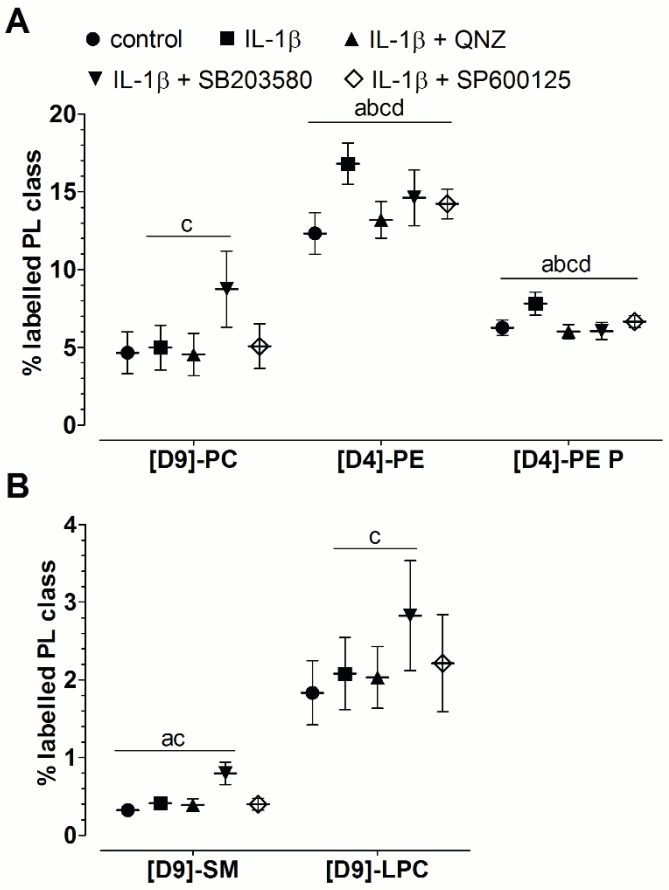

Figure 24. Effect of IL-1β on the biosynthesis of PL classes as modulated by inhibitors of cell signalling pathways. The percentages of labelled PL classes from total corresponding labelled and unlabelled PL class are presented. FLS were treated with 10 ng/ml IL-1β alone or with the inhibitors of signalling pathways QNZ (10 µM, NF-κB), SB203580 (10 µM, p38) and SP600125 (10 µM, JNK) for 16 hours. Data are presented as means ± SDs (n = 5). The significance was tested using t-tests. a = $P \leq 0.05$, control versus IL-1β; b = $P \leq 0.05$, IL-1β versus IL-1β + QNZ; c = $P \leq 0.05$, IL-1β versus IL-1β + SB203580; d = $P \leq 0.05$, IL-1β versus IL-1β + SP600125. PC = phosphatidylcholine; PE = phosphatidylethanolamine; PE P = phosphatidylethanolamine-based plasmalogens; SM = sphingomyelin; LPC = lysophosphatidylcholine.

Ten newly synthesized SM species were identified in human FLS and their concentrations varied between 2±1 pmol/mg protein (SM 36:2) and 39±11 pmol/mg protein (SM 34:1) for untreated control and 3±1 pmol/mg protein (SM 36:2) and 52±13 pmol/mg protein (SM 34:1) for IL-1β treatment (Appendix Table 5). The biosynthesis of four SM species namely SM 34:1 (1.38-fold), SM 35:2 (1.21-fold), SM 36:2 (1.36-fold), and SM 42:2 (1.45-fold) were stimulated by IL-1β. However, inhibition of NF-κB or JNK had no significant impact on SM biosynthesis.

Moreover, only three newly synthesized LPC species were detected, and these were only found at low levels. Their concentrations in the untreated controls were 8±2 pmol/mg protein for LPC 16:0, 5±1 pmol/mg protein for LPC 18:0, and 6±2 pmol/mg protein for LPC 18:1, and in cells treated with IL-1β 8±3 pmol/mg protein for LPC 16:0, 5±1 pmol/mg protein for LPC 18:0, and 6±1 pmol/mg protein for LPC 18:1.

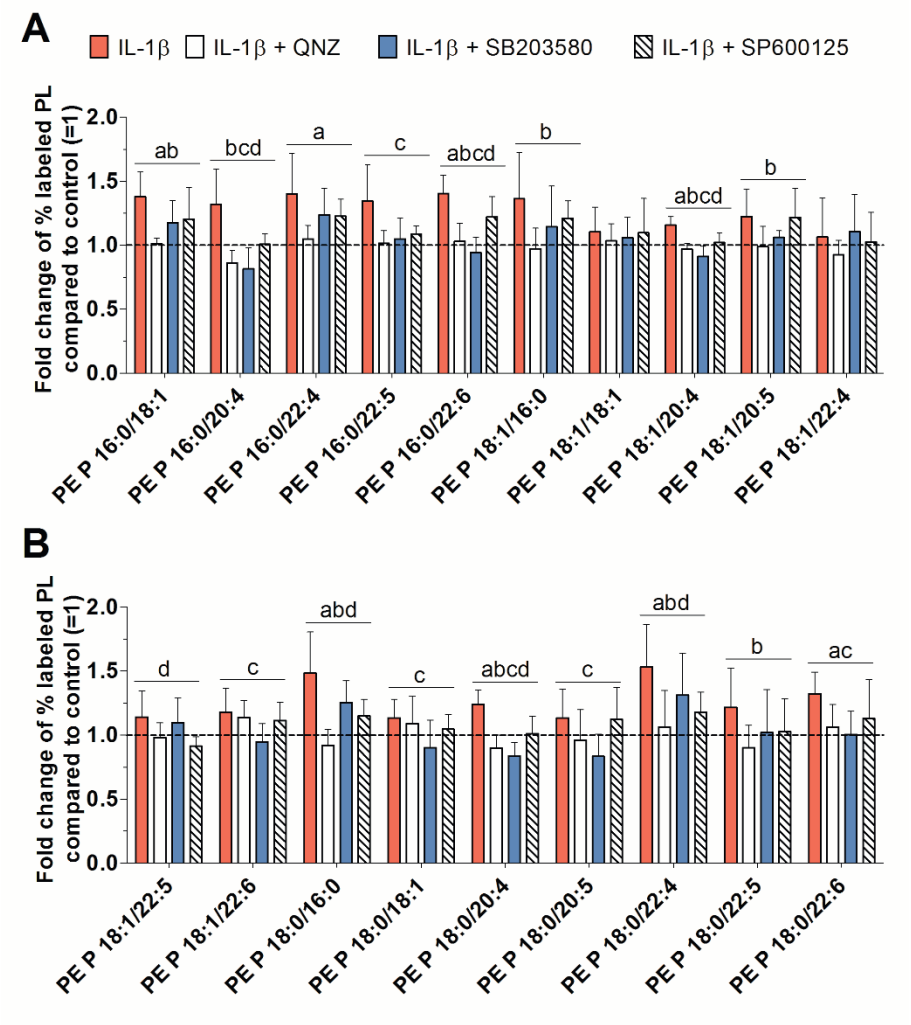

Figure 25. Effect of IL-1β on the biosynthesis of PE-based plasmalogens species as modulated by inhibitors of cell signalling pathways. PE P biosynthesis was monitored with ESI-MS/MS in the presence of IL-1β (red bars) with or without the addition of the JNK inhibitor SP600125 (hatched bars), NF-κB activation inhibitor QNZ (white bars) or the p38 MAPK inhibitor SB203580 (blue bars) for 16 hours. The percentages of stable isotope-labelled PE P species were calculated as a ratio of the corresponding untreated control and are expressed as x-fold change of % labelled PE P species compared to untreated control (=1). Data are presented as means ± SDs (n = 5). The significance was tested using t-tests. a = $P \leq 0.05$, control versus IL-1β; b = $P \leq 0.05$, IL-1β versus IL-1β + QNZ; c = $P \leq 0.05$, IL-1β versus IL-1β + SB203580; d = $P \leq 0.05$, IL-1β versus IL-1β + SP600125. PE P = phosphatidylethanolamine-based plasmalogens.

Nineteen newly synthesized PE-based plasmalogen species of FLS were identified (Figure 25A, B). Their concentrations varied between 36±8 pmol/mg protein (PE P 18:0/18:1)

and 577±77 pmol/mg protein (PE P 18:1/20:4) for untreated controls and 38±7 pmol/mg protein (PE P 18:0/18:1) and 640±66 pmol/mg protein (PE P 18:1/20:4) for IL-1β treated FLS (Appendix Table 5). IL-1β increased the biosynthesis of eight PE-based plasmalogen species from 1.15-fold (PE P 18:1/20:4) up to 1.53- fold (PE P 18:0/22:4). Inhibition of signalling pathways partly abolished the IL-1β effect on the biosynthesis of these species. Inhibition of NF-κB significantly abolished the biosynthesis of six species, of JNK five species, and of p38 MAPK only four species.

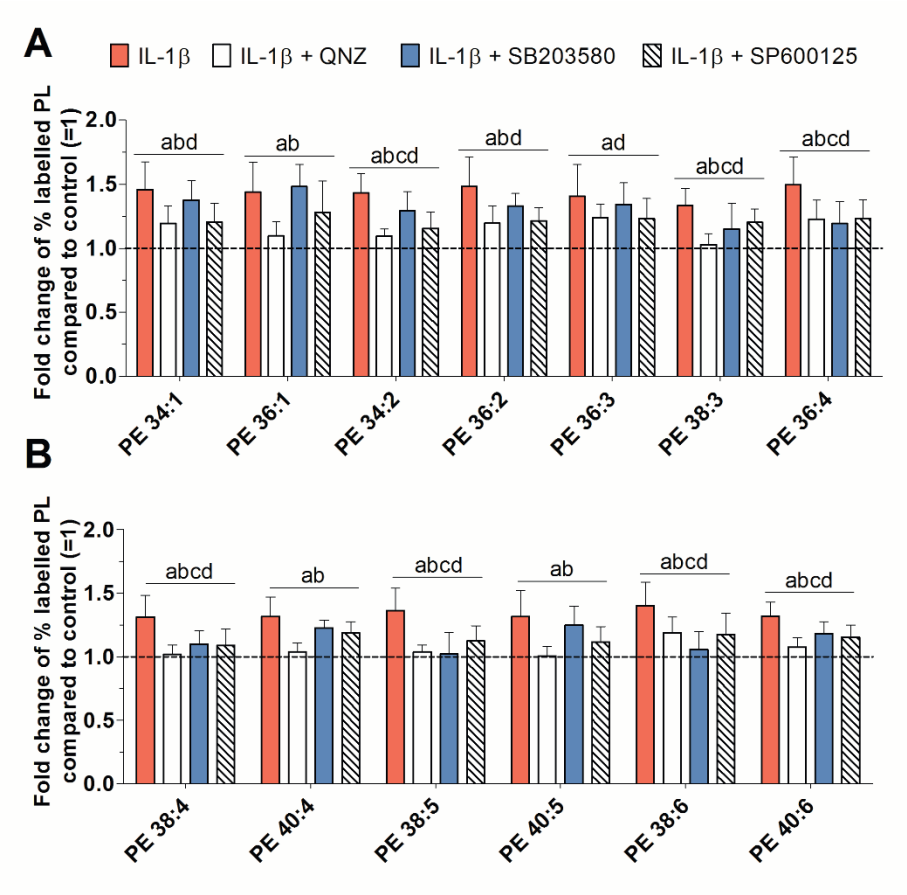

Figure 26. Effect of IL-1β on the biosynthesis of PE species as modulated by inhibitors of cell signalling pathways. PE biosynthesis was monitored with ESI-MS/MS in the presence of IL-1β (red bars) with or without the addition of the JNK inhibitor SP600125 (hatched bars), NF-κB activation inhibitor QNZ (white bars) or the p38 MAPK inhibitor SB203580 (blue bars) for 16 hours. The percentages of stable isotope-labelled PE species were calculated as a ratio of the corresponding untreated control and are expressed as x-fold change of % labelled PE species compared to untreated control (=1). Data are presented as means ± SDs (n = 5). The significance was tested using t-tests. a = $P \leq 0.05$, control versus IL-1β; b = $P \leq 0.05$, IL-1β versus IL-1β + QNZ; c = $P \leq 0.05$, IL-1β versus IL-1β + SB203580; d = $P \leq 0.05$, IL-1β versus IL-1β + SP600125. PE = phosphatidylethanolamine.

Thirteen newly synthesized PE species were identified in human FLS (Figure 26A, B). Their concentrations varied between 35±9 pmol/mg protein (PE 36:4) and 656±97 pmol/mg

protein (PE 38:4) for untreated control and 56±9 pmol/mg protein (PE 36:4) and 871±83 pmol/mg protein (PE 38:4) (Appendix Table 5). IL-1β significantly increased the biosynthesis of all PE species from 1.31-fold (PE 40:5) up to 1.49-fold (PE 36:4). Inhibition of all three signalling pathways abolished the IL-1β effect. QNZ significantly inhibited IL-1β-induced synthesis of twelve PE species, SB203580 of seven PE species, and SP600125 of ten PE species.

4.5.3. Specific effects of TGF-β1

In order to further investigate the effect of TGF-β1 on the PL biosynthesis, FLS from 5 patients were labelled as described previously, pretreated for 30 min with TGF-β type I receptor activin receptor-like kinase ALK5 inhibitor SB432542, and then treated with TGF-β1. In this experiment, "LPDS medium" was enriched with L-serine to ensure access of all amino acid to enzymes. None of these treatments affected the morphology of FLS cultured in medium containing 5% LPDS.

TGF-β1 significantly increased 1.46-fold the biosynthesis of PC (7.65±1.63%; 5.86±1.16 nmol/mg protein) when compared to untreated control (5.25±1.07%; 4.31±0.84 nmol/mg protein) as well as of SM (0.54±0.08%; 0.13±0.02 nmol/mg protein) by 1.29-fold when compared to untreated control (0.42±0.02%; 0.11±0.02 nmol/mg protein). Since SM derives from PC, the ratio of newly synthesized SM to newly synthesized PC was calculated. The analysis shown that SM/PC ratio was decreased (0.07±0.02) when compared to untreated control (0.08±0.02) which suggests that observed effect came only from the increased PC synthesis. Interestingly, the biosynthesis of PE-based plasmalogens decreased (6.12±0.80%; 2.47±0.50 nmol/mg protein) by 0.93-fold when compared to untreated control (6.56±0.91%; 2.78±0.53 nmol/mg protein). Furthermore, inhibition of TGF-β receptor I kinase abolished the TGF-β1 effect on the biosynthesis of PC to untreated control level. Additionally, using SB432542 inhibitor even more decreased the biosynthesis of PE-based plasmalogens by 0.88-fold when compared to sole TGF-β1 treatment (Figure 27A, B, Appendix Table 4).

The concentrations of nineteen newly synthesized PC species varied between 35±12 pmol/mg protein (PC 40:4) and 812±142 pmol/mg protein (PC 34:1) for untreated control and between 39±12 pmol/mg protein (PC 40:4) and 1189±205 pmol/mg protein (PC 34:1) for treatment with TGF-β1 (Appendix Table 6). TGF-β1 significantly enhanced the biosynthesis of all PC species from 1.3-fold up to 1.8-fold when compared to untreated control. Inhibition

of TGF-β receptor I kinase significantly abolished the effect of TGF-β1 on the synthesis of sixteen PC species: PC 30:0, PC 32:0, PC 34:0, PC 32:1, PC 34:1, PC 36:1, PC 34:2, PC 36:2, PC 34:3, PC 36:3, PC 38:4, PC 36:5, PC 38:5, PC 40:5, PC 38:6, and PC 40:6 (Figure 28A, B).

Moreover, ten newly synthesized SM species were identified and their concentrations varied between 3±1 pmol/mg protein (SM 36:2) and 54±10 pmol/mg protein (SM 34:1) for untreated control and 4±1 pmol/mg protein (SM 36:2) and 69±17 pmol/mg protein (SM 34:1) for treatment with TGF-β1 (Appendix Table 6). TGF-β1 significantly increased the biosynthesis only one species SM 36:2 by 1.3-fold. This effect was abolished by the SB432542 inhibitor (Figure 28C).

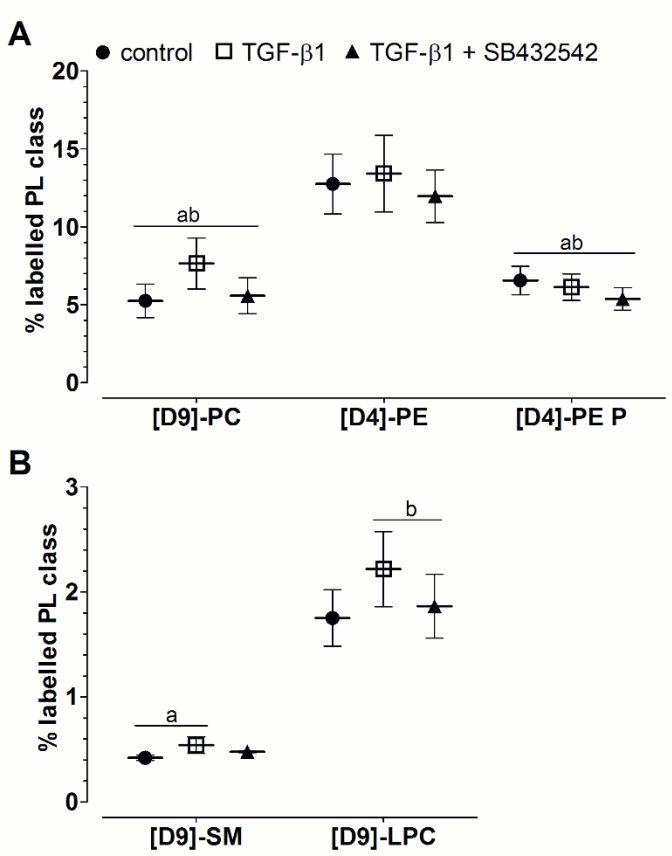

Figure 27. Effect of TGF-β1 on the biosynthesis of PL classes as modulated by TGFβ receptor type I kinase inhibitor. The percentages of labelled PL classes from total corresponding labelled and unlabelled PL class are presented. FLS were treated with 10 ng/ml TGF-β1 alone or with the inhibitor of TGFβ receptor I kinase (10 μM, SB432542) for 16 hours. Data are presented as mean s± SDs (n = 5). The significance was tested using t-tests. a = $P \leq 0.05$, control versus TGF-β1; b = $P \leq 0.05$, TGF-β1 versus TGF-β1 + SB432542. PC = phosphatidylcholine; PE = phosphatidylethanolamine; PE P = phosphatidylethanolamine-based plasmalogens; SM = sphingomyelin; LPC = lysophosphatidylcholine.

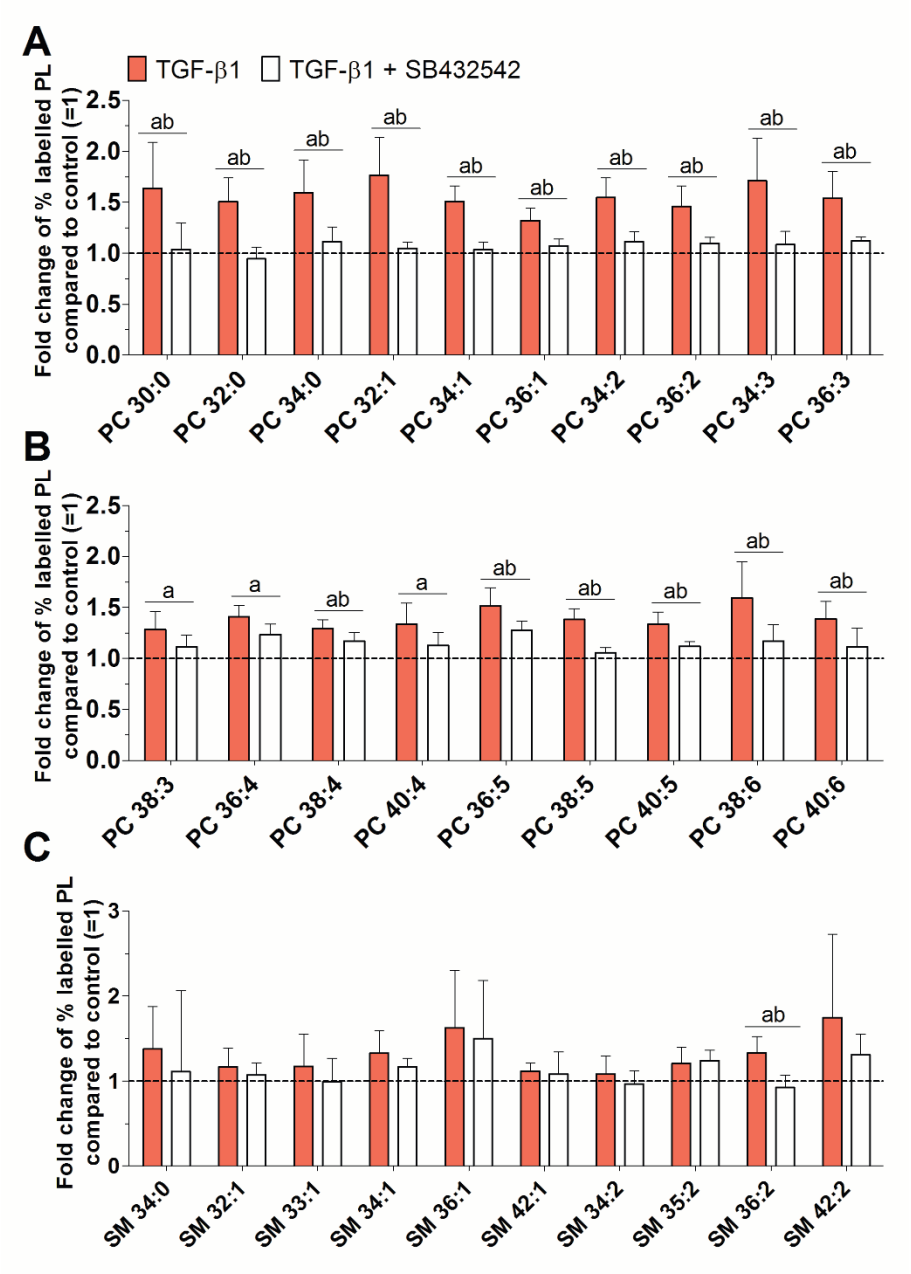

Figure 28. Effect of TGF-β1 on the biosynthesis of PC (A-B) and SM (C) species as modulated by TGFβ receptor I kinase inhibitor. PL biosynthesis was monitored with ESI-MS/MS in the presence of TGF-β1 (red bars) with or without the addition of the TGFβ receptor type I kinase inhibitor SB432542 (white bars) for 16 hours. The percentages of stable isotope-labelled PL species were calculated as a ratio of the corresponding untreated control and are expressed as x-fold change of % labelled PL species compared to untreated control (=1). Data are presented as means ± SDs (n = 5). The significance was tested using t-tests. a = $P \leq 0.05$, control versus TGF-β1; b = $P \leq 0.05$, TGF-β1 versus TGF-β1 + SB432542. PC = phosphatidylcholine; SM = sphingomyelin.

Also, nineteen newly synthesized PE-based plasmalogens species were identified in FLS. Their concentrations varied between 40±14 pmol/mg protein (PE P 18:0/18:1) and 575±105 pmol/mg protein (PE P 18:1/20:4) for untreated control and 37±8 (PE P 18:0/18:1)

and 515±94 pmol/mg protein (PE P 18:1/20:4) for treatment with TGF-β1 (Appendix Table 6). TGF-β1 significantly increased the biosynthesis of only PE P 18:1/20:4 by 1.1-fold and decreased the biosynthesis of PE P 18:0/22:6 specie by 0.9-fold. Inhibition of TGF-β receptor I kinase significantly decreased synthesis of PE P 18:0/22:6 (Figure 29A, B).

Moreover, the biosynthesis of individual PE species was barely affected by TGF-β1. Only the biosynthesis of one specie PE 36:3 was increased by 1.24-fold when compared to untreated control (data not shown).

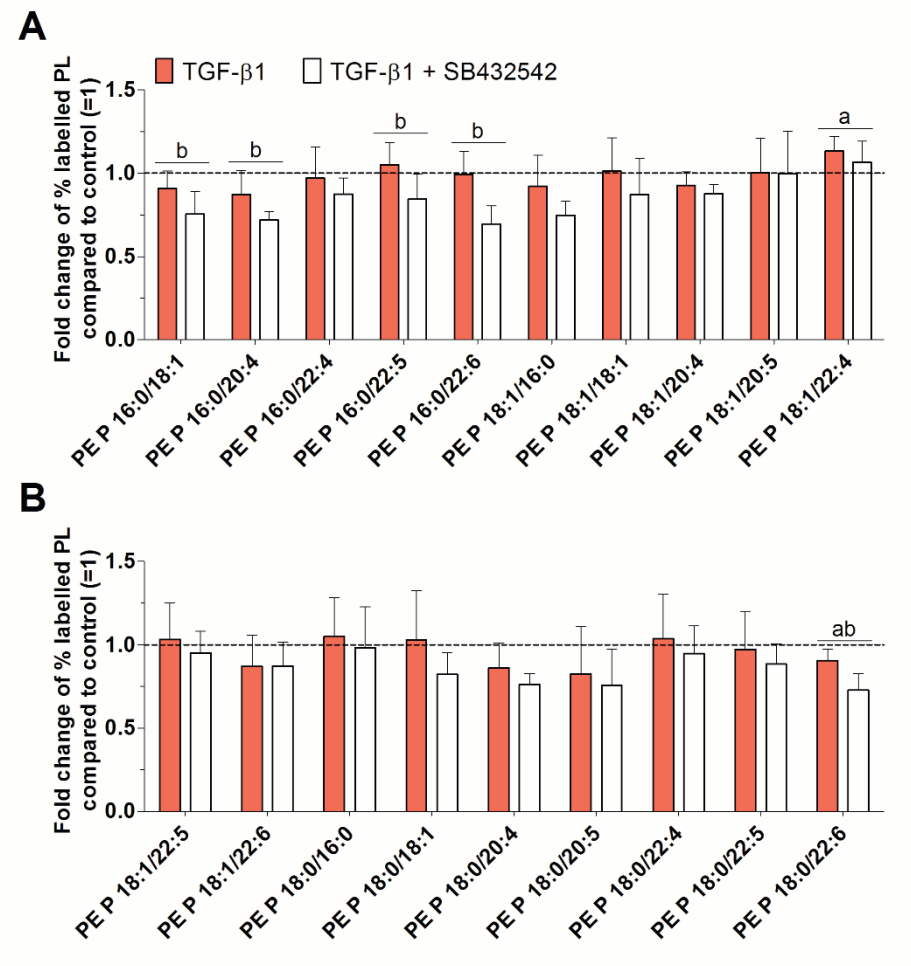

Figure 29. Effect of TGF-β1 on the biosynthesis of PE P species as modulated by TGFβ receptor I kinase inhibitor. PE P biosynthesis was monitored with ESI-MS/MS in the presence of TGF-β1 (red bars) with or without the addition of the TGFβ receptor type I kinase inhibitor SB432542 (white bars) for 16 hours. The percentages of stable isotope-labelled PE P species were calculated as a ratio of the corresponding untreated control and are expressed as x-fold change of % labelled PE P species compared to untreated control (=1). Data are presented as means ± SDs (n = 5). The significance was tested using t-tests. a = $P \leq 0.05$, control versus TGF-β1; b = $P \leq 0.05$, TGF-β1 versus TGF-β1 + SB432542. PE P = phosphatidylethanolamine-based plasmalogens.

4.5.4. Specific effects of IGF-1

Data from our screening experiment lead us to focus on the effect of IGF-1. FLS from 5 patients were labelled as described previously, pretreated for 30 min with signalling pathways inhibitors LY294002 (PI3K) and SCH772984 (ERK), and then treated with IGF-1. In this experiment, "LPDS medium" was enriched with L-serine to ensure access of all amino acid to enzymes. None of these treatments affected the morphology of FLS cultured in medium containing 5% LPDS.

IGF-1 significantly increased 1.28-fold the biosynthesis of PC (6.71±1.53%; 5.06±1.06 nmol/mg protein) when compared to untreated control (5.25±1.07%; 4.31±0.84 nmol/mg protein) as well as of SM (0.59±0.09%; 0.14±0.03 nmol/mg protein) by 1.41-fold when compared to untreated control (0.42±0.02%; 0.11±0.02 nmol/mg protein). However the ratio of newly synthesized SM to newly synthesized PC did not changed, which indicates that the observed effect was not IGF-1 specific. We could determine only a small inhibitory effect of the specific PI3K inhibitor LY294002 on the biosynthesis of PE and SM. Unexpectedly, inhibition of ERK with SCH772984 inhibitor further stimulated the biosynthesis of PC by 1.56-fold, of SM by 1.88-fold, and of LPC by 1.59-fold (Figure 30A, B, Appendix Table 4). Here again, observed effects were not agent specific due to the constant ratio of newly synthesized SM and LPC to newly synthesized PC.

Our analysis allowed us to determine nineteen newly synthesized PC species. Their concentrations varied between 35±12 pmol/mg protein (PC 40:4) and 812±142 pmol/mg protein (PC 34:1) for untreated controls and between 33±9 pmol/mg protein (PC 40:4) and 1036±120 pmol/mg protein (PC 34:1) for treatment with IGF-1 (Appendix Table 7). IGF-1 significantly enhanced the biosynthesis of sixteen PC species from 1.2-fold up to 1.4-fold. Inhibition of PI3K significantly abolished the effect of IGF-1 on the synthesis of four PC species namely PC 32:1, PC 34:1, PC 36:3, and PC 36:4 but increased the synthesis of PC 40:5 (Figure 31A, B).

The concentrations of newly synthesized SM species varied between 3±1 pmol/mg protein (SM 36:2) and 54±10 pmol/mg protein (SM 34:1) for untreated controls and 3±1 pmol/mg protein (SM 36:2) and 70±17 pmol/mg protein (SM 34:1) for treatment with IGF-1 (Appendix Table 7). IGF-1 significantly increased the biosynthesis of SM 34:1 by 1.4-fold, SM 42:1 by 1.7-fold, SM 35:2 by 1.5-fold, and SM 42:2 by 1.9-fold. Inhibition of PI3K

significantly abolished the effect of IGF-1 on the synthesis of SM 34:1 and SM 35:2 (Figure 31C).

Additionally, IGF-1 did not affect the biosynthesis of any PE-based plasmalogen species. However, this growth factor increased the biosynthesis of specie PE 36:3 by 1.09-fold and decreased the biosynthesis of PE 40.4 by 0.88-fold when compared to untreated control (data not shown).

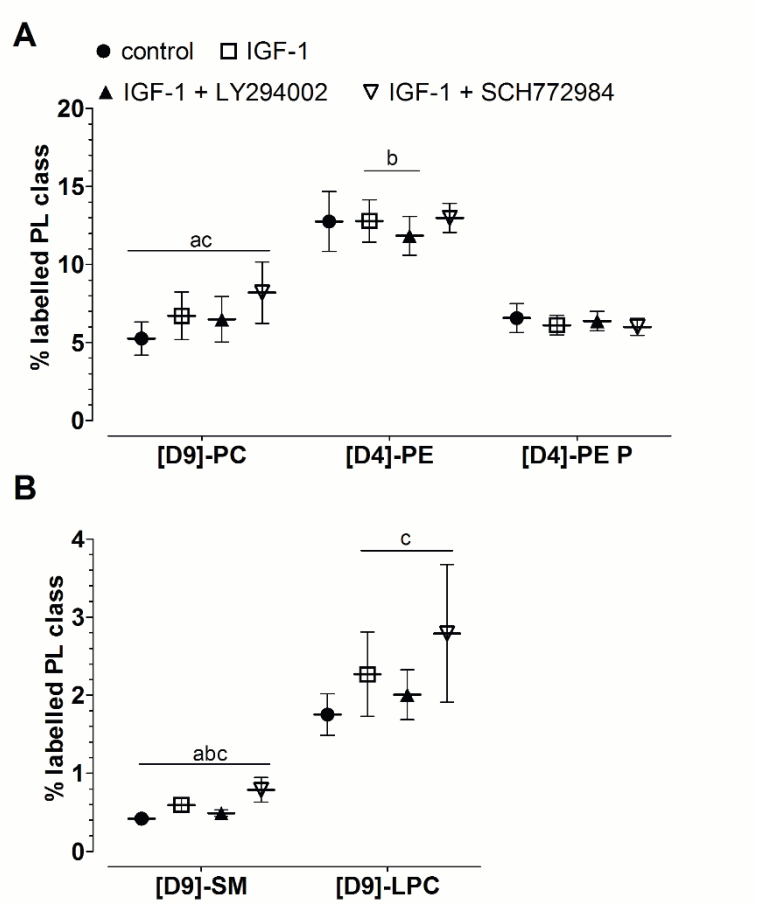

Figure 30. Effect of IGF-1 on the biosynthesis of PL classes as modulated by cell signalling pathways inhibitors. The percentages of labelled PL classes from total corresponding labelled and unlabelled PL class are presented. FLS were treated with 100 ng/ml IGF-1 alone or with the cell signalling pathways inhibitors LY294002 (10 μM, PI3K) and SCH772984 (1μM, ERK) for 16 hours. Data are presented as means ± SDs (n = 5). The significance was tested using t-tests. a = $P \leq 0.05$, control versus IGF-1; b = $P \leq 0.05$, IGF-1 versus IGF1 + LY294002; c = $P \leq 0.05$, IGF-1 versus IGF-1 + SCH772984. PC = phosphatidylcholine; PE = phosphatidylethanolamine; PE P = phosphatidylethanolamine-based plasmalogens; SM = sphingomyelin; LPC = lysophosphatidylcholine.

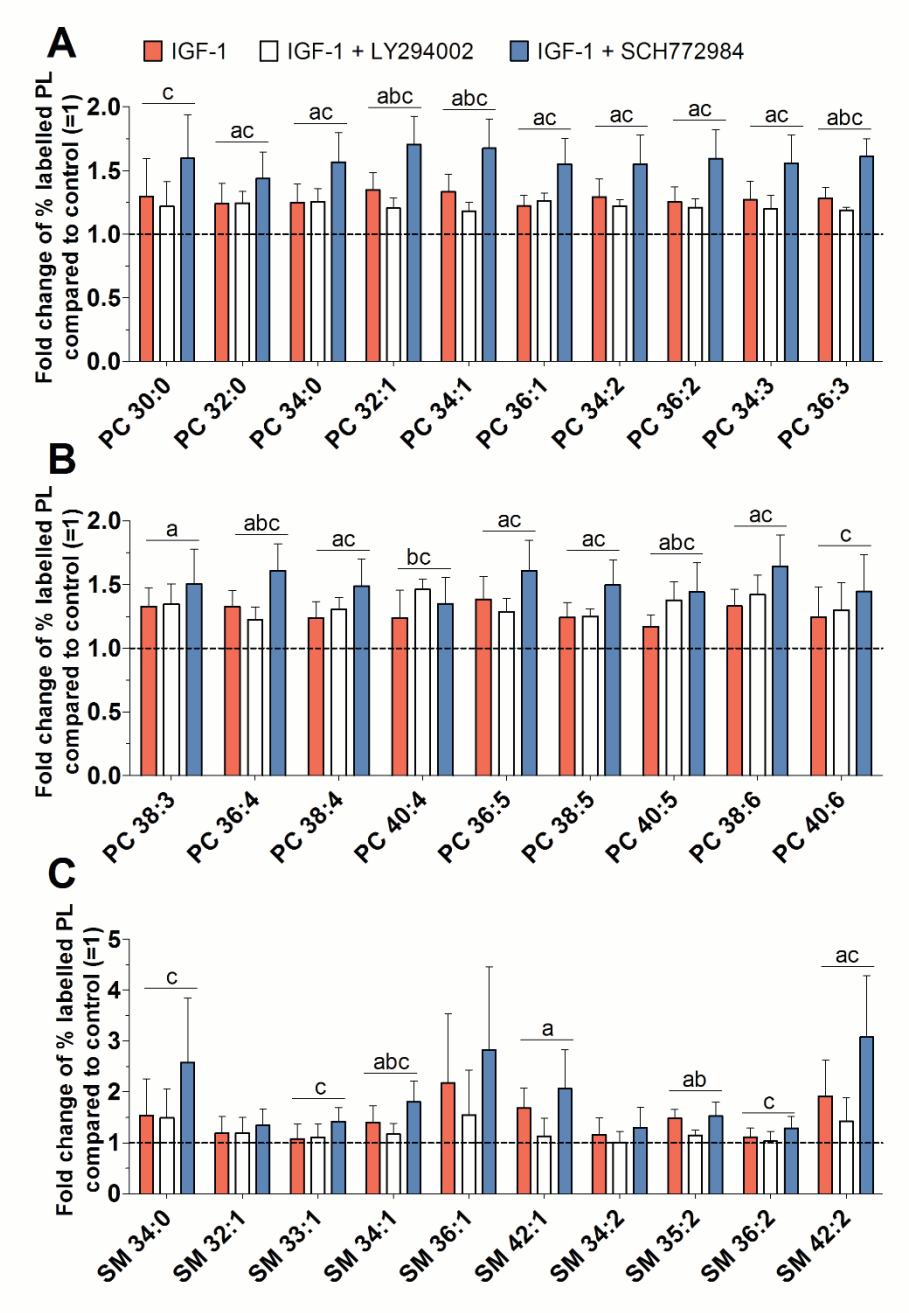

Figure 31. Effect of IGF-1 on the biosynthesis of PC (A-B) and SM (C) species as modulated by signalling pathways inhibitors. PL biosynthesis was monitored with ESI-MS/MS in the presence of IGF-1 (red bars) with or without the addition of the cell signalling pathways inhibitors LY294002 (white bars) and SCH772984 (blue bars) for 16 hours. The percentages of stable isotope-labelled PL species were calculated as a ratio of the corresponding untreated control and are expressed as x-fold change of % labelled PL species compared to untreated control (=1). Data are presented as means ± SDs (n = 5). The significance was tested using t-tests. a = $P \leq 0.05$, control versus IGF-1; b = $P \leq 0.05$, IGF-1 versus IGF1 + LY294002; c = $P \leq 0.05$, IGF-1 versus IGF-1 + SCH772984. PC = phosphatidylcholine; SM = sphingomyelin.

4.5.5. Specific effects of dexamethasone

Our screening experiment revealed that dexamethasone is the only agent which decreased the PL biosynthesis. Thus, we further investigated its effects. FLS from 5 patients were labelled as described previously, pretreated for 30 min with glucocorticoid receptor inhibitor RU 485, and then treated with dexamethasone. In this experiment, "LPDS medium" was enriched with L-serine to ensure access of all amino acid to enzymes. Dexamethasone did not affect the morphology of FLS cultured in medium containing 5% LPDS.

Dexamethasone significantly decreased 0.79-fold the biosynthesis of PE (11.27±1.30%; 2.06±0.29 nmol/mg protein) when compared to untreated control (14.26±1.46%; 3.06±0.54 nmol/mg protein) as well as of SM (0.34±0.01%; 0.08±0.02 nmol/mg protein) by 0.74-fold when compared to untreated control (0.46±0.04%; 0.10±0.01 nmol/mg protein). PC and PE-based plasmalogen biosynthesis was slightly decreased which did not reach statistical significance. Furthermore, blocking the glucocorticoid receptor with RU 486 abolished the dexamethasone effect on the biosynthesis of SM (Figure 32A, B, Appendix Table 4). Since SM derives from PC, the ratios of these newly synthesized SM to its newly synthesized precursor PC were calculated. Our analysis revealed no altered ratios upon treatments suggesting no specific but precursor-dependent stimulatory effect on SM biosynthesis.

Our detailed ESI-MS/MS analysis allowed us to determine nineteen newly synthesized PC species. Their concentrations varied between 39±5 pmol/mg protein (PC 34:3) and 861±90 pmol/mg protein (PC 34:1) for untreated controls and between 28±8 pmol/mg protein (PC 34:3) and 726±206 pmol/mg protein (PC 34:1) for treatment with dexamethasone (Appendix Table 8). Dexamethasone significantly decreased the biosynthesis of only PC 30:3 by 0.77-fold. Moreover, blocking the glucocorticoid receptor with RU 486 abolished this effect (Figure 33A, B).

Moreover, ten newly synthesized SM species were identified and their concentrations varied between 3±1 pmol/mg protein (SM 36:2) and 54±8 pmol/mg protein (SM 34:1) for untreated controls and 2±0 pmol/mg protein (SM 36:2) and 37±11 pmol/mg protein (SM 34:1) for treatment with dexamethasone (Appendix Table 8). Dexamethasone significantly decreased the biosynthesis of four SM species namely SM 33:1 by 0.88-fold, SM 42:1 by 0.65-fold, SM 36:2 by 0.78-fold, and SM 42:2 by 0.53-fold. Blocking the glucocorticoid

receptor with RU 486 significantly abolished the dexamethasone effect on the synthesis of SM 34:1 (Figure 33C).

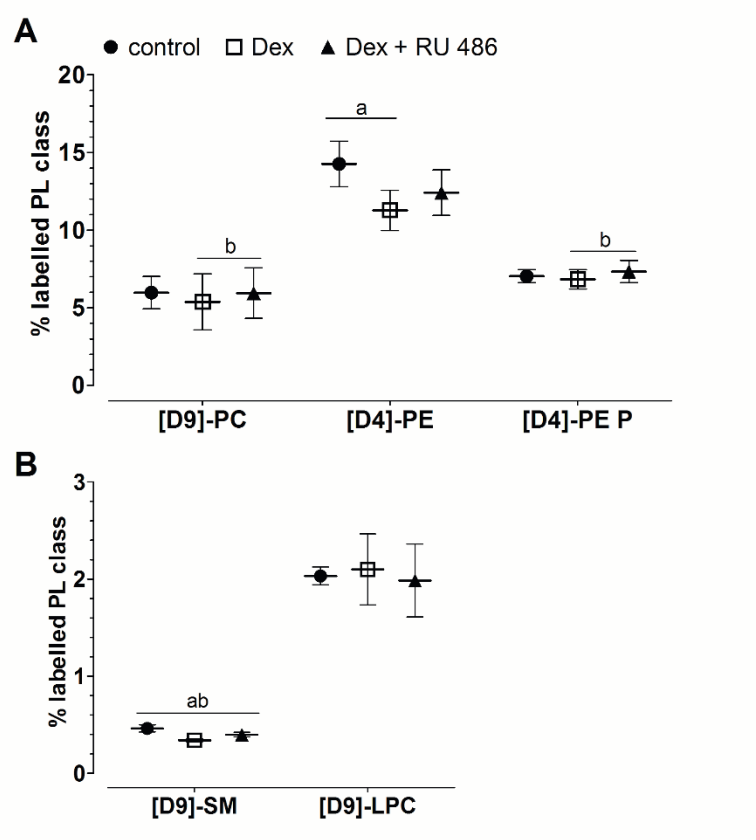

Figure 32. Effect of dexamethasone on the biosynthesis of PL classes as modulated by a glucocorticoid receptor inhibitor. The percentages of labelled PL classes from total corresponding labelled and unlabelled PL class are presented. FLS were treated with dexamethasone (10 µM) alone or with the glucocorticoid receptor inhibitor RU 486 (1 µM) for 16 hours. Data are presented as means ± SDs (n = 5). The significance was tested using t-tests. a = $P \leq 0.05$, control versus Dex; b = $P \leq 0.05$, Dex versus Dex + RU 486. PC = phosphatidylcholine; PE = phosphatidylethanolamine; PE P = phosphatidylethanolamine-based plasmalogens; SM = sphingomyelin; LPC = lysophosphatidylcholine; Dex = dexamethasone.

In addition, thirteen newly synthesized PE species were identified and their concentrations varied between 37±16 pmol/mg protein (PE 34:2) and 722±134 pmol/mg protein (PE 38:4) for untreated controls and 18±8 pmol/mg protein (PE 34:2) and 558±125 pmol/mg protein (PE 38:4) for dexamethasone (Appendix Table 8). Dexamethasone significantly decreased the biosynthesis of eleven PE species from 0.67-fold (PE 34:1) down to 0.85-fold (PE 40:5). Blocking the glucocorticoid receptor with RU 486 significantly abolished the dexamethasone effect on the synthesis of five PE species: PE 34:1, PE 36:1, PE 38:3, PE 40:4, and PE 40:6 (Figure 34A, B).

Additionally, dexamethasone did not significantly affect the biosynthesis of any of detected nineteen PE-based plasmalogen species (data not shown).

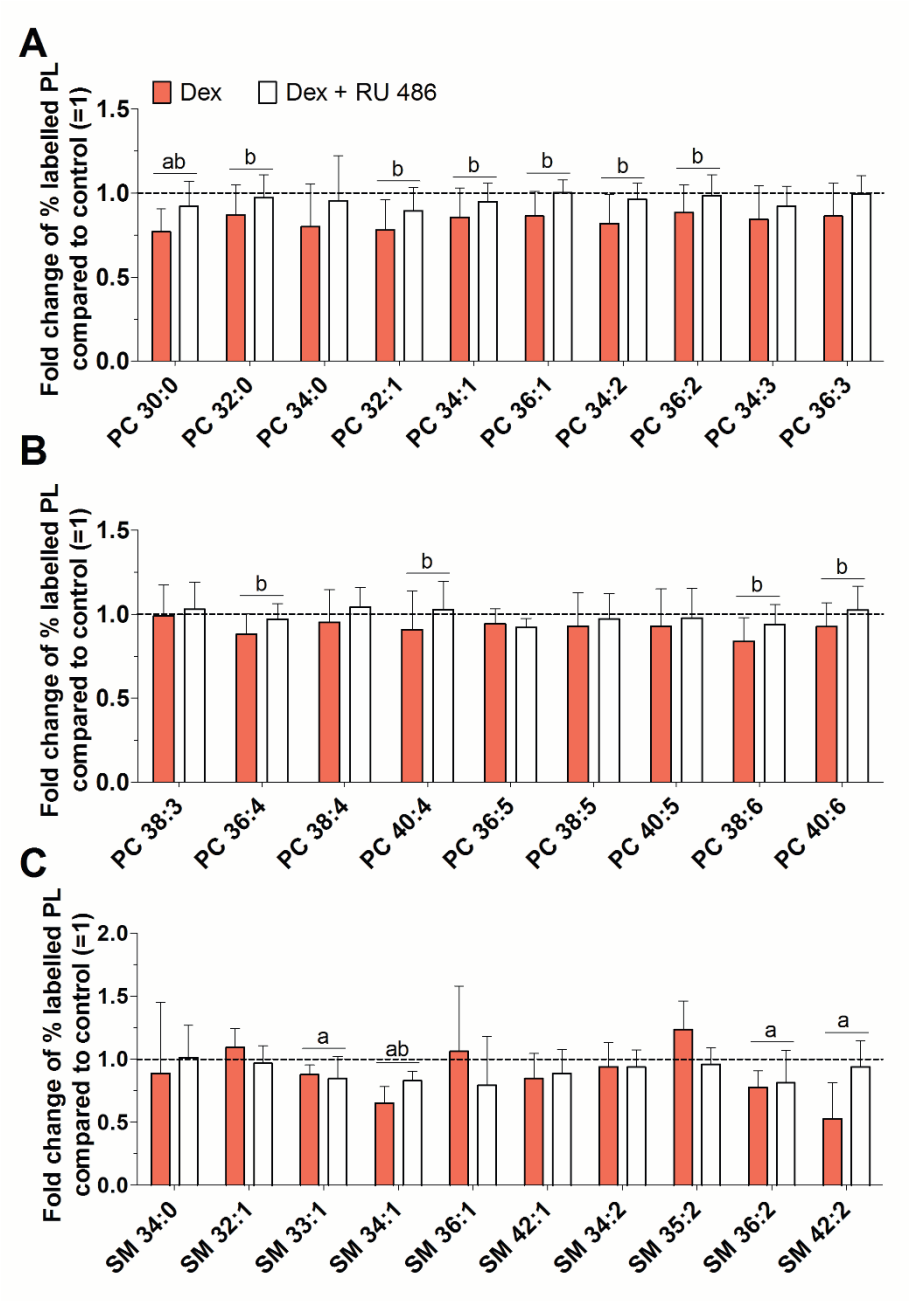

Figure 33. Effect of dexamethasone on the biosynthesis of PC (A-B) and SM (C) species as modulated by a glucocorticoid receptor inhibitor. PL biosynthesis was monitored with ESI-MS/MS in the presence of dexamethasone (red bars) with or without the addition of the glucocorticoid receptor inhibitor RU 486 (white bars) for 16 hours. The percentages of stable isotope-labelled PL species were calculated as a ratio of the corresponding untreated control and are expressed as x-fold change of % labelled PL species compared to untreated control (=1). Data are presented as means ± SDs (n = 5). The significance was tested using t-tests. a = $P \leq 0.05$, control versus Dex; b = $P \leq 0.05$, Dex versus Dex + RU 486. PC = phosphatidylcholine; SM = sphingomyelin; Dex = dexamethasone.

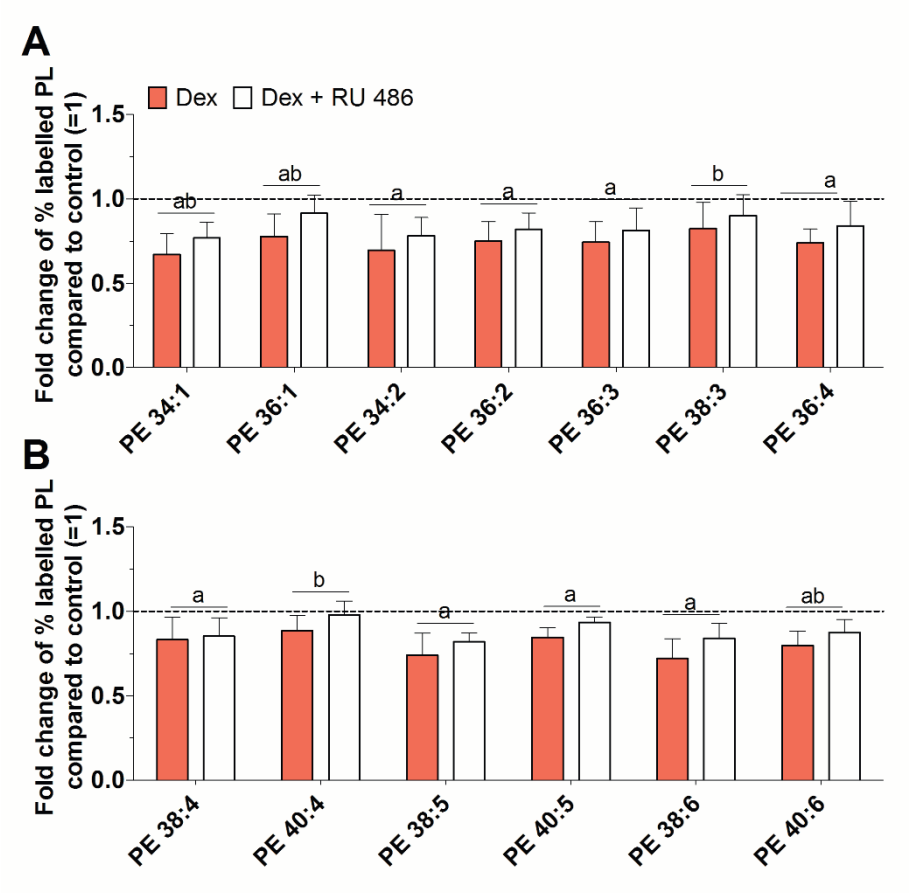

Figure 34. Effect of dexamethasone on the biosynthesis of PE species as modulated by a glucocorticoid receptor inhibitor. PE biosynthesis was monitored with ESI-MS/MS in the presence of dexamethasone (red bars) with or without the addition of the glucocorticoid receptor inhibitor RU 486 (white bars) for 16 hours. The percentages of stable isotope-labelled PE species were calculated as a ratio of the corresponding untreated control and are expressed as x-fold change of % labelled PE species compared to untreated control (=1). Data are presented as means ± SDs (n = 5). The significance was tested using t-tests. a = $P \leq 0.05$, control versus Dex; b = $P \leq 0.05$, Dex versus Dex + RU 486. PE = phosphatidylethanolamine; Dex = dexamethasone.

4.6. The effects of agents on the release of PLs from FLS

We have used our established release model to investigate the effects of various agents on the PL release from FLS into culture media.

4.6.1. Screening the effects of agents on the release of PLs

Because current knowledge about PL release of FLS is limited, we screened the effects of various agents known to be associated with the pathogenesis of OA (Table 13). Similar to the biosynthesis model we have investigated the effect of cytokines, growth factors,

corticosteroids, β-adrenergic agonists, muscarinic receptor agonists, inhibitor of phospholipase A2, inhibitor of choline transporter, and inhibitors of sirtuins. Moreover, we wanted to enhance the release of PLs from FLS using apolipoproteins, since they transport cholesterol and PLs (104).

In general, the release of [^{3}H]-choline-labelled PLs was 2.3-fold higher than [^{14}C]-ethanolamine-labelled PLs. From all tested agents only IL-1β and TNFα enhanced the release of [^{3}H]-choline-labelled PLs into DMEM containing 2% FBS. However, FLS treated with IL-1β and TNFα displayed more rounded morphology of spindle-shaped cells. Other treatments did not affected the morphology of FLS cultured in medium containing 2% or 5% FBS. Nevertheless, all other agents had no impact on the release of PLs.

4.6.2. Specific effect of IL-1β

Data from the screening experiment lead us to focus on the effect of IL-1β. Due to the altered cell morphology during treatment of FLS with 10 ng/ml IL-1β we reduced finally the concentration to 2 ng/ml. Simultaneously, the serum content of nutrient media was increased up to 10%. In order to identify the mechanism of action of IL-1β on PL release, inhibitors of specific signalling pathway were used (Table 14).

Despite improvements in this experiment, FLS still displayed some altered morphology upon IL-1β treatment. Only cells treated with 5 ng/ml IL-1β and 10 μM SB203580 had normal spindled-shaped cell morphology. IL-1β did not stimulate PL release in DMEM containing 5% or 10% FBS. Additionally, we could not observe any concentration-dependent effect. Inhibition of signalling pathways did not influence the effect of IL-1β. However, an increased release of [^{14}C]-ethanolamine-labelled PLs into DMEM containing 5% FBS was determined after blocking the p38 MAPK signalling pathway with SB203580 (2.4±0.4%) when compared to IL-1β (1.8±0.7%).

Treatment	[^{3}H]-choline-labelled PLs		[^{14}C]-ethanolamine-labelled PLs	
	% released PLs	*P*-values	% released PLs	*P*-values
2% FBS	n= 5		n = 5	
control + 40 µl 5% trehalose	**4.7±0.9**	**-**	**2.0±0.5**	**-**
IL-1β (10 ng/ml)	5.9±1.1	**	1.7±0.5	NS
TNFα (100 ng/ml)	5.7±1.2	**	2.2±0.5	NS
IL-6 (10 ng/ml)	5.3±1.5	NS	2.2±0.6	NS
TGF-β1 (10 ng/ml)	5.6±2.2	NS	-	-
IGF-1 (100 ng/ml)	5.0±1.3	NS	-	-
control + 20 µl 95% ethanol	**5.0±1.0**	**-**	**2.2±0.7**	**-**
Dexamethasone (10 µM)	4.8±1.4	NS	2.1±0.7	NS
control + 20 µl H_2O	**5.0±0.8**	**-**	**1.8±0.3**	**-**
Terbutaline (10 µM)	5.0±1.2	NS	2.1±0.6	NS
Epinephrine (10 µM)	5.1±1.2	NS	-	-
Carbachol (10 µM)	4.7±1.2	NS	2.1±0.7	NS
Pilocarpine (10 µM)	5.2±1.6	NS	-	-
Quinacrine (5 µM)	4.1±0.7	NS	-	-
control + 2 µl DMSO	**5.4±1.5**	**-**	**2.1±0.5**	**-**
Sirtinol (1 µM)	5.2±1.6	NS	3.1±1.0	NS
control + 100 µl H_2O	**6.9±2.8**	**-**	**-**	**-**
Hemicholinium-3 (50 µM)	5.1±1.2	NS	-	-
Treatment	**[^{3}H]-choline-labelled PLs**		**[^{14}C]-ethanolamine-labelled PLs**	
	% released PLs	***P*-values**	**% released PLs**	***P*-values**
5% FBS	n = 6		n = 6	
control + 40 µl 5% trehalose + 4 µl DMSO	**5.7±0.8**	**-**	**2.2±0.4**	**-**
EX 527 (1 µM)	5.5±1.1	NS	2.1±0.5	NS
control + 8 µl gelatin-PBS + 20 µl 5% terhalose	**6.9±2.1**	**-**	**2.6±0.9**	**-**
Apo A-I (10 µg/ml)	6.5±0.9	NS	2.5±0.8	NS
Apo E4 (10 µg/ml)	6.2±0.9	NS	2.0±0.4	NS

Table 13. The effects of agents on the release of PLs from FLS. Our *in vitro* model to study the efflux of PLs from FLS was applied. The release of radiolabelled PLs from confluent FLS into media during a 24 hours period was monitored in the presence of agents at the final concentration indicated in the table. The quantitative dpm values were normalized to the cellular protein content. Data presented are the percentages of radiolabelled PLs being released from total radiolabelled PLs found in media and cellular lysates (=100%) which were calculated separately for [^{3}H]- as well as [^{14}C]-labelled PLs. ** = $P \leq 0.01$. Data are presented as means ± SDs (n = 5-6). The significance was tested using t-tests and further Bonferroni correction for multiple testing was applied. NS = not significant.

Treatment	[^{3}H]-choline-labelled PLs		[^{14}C]-ethanolamine-labelled PLs	
	% released PLs	*P*-values	% released PLs	*P*-values
5% FBS	n = 6		n = 6	
control	**6.2±1.0**	-	**2.3±0.6**	-
IL-1β (5 ng/ml)	6.9±1.8	NS	1.8±0.7	NS
IL-1β (5 ng/ml) + SB203580 (10 µM)	7.3±1.1	NS	2.4±0.4	#
Treatment	**[^{3}H]-choline-labelled PLs**		**[^{14}C]-ethanolamine-labelled PLs**	
	% released PLs	***P*-values**	**% released PLs**	***P*-values**
10% FBS	n = 3		n = 2	
control	**6.8±0.5**	-	-	-
IL-1β (2 ng/ml)	10.8±3.7	NS	-	-
control	**7.1±1.5**	-	**2.0±0.1**	-
IL-1β (5 ng/ml)	7.7±1.5	NS	1.9±0.2	NS
IL-1β (5 ng/ml) + SB203580 (10 µM)	7.9±1.6	NS	3.1±1.9	NS
IL-1β (5 ng/ml) + QNZ (10 µM)	7.8±1.8	NS	2.3±0.0	NS
control	**7.4±0.6**	-	-	-
IL-1β (10 ng/ml)	9.2±2.1	NS	-	-

Table 14. The effect of IL-1β on the release of PLs from FLS. Our *in vitro* model to study the efflux of PLs from FLS was applied. The release of radiolabelled PLs from confluent FLS into media during a 24 hours period was monitored in the presence of agents at the final concentration indicated in the table. The quantitative dpm values were normalized to the cellular protein content. Data presented are the percentages of radiolabelled PLs being released from total radiolabelled PLs found in media and cellular lysates (=100%) which were calculated separately for [^{3}H]- as well as [^{14}C]-labelled PLs. # = $P \leq 0.05$, IL-1β versus IL-1β + SB203580. Data are presented as means ± SDs (n = 2-6). The significance was tested using t-tests. NS = not significant.

5. DISCUSSION

The main goal of this study was to determine the effects of cytokines, growth factors as well as pharmacological agents on the biosynthesis and release of PL classes and species from human FLS and further elucidate the underlying cell transduction mechanism. This study provides the first detailed overview of PLs being synthesized and released from human FLS using two newly developed *in vitro* models. Furthermore, our data indicate that cytokines and growth factors differently regulate PL metabolism. The obtained results suggest that PL biosynthesis and release is regulated by some cytokines and growth factors being present at the elevated levels in the synovial fluid of osteoarthritic articular joints.

5.1. Comparison of PLs from SF and FLS

PLs together with HA and lubricin were reported to provide boundary lubrication within human articular joints (52, 54, 61, 62, 105). Recent studies have shown that lubricin interacts with HA complexed with PLs, which can slide past similar groups from opposing surfaces with low friction via boundary lubrication mechanism (106, 107). The lipid profile of SF is well described and related to the health status of the joint. Our previous studies have reported that SF from patients with OA and RA displayed higher levels of PLs compared to healthy controls, whereas the concentrations of HA and lubricin were reduced in these diseases (53, 54, 82). The balance between these three compounds is necessary for proper lubrication. Moreover, PLs are involved in many other processes in human body including membrane constitutes, cell signalling, inflammation, and anti-oxidative processes (67, 68, 70, 78).

Our analysis showed for the first time the composition of PLs in human OA FLS. Using ESI-MS/MS we were able to determine nine PL classes. PC was found to be a major PL class constituting 33% of all PLs. We previously reported that in human SF 67% of total PLs is PC, and that 94% of all PLs contain choline. Interestingly, in our study PE-based plasmalogen was the second major class constituting 18% of all PLs, whereas in SF this class constituted only 2.5% of all PLs (53). PC is considered to be a major lipid class playing a role in joint lubrication. Within cells PLs are membrane components and they are also involved in many processes such as cell signalling and inflammation, which may explain their greater diversity.

In a lipidomic study by Kosinska *et al.* 23 PC, 21 PE species, and 24 PE-based plasmalogen were found in human SF from healthy donors (53). In this study, we demonstrated that untreated FLS synthesized 19 PC, 13 PE species, and 17 PE-based plasmalogen from those species being present in SF. We could observe similarities between SF and FLS in individual species composition. PC 34:2, PC 34:1 and PC 36:2 are the major species being present in SF, while PC 34:1, PC 32:0 and PC 38:4 are in untreated FLS. The most abundant PE species for both SF and untreated FLS is PE 38:4. Also, the main PE-based plasmalogen species are the same for SF and untreated FLS, which are PE P 16:0/20:4, PE P 18:1/20:4, and PE P 18:0/20:4. This indicates that at least part of PLs being present in SF may derive from FLS.

Furthermore, human knee joint contains about 0.5-4 ml of SF. The concentrations of PLs being present in SF are at high levels and are expressed as nmol/ml of SF. In our study, the concentrations of PLs are much lower and are expressed as nmol/mg cellular protein. According to our experiments one million of FLS produce approximately 0.14±0.03 µg protein. The whole synovial membrane contains 1-2 layers of FLS. In order to be the sole source of the most abundant PC species in SF, namely PC 34:2 (26.1 nmol/ml), approximately 600 billions of cultured FLS are needed. This calculation is based on the assumption that the same rate of synthesis and degradation is present *in vivo* and *in vitro*. Therefore, it seems unlikely that all PLs present in SF derive from FLS.

5.2. Biosynthesis of PLs

PLs were reported to be synthesized and stored in lamellar bodies of FLS (59, 108-110). These cells can also secrete hyaluronan and lubricin, molecules which contribute to lubrication of articular joints (58, 111). They also produce and release cytokines, mediators of inflammations and matrix metalloproteinases (55).

Our data confirm that non-proliferating, confluent FLS indeed synthesize PLs. The application of stable isotope-labelled precursors of PLs combined with ESI-MS/MS technology allowed us to analyse a great variety of individual lipid species. Using our newly developed model to study the biosynthesis of PLs, we were able to determine 74 newly synthesized PL species belonging to five PL classes. However, using stable isotope-labelled precursors of choline and ethanolamine limited our investigation about the *de novo* synthesis of PLs to only PC and PE synthesis via the Kennedy pathway. Other newly synthesized lipids

such as PE-based plasmalogens, SM, and LPC were generated in our study only from their precursors PC and PE, which must be taken into account when interpreting our data. The biosynthesis of PL is highly correlated with time. After 16 hours of labelling, we found more PE than PC being labelled with their stable isotope-labelled precursors. Our data suggest that synthesis and remodelling of PC require more time than synthesis of PE. Since in our experiments we used 100% confluent FLS and a starvation period, we assume that the observed effect on the biosynthesis of PLs does not derive from lipids produced for cell membranes of dividing cells.

Several studies have suggested that the fatty acid chain length and saturation have an impact on the lubricating properties of PC. It is believed that the most important surfactant in the lung is saturated dipalmityol-phosphatidylcholine (DPPC) (64). However, DPPC was found only in small amounts on the surface of articular cartilage (112, 113). Moreover, Kosinska *et al.* reported elevated levels of polyunsaturated PC species such as PC 34:1, PC 36:1, PC 34:2, PC 36:2, PC 36:3, PC 36:4, PC 38:4, and PC 38:5 within human SF (53). Similarly, our data indicate that FLS mostly produce the same unsaturated PC species. We assume that these polyunsaturated species might be involved in boundary lubrication. Here we showed that newly synthesized PC species exist mostly in unsaturated form and their FA chains contain equal or less than 36 carbon atoms, which might derive from the FAs such as palmitic, palmitoleic, stearic and oleic acids being present in the culture media. Also, the preferred synthesized PE species were polyunsaturated and contained more than 36 carbon atoms in their FA chains.

5.2.1. Effect of cytokines on the biosynthesis of PLs

IL-1β, TNFα and IL-6 are thought to be key pro-inflammatory cytokines involved in the pathogenesis of OA, and elevated levels of these cytokines were found in SF and sera of OA patients (11, 12, 15). We therefore tested the effect of these cytokines on the biosynthesis of PLs. Kronqvist *et al*. (114) focused on IL-1β using human skin fibroblasts to show that this cytokine inhibits the synthesis of SM class but not PC class. Angel *et al.* (102) reported that IL-1β induced the degradation of PC, PE, and PI through the activation of phospholipase A2 and release of arachidonic acid using human FLS. We did not observe this effect in our study. Here, IL-1β stimulated PE biosynthesis and did not reduce levels of PC species, even of those PC species that might contain arachidonic acid such as PC 36:4 and PC 38:4. Our results

show that IL-1β enhanced the synthesis of PE and PE-based plasmalogen when compared to untreated control. Interestingly, it only slightly influenced the synthesis of PLs containing choline. Moreover, we have shown that TNFα only slightly contributes to changes in the biosynthesis of PLs, whereas IL-6 has no impact. Also, our data are partly in contrast to those obtained by Kronqvist *et al*. (114), a difference which might have been due to methodological differences. We used a shorter time period to determine the *de novo* synthesis of PLs in order to avoid any degradation and reuptake of newly synthesized lipids. Also, our study used highly differentiated human FLS which are cells known to secrete many factors including lubricants. Furthermore, Kronqvist *et al.* (34) used a culture medium supplemented with 12% FBS which contains LDL and cholesterol, whereas we used lipoprotein deficient serum. It is known that less SM is found wherever increased levels of cholesterol esters are seen (115) and this interaction might be one of the reasons for the divergence.

During this study we could notice the advantage of ESI-MS/MS, because we were able to see the differences on the individual species levels, which was sometimes not visible when only looking at the overall effect on the corresponding PL class. Here we could demonstrate e.g. for PC that a marked stimulation of individual PC species does not necessarily result in an elevated level of the corresponding PL class. A detailed view of PL species being regulated individually might be important for future experiments designed to elucidate their individual roles.

IL-1β can stimulate the production of ROS which leads to damage of articular cartilage (21, 22, 116). In our study, IL-1β markedly elevated the levels of PE and PE-based plasmalogens which can act as an antioxidant (67). Moreover, our previous study reported elevated levels of PE-based plasmalogen in human OA SF (53). Our data support the concept of a protective role of PE-based plasmalogen against ROS-induced damage by equilibrating the IL-1β effect on ROS.

To further understand the role of IL-1β in PL synthesis, we searched for the molecular mechanism underlying its effect. We focused on the signalling pathways such as NF-κB, p38 MAPK, and JNK known to be involved in IL-1β cellular signalling. Our results demonstrate that IL-1β enhance the biosynthesis of PE and PE-based plasmalogen via NF-κB, p38 MAPK, and JNK pathways without any preference. However, inhibition of p38 MAPK unexpectedly enhanced the biosynthesis of PLs containing choline during treatment with IL-1β. There are two explanations of this: First, p38 MAPK signalling pathway is negatively involved in the biosynthesis of PLs. Second, that an agent specific effect was determined. Further analyses

containing proper control and inhibitor alone are required to explain the role of p38 MAPK signalling in the biosynthesis of PLs containing choline.

We compared species found to be altered in early OA SF (53) with IL-1β treated FLS. The concentrations of 19 PC species were elevated during early OA, from which the biosynthesis of only PC 34:0 and PC 36:1 was also found to be enhanced after IL-1β treatment (Appendix Table 9). Moreover, 10 PE species were elevated in early OA SF. The biosynthesis of 9 of them was found to be enhanced by treatment with IL-1β (Appendix Table 10). In addition, 8 PE-based plasmalogen species were found to be elevated in both early OA SF and FLS, but only 3 of them were common, which were PE P 16:0/22:6, PE P 18:0/20:4, and PE P 18:0/22:6 (Appendix Table 11). Taken together our data indicate that the effect of IL-1β on PL biosynthesis in FLS partly parallels those of the PL alterations seen in SF during early OA (53). Moreover, the observed effect might be due to the adaptation of FLS to elevated levels of IL-1β in OA SF (12, 15).

IL-1β and TNFα significantly enhanced the biosynthesis of PLs containing ethanolamine in cultured FLS. IL-1β increased the biosynthesis of PE, PE-based plasmalogens as well as SM, whereas TNFα elevated only the synthesis of PE. A main biological function of PE and PE-based plasmalogen is the maintenance of the cell membrane dynamic (70). Since in our study non-proliferating, confluent FLS were used, we can assume that changes in PLs levels did not derive from PLs constituting cell membranes. Also, PLs take part in many other biological processes. For instance, PE is the precursor of molecules which modulate pain perception (e.g. anandamide, *N*-arachidonylethanolamine), inflammation (e.g. *N*-palmitoylethanolamine), autophagy (e.g. PE-modified microtubule-associated protein light-chain 3), and apoptosis (e.g. *N*-stearoylethanolamine, diarachidonoylphosphoethanolamine) (70, 117-120). PE-based plasmalogens can act as antioxidants during oxidative stress (67, 121). Furthermore, PE and PE-based plasmalogens are source of DAGs which are intracellular messengers and play a role in intracellular signalling involving protein kinase C (67, 117, 122). SM species and their metabolites such as ceramides (e.g. C1P, C2-, C6-ceramides) and sphingosine (e.g. S1P) play also important roles in cell signalling involving protein kinase C, phospholipase D, and MAPK, as well as in cell differentiation, survival, and apoptosis (84, 123).

In conclusion, our data indicate that elevated levels of PE, PE-based plasmalogens, and SM induced by elevated levels of IL-1β could turn on defence or survival mechanisms against the harmful effect of this cytokine. For instance elevated levels of PE-based

plasmalogens might protect against cartilage destruction by scavenging ROS (67, 121). PE containing arachidonic and stearic acid (e.g. PE 36:4, PE 38:4) and SM metabolites could induce the apoptosis either of FLS to reduce synovial hyperplasia, or of osteophytes by altering mitochondria function and inducing caspase activation. Our study showed that the biosynthesis of PE and PE-based plasmalogen is mediated via NF-κB, p38 MAPK, and JNK signalling pathways. Moreover, these cell transduction pathways are involved in the response to cellular stress, cytokines, and free radicals and were also found to be activated in other cells of OA synovial joint (124-126). This suggests that PLs could also activate pathways which could transfer the signal from FLS further to other cells within the joint. However, additional studies are required to confirm these possible effects.

5.2.2. Effect of growth factors on the biosynthesis of PLs

Current research also focus on the anabolic growth factors in rheumatic disorders (32). Since elevated levels of TGF-β1, IGF-1, BMP-2, and BMP-7 were found in OA SF (44, 127-129), we tested the effect of these growth factors on PL biosynthesis in FLS. The growth factors investigated in this study significantly increased the biosynthesis of PC and SM in human FLS. Our analysis focused mainly on the PC as a major PL class being synthesized *de novo* via the Kennedy pathway. In this section we do not focus on the SM, because we were able to measure its synthesis only indirectly and individual species were at low concentrations. The highest stimulation of PC occurred with TGF-β1 treatment, resulting in the increased synthesis of 19 PC species. We have also shown that the TGF-β1 effect was mediated by TGFβ receptor type I. The second most stimulating growth factor was IGF-1, which increased the biosynthesis of 16 PC species. The least effective factor was BMP-2, stimulating the biosynthesis of 13 species (Appendix Table 12). BMP-4 and BMP-7 stimulated synthesis of some individual PC species which had no impact on the overall synthesis rate of the PC class. Our data indicate that various growth factors affect differently the PL biosynthesis of FLS.

We could observe some differences of the effects of TGF-β1 between experiments. In our screening experiment TGF-β1 increased the biosynthesis of PLs, however the values did not reach statistical significance. In our main experiment TGF-β1 was found to strongly influence PC biosynthesis. The differences might be due to the Bonferroni correction used in the statistical analysis of the screening experiment.

Due to the increased biosynthesis of PC upon IGF-1 treatment, we searched for a possible mechanism underlying this effect. We have focused on the canonical signalling pathways being activated by IGF-1 which were PI3K and ERK. Inhibition of PI3K abolished the effect of IGF-1 only on the biosynthesis of four PC species which suggest a small contribution of this signalling pathway to PC biosynthesis. Unexpectedly, the inhibition of ERK enhanced the biosynthesis of 17 PC species. Similar to the p38 MAPK inhibition, this signalling pathway might be negatively involved in PL biosynthesis or we observed an agent specific effect. However, IGF-1 can also act through other non-canonical signalling pathways, and further analyses are needed to better understand its mechanism of action.

According to our study, BMPs are not as potent as TGF-β1 or IGF-1. Nevertheless, we could observe some specific effect on the biosynthesis of PLs. BMP-2, the most effective factor, enhanced the biosynthesis of 13 PC, 3 PE and 6 PE-based plasmalogen species. BMP-7 induced the biosynthesis of 10 PC, 6 PE and 3 PE-based plasmalogen species, whereas BMP-4 affected the biosynthesis of 9 PC, 4 PE and 2 PE-based plasmalogen species (Appendix Tables 12-14).

The accumulation of lubricin has been intensively studied (130-132). Both TGF-β1 and IGF-1 were found to increase the accumulation of lubricin in bovine chondrocytes and FLS. Niikura *et al.* have shown that FLS were more sensitive to BMP family members than chondrocytes (132). It is well known that lubricin plays an important role in lubrication. Also, it has been shown that TGF-β upregulates synthesis of HA in human FLS (133, 134). In our study of human FLS, we focused on the effect of growth factors on the biosynthesis of another lubricant. Our data showed that TGF-β1 and IGF-1 upregulates the biosynthesis of PC in non-proliferating, confluent FLS. Moreover, in our study FLS rather poorly responded to BMPs. Since PC is considered as a main PL participating in lubrication (112), the effect of growth factors speaks for their beneficial effect on lubricating properties within synovial joints.

Furthermore, we compared PC species found to be altered in early and late OA SF (53) and found them to be similar to those of FLS treated with growth factors. 19 PC species were elevated during early OA, and 18 among them were even more increased during late OA. Remarkably, the biosynthesis of 16 from those 19 PC species was also stimulated by TGF-β1 in FLS. Moreover, IGF-1 stimulated the biosynthesis of 14 from those 19 PC species being elevated in OA SF (Appendix Table 9). In addition, increased levels of 10, 9, and 10 PC species were found in OA SF as well as upon BMP-2, BMP-4, and BMP-7 treatment,

respectively (Appendix Table 12). Interestingly, five PC species (PC 34:0, PC 34:1, PC 36:2, PC 36:3 and PC 36:4) were commonly upregulated by all growth factors and also found to be elevated in SF during early and late OA. Taken into account that growth factors being present in SF are elevated during OA, our results suggest that PL alterations observed in diseased SF might derive from FLS influenced by those factors. However, all growth factors did not modulate the release of PLs from cultured FLS into nutrient media. Further culture parameters need to be tested to confirm these preliminary results.

Interestingly, TGF-β1 acts differently on the surfactant production within the pulmonary system. Beers *et al.* have shown that TGF-β1 inhibits surfactant proteins and fatty acid synthetase expression as well as phospholipid production in human fetal lung explants (135). The rate of [^{3}H]-choline incorporation into PC was significantly decreased. Moreover, epithelial cells treated with TGF-β1 did not display lamellar bodies responsible for lipid secretion. This indicates that the response to TGF-β1 is dependent on the cell type and that the surfactant system of the lung is differently regulated than the lubricating system within articular joints.

Growth factors investigated in this study significantly increased the biosynthesis of 19 PC species. TGF-β1 and IGF-1 also enhanced the biosynthesis of SM and LPC. Additionally, BMPs enhanced the biosynthesis of some PE and PE-based plasmalogen species. Since, non-proliferating, confluent cells were used we can exclude the membrane building function of these newly produced PC. However, some PC species produced by FLS could be responsible for lubricating properties, especially polyunsaturated PC species, which are highly present within human SF. The remaining PC species and metabolites such as PA and DAGs participate in cell signalling involving protein kinase C and G-proteins, or can be used as a precursor of other lipids (70, 136, 137). LPC species are also important molecules in cell signalling pathways such as ERK, MAPK, PI3K, and Rho, and have some pro-inflammatory properties including increasing the IL-1β production and activation of macrophages (76).

In conclusion, our data indicate that the enhanced production of polyunsaturated PC species stimulated by elevated levels of growth factors could improve lubrication of the articular joint. In our study we showed that activation of TGF-β/BMP signalling was involved in the biosynthesis of PC. These signalling pathways are also activated in articular cartilage and subchondral bone during OA (138). Second messengers such as DAGs, PA, and arachidonic acid can be also generated from PC, thus elevated PC species might be involved in downstream signalling. Moreover, DAGs and PAs might also passage from one tissue to

another, affecting metabolic homeostasis of the neighbour tissue. Also individual PC species can act as signalling molecules, for instance palmitoyl-oleoyl-phosphatidylcholine (PC 34:1) was recently found to be a ligand for peroxisome proliferator-activated receptors (PPARs) which regulate expression of many genes that govern lipid metabolism including triglyceride turnover, as well as uptake, activation, and oxidation of fatty acids (139, 140). This suggests that PC 34:1 species, which is a major PC species being present in both FLS and SF, can affect the final composition of PL being present within the synovial joint. Furthermore, elevated LPC species could activate macrophage-like synoviocytes within the synovial membrane leading to production and secretion of cytokines and chemokines. Moreover, PE and PE-based plasmalogen species induced by BMPs could also take part in defence mechanism in response to diseased joint environment. For instance PE-based plasmalogens can protect cartilage against ROS by scavenging free radicals (67, 121) or PE can induce caspase activity leading to apoptosis of hypertrophic FLS and inhibition of osteophyte formation (119, 120). Further studies are needed to confirm these possible functions.

5.2.3. Effect of dexamethasone on the biosynthesis of PLs

Intra-articular injections of dexamethasone are commonly used in OA and RA treatment (100, 141). Several studies have shown that dexamethasone inhibits the induction of MMPs, prostaglandins, inflammatory cytokines, and oxygen-derived radicals (142-145). Moreover, it has been reported that glucocorticoids stimulate synthesis and secretion of pulmonary surfactants (99, 146). PLs are part of the lubricating system in synovial joints, however not much is known about the impact of dexamethasone on PL metabolism. Hills *et al.* demonstrated that administration of glucocorticosteroids into the equine joint increases the quantity of PLs in SF (147) and proposed that improvement in joint mobility may be derived from improved lubrication. However, Hills *et al.* used DPPC as a standard for surfactant levels measurements. We have already mentioned that DPPC was found in human SF in small amounts (53). Our study aimed to investigate the effect of dexamethasone on the biosynthesis of various PLs.

Dexamethasone significantly decreased the biosynthesis of 11 PE species. Even though dexamethasone slightly decreased the biosynthesis of other PL classes, this did not reach statistical significance. However, in our screening experiment dexamethasone was found to be a more potent inhibitor in PL biosynthesis indicating interindividual differences

between results. Nevertheless, the observed trend was similar in both cases. We also have shown that the dexamethasone action was at least partly mediated through the glucocorticoid receptor. Blocking of the glucocorticoid receptor abolished dexamethasone effect on the biosynthesis of 1 PC specie and 4 PE species. According to current knowledge glucocorticoids act through two types of nuclear receptors: glucocorticoid receptor (GR, NR3C1) as well as mineralocorticoid receptor (MR, NR3C2) (148). Further analysis is needed to verify whether dexamethasone might also bind to MR in FLS to modulate PL biosynthesis.

Moreover, within human fetal lungs, dexamethasone significantly increased [^{3}H]-choline incorporation into PC (135). In our study of human FLS, dexamethasone decreased PL synthesis. This data indicate different effects of dexamethasone on PL synthesis depending on the cell type.

Dexamethasone inhibits synovial inflammation (149, 150). We have shown that IL-1β increases the biosynthesis of PE and PE-based plasmalogens. Here, we demonstrated that dexamethasone could abolish this effect. The biosynthesis of the same 11 PE species was upregulated by IL-1β and downregulated by dexamethasone (Appendix Table 9). This effect might be due to the cross-talk of dexamethasone and IL-1β in signalling transduction pathway NF-κB in synovium (150). In our experiments, we used relatively short time to study the effect of agents on the biosynthesis of PLs, however *in vivo* higher inhibitory effect of dexamethasone could be observed. Further studies are necessary to confirm this effect. Moreover, it has been reported that IGF-1 and dexamethasone together have greater beneficial effect than alone in preventing cytokine-induced cartilage degradation in human and bovine cartilage (151). It would be worth to investigate the combined effect of these agents on the PL biosynthesis.

We also compared PL species found to be altered in early OA SF (53) and found them to be opposite to those of FLS treated with dexamethasone. The biosynthesis of 9 PE species which were elevated during early OA was decreased by dexamethasone treatment (Appendix Table 10). This suggests a possible therapeutic use of dexamethasone in OA in order to balance PL composition.

In this study dexamethasone was found to be an inhibitor of PE and SM biosynthesis. PE is a precursor of molecules such as anandamide, *N*-palmitoylethanolamine, *N*-stearoylethanolamine, and DAG, which modulate pain perception, inflammation, autophagy,

and apoptosis (70, 117-120), while SM species and their metabolites such as ceramides and sphingosine play roles in cell signalling, apoptosis, and survival (84, 123).

In conclusion, decreased levels of PE and SM in FLS could prevent turning on NF-κB signalling transduction pathway (150), which is involved in the pathogenesis of OA and transcription of genes encoding pro-inflammatory mediators. Low levels of PE species could suppress the inflammation by inhibition of the expression of pro-inflammatory cytokines within synovial joint. Low levels of SM could prevent induction of apoptosis of chondrocytes in order to reduce cartilage loss. This could speak for the beneficial effect of dexamethasone on altered lipid metabolism during diseases such as OA. Additional experiments are required to confirm these effects.

5.2.4. Effect of adrenergic and cholinergic agonists on the biosynthesis of PLs

The pulmonary surfactant system has been intensively studied (101) but there is still not much known about the synovial joint lubricating system, especially surface-active PLs. Adrenergic and cholinergic agonists have been found to stimulate pulmonary surfactant production and release from alveolar type II cells (146, 152-155). In our study of FLS, we investigated the effect of adrenergic agonists such as terbutaline and epinephrine as well as cholinergic agonists such as carbachol and pilocarpine on the biosynthesis of PLs. Our data revealed that tested agents did not influence the biosynthesis of PLs by FLS. However, in the pulmonary surfactant system adrenergic agonists act directly on alveolar type II cells, which are responsible for the production and secretion of surfactants, as well as interstitial fibroblasts. Cholinergic agonists act indirectly on the lung surfactant synthesis and release by stimulation of the release of epinephrine by adrenal glands or by contraction of smooth muscle cells which in turn stimulate surfactant secretion (146). Taken together, we can conclude that the effects of adrenergic and cholinergic agonists are dependent on the cell type and, therefore, different mechanisms are involved in the biosynthesis of PLs within synovial joints and the lung.

5.2.5. Effect of inhibition of phospholipase A2 on the biosynthesis of PLs

The enzyme phospholipase hydrolyse PLs to liberate FAs (156). Angel *et al*. reported that blocking of phospholipase A2 activation with quinacrine abolished the IL-1β-induced

hydrolysis of PC and PE in synovial cells (102). Our data show that quinacrine increased the biosynthesis of PLs. We assume that inhibition of endogenous phospholipase A2 activity prevented the hydrolysis of PLs resulting in elevated percentage of labelled PC and PE. Thus, our data are consistent with those of the literature (102).

5.2.6. Effect of inhibition of choline kinase on the biosynthesis of PLs

In our study, we also investigated the effect of choline kinase (CK) inhibition on the biosynthesis of PLs. CK is an enzyme which can use both choline and ethanolamine as substrates in the first step of the Kennedy pathway. Several studies have shown that choline kinase can influence the rate of PC synthesis (70, 71). Another group reported that this enzyme is expressed in human RA synovial tissue, and that its inhibition decreases the severity of inflammation in arthritic mice (157). Our data revealed that choline kinase does not affect the rate of synthesis of any PL class. Therefore, we share the opinion with Gibellini *et al.* (70) and Fagone *et al.* (71) that choline kinase is not a rate-limiting step in the biosynthesis of PLs.

5.2.7. Effect of inhibition of choline transporter on the biosynthesis of PLs

The biosynthesis of PC begins from the uptake of extracellular choline into the cell, which is mediated by choline transporters (71). Thus, we investigated whether the inhibition of the high-affinity choline transporter 1 (CHT1) has an impact on the biosynthesis of PLs containing choline. Inhibition of CHT1 with hemicholinium-3 did not influence the biosynthesis of choline-based PLs, but unexpectedly increased the biosynthesis of ethanolamine-based PLs. Probably other choline transporters took over the complete choline uptake. Recently, Seki *et al.* reported about the expression of choline transporter-like protein 1 (CTL1) in RA FLS and choline uptake by this transporter (158). As expected, they observed an inhibition of choline uptake by hemicholinium-3. The increase in ethanolamine-based PLs synthesis in our cultured FLS might be caused by a switch of the cell metabolism to PE synthesis due to a disturbances in the choline uptake.

5.2.8. Effect of inhibition of sirtuins on the biosynthesis of PLs

Recently, several studies have investigated the role of sirtuins in OA (50, 103, 159). SIRT1 has a positive effect in maintaining cartilage homeostasis during OA. On the other hand, study on RA FLS showed that elevated SIRT1 contribute to chronic inflammation (160). Since sirtuins were found to regulate lipid metabolism (161), our research focus on their role in the biosynthesis of PLs by OA FLS. Treatment with sirtinol, which inhibits SIRT 1 and 2, at low concentration slightly increased the biosynthesis of PE and LPC, while at higher concentration the biosynthesis of more PL classes was enhanced. Interestingly, another sirtuin inhibitor, EX 527 combined with NAM, which blocks all sirtuins, caused a decrease in PC biosynthesis. However, EX 527 alone did not have an impact on the PL biosynthesis. Here we showed that different sirtuins inhibitors display different specificity. Sirtinol, which blocks SIRT1 and SIRT 2, enhanced the biosynthesis of PLs, while more potent inhibitor EX 527, which blocks all sirtuins, reduced the biosynthesis of PC. However, additional experiments are required to better understand the role of individual sirtuins on PL biosynthesis in human articular joints. Nevertheless, our data indicate that sirtuins are involved in the biosynthesis of PLs.

5.3. Release of PLs

PLs in SF are thought to derive from FLS and from blood by diffusion. However, there is not much known how the release of PLs into synovial joint cavity is controlled. Dobbie *et al.* provided an evidence of FLS activity in secreting PLs (109). Also, treatment with glucocorticosteroids has been reported to enhance the release of PLs into equine SF (147). One of the aims of this study was to investigate the release of PLs from FLS into the cell culture media.

We have developed a new *in vitro* model to study the release of PLs. Using radioactive isotope-labelled precursors of PLs allowed us to determine the release of two lipid fractions: choline-labelled PLs including PC, LPC, and SM and ethanolamine-labelled PLs including PE and PE-based plasmalogens. We have demonstrated that the release of both PL fractions is time-dependent. Moreover, the release of choline-labelled PLs is higher than ethanolamine-labelled PLs. This finding implicates that higher efflux of PLs based on choline can explain the high amount of PC found within human SF (53). However, the lipid secretion mechanism of FLS was not further investigated in our study.

The newly developed model already enabled us to show that tested agents seem to not stimulate the release of PLs into cell culture media. In our study we used a relatively short time to investigate the release of PLs. Further experiments are needed to show whether transporters or enzymes must be first activated to enhance the release of PLs. Kronqvist *et al.* (114) reported that IL-1β markedly increased efflux of SM and PC to lipid-free Apo A-I in human skin fibroblast. In our study, IL-1β and TNFα treatments in combination with low serum content and radioactive isotopes were found to be toxic for FLS. Even FLS cultured in medium containing higher amount of FBS displayed a changed rounded morphology. All other treatments did not change the morphology of cells. Apolipoprotein have been reported to induce PL efflux (162, 163), but in our study even the addition of apolipoprotein A-I and E4 did not enhance the release of PLs. Moreover IL-6, IGF-1 and TGF-β1 did not affect the release of PLs. In the pulmonary surfactant system, dexamethasone as well as cholinergic and adrenergic agonists have stimulated secretion of surfactant from alveolar type II cells (99, 101, 146). In our experiment using cultured FLS, none of these agents had an effect on PL release. Also, our results differ from those obtained *in vivo* by Hills *et al.* (147). In our study dexamethasone did not enhance the release of PLs into nutrient media. The divergence might be due to the species differences as well as applied methodology. Hills *et al.* used DPPC, which was found in small amounts in human SF, as a standard for surfactant levels measurements in equine SF. We investigated the release of [3H]-choline-labelled PLs fraction from cultured human FLS which includes PC, LPC, and SM.

5.4. Limitations

The great diversity of lipid structures and their characteristics is a challenge of any lipidomic study. In the last few years, the methods of lipid analysis were improved. ESI-MS/MS allows to identify and quantify hundreds of lipid molecules from a single biological sample (66). Stable isotope labelling is commonly used to investigate lipid metabolism (164). In our study, we have used only two stable isotopes namely [D9]-choline and [D4]-ethanolamine, which narrows the PL biosynthesis investigation to *de novo* synthesis of PC and PE, produced via the Kennedy pathway. Other PL classes such as SM, LPC, and PE-based plasmalogens were labelled indirectly, because they origin in our study from newly synthesized PC and PE. There are many cross-talks between the PL biosynthesis pathways. Thus, the interpretation of these data is difficult. For instance, PC can be also synthesized from PE, and PE can be also synthesized from PS. So, we do not know the amounts of PE and

PC generated from other PL classes. The addition of third and fourth stable isotopes, [D3]-serine and [D6]-*myo*-inositol, to the cell culture would allow us to measure also newly synthesized PS and PI, respectively. In our study, we did not focus on PL remodelling. This could be done by using stable isotope-labelled FAs. However, this approach would need to be established first. Nevertheless, our method allowed us to quantify over 40 newly synthesized PC and PE species, which is still a lot.

During the investigation of mechanisms underlying specific effects of IL-1β and IGF-1 on the biosynthesis of PLs, we have obtained unexpected results. Inhibition of p38 MAPK during IL-1β treatment enhanced PL biosynthesis. A similar effect was observed after inhibition of ERK during IGF-1 treatment. We can not make any final conclusions from these data, since the signalling pathways might be involved in the IL-1β- or IGF-1-induced PL synthesis or are just inhibitor specific effects. To verify that additional experiments containing proper controls as well as inhibitors alone are required.

We could also observe differences in PL detection between experiments. Especially during the screening biosynthesis experiment, the concentrations of labelled and unlabelled lipids were higher. This might be due to differences between patients as well as PL standards and conditions used during ESI-MS/MS measurements. To avoid misinterpretation, the most appropriate approach would be to compare data only within the same bench of samples. Nevertheless, data from different experiments display the same tendency.

In our release model, we have used two radioactive isotopes namely [^{3}H]-choline and [^{14}C]-ethanolamine, which allowed us to study the release of the PLs containing only choline or ethanolamine. Therefore, within the fraction containing choline-based PLs we were actually measuring [^{3}H]-labelled PC, SM, and LPC, while within fraction containing ethanolamine-based PLs we were measuring [^{14}C]-labelled PE and PE-based plasmalogens. TLC or HPLC techniques could be applied to separate individual PL classes from each sample. Also, using radioactive isotopes is laborious and hazardous. Therefore, we have undertaken an attempt to investigate the release of stable isotope-labelled PLs, but lipids found in the media were at low concentrations, far under the detection limit of ESI-MS/MS. Maybe in a few years this technology improves and will enable us to investigate the release of even PL species.

Our *in vitro* model of release may still need some optimization to measure release of PLs as modulated by cytokines like improvement of cell culture conditions. In the release

experiments IL-1β and TNFα were found to be toxic for cells, since we observed a more rounded morphology of originally spindle-shaped cells. Interestingly, IL-1β and TNFα did not influence the morphology of cells in our experiments using the biosynthesis model. However, it seems that these cytokines combined with low serum content and the presence of radioactive isotopes affected cells using the release model. Nevertheless, the increase of serum content in our release model only slightly improved altered morphology upon IL-1β and TNFα treatments, and most of the cells were still rounded. Therefore, the conditions in the release model for treatment with IL-1β and TNFα still need to be optimized. Also, the impact of IL-1β and TNFα on FLS viability and apoptosis in these conditions should be verified.

5.5. Summary

1. In this study, we have identified nine PL classes being present within FLS. The same classes were found in SF. PC is a major PL class for both FLS and SF. However, the diversity of PLs in FLS is greater.

2. We confirmed that non-proliferating, confluent FLS indeed synthesise PLs. We were able to measure the biosynthesis of 74 PL species belonging to five PL classes. The biosynthesis of PLs is highly correlated with time. Moreover, the PC biosynthesis and remodelling requires more time than PE biosynthesis. We assume that at least part of PL being present in SF derives from FLS.

3. Cytokines affect differently the biosynthesis of PLs. IL-1β induces the biosynthesis of PE and PE-based plasmalogen via NF-κB, p38 MAPK, and JNK pathways. Elevated levels of PE-based plasmalogen were also found in OA SF which might result in a protective effect of plasmalogens against cartilage damage. TNFα slightly induces the biosynthesis of PE, whereas IL-6 has no impact on the PL biosynthesis and release.

4. Growth factors affect differently the biosynthesis of PLs, mostly inducing the biosynthesis of PC, which indicates their beneficial effect on synovial joint lubrication. TGF-β1 and IGF-1 are more potent than BMPs. However, growth factors were found not to influence the release of PLs using our *in vitro* model.

5. Dexamethasone decreases the biosynthesis of PE and partly acts through the glucocorticoid receptor. We assume that, dexamethasone could inhibit the effect of IL-1β on PE biosynthesis. Moreover, dexamethasone does not influence PL release using our *in vitro* model.

6. Adrenergic and cholinergic agonists influence neither the biosynthesis nor release of PLs from FLS. This indicates that pulmonary surfactant system differs from the synovial joint lubricating system.

7. Inhibition of phospholipase A2 activity causes an increase of PL biosynthesis. We assume that blocking of phospholipase A2 activity could prevent the hydrolysis of PLs and thus results in a seemingly increased rate of PL synthesis.

8. Inhibition of high-affinity choline transporter CHT1 does not block the uptake of extracellular choline into the cell. We assume that other choline transporters took over the complete uptake of choline. Moreover, the activity of the choline kinase (CK) appears to be not a rate-limiting step in the PL biosynthesis via the Kennedy pathway.

9. We showed that sirtuins are involved in PL biosynthesis. Inhibition of SIRT1 and SIRT2 increases PL biosynthesis, whereas inhibition of all sirtuins decreases the biosynthesis of PC. Further studies are required to identify the roles of individual sirtuins in the biosynthesis of PLs in OA FLS.

10. The release of PLs is a time-dependent process. More PLs containing choline are released from FLS than PLs containing ethanolamine, which might partly explain the high amount of PC being found within human SF. Using our in *vitro model* to study PL release, we were not able to demonstrate that cytokines, growth factors, and pharmacological agents associated with OA influence the release of PLs from FLS. Further studies may be needed to optimize this model for studying PL release as modulated by cytokines.

5.6. Future perspectives

In this study, we investigated the PL biosynthesis and release of human FLS from OA patients. Our study revealed that biosynthesis of PLs is regulated by some cytokines such IL-

1β, as well as growth factors such as TGF-β1, IGF-1, and BMPs, which are present at elevated levels in OA SF. Nevertheless, more research on this topic need to be undertaken before we will fully understand the complex lipid metabolism within OA synovial joint.

First of all, further investigation should focus on the function of certain PL classes or even species. It is known that PC possess lubricating properties, and plasmalogens can act as antioxidants. Nevertheless, the functions of many lipids remain unknown. They can also act differently in various tissues. The synovial joint is a complex organ, thus we should not focus only on FLS. The function of PLs in other cell types such as chondrocytes, osteoblast, and macrophages should be also investigated. This knowledge could provide us with new targets and treatments for OA.

Also, we have only partly focused on the signalling pathways through which tested agents could act. This opens another important area of cell signalling research. Since we have obtained unexpected results after inhibition of p38 MAPK and ERK, the role of these signalling pathways in the biosynthesis of PLs should be determined. In our study, we showed the role of TGFβ receptor type I in the PC biosynthesis. Further investigations could focus on the activation of receptor-regulated SMAD proteins (SMAD2 and 3) and genes which are afterwards upregulated. This could give us a more detailed overview on TGF-β signalling in PL biosynthesis of FLS. Besides that, the non-canonical signalling pathways of IGF-1 signalling need to be also investigated.

In our study, we could observe some specific effects on the biosynthesis of PLs, especially during IL-1β, TGF-β1, IGF-1, and dexamethasone treatments. Since FLS are exposed to a mixture of cytokines and growth factors present within SF of articular joint, it would be worth to investigate the combined effects of these agents. For instance, growth factor or dexamethasone could reverse or block the effect of IL-1β. Additionally, Loeser *et al.* have shown that the combination of IGF-1 and BMP-7 resulted in a greater cartilage repair (49).

Finally, we still do not know how the release of PLs is regulated. One way to improve our *in vitro* release model would be to preload cells with labelled lipids or cholesterol. Several studies have investigated apolipoprotein-mediated efflux of PLs in lipid enriched cells (162, 163). The other idea would be to upregulate the lipid transporters. Maybe if they would be present in larger amounts, the efflux of PLs would be enhanced, and then we would be able to observe differences and thus investigate the effect of various agents on the release of PLs. The

last possibility would be the addition of other lipid transfer proteins such as phospholipid transfer protein (PLTP) or other apolipoproteins (for instance Apo B, C) to the cell culture. In the near future, also the ESI-MS/MS technology will be more advanced and maybe at that time we will be able to measure the release of even newly synthesized PL species into media.

Taken together, this study reported for the first time the composition of PLs being synthesized and released from human OA FLS using two newly developed *in vitro* models. Moreover, we showed that cytokines, growth factors and dexamethasone differently regulate the biosynthesis of PLs. Furthermore, similar PL species were elevated in OA SF as well as in OA FLS treated with IL-1β, TGF-β1, IGF-1, and BMPs. Our findings suggest that PL alterations of OA SF might derive at least partly from FLS influenced by mentioned factors, which are present at elevated levels in OA SF. Further studies concerning the effect of cytokines and growth factors on PL metabolism in human articular joints could help us to better understand the mechanism of OA pathogenesis and to find novel targets to treat OA. Also, our newly developed *in vitro* models can be further used to investigate the effects of other agents on the PL metabolism as well as to test possible new treatments for OA. The challenge of OA research includes the recognition of functions of individual PLs in humans, investigation of the signal transduction mechanism in PL metabolism, as well as finding novel targets to treat lipid-related disease mechanisms. Thus, lipidomics brings new perspectives to scientific research on OA.

6. APPENDIX

Appendix Table 1. PL background of the experimental media.
(see chapter 4.1.1. and 4.2.1.)

PL class	10% FBS medium	5% LPDS medium w/o L-serine [nmol/ml medium]	2% FBS medium
PC	14.56±0.31	1.11±0.01	2.56±0.07
PE	0.40±0.02	0.07±0.00	0.25±0.01
PE P	0.62±0.06	0.14±0.00	0.41±0.02
SM	5.64±0.06	0.16±0.00	1.04±0.04
LPC	5.05±0.02	3.66±0.02	0.77±0.03
Cer	0.12±0.00	0.01±0.00	0.05±0.00
PS	2.49±0.70	0.23±0.03	0.89±0.13
PI	1.16±0.14	0.39±0.01	0.37±0.11
PG	0.00±0.00	0.00±0.00	0.00±0.00

The quantitative values obtained for PL class were normalized to the volume of cell culture media and are expressed as nmol/ml of medium.
Data are presented as means ± SDs (n = 3).

Appendix Table 2. Time-dependent expression of reference genes from cultured FLS.
(see chapter 4.3.5. and 4.4.3.)

		10% FBS	5% LPDS		10% FBS	2% FBS	10% FBS	5% FBS
ACTB Ct value	**8 h**	21.0±0.4	20.2±0.6	**12 h**	20.1±0.3	20.8±0.4	26.1±0.5	25.6±1.9
	16 h	20.2±0.7	21.2±1.1	**24 h**	21.1±0.1	21.7±1.2	27.1±2.4	29.9±3.4
	24 h	21.1±0.1	21.6±0.8	**36 h**	20.4±1.3	21.1±1.1	26.3±0.9	30.5±2.4
B2M Ct value	**8 h**	22.8±0.4	22.1±0.9	**12 h**	21.9±0.8	22.2±0.6	29.0±0.7	27.8±2.3
	16 h	21.8±0.5	22.1±0.8	**24 h**	22.3±0.4	22.4±1.0	28.4±3.4	30.8±4.0
	24 h	22.3±0.4	22.7±0.6	**36 h**	22.2±0.08	22.3±1.0	27.3±1.0	31.0±2.5
GAPDH Ct value	**8 h**	27.3±0.5	26.8±1.4	**12 h**	26.2±0.5	26.8±0.9	35.2±0.8	33.4±2.8
	16 h	25.5±1.5	26.6±0.3	**24 h**	26.1±0.8	27.4±1.3	24.8±6.3	34.3±4.7
	24 h	26.1±0.8	27.0±1.0	**36 h**	26.4±1.0	26.8±0.8	32.5±2.9	37.5±1.8

The Ct values of reference genes of FLS cultured according to the methods used in the biosynthesis and release models were obtained from quantitative real-time PCR.
Data are presented as means ± SDs (n = 3).

Appendix Table 3. The concentrations of newly synthesized PL classes of FLS treated with various agents.
(see chapter 3.4.1. and 4.5.1.)

Treatment (n = 6)	[D9]-PC [nmol/mg]	[D4]-PE [nmol/mg]	[D4]-PE P [nmol/mg]	[D9]-SM [nmol/mg]	[D9]-LPC [nmol/mg]
control + 40 µl 5% trehalose	**13.3±6.10**	**8.16±2.32**	**2.25±0.52**	**0.25±0.09**	**0.07±0.04**
IL-1β (10 ng/ml)	12.6±5.34	10.6±2.14	2.80±0.42	0.24±0.09	0.06±0.03
TNFα (100 ng/ml)	15.1±5.06	10.8±1.92	2.29±0.35	0.26±0.06	0.06±0.03
IL-6 (10 ng/ml)	11.9±4.36	7.51±1.86	2.02±0.18	0.22±0.08	0.06±0.02
TGF-β1 (10 ng/ml)	15.4±5.88	8.82±3.77	2.20±0.67	0.30±0.11	0.08±0.03
IGF-I (100 ng/ml)	13.9±2.86	8.27±2.09	2.18±0.61	0.36±0.07	0.07±0.02
control + 20 µl 95% ethanol	**12.8±4.71**	**8.18±1.58**	**2.24±0.17**	**0.25±0.07**	**0.06±0.02**
Dexamethasone (10 µM)	10.7±3.07	6.56±2.43	2.10±0.42	0.16±0.06	0.08±0.03
control + 20 µl H_2O	**11.9±3.88**	**7.58±2.62**	**2.07±0.40**	**0.22±0.06**	**0.06±0.02**
Terbutaline (10 µM)	11.5±4.65	7.12±1.22	1.96±0.26	0.20±0.07	0.07±0.02
Epinephrine (10 µM)	11.3±4.26	7.16±1.35	1.99±0.11	0.20±0.06	0.08±0.03
Carbachol (10 µM)	12.1±5.74	7.72±2.76	2.06±0.60	0.22±0.09	0.08±0.04
Pilocarpine (10 µM)	12.5±4.91	8.41±3.66	2.15±0.71	0.24±0.09	0.09±0.04
Quinacrine (5 µM)	16.7±4.51	9.43±2.18	2.02±0.45	0.30±0.06	0.19±0.09
control + 20 µl DMSO	**15.6±4.27**	**9.21±1.95**	**2.87±0.33**	**0.29±0.06**	**0.07±0.02**
CK37 (10 µM)	16.0±5.09	7.55±2.25	2.81±0.46	0.31±0.09	0.08±0.03
CK 37 (5 µM)	14.1±4.64	7.81±2.62	2.32±0.50	0.28±0.08	0.07±0.03
control + 2 µl DMSO	**13.1±5.17**	**8.06±1.94**	**2.21±0.25**	**0.25±0.08**	**0.06±0.03**
CK37 (1 µM)	12.4±5.18	7.20±1.32	2.03±0.17	0.23±0.08	0.06±0.02
Sirtinol (1 µM)	14.2±4.08	9.02±3.19	2.48±0.55	0.27±0.07	0.09±0.03
Sirtinol (10 µM)	13.9±3.63	9.36±3.04	2.65±0.69	0.28±0.07	0.09±0.02
control + 100 µl H_2O	**10.5±3.41**	**6.67±1.32**	**1.84±0.25**	**0.19±0.04**	**0.05±0.01**
Hemicholinium-3 (50 µM)	12.3±4.92	7.72±2.26	2.30±0.52	0.23±0.08	0.08±0.03
Treatment (n = 5)	**[D9]-PC [nmol/mg]**	**[D4]-PE [nmol/mg]**	**[D4]-PE P [nmol/mg]**	**[D9]-SM [nmol/mg]**	**[D9]-LPC [nmol/mg]**
control + 40 µl 5% trehalose + 4 µl DMSO	**4.3±0.84**	**2.74±0.50**	**2.79±0.53**	**0.11±0.02**	**0.02±0.00**
EX 527 (1 µM)	4.4±0.73	3.02±0.54	2.59±0.29	0.10±0.01	0.02±0.00
EX 527 (50 µM) + NAM (10 mM)	3.6±1.34	2.85±0.75	2.48±0.34	0.09±0.03	0.02±0.01
control + 40 µl 5% trehalose	**3.5±0.72**	**2.07±0.47**	**2.28±0.46**	**0.08±0.01**	**0.02±0.00**
BMP-2 (100 ng/ml)	3.9±0.72	2.25±0.69	2.36±0.41	0.08±0.01	0.02±0.00
BMP-4 (100 ng/ml)	3.8±0.97	2.21±0.51	2.29±0.32	0.08±0.02	0.02±0.01
BMP-7 (100 ng/ml)	4.2±0.77	2.38±0.58	2.47±0.39	0.09±0.01	0.02±0.00

The quantitative values obtained for each stable isotope-labelled PL class were normalized to cellular protein content and are expressed as nmol/mg protein. Data are presented as means ± SDs (n = 5-6).

Appendix Table 4. The concentrations of newly synthesized PL classes of FLS treated with various agents.
(see chapter 3.4.2. and 4.5.2-5.)

Treatment	[D9]-PC [nmol/mg]	[D4]-PE [nmol/mg]	[D4]-PE P [nmol/mg]	[D9]-SM [nmol/mg]	[D9]-LPC [nmol/mg]
control	**3.74±1.05**	**2.66±0.34**	**2.62±0.30**	**0.08±0.02**	**0.02±0.00**
IL-1β (10 ng/ml)	4.19±1.14	3.84±0.36	3.29±0.36	0.10±0.02	0.02±0.00
IL-1β (10 ng/ml) + QNZ (10 μM)	3.56±1.06	2.93±0.23	2.33±0.21	0.09±0.02	0.02±0.01
IL-1β (10 ng/ml) + SB203580 (10 μM)	6.70±1.82	3.39±0.60	2.49±0.38	0.20±0.05	0.03±0.01
IL-1β (10 ng/ml) + SP600125 (10 μM)	3.87±1.15	2.99±0.34	2.56±0.51	0.09±0.03	0.02±0.00
control	**4.31±0.84**	**2.74±0.50**	**2.78±0.53**	**0.11±0.02**	**0.02±0.01**
TGF-β1 (10 ng/ml)	5.86±1.16	3.02±0.55	2.47±0.50	0.13±0.02	0.02±0.00
TGF-β1 (10 ng/ml) + SB432542 (10 μM)	4.19±0.82	2.56±0.46	2.15±0.34	0.12±0.02	0.02±0.00
IGF-1 (100 ng/ml)	5.06±1.06	2.84±0.50	2.39±0.34	0.14±0.03	0.02±0.00
IGF-1 (100 ng/ml) + LY294002 (10 μM)	5.28±1.25	2.63±0.45	2.68±0.31	0.12±0.02	0.02±0.01
IGF-1 (100 ng/ml) + SCH772984 (1 μM)	6.07±1.51	3.01±0.54	2.35±0.34	0.19±0.06	0.03±0.01
control	**4.57±0.82**	**2.90±0.55**	**2.76±0.32**	**0.10±0.01**	**0.02±0.00**
Dex (10 μM)	3.96±1.40	2.06±0.29	2.68±0.41	0.08±0.02	0.02±0.01
Dex (10 μM) + RU 486 (1 μM)	4.54±1.37	2.26±0.42	3.00±0.39	0.09±0.02	0.03±0.01

The quantitative values obtained for each stable isotope-labelled PL class were normalized to cellular protein content and are expressed as nmol/mg protein. Data are presented as means ± SDs (n = 5).

Appendix Table 5. Effect of IL-1β on newly synthesized PL species.
(see chapter 3.4.2. and 4.5.2.)

Species	control			IL-1β			IL-1β + QNZ	IL-1β + SB203580	IL-1β + SP600125
	[pmol/mg]	% lab. PL	Fold of change	[pmol/mg]	% lab. PL	Fold of change	Fold of change	Fold of change	Fold of change
PC 30:0	41±13	3.7±1.1	1.0	50±14	4.1±1.2	1.1±0.1	1.2±0.1	**2.2±0.3**	**1.2±0.1**
PC 32:0	431±145	5.4±1.5	1.0	565±193	6.1±1.7	**1.1±0.1**	**1.0±0.1**	**1.7±0.2**	1.1±0.1
PC 34:0	54±21	4.8±1.5	1.0	95±42	6.7±2.1	**1.4±0.2**	1.1±0.1	**2.6±0.2**	1.5±0.2
PC 32:1	135±34	4.7±1.4	1.0	165±40	5.6±1.7	**1.2±0.1**	1.1±0.1	**1.9±0.2**	1.2±0.1
PC 34:1	677±151	4.6±1.5	1.0	757±168	4.9±1.7	1.1±0.1	**1.0±0.1**	**1.9±0.1**	1.1±0.1
PC 36:1	170±29	2.9±1.0	1.0	211±40	3.6±1.3	**1.3±0.2**	**1.1±0.0**	**1.9±0.2**	1.2±0.1
PC 34:2	309±74	7.4±2.0	1.0	386±97	7.7±2.1	1.0±0.0	1.0±0.1	**1.9±0.2**	1.1±0.1
PC 36:2	250±48	4.3±1.4	1.0	300±64	4.6±1.5	1.1±0.2	1.0±0.1	**2.0±0.2**	1.1±0.1
PC 34:3	36±05	9.7±2.1	1.0	44±9	10.7±2.7	1.1±0.1	1.1±0.1	**1.7±0.2**	1.1±0.1
PC 36:3	170±54	5.6±1.9	1.0	200±56	5.7±1.8	1.0±0.1	1.0±0.1	**2.2±0.2**	1.1±0.1
PC 38:3	66±22	3.9±1.2	1.0	77±23	4.7±1.5	1.2±0.2	**1.0±0.2**	**1.8±0.2**	1.2±0.2
PC 36:4	301±127	4.9±1.1	1.0	291±121	4.4±1.0	0.9±0.1	0.9±0.1	**2.1±0.2**	0.9±0.1
PC 38:4	376±172	4.1±1.1	1.0	330±137	4.2±1.1	1.0±0.2	0.9±0.1	**1.9±0.3**	1.0±0.1
PC 40:4	32±12	6.5±2.3	1.0	33±11	7.3±2.3	1.1±0.2	**1.0±0.1**	**1.7±0.3**	1.3±0.2
PC 36:5	42±14	5.9±1.3	1.0	39±13	5.1±1.0	0.9±0.1	0.9±0.0	**2.1±0.3**	0.9±0.1
PC 38:5	226±100	5.3±1.5	1.0	194±69	5.1±1.2	1.0±0.2	0.9±0.1	**1.9±0.2**	1.0±0.2
PC 40:5	47±15	5.8±1.7	1.0	47±16	6.6±2.2	1.1±0.1	**0.9±0.1**	**1.5±0.2**	1.1±0.1
PC 38:6	59±19	4.3±1.0	1.0	58±21	3.7±1.1	0.9±0.1	0.8±0.1	**1.8±0.2**	0.8±0.2
PC 40:6	35±10	5.2±1.2	1.0	30±9	4.6±1.2	0.9±0.1	0.9±0.2	**1.5±0.1**	0.9±0.1
SM 34:0	3±1	0.4±0.1	1.0	4±2	0.5±0.3	1.2±0.6	3.4±2.3	3.8±2.7	1.8±0.8
SM 32:1	5±1	1.2±0.2	1.0	5±1	1.2±0.2	1.0±0.1	1.0±0.1	**1.6±0.1**	1.1±0.1
SM 33:1	4±1	0.7±0.1	1.0	5±1	0.8±0.1	1.2±0.3	1.1±0.2	**1.6±0.2**	1.1±0.2
SM 34:1	39±11	0.3±0.1	1.0	52±13	0.4±0.1	**1.4±0.2**	**1.0±0.1**	**2.6±0.4**	1.3±0.1
SM 36:1	3±2	0.3±0.2	1.0	5±2	0.3±0.1	0.9±0.6	0.8±0.6	2.1±1.8	0.8±0.6
SM 42:1	5±2	0.2±0.1	1.0	6±1	0.3±0.1	1.5±0.7	1.5±0.5	**3.2±1.7**	1.3±0.7
SM 34:2	4±1	1.2±0.4	1.0	4±1	1.1±0.3	1.0±0.2	1.0±0.2	**1.8±0.5**	1.1±0.2
SM 35:2	6±1	0.8±0.1	1.0	7±1	1.0±0.1	1.2±0.1	1.1±0.2	**1.5±0.2**	1.2±0.2
SM 36:2	2±1	1.5±0.4	1.0	3±1	1.9±0.2	**1.4±0.3**	1.1±0.5	**2.5±0.9**	1.5±0.5
SM 42:2	7±3	0.3±0.1	1.0	9±2	0.4±0.0	**1.5±0.3**	1.5±0.5	**3.4±1.2**	1.2±0.4
PE 34:1	122±2	11.2±1.8	1.0	182±44	16.0±1.3	**1.5±0.2**	**1.2±0.1**	1.4±0.1	**1.2±0.1**
PE 36:1	99±47	6.7±1.4	1.0	147±63	9.5±1.4	**1.4±0.2**	**1.1±0.1**	1.5±0.2	1.3±0.2
PE 34:2	38±15	15.7±2.4	1.0	64±17	22.1±1.4	**1.4±0.1**	**1.1±0.1**	**1.3±0.1**	**1.2±0.1**
PE 36:2	93±31	10.3±1.8	1.0	143±32	15.0±0.7	**1.5±0.2**	**1.2±0.1**	1.3±0.1	**1.2±0.1**
PE 36:3	40±10	16.1±3.1	1.0	63±7	22.1±2.3	**1.4±0.2**	1.2±0.1	1.3±0.2	**1.2±0.1**
PE 38:3	171±13	13.2±1.3	1.0	234±23	17.6±2.0	**1.3±0.1**	**1.0±0.1**	**1.1±0.2**	**1.2±0.1**
PE 36:4	35±9	11.6±1.9	1.0	56±9	17.2±2.5	**1.5±0.2**	**1.2±0.1**	**1.2±0.2**	**1.2±0.2**
PE 38:4	656±97	8.1±1.1	1.0	871±83	10.6±1.2	**1.3±0.2**	**1.0±0.1**	**1.1±0.1**	**1.1±0.1**
PE 40:4	270±23	16.5±2.0	1.0	382±44	21.6±2.6	**1.3±0.1**	**1.0±0.1**	1.2±0.1	1.2±0.1

Continuation of Appendix Table 5. Effect of IL-1β on newly synthesized PL species.

(see chapter 3.4.2. and 4.5.2.)

Species	control			IL-1β			IL-1β + QNZ	IL-1β + SB203580	IL-1β + SP600125
	[pmol/mg]	% lab. PL	Fold of change	[pmol/mg]	% lab. PL	Fold of change	Fold of change	Fold of change	Fold of change
PE 38:5	276±42	12.7±1.5	1.0	374±41	17.2±1.8	**1.4±0.2**	**1.0±0.1**	**1.0±0.2**	**1.1±0.1**
PE 40:5	297±52	18.1±2.1	1.0	415±96	23.5±3.2	**1.3±0.3**	**1.0±0.1**	1.3±0.1	1.1±0.1
PE 38:6	234±63	25.8±4.7	1.0	412±66	35.5±2.4	**1.4±0.2**	**1.2±0.1**	**1.1±0.1**	**1.2±0.2**
PE 40:6	326±53	20.8±3.1	1.0	499±91	27.2±2.4	**1.3±0.1**	**1.1±0.1**	**1.2±0.1**	**1.2±0.1**
PE P 16:0/18:1	44±16	2.9±0.4	1.0	60±121	4.0±0.6	**1.4±0.2**	**1.0±0.4**	1.2±0.2	1.2±0.3
PE P 16:0/20:4	364±78	4.2±0.4	1.0	477±105	5.5±1.1	1.3±0.3	**0.9±0.1**	**0.8±0.2**	**1.0±0.1**
PE P 16:0/22:4	147±21	8.4±1.0	1.0	205±16	11.5±1.5	**1.4±0.3**	1.1±0.1	1.2±0.2	1.2±0.1
PE P 16:0/22:5	134±26	8.8±1.1	1.0	192±66	11.7±1.9	1.4±0.3	1.0±0.1	**1.0±0.2**	1.1±0.1
PE P 16:0/22:6	128±23	8.0±0.9	1.0	187±16	11.2±0.4	**1.4±0.1**	**1.0±0.1**	**0.9±0.1**	**1.2±0.2**
PE P 18:1/16:0	70±12	8.5±2.2	1.0	91±6	11.0±0.7	1.4±0.4	**1.0±0.2**	1.1±0.3	1.2±0.1
PE P 18:1/18:1	55±13	7.8±1.4	1.0	55±12	8.4±1.5	1.1±0.2	1.0±0.1	1.1±0.2	1.1±0.3
PE P 18:1/20:4	577±77	11.2±0.7	1.0	640±66	12.9±0.5	**1.2±0.1**	**1.0±0.0**	**0.9±0.1**	**1.0±0.1**
PE P 18:1/20:5	58±14	14.6±0.8	1.0	72±15	17.7±2.7	1.2±0.2	**1.0±0.2**	1.1±0.1	1.2±0.2
PE P 18:1/22:4	87±14	16.2±4.0	1.0	91±10	16.3±1.9	1.1±0.3	0.9±0.1	1.1±0.3	1.0±0.2
PE P 18:1/22:5	83±23	16.1±2.1	1.0	97±19	18.1±2.0	1.1±0.2	1.0±0.1	1.1±0.2	**0.9±0.1**
PE P 18:1/22:6	89±12	12.3±1.4	1.0	113±12	14.4±1.8	1.2±0.2	1.1±0.1	**1.0±0.1**	1.1±0.1
PE P 18:0/16:0	44±6	13.0±2.1	1.0	73±7	19.0±3.8	**1.5±0.3**	**0.9±0.1**	1.3±0.2	**1.1±0.1**
PE P 18:0/18:1	36±8	4.1±0.4	1.0	38±7	4.6±0.7	1.1±0.1	1.1±0.2	**0.9±0.2**	1.0±0.1
PE P 18:0/20:4	398±85	3.5±0.7	1.0	488±95	4.3±0.9	**1.2±0.1**	**0.9±0.1**	**0.8±0.1**	**1.0±0.1**
PE P 18:0/20:5	48±14	5.6±0.8	1.0	56±13	6.2±0.7	1.1±0.2	1.0±0.2	**0.8±0.2**	1.1±0.2
PE P 18:0/22:4	76±15	6.0±1.4	1.0	116±12	8.9±1.7	**1.5±0.3**	**1.1±0.3**	1.3±0.3	**1.2±0.2**
PE P 18:0/22:5	98±19	7.2±1.8	1.0	119±39	8.5±1.7	1.2±0.3	**0.9±0.2**	1.0±0.3	1.0±0.3
PE P 18:0/22:6	84±11	5.3±1.1	1.0	118±15	7.0±1.5	**1.3±0.2**	1.1±0.2	**1.0±0.2**	1.1±0.3

The quantitative values obtained for each stable isotope-labelled PL species were normalized to cellular protein content and are expressed as pmol/mg protein. For each PL specie the percentage of stable isotope-labelled PL from total labelled and unlabelled PL was calculated. The percentages of stable isotope-labelled species were then calculated as a ratio of corresponding untreated control (=1). Bold data represent significantly altered x-fold of changes with $P \leq 0.05$. Data are presented as means ± SDs of these ratios (n = 5).

Appendix Table 6. Effect of TGF-β1 on newly synthesized PL species.
(see chapter 3.4.2. and 4.5.3.)

Species	control			TGF-β1			TGF-β1 + SB432542
	[pmol/mg]	% lab. PL	Fold of change	[pmol/mg]	% lab. PL	Fold of change	Fold of change
PC 30:0	46±16	4.3±1.4	1.0	73±21	6.6±1.6	**1.6±0.5**	**1.0±0.3**
PC 32:0	426±105	5.7±1.2	1.0	584±200	8.6±2.3	**1.5±0.2**	**0.9±0.1**
PC 34:0	59±22	5.4±1.5	1.0	82±36	8.4±2.4	**1.6±0.3**	**1.1±0.1**
PC 32:1	148±27	5.1±0.9	1.0	267±60	8.8±2.3	**1.8±0.4**	**1.0±0.1**
PC 34:1	812±142	5.3±1.3	1.0	1189±205	8.0±2.3	**1.5±0.2**	**1.0±0.1**
PC 36:1	208±33	3.3±0.7	1.0	255±42	4.3±0.9	**1.3±0.1**	**1.1±0.1**
PC 34:2	332±58	8.0±1.6	1.0	527±101	12.4±2.8	**1.5±0.2**	**1.1±0.1**
PC 36:2	315±27	5.2±1.4	1.0	438±64	7.5±2.1	**1.5±0.2**	**1.1±0.1**
PC 34:3	37±6	10.0±2.3	1.0	74±25	16.6±3.9	**1.7±0.4**	**1.1±0.1**
PC 36:3	210±37	7.0±1.8	1.0	309±67	10.6±2.6	**1.5±0.3**	**1.1±0.0**
PC 38:3	78±25	4.3±1.0	1.0	88±24	5.4±1.1	**1.3±0.2**	1.1±0.1
PC 36:4	350±122	5.9±0.7	1.0	435±145	8.3±0.9	**1.4±0.1**	1.2±0.1
PC 38:4	448±182	4.6±0.8	1.0	506±194	5.9±0.8	**1.3±0.1**	**1.2±0.1**
PC 40:4	35±12	6.3±1.6	1.0	39±12	8.3±2.0	**1.3±0.2**	1.1±0.1
PC 36:5	43±12	6.5±1.1	1.0	60±15	9.8±1.2	**1.5±0.2**	**1.3±0.1**
PC 38:5	282±93	6.5±1.2	1.0	337±105	9.0±1.3	**1.4±0.1**	**1.1±0.1**
PC 40:5	54±15	5.7±1.2	1.0	62±17	7.6±1.4	**1.3±0.1**	**1.1±0.0**
PC 38:6	65±18	5.5±1.1	1.0	83±19	8.5±1.2	**1.6±0.4**	**1.2±0.2**
PC 40:6	42±15	5.6±1.4	1.0	49±12	7.6±1.4	**1.4±0.2**	**1.1±0.2**
SM 34:0	5±2	0.5±0.2	1.0	6±2	0.7±0.2	1.4±0.5	1.1±1.0
SM 32:1	6±1	1.3±0.2	1.0	6±0	1.5±0.2	1.2±0.2	1.1±0.1
SM 33:1	5±2	0.8±0.2	1.0	5±1	0.9±0.2	1.2±0.4	1.0±0.3
SM 34:1	54±10	0.4±0.0	1.0	69±17	0.5±0.1	1.3±0.3	1.2±0.1
SM 36:1	4±2	0.3±0.1	1.0	6±1	0.4±0.1	1.6±0.7	1.5±0.7
SM 42:1	8±3	0.3±0.1	1.0	8±2	0.3±0.1	1.1±0.1	1.1±0.3
SM 34:2	5±1	1.4±0.2	1.0	5±1	1.5±0.3	1.1±0.2	1.0±0.2
SM 35:2	6±1	0.8±0.1	1.0	7±1	1.0±0.2	1.2±0.2	1.2±0.1
SM 36:2	3±1	1.8±0.3	1.0	4±1	2.4±0.4	**1.3±0.2**	**0.9±0.2**
SM 42:2	10±4	0.4±0.1	1.0	16±4	0.6±0.2	1.7±1.0	1.3±0.2
PE P 16:0/18:1	57±26	3.8±0.4	1.0	48±20	3.4±0.3	0.9±0.1	**0.8±0.1**
PE P 16:0/20:4	360±97	4.1±0.7	1.0	304±105	3.6±0.9	0.9±0.1	**0.7±0.1**
PE P 16:0/22:4	158±34	8.8±1.6	1.0	143±38	8.5±2.0	1.0±0.2	0.9±0.1
PE P 16:0/22:5	145±47	9.0±1.8	1.0	152±53	9.4±1.7	1.1±0.1	**0.8±0.1**
PE P 16:0/22:6	137±34	8.8±1.5	1.0	131±28	8.6±1.1	1.0±0.1	**0.7±0.1**
PE P 18:1/16:0	80±9	9.8±1.7	1.0	75±19	9.1±2.7	0.9±0.2	0.7±0.1
PE P 18:1/18:1	61±20	9.1±1.0	1.0	61±23	9.1±1.5	1.0±0.2	0.9±0.2
PE P 18:1/20:4	575±105	11.3±1.2	1.0	515±94	10.4±0.9	0.9±0.1	0.9±0.1
PE P 18:1/20:5	62±22	15.6±3.6	1.0	59±13	15.4±3.6	1.0±0.2	1.0±0.3

Continuation of Appendix Table 6. Effect of TGF-β1 on newly synthesized PL species.
(see chapter 3.4.2. and 4.5.3.)

Specie	control			TGF-β1			TGF-β1 + SB432542
	[pmol/mg]	% lab. PL	Fold of change	[pmol/mg]	% lab. PL	Fold of change	Fold of change
PE P 18:1/22:4	86±15	14.8±1.8	1.0	96±12	16.7±1.2	**1.1±0.1**	1.1±0.1
PE P 18:1/22:5	89±23	16.6±3.1	1.0	89±25	16.5±1.8	1.0±0.2	1.0±0.1
PE P 18:1/22:6	108±31	14.3±3.1	1.0	88±10	12.0±1.6	0.9±0.2	0.9±0.1
PE P 18:0/16:0	45±13	12.7±4.1	1.0	40±10	13.2±4.8	1.1±0.2	1.0±0.2
PE P 18:0/18:1	40±14	4.9±0.8	1.0	37±8	4.8±1.0	1.0±0.3	0.8±0.1
PE P 18:0/20:4	438±112	3.7±0.8	1.0	341±84	3.1±0.7	0.9±0.2	0.8±0.1
PE P 18:0/20:5	61±31	7.2±2.8	1.0	44±11	5.3±0.4	0.8±0.3	0.8±0.2
PE P 18:0/22:4	96±22	7.0±1.9	1.0	87±16	7.0±1.2	1.0±0.3	0.9±0.2
PE P 18:0/22:5	94±35	6.5±1.8	1.0	80±19	6.1±1.5	1.0±0.2	0.9±0.1
PE P 18:0/22:6	94±18	5.8±0.9	1.0	77±10	5.3±1.1	**0.9±0.1**	**0.7±0.1**
PE 34:1	132±63	12.4±2.1	1.0	160±63	13.7±2.6	1.1±0.2	1.0±0.1
PE 36:1	117±66	7.9±1.3	1.0	120±62	7.9±1.9	1.0±0.2	1.0±0.1
PE 34:2	33±14	15.1±3.0	1.0	51±22	18.7±3.5	1.3±0.4	1.1±0.1
PE 36:2	108±48	12.3±2.3	1.0	140±62	14.0±2.7	1.1±0.2	0.9±0.1
PE 36:3	42±10	17.9±1.6	1.0	69±28	22.2±4.1	**1.2±0.3**	1.1±0.1
PE 38:3	180±29	13.6±2.5	1.0	198±36	14.4±2.3	1.1±0.2	1.0±0.1
PE 36:4	39±13	13.0±3.1	1.0	45±9	14.4±3.4	1.1±0.3	1.0±0.2
PE 38:4	684±93	8.4±1.6	1.0	755±103	9.0±1.9	1.1±0.21	0.9±0.1
PE 40:4	301±54	18.3±3.7	1.0	282±40	17.3±3.6	0.9±0.1	0.9±0.1
PE 38:5	268±67	12.6±2.6	1.0	318±68	14.0±3.2	1.1±0.2	0.9±0.0
PE 40:5	301±62	18.2±2.2	1.0	324±53	19.0±3.4	1.0±0.1	1.0±0.0
PE 38:6	189±48	24.3±3.6	1.0	235±49	26.6±4.2	1.1±0.1	0.9±0.1
PE 40:6	348±43	21.4±3.2	1.0	328±37	20.1±3.2	0.9±0.1	1.0±0.1

The quantitative values obtained for each stable isotope-labelled PL species were normalized to cellular protein content and are expressed as pmol/mg protein. For each PL specie the percentage of stable isotope-labelled PL from total labelled and unlabelled PL was calculated. The percentages of stable isotope-labelled species were then calculated as a ratio of corresponding untreated control (=1). Bold data represent significantly altered x-fold of changes with $P \leq 0.05$. Data are presented as means ± SDs of these ratios (n = 5).

Appendix Table 7. Effect of IGF-1 on newly synthesized PL species.
(see chapter 3.4.2. and 4.5.4.)

Species	control			IGF-1			IGF-1 + LY294002	IGF-1 + SCH772984
	[pmol/mg]	% lab. PL	Fold of change	[pmol/mg]	% lab. PL	Fold of change	Fold of change	Fold of change
PC 30:0	46±16	4.3±1.4	1.0	56±13	5.3±1.3	1.3±0.3	1.2±0.2	**1.6±0.3**
PC 32:0	426±105	5.7±1.2	1.0	477±137	7.0±1.3	**1.2±0.2**	1.2±0.1	**1.4±0.2**
PC 34:0	59±22	5.4±1.5	1.0	65±27	6.6±1.5	**1.3±0.1**	1.3±0.1	**1.6±0.2**
PC 32:1	148±27	5.1±0.9	1.0	193±24	6.8±1.5	**1.3±0.1**	**1.2±0.1**	**1.7±0.2**
PC 34:1	812±142	5.3±1.3	1.0	1036±120	7.1±2.0	**1.3±0.1**	**1.2±0.1**	**1.7±0.2**
PC 36:1	208±33	3.3±0.7	1.0	230±26	4.0±1.0	**1.2±0.1**	1.3±0.1	**1.5±0.2**
PC 34:2	332±58	8.0±1.6	1.0	419±67	10.3±2.3	**1.3±0.1**	1.2±0.1	**1.5±0.2**
PC 36:2	315±27	5.2±1.4	1.0	379±52	6.4±1.7	**1.2±0.1**	1.2±0.1	**1.6±0.2**
PC 34:3	37±6	10.0±2.3	1.0	46±7	12.5±2.4	**1.3±0.1**	1.2±0.1	**1.6±0.2**
PC 36:3	210±37	7.0±1.8	1.0	254±72	9.1±2.8	**1.3±0.1**	**1.2±0.0**	**1.6±0.1**
PC 38:3	78±25	4.3±1.0	1.0	87±22	5.6±1.2	**1.3±0.1**	1.3±0.2	1.5±0.3
PC 36:4	350±122	5.9±0.7	1.0	428±167	7.8±1.3	**1.3±0.1**	**1.2±0.1**	**1.6±0.2**
PC 38:4	448±182	4.6±0.8	1.0	479±190	5.7±0.9	**1.2±0.1**	1.3±0.1	**1.5±0.2**
PC 40:4	35±12	6.3±1.6	1.0	33±9	7.6±1.6	1.2±0.2	**1.5±0.1**	1.3±0.2
PC 36:5	43±12	6.5±1.1	1.0	51±16	8.9±1.3	**1.4±0.2**	1.3±0.1	**1.6±0.2**
PC 38:5	282±93	6.5±1.2	1.0	302±105	8.1±1.5	**1.2±0.1**	1.2±0.1	**1.5±0.2**
PC 40:5	54±15	5.7±1.2	1.0	51±15	6.7±1.5	**1.2±0.1**	**1.4±0.1**	**1.4±0.2**
PC 38:6	65±18	5.5±1.1	1.0	68±24	7.3±1.6	**1.3±0.1**	1.4±0.2	**1.6±0.2**
PC 40:6	42±15	5.6±1.4	1.0	42±13	6.8±1.4	1.2±0.2	1.3±0.2	**1.4±0.3**
SM 34:0	5±2	0.5±0.2	1.0	7±3	0.8±0.3	1.5±0.7	1.5±0.6	**2.6±1.3**
SM 32:1	6±1	1.3±0.2	1.0	6±1	1.5±0.3	1.2±0.3	1.2±0.3	1.3±0.3
SM 33:1	5±2	0.8±0.2	1.0	4±1	0.8±0.1	1.1±0.3	1.1±0.3	**1.4±0.3**
SM 34:1	54±10	0.4±0.0	1.0	70±17	0.5±0.1	**1.4±0.3**	**1.2±0.2**	**1.8±0.4**
SM 36:1	4±2	0.3±0.1	1.0	7±2	0.5±0.1	2.2±1.4	1.5±0.9	2.8±1.6
SM 42:1	8±3	0.3±0.1	1.0	12±2	0.5±0.1	**1.7±0.4**	1.1±0.4	2.1±0.8
SM 34:2	5±1	1.4±0.2	1.0	5±1	1.6±0.4	1.2±0.3	1.0±0.2	1.3±0.4
SM 35:2	6±1	0.8±0.1	1.0	9±2	1.2±0.1	**1.5±0.2**	**1.2±0.1**	1.5±0.3
SM 36:2	3±1	1.8±0.3	1.0	3±1	2.0±0.3	1.1±0.2	1.0±0.2	**1.3±0.2**
SM 42:2	10±4	0.4±0.1	1.0	18±6	0.7±0.1	**1.9±0.7**	1.4±0.5	**3.1±1.2**

The quantitative values obtained for each stable isotope-labelled PL species were normalized to cellular protein content and are expressed as pmol/mg protein. For each PL specie the percentage of stable isotope-labelled PL from total labelled and unlabelled PL was calculated. The percentages of stable isotope-labelled species were then calculated as a ratio of corresponding untreated control (=1). Bold data represent significantly altered x-fold of changes with $P \leq 0.05$. Data are presented as means ± SDs of these ratios (n = 5).

Appendix Table 8. Effect of dexamethasone on newly synthesized PL species.
(see chapter 3.4.2. and 4.5.5.)

Species	control			Dex			Dex + RU 486
	[pmol/mg]	% lab. PL	Fold of change	[pmol/mg]	% lab.PL	Fold of change	Fold of change
PC 30:0	48±10	4.8±0.7	1.0	35±12	3.7±1.0	**0.8±0.1**	**0.9±0.1**
PC 32:0	438±102	6.4±0.9	1.0	344±135	5.6±1.7	0.9±0.2	**1.0±0.1**
PC 34:0	59±11	6.3±1.1	1.0	43±20	5.1±1.8	0.8±0.3	1.0±0.3
PC 32:1	158±10	5.7±0.8	1.0	119±39	4.6±1.5	0.8±0.2	**0.9±0.1**
PC 34:1	861±90	6.0±1.4	1.0	726±206	5.3±2.1	0.9±0.2	**0.9±0.1**
PC 36:1	218±23	3.8±0.8	1.0	189±25	3.3±1.2	0.9±0.1	**1.0±0.1**
PC 34:2	358±34	9.0±1.7	1.0	275±88	7.6±2.6	0.8±0.2	**1.0±0.1**
PC 36:2	332±31	5.8±1.4	1.0	278±65	5.3±1.9	0.9±0.2	**1.0±0.1**
PC 34:3	39±5	10.9±1.2	1.0	28±8	9.4±3.0	0.8±0.2	0.9±0.1
PC 36:3	218±43	7.8±1.8	1.0	173±69	6.9±2.7	0.9±0.2	1.0±0.1
PC 38:3	84±24	4.9±0.7	1.0	82±31	5.0±1.5	1.0±0.2	1.0±0.2
PC 36:4	394±133	6.9±0.7	1.0	366±168	6.1±1.3	0.9±0.1	**1.0±0.1**
PC 38:4	482±186	5.3±0.7	1.0	474±246	5.1±1.5	1.0±0.2	1.0±0.1
PC 40:4	40±14	7.7±1.7	1.0	37±17	7.1±2.4	0.9±0.2	**1.0±0.2**
PC 36:5	52±17	8.0±1.6	1.0	46±19	7.5±1.4	0.9±0.1	0.9±0.1
PC 38:5	284±94	7.2±1.0	1.0	267±137	6.8±2.2	0.9±0.2	1.0±0.2
PC 40:5	60±19	7.0±1.6	1.0	58±29	6.7±2.6	0.9±0.2	1.0±0.2
PC 38:6	69±21	6.5±1.3	1.0	55±26	5.6±1.8	0.8±0.1	**0.9±0.1**
PC 40:6	42±15	6.1±1.3	1.0	39±20	5.7±1.9	0.9±0.1	**1.0±0.1**
SM 34:0	3±2	0.3±0.2	1.0	2±2	0.2±0.2	0.7±0.6	1.0±0.3
SM 32:1	5±1	1.2±0.1	1.0	5±1	1.4±0.2	1.1±0.2	1.0±0.1
SM 33:1	5±1	0.9±0.2	1.0	4±1	0.8±0.1	**0.9±0.1**	0.8±0.2
SM 34:1	54±8	0.4±0.0	1.0	37±11	0.3±0.0	**0.7±0.1**	**0.8±0.1**
SM 36:1	5±2	0.4±0.2	1.0	5±1	0.4±0.1	1.1±0.5	0.8±0.4
SM 42:1	8±2	0.3±0.0	1.0	7±1	0.3±0.1	0.8±0.2	0.9±0.2
SM 34:2	4±0	1.3±0.2	1.0	3±1	1.2±0.3	0.9±0.2	0.9±0.1
SM 35:2	7±1	1.0±0.3	1.0	9±2	1.3±0.7	1.2±0.2	1.0±0.1
SM 36:2	3±1	2.1±0.6	1.0	2±0	1.5±0.1	**0.8±0.1**	0.8±0.3
SM 42:2	12±4	0.5±0.1	1.0	6±2	0.2±0.1	**0.5±0.3**	0.9±0.2
PE 34:1	129±54	13.3±1.4	1.0	70±22	8.9±1.8	**0.7±0.1**	**0.8±0.1**
PE 36:1	122±67	8.8±1.3	1.0	83±31	6.8±1.5	**0.8±0.1**	**0.9±0.1**
PE 34:2	37±16	17.4±1.4	1.0	18±8	12.2±4.2	**0.7±0.2**	0.8±0.1
PE 36:2	108±42	13.3±1.9	1.0	66±19	9.9±1.8	**0.7±0.1**	0.8±0.1
PE 36:3	46±13	20.8±2.8	1.0	26±8	15.5±3.5	**0.7±0.1**	0.8±0.1
PE 38:3	208±42	16.1±1.9	1.0	155±19	13.0±1.7	0.8±0.1	**0.9±0.1**
PE 36:4	42±9	14.4±1.6	1.0	26±07	10.7±2.0	**0.7±0.1**	0.8±0.1
PE 38:4	722±134	9.4±1.4	1.0	558±125	7.7±1.1	**0.8±0.1**	0.9±0.1
PE 40:4	303±56	19.2±2.2	1.0	258±16	17.0±2.1	0.9±0.1	**1.0±0.1**
PE 38:5	288±67	14.7±2.6	1.0	183±54	10.8±2.3	**0.7±0.1**	0.8±0.1
PE 40:5	324±67	20.7±1.5	1.0	249±33	17.5±1.8	**0.8±0.1**	0.9±0.0

Continuation of Appendix Table 8. Effect of dexamethasone on newly synthesized PL species.

(see chapter 3.4.2. and 4.5.5.)

Species	control			Dex			Dex + RU 486
	[pmol/mg]	% lab. PL	Fold of change	[pmol/mg]	% lab.PL	Fold of change	Fold of change
PE 38:6	198±44	26.6±3.7	1.0	106±30	19.0±2.8	**0.7±0.1**	0.8±0.1
PE 40:6	376±85	23.9±2.7	1.0	263±52	18.9±2.32	**0.8±0.1**	**0.9±0.1**

The quantitative values obtained for each stable isotope-labelled PL species were normalized to cellular protein content and are expressed as pmol/mg protein. For each PL specie the percentage of stable isotope-labelled PL from total labelled and unlabelled PL was calculated. The percentages of stable isotope-labelled species were then calculated as a ratio of corresponding untreated control (=1). Bold data represent significantly altered x-fold of changes with $P \leq 0.05$. Data are presented as means ± SDs of these ratios (n = 5). Dex = dexamethasone.

Appendix Table 9. Comparison of PC species between SF and treated FLS.

Specie	control [pmol/mg]	IL-1β	TGF-β1	IGF-1	Dex	Specie	healthy SF [nmol/ml]	early OA SF [nmol/ml]
[D9]-PC 30:0	41±11	NS	*↑	NS	*↓	PC 30:0	1.21	1.85
[D9]-PC 32:0	408±142	*↑	**↑	*↑	NS	PC 32:0	5.01	12.8
[D9]-PC 34:0	58±29	*↑	*↑	*↑	NS	PC 34:0	0.25	0.74↑
[D9]-PC 36:0	ND	ND	ND	ND	ND	PC 36:0	0.30	0.60↑
[D9]-PC 32:1	131±29	**↑	**↑	**↑	NS	PC 32:1	2.56	4.48
[D9]-PC 34:1	780±208	NS	**↑	**↑	NS	PC 34:1	25.4	56.9↑
[D9]-PC 36:1	330±115	*↑	**↑	**↑	NS	PC 36:1	4.43	12.4↑
[D9]-PC 38:1	ND	ND	ND	ND	ND	PC 38:1	0.22	0.56↑
[D9]-PC 32:2	ND	ND	ND	ND	ND	PC 32:2	0.21	0.54
[D9]-PC 34:2	305±84	NS	**↑	*↑	NS	PC 34:2	26.1	61.0↑
[D9]-PC 36:2	322±96	NS	**↑	**↑	NS	PC 36:2	16.5	43.8↑
[D9]-PC 38:2	ND	ND	ND	ND	ND	PC 38:2	0.48	1.09↑
[D9]-PC 34:3	33±8	NS	*↑	*↑	NS	PC 34:3	0.84	1.95↑
[D9]-PC 36:3	184±59	NS	*↑	**↑	NS	PC 36:3	8.10	20.2↑
[D9]-PC 38:3	131±58	NS	*↑	**↑	NS	PC 38:3	1.88	6.50↑
[D9]-PC 36:4	352±156	NS	**↑	**↑	NS	PC 36:4	10.9	30.9↑
[D9]-PC 38:4	624±322	NS	**↑	*↑	NS	PC 38:4	9.56	24.4↑
[D9]-PC 40:4	72±41	NS	*↑	NS	NS	PC 40:4	0.40	1.23↑
[D9]-PC 36:5	44±17	NS	**↑	**↑	NS	PC 36:5	0.85	2.86↑
[D9]-PC 38:5	280±119	NS	**↑	**↑	NS	PC 38:5	3.36	10.4↑
[D9]-PC 40:5	99±54	NS	**↑	*↑	NS	PC 40:5	0.75	2.65↑
[D9]-PC 38:6	61±23	NS	*↑	**↑	NS	PC 38:6	3.17	9.78↑
[D9]-PC 40:6	50±25	*↓	**↑	NS	NS	PC 40:6	1.60	4.51↑

The quantitative values obtained from each stable-isotope-labelled sample were normalized to cellular protein content and expressed as pmol/mg protein. For each PL specie the percentage of stable isotope-labelled PL from total labelled and unlabelled PL was calculated. The percentages of stable isotope-labelled species were then calculated as a ratio of corresponding untreated control (=1). Marked data correspond to the significantly elevated x-fold of changes. Data are presented as means ± SDs of these ratios (n = 5). * = $P < 0.05$; ** = $P \leq 0.01$. PL species of SF are expressed as median of nmol/ml of SF (healthy, n = 9; early OA, n =17) as described in (53). Marked data correspond to elevated concentrations of PL in early OA SF. PC = phosphatidylcholine; NS = not significant; ND = not determined; Dex = dexamethasone.

Appendix Table 10. Comparison of PE species between SF and treated FLS.

Specie	control [pmol/mg]	IL-1β	TGF-β1	IGF-1	Dex	Specie	healthy SF [nmol/ml]	early OA SF [nmol/ml]
[D4]-PE 32:0	ND	ND	ND	ND	ND	PE 32:0	0.02	0.03
[D4]-PE 34:0	ND	ND	ND	ND	ND	PE 34:0	0.03	0.04
[D4]-PE 32:1	ND	ND	ND	ND	ND	PE 32:1	0.03	0.03
[D4]-PE 34:1	132±54	**↑	NS	NS	**↓	PE 34:1	0.07	0.13
[D4]-PE 36:1	154±73	*↑	NS	NS	*↓	PE 36:1	0.07	0.12
[D4]-PE 38:1	ND	ND	ND	ND	ND	PE 38:1	0.06	0.07↑
[D4]-PE 32:2	ND	ND	ND	ND	ND	PE 32:2	0.03	0.03
[D4]-PE 34:2	31±13	**↑	NS	NS	*↓	PE 34:2	0.09	0.17↑
[D4]-PE 36:2	100±39	**↑	NS	NS	**↓	PE 36:2	0.16	0.38↑
[D4]-PE 38:2	ND	ND	ND	ND	ND	PE38:2	0.06	0.07
[D4]-PE 34:3	ND	ND	ND	ND	ND	PE 34:3	0.03	0.03
[D4]-PE 36:3	36±11	*↑	*↑	*↑	**↓	PE 36:3	0.07	0.12↑
[D4]-PE 38:3	206±38	**↑	NS	NS	NS	PE 38:3	0.06	0.11
[D4]-PE 36:4	41±11	**↑	NS	NS	**↓	PE 36:4	0.08	0.19↑
[D4]-PE 38:4	765±176	*↑	NS	NS	*↓	PE 38:4	0.32	0.85↑
[D4]-PE 40:4	338±65	**↑	NS	*↓	NS	PE 40:4	0.08	0.10
[D4]-PE 36:5	ND	ND	ND	ND	ND	PE 36:5	0.03	0.04
[D4]-PE 38:5	258±65	**↑	NS	NS	*↓	PE 38:5	0.13	0.28↑
[D4]-PE 40:5	323±78	*↑	NS	NS	**↓	PE 40:5	0.08	0.14↑
[D4]-PE 38:6	187±57	**↑	NS	NS	**↓	PE 38:6	0.16	0.45↑
[D4]-PE 40:6	383±84	**↑	NS	NS	**↓	PE 40:6	0.10	0.28↑

The quantitative values obtained from each stable-isotope-labelled sample were normalized to cellular protein content and expressed as pmol/mg protein. For each PL specie the percentage of stable isotope-labelled PL from total labelled and unlabelled PL was calculated. The percentages of stable isotope-labelled species were then calculated as a ratio of corresponding untreated control (=1). Marked data correspond to the significantly elevated x-fold of changes. Data are presented as means ± SDs of these ratios (n = 5). * = $P < 0.05$; ** = $P \leq 0.01$. PL species of SF are expressed as median of nmol/ml of SF (healthy, n = 9; early OA, n =17) as described in (53). Marked data correspond to elevated concentrations of PL in early OA SF. PE = phosphatidylethanolamine; NS = not significant; ND = not determined; Dex = dexamethasone.

Appendix Table 11. Comparison of PE-based plasmalogen species between SF and treated FLS.

Specie	control [pmol/mg]	IL-1β	TGF-β1	IGF-1	Dex	Specie	healthy SF [nmol/ml]	early OA SF [nmol/ml]
[D4]-PE P 16:0/18:1	44±17	*↑	NS	NS	NS	PE P 16:0/18:1	0.26	0.31
[D4]-PE P 16:0/18:2	ND	ND	ND	ND	ND	PE P 16:0/18:2	0.34	0.54
[D4]-PE P 16:0/20:3	ND	ND	ND	ND	ND	PE P 16:0/20:3	0.14	0.22
[D4]-PE P 16:0/20:4	308±75	*↑	NS	NS	NS	PE P 16:0/20:4	0.71	1.07
[D4]-PE P 16:0/22:4	139±31	NS	NS	NS	NS	PE P 16:0/22:4	0.28	0.27
[D4]-PE P 16:0/20:5	ND	ND	ND	ND	ND	PE P 16:0/20:5	0.20	0.25
[D4]-PE P 16:0/22:5	119±29	NS	NS	NS	NS	PE P 16:0/22:5	0.25	0.42↑
[D4]-PE P 16:0/22:6	90±22	**↑	NS	NS	NS	PE P 16:0/22:6	0.28	0.83↑
[D4]-PE P 18:1/16:0	51±9	NS	NS	NS	NS	PE P 18:1/16:0	ND	ND
[D4]-PE P 18:1/18:1	55±14	NS	NS	NS	NS	PE P 18:1/18:1	0.23	0.28
[D4]-PE P 18:1/18:2	ND	ND	ND	ND	ND	PE P 18:1/18:2	0.24	0.30
[D4]-PE P 18:1/20:3	ND	ND	ND	ND	ND	PE P 18:1/20:3	0.14	0.16
[D4]-PE P 18:1/20:4	556±87	**↑	NS	NS	NS	PE P 18:1/20:4	0.47	0.84
[D4]-PE P 18:1/20:5	59±15	NS	NS	NS	NS	PE P 18:1/20:5	0.14	0.19
[D4]-PE P 18:1/22:4	91±8	NS	*↑	NS	NS	PE P 18:1/22:4	0.13	0.13
[D4]-PE P 18:1/22:5	79±19	NS	NS	NS	NS	PE P 18:1/22:5	0.10	0.18
[D4]-PE P 18:1/22:6	95±4	NS	NS	NS	NS	PE P 18:1/22:6	0.22	0.40↑
[D4]-PE P 18:0/16:0	41±4	*↑	NS	NS	NS	PE P 18:0/16:0	ND	ND
[D4]-PE P 18:0/18:1	30±5	NS	NS	NS	NS	PE P 18:0/18:1	0.22	0.26
[D4]-PE P 18:0/18:2	ND	ND	ND	ND	ND	PE P 18:0/18:2	0.30	0.50↑
[D4]-PE P 18:0/20:3	ND	ND	ND	ND	ND	PE P 18:0/20:3	0.13	0.20
[D4]-PE P 18:0/20:4	367±70	**↑	NS	NS	NS	PE P 18:0/20:4	0.44	1.31↑
[D4]-PE P 18:0/20:5	51±5	NS	NS	NS	NS	PE P 18:0/20:5	0.12	0.29↑
[D4]-PE P 18:0/22:4	67±5	*↑	NS	NS	NS	PE P 18:0/22:4	0.14	0.14
[D4]-PE P 18:0/22:5	76±17	NS	NS	NS	NS	PE P 18:0/22:5	0.12	0.25↑
[D4]-PE P 18:0/22:6	66±17	*↑	*↓	NS	NS	PE P 18:0/22:6	0.22	0.43↑

The quantitative values obtained from each stable-isotope-labelled sample were normalized to cellular protein content and expressed as pmol/mg protein. For each PL specie the percentage of stable

isotope-labelled PL from total labelled and unlabelled PL was calculated. The percentages of stable isotope-labelled species were then calculated as a ratio of corresponding untreated control (=1). Marked data correspond to the significantly elevated x-fold of changes. Data are presented as means ± SDs of these ratios (n = 5). * = $P < 0.05$; ** = $P \leq 0.01$. PL species of SF are expressed as median of nmol/ml of SF (healthy, n = 9; early OA, n =17) as described in (53). Marked data correspond to elevated concentrations of PL in early OA SF. PE P = PE-based plasmalogen; NS = not significant; ND = not determined; Dex = dexamethasone.

Appendix Table 12. Comparison of PC species between SF and FLS treated with BMPs.

Specie	control [pmol/mg]	BMP-2	BMP-4	BMP-7	Specie	healthy SF [nmol/ml]	early OA SF [nmol/ml]
[D9]-PC 30:0	41±11	**↑	NS	NS	PC 30:0	1.21	1.85
[D9]-PC 32:0	408±142	**↑	NS	NS	PC 32:0	5.01	12.8
[D9]-PC 34:0	58±29	*↑	*↑	*↑	PC 34:0	0.25	0.74↑
[D9-]-PC 36:0	ND	ND	ND	ND	PC 36:0	0.30	0.60↑
[D9]-PC 32:1	131±29	*↑	NS	NS	PC 32:1	2.56	4.48
[D9]-PC 34:1	780±208	*↑	*↑	*↑	PC 34:1	25.4	56.9↑
[D9]-PC 36:1	330±115	NS	NS	*↑	PC 36:1	4.43	12.4↑
[D9]-PC 38:1	ND	ND	ND	ND	PC 38:1	0.22	0.56↑
[D9]-PC 32:2	ND	ND	ND	ND	PC 32:2	0.21	0.54
[D9]-PC 34:2	305±84	*↑	*↑	NS	PC 34:2	26.1	61.0↑
[D9]-PC 36:2	322±96	*↑	*↑	*↑	PC 36:2	16.5	43.8↑
[D9]-PC 38:2	ND	ND	ND	ND	PC 38:2	0.48	1.09↑
[D9]-PC 34:3	33±8	*↑	NS	NS	PC 34:3	0.84	1.95↑
[D9]-PC 36:3	184±59	*↑	*↑	*↑	PC 36:3	8.10	20.2↑
[D9]-PC 38:3	131±58	NS	NS	NS	PC 38:3	1.88	6.50↑
[D9]-PC 36:4	352±156	**↑	*↑	*↑	PC 36:4	10.9	30.9↑
[D9]-PC 38:4	624±322	*↑	*↑	NS	PC 38:4	9.56	24.4↑
[D9]-PC 40:4	72±41	NS	NS	NS	PC 40:4	0.40	1.23↑
[D9]-PC 36:5	44±17	NS	*↑	*↑	PC 36:5	0.85	2.86↑
[D9]-PC 38:5	280±119	*↑	*↑	NS	PC 38:5	3.36	10.4↑
[D9]-PC 40:5	99±54	NS	NS	*↑	PC 40:5	0.75	2.65↑
[D9]-PC 38:6	61±23	*↑	NS	*↑	PC 38:6	3.17	9.78↑
[D9]-PC 40:6	50±25	NS	NS	**↑	PC 40:6	1.60	4.51↑

The quantitative values obtained from each stable-isotope-labelled sample were normalized to cellular protein content and expressed as pmol/mg protein. For each PL specie the percentage of stable isotope-labelled PL from total labelled and unlabelled PL was calculated. The percentages of stable isotope-labelled species were then calculated as a ratio of corresponding untreated control (=1). Marked data correspond to the significantly elevated x-fold of changes. Data are presented as means ± SDs of these ratios (n = 5). * = $P < 0.05$; ** = $P \leq 0.01$. PL species of SF are expressed as median of nmol/ml of SF (healthy, n = 9; early OA, n =17) as described in (53). Marked data correspond to elevated concentrations of PL in early OA SF. PC = phosphatidylcholine; NS = not significant; ND = not determined.

Appendix Table 13. Comparison of PE species between SF and FLS treated with BMPs.

Specie	control [pmol/mg]	BMP-2	BMP-4	BMP-7	Specie	healthy SF [nmol/ml]	early OA SF [nmol/ml]
[D4]-PE 32:0	ND	ND	ND	ND	PE 32:0	0.02	0.03
[D4]-PE 34:0	ND	ND	ND	ND	PE 34:0	0.03	0.04
[D4]-PE 32:1	ND	ND	ND	ND	PE 32:1	0.03	0.03
[D4]-PE 34:1	132±54	NS	*↑	NS	PE 34:1	0.07	0.13
[D4]-PE 36:1	154±73	*↑	*↑	*↑	PE 36:1	0.07	0.12
[D4]-PE 38:1	ND	ND	ND	ND	PE 38:1	0.06	0.07↑
[D4]-PE 32:2	ND	ND	ND	ND	PE 32:2	0.03	0.03
[D4]-PE 34:2	31±13	NS	NS	NS	PE 34:2	0.09	0.17↑
[D4]-PE 36:2	100±39	NS	NS	*↑	PE 36:2	0.16	0.38↑
[D4]-PE 38:2	ND	ND	ND	ND	PE38:2	0.06	0.07
[D4]-PE 34:3	ND	ND	ND	ND	PE 34:3	0.03	0.03
[D4]-PE 36:3	36±11	NS	NS	NS	PE 36:3	0.07	0.12↑
[D4]-PE 38:3	206±38	NS	NS	*↑	PE 38:3	0.06	0.11
[D4]-PE 36:4	41±11	NS	NS	NS	PE 36:4	0.08	0.19↑
[D4]-PE 38:4	765±176	NS	NS	NS	PE 38:4	0.32	0.85↑
[D4]-PE 40:4	338±65	NS	NS	*↑	PE 40:4	0.08	0.10
[D4]-PE 36:5	ND	ND	ND	ND	PE 36:5	0.03	0.04
[D4]-PE 38:5	258±65	NS	NS	*↑	PE 38:5	0.13	0.28↑
[D4]-PE 40:5	323±78	**↑	*↑	NS	PE 40:5	0.08	0.14↑
[D4]-PE 38:6	187±57	NS	NS	NS	PE 38:6	0.16	0.45↑
[D4]-PE 40:6	383±84	*↑	*↑	*↑	PE 40:6	0.10	0.28↑

The quantitative values obtained from each stable-isotope-labelled sample were normalized to cellular protein content and expressed as pmol/mg protein. For each PL specie the percentage of stable isotope-labelled PL from total labelled and unlabelled PL was calculated. The percentages of stable isotope-labelled species were then calculated as a ratio of corresponding untreated control (=1). Marked data correspond to the significantly elevated x-fold of changes. Data are presented as means ± SDs of these ratios (n = 5). * = $P < 0.05$; ** = $P \leq 0.01$. PL species of SF are expressed as median of nmol/ml of SF (healthy, n = 9; early OA, n =17) as described in (53). Marked data correspond to elevated concentrations of PL in early OA SF. PE = phosphatidylethanolamine; NS = not significant; ND = not determined.

Appendix Table 14. Comparison of PE-based plasmalogen species between SF and FLS treated with BMPs.

Specie	control [pmol/mg]	BMP-2	BMP-4	BMP-7	Specie	healthy SF [nmol/ml]	early OA SF [nmol/ml]
[D4]-PE P 16:0/18:1	44±17	NS	NS	*↑	PE P 16:0/18:1	0.26	0.31
[D4]-PE P 16:0/18:2	ND	ND	ND	ND	PE P 16:0/18:2	0.34	0.54
[D4]-PE P 16:0/20:3	ND	ND	ND	ND	PE P 16:0/20:3	0.14	0.22
[D4]-PE P 16:0/20:4	308±75	*↑	*↑	NS	PE P 16:0/20:4	0.71	1.07
[D4]-PE P 16:0/22:4	139±31	NS	NS	NS	PE P 16:0/22:4	0.28	0.27
[D4]-PE P 16:0/20:5	ND	ND	ND	ND	PE P 16:0/20:5	0.20	0.25
[D4]-PE P 16:0/22:5	119±29	*↑	NS	NS	PE P 16:0/22:5	0.25	0.42↑
[D4]-PE P 16:0/22:6	90±22	NS	NS	NS	PE P 16:0/22:6	0.28	0.83↑
[D4]-PE P 18:1/16:0	51±9	NS	NS	NS	PE P 18:1/16:0	ND	ND
[D4]-PE P 18:1/18:1	55±14	NS	NS	NS	PE P 18:1/18:1	0.23	0.28
[D4]-PE P 18:1/18:2	ND	ND	ND	ND	PE P 18:1/18:2	0.24	0.30
[D4]-PE P 18:1/20:3	ND	ND	ND	ND	PE P 18:1/20:3	0.14	0.16
[D4]-PE P 18:1/20:4	556±87	NS	NS	*↑	PE P 18:1/20:4	0.47	0.84
[D4]-PE P 18:1/20:5	59±15	NS	NS	NS	PE P 18:1/20:5	0.14	0.19
[D4]-PE P 18:1/22:4	91±8	NS	NS	NS	PE P 18:1/22:4	0.13	0.13
[D4]-PE P 18:1/22:5	79±19	NS	NS	NS	PE P 18:1/22:5	0.10	0.18
[D4]-PE P 18:1/22:6	95±4	*↑	NS	NS	PE P 18:1/22:6	0.22	0.40↑
[D4]-PE P 18:0/16:0	41±4	NS	NS	NS	PE P 18:0/16:0	ND	ND
[D4]-PE P 18:0/18:1	30±5	*↑	*↑	NS	PE P 18:0/18:1	0.22	0.26
[D4]-PE P 18:0/18:2	ND	ND	ND	ND	PE P 18:0/18:2	0.30	0.50↑
[D4]-PE P 18:0/20:3	ND	ND	ND	ND	PE P 18:0/20:3	0.13	0.20
[D4]-PE P 18:0/20:4	367±70	*↑	NS	*↑	PE P 18:0/20:4	0.44	1.31↑
[D4]-PE P 18:0/20:5	51±5	NS	NS	NS	PE P 18:0/20:5	0.12	0.29↑
[D4]-PE P 18:0/22:4	67±5	NS	NS	NS	PE P 18:0/22:4	0.14	0.14
[D4]-PE P 18:0/22:5	76±17	*↑	NS	NS	PE P 18:0/22:5	0.12	0.25↑
[D4]-PE P 18:0/22:6	66±17	NS	NS	NS	PE P 18:0/22:6	0.22	0.43↑

The quantitative values obtained from each stable-isotope-labelled sample were normalized to cellular protein content and expressed as pmol/mg protein. For each PL specie the percentage of stable isotope-labelled PL from total labelled and unlabelled PL was calculated. The percentages of stable

isotope-labelled species were then calculated as a ratio of corresponding untreated control (=1). Marked data correspond to the significantly elevated x-fold of changes. Data are presented as means ± SDs of these ratios (n = 5). * = $P < 0.05$; ** = $P \leq 0.01$. PL species of SF are expressed as median of nmol/ml of SF (healthy, n = 9; early OA, n =17) as described in (53). Marked data correspond to elevated concentrations of PL in early OA SF. PE P = PE-based plasmalogen; NS = not significant; ND = not determined.

7. REFERENCES

1. Allen KD, Golightly YM. Epidemiology of osteoarthritis: state of the evidence. Curr Opin Rheumatol 2015;27(3):276-83.

2. Wieland HA, Michaelis M, Kirschbaum BJ, Rudolphi KA. Osteoarthritis - an untreatable disease? Nat Rev Drug Discov 2005;4(4):331-44.

3. Ondresik M, Azevedo Maia FR, da Silva Morais A, Gertrudes AC, Dias Bacelar AH, Correia C, Goncalves C, Radhouani H, Amandi Sousa R, Oliveira JM, Reis RL. Management of knee osteoarthritis. Current status and future trends. Biotechnol Bioeng 2016.

4. Aigner T, Sachse A, Gebhard PM, Roach HI. Osteoarthritis: pathobiology-targets and ways for therapeutic intervention. Adv Drug Deliv Rev 2006;58(2):128-49.

5. Steinmeyer J, Konttinen YT. Oral treatment options for degenerative joint disease--presence and future. Adv Drug Deliv Rev 2006;58(2):168-211.

6. Crema MD, Roemer FW, Marra MD, Burstein D, Gold GE, Eckstein F, Baum T, Mosher TJ, Carrino JA, Guermazi A. Articular cartilage in the knee: current MR imaging techniques and applications in clinical practice and research. Radiographics 2011;31(1):37-61.

7. Haq I, Murphy E, Dacre J. Osteoarthritis. Postgrad Med J 2003;79(933):377-83.

8. Madry H, Kon E, Condello V, Peretti GM, Steinwachs M, Seil R, Berruto M, Engebretsen L, Filardo G, Angele P. Early osteoarthritis of the knee. Knee Surg Sports Traumatol Arthrosc 2016;24(6):1753-62.

9. Lee AS, Ellman MB, Yan D, Kroin JS, Cole BJ, van Wijnen AJ, Im HJ. A current review of molecular mechanisms regarding osteoarthritis and pain. Gene 2013;527(2):440-7.

10. Tetlow LC, Adlam DJ, Woolley DE. Matrix metalloproteinase and proinflammatory cytokine production by chondrocytes of human osteoarthritic cartilage: associations with degenerative changes. Arthritis Rheum 2001;44(3):585-94.

11. Berenbaum F. Osteoarthritis as an inflammatory disease (osteoarthritis is not osteoarthrosis!). Osteoarthritis Cartilage 2013;21(1):16-21.

12. Rahmati M, Mobasheri A, Mozafari M. Inflammatory mediators in osteoarthritis: A critical review of the state-of-the-art, current prospects, and future challenges. Bone 2016;85:81-90.

13. Attur MG, Dave M, Akamatsu M, Katoh M, Amin AR. Osteoarthritis or osteoarthrosis: the definition of inflammation becomes a semantic issue in the genomic era of molecular medicine. Osteoarthritis Cartilage. England; 2002. p. 1-4.

14. Pelletier JP, Martel-Pelletier J, Abramson SB. Osteoarthritis, an inflammatory disease: potential implication for the selection of new therapeutic targets. Arthritis Rheum 2001;44(6):1237-47.

15. Wojdasiewicz P, Poniatowski LA, Szukiewicz D. The role of inflammatory and anti-inflammatory cytokines in the pathogenesis of osteoarthritis. Mediators Inflamm 2014;2014:561459.

16. Martel-Pelletier J, Alaaeddine N, Pelletier JP. Cytokines and their role in the pathophysiology of osteoarthritis. Front Biosci 1999;4:D694-703.

17. Kapoor M, Martel-Pelletier J, Lajeunesse D, Pelletier JP, Fahmi H. Role of proinflammatory cytokines in the pathophysiology of osteoarthritis. Nat Rev Rheumatol 2011;7(1):33-42.

18. Kokebie R, Aggarwal R, Lidder S, Hakimiyan AA, Rueger DC, Block JA, Chubinskaya S. The role of synovial fluid markers of catabolism and anabolism in osteoarthritis, rheumatoid arthritis and asymptomatic organ donors. Arthritis Res Ther 2011;13(2):R50.

19. Lettesjo H, Nordstrom E, Strom H, Nilsson B, Glinghammar B, Dahlstedt L, Moller E. Synovial fluid cytokines in patients with rheumatoid arthritis or other arthritic lesions. Scand J Immunol 1998;48(3):286-92.

20. Fernandes JC, Martel-Pelletier J, Pelletier JP. The role of cytokines in osteoarthritis pathophysiology. Biorheology 2002;39(1-2):237-46.

21. Afonso V, Champy R, Mitrovic D, Collin P, Lomri A. Reactive oxygen species and superoxide dismutases: role in joint diseases. Joint Bone Spine 2007;74(4):324-9.

22. Rousset F, Hazane-Puch F, Pinosa C, Nguyen MV, Grange L, Soldini A, Rubens-Duval B, Dupuy C, Morel F, Lardy B. IL-1beta mediates MMP secretion and IL-1beta neosynthesis via upregulation of p22(phox) and NOX4 activity in human articular chondrocytes. Osteoarthritis Cartilage 2015;23(11):1972-80.

23. Alcaraz MJ, Megias J, Garcia-Arnandis I, Clerigues V, Guillen MI. New molecular targets for the treatment of osteoarthritis. Biochem Pharmacol 2010;80(1):13-21.

24. Kwan Tat S, Padrines M, Theoleyre S, Heymann D, Fortun Y. IL-6, RANKL, TNF-alpha/IL-1: interrelations in bone resorption pathophysiology. Cytokine Growth Factor Rev 2004;15(1):49-60.

25. Honorati MC, Neri S, Cattini L, Facchini A. Interleukin-17, a regulator of angiogenic factor release by synovial fibroblasts. Osteoarthritis Cartilage 2006;14(4):345-52.

26. Lubberts E, Joosten LA, van de Loo FA, van den Gersselaar LA, van den Berg WB. Reduction of interleukin-17-induced inhibition of chondrocyte proteoglycan synthesis in intact murine articular cartilage by interleukin-4. Arthritis Rheum 2000;43(6):1300-6.

27. Steinmeyer J. Cytokines in osteoarthritis-current status on the pharmacological intervention. Front Biosci 2004;9:575-80.

28. Yorimitsu M, Nishida K, Shimizu A, Doi H, Miyazawa S, Komiyama T, Nasu Y, Yoshida A, Watanabe S, Ozaki T. Intra-articular injection of interleukin-4 decreases nitric oxide production by chondrocytes and ameliorates subsequent destruction of cartilage in

instability-induced osteoarthritis in rat knee joints. Osteoarthritis Cartilage 2008;16(7):764-71.

29. Alaaeddine N, Di Battista JA, Pelletier JP, Kiansa K, Cloutier JM, Martel-Pelletier J. Inhibition of tumor necrosis factor alpha-induced prostaglandin E2 production by the antiinflammatory cytokines interleukin-4, interleukin-10, and interleukin-13 in osteoarthritic synovial fibroblasts: distinct targeting in the signaling pathways. Arthritis Rheum 1999;42(4):710-8.

30. Yeh LA, Augustine AJ, Lee P, Riviere LR, Sheldon A. Interleukin-4, an inhibitor of cartilage breakdown in bovine articular cartilage explants. J Rheumatol 1995;22(9):1740-6.

31. Jovanovic D, Pelletier JP, Alaaeddine N, Mineau F, Geng C, Ranger P, Martel-Pelletier J. Effect of IL-13 on cytokines, cytokine receptors and inhibitors on human osteoarthritis synovium and synovial fibroblasts. Osteoarthritis Cartilage 1998;6(1):40-9.

32. Blaney Davidson EN, van Caam AP, van der Kraan PM. Osteoarthritis year in review 2016: biology. Osteoarthritis Cartilage 2017;25(2):175-80.

33. Zhai G, Dore J, Rahman P. TGF-beta signal transduction pathways and osteoarthritis. Rheumatol Int 2015;35(8):1283-92.

34. Fortier LA, Barker JU, Strauss EJ, McCarrel TM, Cole BJ. The role of growth factors in cartilage repair. Clin Orthop Relat Res 2011;469(10):2706-15.

35. Shen J, Li S, Chen D. TGF-beta signaling and the development of osteoarthritis. Bone Res 2014;2.

36. Waly NE, Refaiy A, Aborehab NM. IL-10 and TGF-beta: Roles in chondroprotective effects of Glucosamine in experimental Osteoarthritis? Pathophysiology 2017;24(1):45-9.

37. Massicotte F, Lajeunesse D, Benderdour M, Pelletier JP, Hilal G, Duval N, Martel-Pelletier J. Can altered production of interleukin-1beta, interleukin-6, transforming growth factor-beta and prostaglandin E(2) by isolated human subchondral osteoblasts identify two subgroups of osteoarthritic patients. Osteoarthritis Cartilage 2002;10(6):491-500.

38. Bakker AC, van de Loo FA, van Beuningen HM, Sime P, van Lent PL, van der Kraan PM, Richards CD, van den Berg WB. Overexpression of active TGF-beta-1 in the murine knee joint: evidence for synovial-layer-dependent chondro-osteophyte formation. Osteoarthritis Cartilage 2001;9(2):128-36.

39. Xie L, Tintani F, Wang X, Li F, Zhen G, Qiu T, Wan M, Crane J, Chen Q, Cao X. Systemic neutralization of TGF-beta attenuates osteoarthritis. Ann N Y Acad Sci 2016;1376(1):53-64.

40. Biver E, Hardouin P, Caverzasio J. The "bone morphogenic proteins" pathways in bone and joint diseases: translational perspectives from physiopathology to therapeutic targets. Cytokine Growth Factor Rev 2013;24(1):69-81.

41. Bandyopadhyay A, Yadav PS, Prashar P. BMP signaling in development and diseases: a pharmacological perspective. Biochem Pharmacol 2013;85(7):857-64.

42. Nakase T, Miyaji T, Tomita T, Kaneko M, Kuriyama K, Myoui A, Sugamoto K, Ochi T, Yoshikawa H. Localization of bone morphogenetic protein-2 in human osteoarthritic cartilage and osteophyte. Osteoarthritis Cartilage 2003;11(4):278-84.

43. Blaney Davidson EN, Vitters EL, van Lent PL, van de Loo FA, van den Berg WB, van der Kraan PM. Elevated extracellular matrix production and degradation upon bone morphogenetic protein-2 (BMP-2) stimulation point toward a role for BMP-2 in cartilage repair and remodeling. Arthritis Res Ther 2007;9(5):R102.

44. Honsawek S, Chayanupatkul M, Tanavalee A, Sakdinakiattikoon M, Deepaisarnsakul B, Yuktanandana P, Ngarmukos S. Relationship of plasma and synovial fluid BMP-7 with disease severity in knee osteoarthritis patients: a pilot study. Int Orthop 2009;33(4):1171-5.

45. Fan Z, Chubinskaya S, Rueger DC, Bau B, Haag J, Aigner T. Regulation of anabolic and catabolic gene expression in normal and osteoarthritic adult human articular chondrocytes by osteogenic protein-1. Clin Exp Rheumatol 2004;22(1):103-6.

46. Im HJ, Pacione C, Chubinskaya S, Van Wijnen AJ, Sun Y, Loeser RF. Inhibitory effects of insulin-like growth factor-1 and osteogenic protein-1 on fibronectin fragment- and interleukin-1beta-stimulated matrix metalloproteinase-13 expression in human chondrocytes. J Biol Chem 2003;278(28):25386-94.

47. Denko CW, Malemud CJ. Role of the growth hormone/insulin-like growth factor-1 paracrine axis in rheumatic diseases. Semin Arthritis Rheum 2005;35(1):24-34.

48. Fortier LA, Mohammed HO, Lust G, Nixon AJ. Insulin-like growth factor-I enhances cell-based repair of articular cartilage. J Bone Joint Surg Br 2002;84(2):276-88.

49. Loeser RF, Pacione CA, Chubinskaya S. The combination of insulin-like growth factor 1 and osteogenic protein 1 promotes increased survival of and matrix synthesis by normal and osteoarthritic human articular chondrocytes. Arthritis Rheum 2003;48(8):2188-96.

50. Berenbaum F, Griffin TM, Liu-Bryan R. Review: Metabolic Regulation of Inflammation in Osteoarthritis. Arthritis Rheumatol 2017;69(1):9-21.

51. Malfait AM. Osteoarthritis year in review 2015: biology. Osteoarthritis Cartilage 2016;24(1):21-6.

52. Hui AY, McCarty WJ, Masuda K, Firestein GS, Sah RL. A systems biology approach to synovial joint lubrication in health, injury, and disease. Wiley Interdiscip Rev Syst Biol Med 2012;4(1):15-37.

53. Kosinska MK, Liebisch G, Lochnit G, Wilhelm J, Klein H, Kaesser U, Lasczkowski G, Rickert M, Schmitz G, Steinmeyer J. A lipidomic study of phospholipid classes and species in human synovial fluid. Arthritis Rheum 2013;65(9):2323-33.

54. Kosinska MK, Ludwig TE, Liebisch G, Zhang R, Siebert HC, Wilhelm J, Kaesser U, Dettmeyer RB, Klein H, Ishaque B, Rickert M, Schmitz G, Schmidt TA, Steinmeyer J. Articular Joint Lubricants during Osteoarthritis and Rheumatoid Arthritis Display Altered Levels and Molecular Species. PLoS One 2015;10(5):e0125192.

55. Bartok B, Firestein GS. Fibroblast-like synoviocytes: key effector cells in rheumatoid arthritis. Immunol Rev 2010;233(1):233-55.

56. Revell PA. Synovial lining cells. Rheumatol Int 1989;9(2):49-51.

57. Clark RB, Schmidt T, Sachse FB, Boyle D, Firestein GS, Giles WR. Cellular electrophysiological principles that modulate secretion from synovial fibroblasts. J Physiol 2017;595(3):635-65.

58. Nagaoka A, Yoshida H, Nakamura S, Morikawa T, Kawabata K, Kobayashi M, Sakai S, Takahashi Y, Okada Y, Inoue S. Regulation of Hyaluronan (HA) Metabolism Mediated by HYBID (Hyaluronan-binding Protein Involved in HA Depolymerization, KIAA1199) and HA Synthases in Growth Factor-stimulated Fibroblasts. J Biol Chem 2015;290(52):30910-23.

59. Schwarz IM, Hills BA. Synovial surfactant: lamellar bodies in type B synoviocytes and proteolipid in synovial fluid and the articular lining. Br J Rheumatol 1996;35(9):821-7.

60. Daniel M. Boundary cartilage lubrication: review of current concepts. Wien Med Wochenschr 2014;164(5-6):88-94.

61. Jahn S, Seror J, Klein J. Lubrication of Articular Cartilage. Annu Rev Biomed Eng 2016;18:235-58.

62. Hills BA. Identity of the joint lubricant. J Rheumatol 2002;29(1):200-1.

63. Hills BA. Surface-active phospholipid: a Pandora's box of clinical applications. Part II. Barrier and lubricating properties. Intern Med J 2002;32(5-6):242-51.

64. Hills BA, Crawford RW. Normal and prosthetic synovial joints are lubricated by surface-active phospholipid: a hypothesis. J Arthroplasty 2003;18(4):499-505.

65. Vance JE. Phospholipid synthesis and transport in mammalian cells. Traffic 2015;16(1):1-18.

66. Rolim AE, Henrique-Araujo R, Ferraz EG, de Araujo Alves Dultra FK, Fernandez LG. Lipidomics in the study of lipid metabolism: Current perspectives in the omic sciences. Gene 2015;554(2):131-9.

67. Nagan N, Zoeller RA. Plasmalogens: biosynthesis and functions. Prog Lipid Res 2001;40(3):199-229.

68. Bartke N, Hannun YA. Bioactive sphingolipids: metabolism and function. J Lipid Res 2009;50 Suppl:S91-6.

69. Postle AD. Phospholipid lipidomics in health and disease. European Journal of Lipid Science and Technology 2016;111(1):2-13.

70. Gibellini F, Smith TK. The Kennedy pathway--De novo synthesis of phosphatidylethanolamine and phosphatidylcholine. IUBMB Life 2010;62(6):414-28.

71. Fagone P, Jackowski S. Phosphatidylcholine and the CDP-choline cycle. Biochim Biophys Acta 2013;1831(3):523-32.

72. Agassandian M, Mallampalli RK. Surfactant phospholipid metabolism. Biochim Biophys Acta 2013;1831(3):612-25.

73. Calzada E, Onguka O, Claypool SM. Phosphatidylethanolamine Metabolism in Health and Disease. Int Rev Cell Mol Biol 2016;321:29-88.

74. Kennedy EP. Metabolism of lipides. Annu Rev Biochem 1957;26:119-48.

75. van der Veen JN, Lingrell S, da Silva RP, Jacobs RL, Vance DE. The concentration of phosphatidylethanolamine in mitochondria can modulate ATP production and glucose metabolism in mice. Diabetes 2014;63(8):2620-30.

76. Schmitz G, Ruebsaamen K. Metabolism and atherogenic disease association of lysophosphatidylcholine. Atherosclerosis 2010;208(1):10-8.

77. Hailey DW, Rambold AS, Satpute-Krishnan P, Mitra K, Sougrat R, Kim PK, Lippincott-Schwartz J. Mitochondria supply membranes for autophagosome biogenesis during starvation. Cell 2010;141(4):656-67.

78. Vance JE, Tasseva G. Formation and function of phosphatidylserine and phosphatidylethanolamine in mammalian cells. Biochim Biophys Acta 2013;1831(3):543-54.

79. Sundler R, Akesson B. Regulation of phospholipid biosynthesis in isolated rat hepatocytes. Effect of different substrates. J Biol Chem 1975;250(9):3359-67.

80. Lykidis A, Wang J, Karim MA, Jackowski S. Overexpression of a mammalian ethanolamine-specific kinase accelerates the CDP-ethanolamine pathway. J Biol Chem 2001;276(3):2174-9.

81. Jang DJ, Lee JA. The roles of phosphoinositides in mammalian autophagy. Arch Pharm Res 2016;39(8):1129-36.

82. Kosinska MK, Liebisch G, Lochnit G, Wilhelm J, Klein H, Kaesser U, Lasczkowski G, Rickert M, Schmitz G, Steinmeyer J. Sphingolipids in human synovial fluid--a lipidomic study. PLoS One 2014;9(3):e91769.

83. Adam D, Heinrich M, Kabelitz D, Schutze S. Ceramide: does it matter for T cells? Trends Immunol 2002;23(1):1-4.

84. Cutler RG, Mattson MP. Sphingomyelin and ceramide as regulators of development and lifespan. Mech Ageing Dev 2001;122(9):895-908.

85. Chalfant CE, Spiegel S. Sphingosine 1-phosphate and ceramide 1-phosphate: expanding roles in cell signaling. J Cell Sci 2005;118(Pt 20):4605-12.

86. Spiegel S, Milstien S. Sphingosine-1-phosphate: an enigmatic signalling lipid. Nat Rev Mol Cell Biol 2003;4(5):397-407.

87. Stradner MH, Hermann J, Angerer H, Setznagl D, Sunk I, Windhager R, Graninger WB. Spingosine-1-phosphate stimulates proliferation and counteracts interleukin-1 induced nitric oxide formation in articular chondrocytes. Osteoarthritis Cartilage 2008;16(3):305-11.

88. Stradner MH, Gruber G, Angerer H, Huber V, Setznagl D, Kremser ML, Moazedi-Furst FC, Windhager R, Graninger WB. Sphingosine 1-phosphate counteracts the effects of interleukin-1beta in human chondrocytes. Arthritis Rheum 2013;65(8):2113-22.

89. Neumann E, Riepl B, Knedla A, Lefevre S, Tarner IH, Grifka J, Steinmeyer J, Scholmerich J, Gay S, Muller-Ladner U. Cell culture and passaging alters gene expression pattern and proliferation rate in rheumatoid arthritis synovial fibroblasts. Arthritis Res Ther 2010;12(3):R83.

90. Chomczynski P, Sacchi N. Single-step method of RNA isolation by acid guanidinium thiocyanate-phenol-chloroform extraction. Anal Biochem 1987;162(1):156-9.

91. Smith PK, Krohn RI, Hermanson GT, Mallia AK, Gartner FH, Provenzano MD, Fujimoto EK, Goeke NM, Olson BJ, Klenk DC. Measurement of protein using bicinchoninic acid. Anal Biochem 1985;150(1):76-85.

92. Bligh EG, Dyer WJ. A rapid method of total lipid extraction and purification. Can J Biochem Physiol 1959;37(8):911-7.

93. Liebisch G, Lieser B, Rathenberg J, Drobnik W, Schmitz G. High-throughput quantification of phosphatidylcholine and sphingomyelin by electrospray ionization tandem mass spectrometry coupled with isotope correction algorithm. Biochim Biophys Acta 2004;1686(1-2):108-17.

94. Brugger B, Erben G, Sandhoff R, Wieland FT, Lehmann WD. Quantitative analysis of biological membrane lipids at the low picomole level by nano-electrospray ionization tandem mass spectrometry. Proc Natl Acad Sci U S A 1997;94(6):2339-44.

95. Zemski Berry KA, Murphy RC. Electrospray ionization tandem mass spectrometry of glycerophosphoethanolamine plasmalogen phospholipids. J Am Soc Mass Spectrom 2004;15(10):1499-508.

96. Matyash V, Liebisch G, Kurzchalia TV, Shevchenko A, Schwudke D. Lipid extraction by methyl-tert-butyl ether for high-throughput lipidomics. J Lipid Res 2008;49(5):1137-46.

97. Liebisch G, Drobnik W, Reil M, Trumbach B, Arnecke R, Olgemoller B, Roscher A, Schmitz G. Quantitative measurement of different ceramide species from crude cellular extracts by electrospray ionization tandem mass spectrometry (ESI-MS/MS). J Lipid Res 1999;40(8):1539-46.

98. Liebisch G, Vizcaino JA, Kofeler H, Trotzmuller M, Griffiths WJ, Schmitz G, Spener F, Wakelam MJ. Shorthand notation for lipid structures derived from mass spectrometry. J Lipid Res 2013;54(6):1523-30.

99. King G, Damas JE, Cake MH, Berryman D, Maker GL. Influence of glucocorticoids, neuregulin-1beta, and sex on surfactant phospholipid secretion from type II cells. Am J Physiol Lung Cell Mol Physiol 2014;306(3):L292-8.

100. Creamer P. Intra-articular corticosteroid treatment in osteoarthritis. Curr Opin Rheumatol 1999;11(5):417-21.

101. Sullivan LC, Orgeig S, Daniels CB. The role of extrinsic and intrinsic factors in the evolution of the control of pulmonary surfactant maturation during development in the amniotes. Physiol Biochem Zool 2003;76(3):281-95.

102. Angel J, Colard O, Chevy F, Fournier C. Interleukin-1-mediated phospholipid breakdown and arachidonic acid release in human synovial cells. Arthritis Rheum 1993;36(2):158-67.

103. Dvir-Ginzberg M, Steinmeyer J. Towards elucidating the role of SirT1 in osteoarthritis. Front Biosci (Landmark Ed) 2013;18:343-55.

104. Erkelens DW. Apolipoproteins in lipid transport, an impressionist view. Postgrad Med J 1989;65(763):275-81.

105. Schmidt TA, Gastelum NS, Nguyen QT, Schumacher BL, Sah RL. Boundary lubrication of articular cartilage: role of synovial fluid constituents. Arthritis Rheum 2007;56(3):882-91.

106. Seror J, Zhu L, Goldberg R, Day AJ, Klein J. Supramolecular synergy in the boundary lubrication of synovial joints. Nat Commun 2015;6:6497.

107. Raviv U, Klein J. Fluidity of bound hydration layers. Science 2002;297(5586):1540-3.

108. Schmitz G, Muller G. Structure and function of lamellar bodies, lipid-protein complexes involved in storage and secretion of cellular lipids. J Lipid Res 1991;32(10):1539-70.

109. Dobbie JW, Hind C, Meijers P, Bodart C, Tasiaux N, Perret J, Anderson JD. Lamellar body secretion: ultrastructural analysis of an unexplored function of synoviocytes. Br J Rheumatol 1995;34(1):13-23.

110. Crockett R. Boundary Lubrication in Natural Articular Joints. Tribology Letters 2016;35(2):77-84.

111. Clark RB, Schmidt T, Sachse FB, Boyle D, Firestein GS, Giles WR. Cellular electrophysiological principles that modulate secretion from synovial fibroblasts. J Physiol 2016.

112. Chen Y, Crawford RW, Oloyede A. Unsaturated phosphatidylcholines lining on the surface of cartilage and its possible physiological roles. J Orthop Surg Res 2007;2:14.

113. Gale LR, Chen Y, Hills BA, Crawford R. Boundary lubrication of joints: characterization of surface-active phospholipids found on retrieved implants. Acta Orthop 2007;78(3):309-14.

114. Kronqvist R, Leppimaki P, Mehto P, Slotte JP. The effect of interleukin 1 beta on the biosynthesis of cholesterol, phosphatidylcholine, and sphingomyelin in fibroblasts, and on their efflux from cells to lipid-free apolipoprotein A-I. Eur J Biochem 1999;262(3):939-46.

115. Slotte JP. Sphingomyelin-cholesterol interactions in biological and model membranes. Chem Phys Lipids 1999;102(1-2):13-27.

116. Grange L, Nguyen MV, Lardy B, Derouazi M, Campion Y, Trocme C, Paclet MH, Gaudin P, Morel F. NAD(P)H oxidase activity of Nox4 in chondrocytes is both inducible and involved in collagenase expression. Antioxid Redox Signal 2006;8(9-10):1485-96.

117. Momchilova A, Markovska T. Phosphatidylethanolamine and phosphatidylcholine are sources of diacylglycerol in ras-transformed NIH 3T3 fibroblasts. Int J Biochem Cell Biol 1999;31(2):311-8.

118. Okamoto Y, Morishita J, Tsuboi K, Tonai T, Ueda N. Molecular characterization of a phospholipase D generating anandamide and its congeners. J Biol Chem 2004;279(7):5298-305.

119. Carver KA, Yang D. N-Acetylcysteine Amide Protects Against Oxidative Stress-Induced Microparticle Release From Human Retinal Pigment Epithelial Cells. Invest Ophthalmol Vis Sci 2016;57(2):360-71.

120. Emoto K, Toyama-Sorimachi N, Karasuyama H, Inoue K, Umeda M. Exposure of phosphatidylethanolamine on the surface of apoptotic cells. Exp Cell Res 1997;232(2):430-4.

121. Engelmann B. Plasmalogens: targets for oxidants and major lipophilic antioxidants. Biochem Soc Trans 2004;32(Pt 1):147-50.

122. Pettitt TR, Martin A, Horton T, Liossis C, Lord JM, Wakelam MJ. Diacylglycerol and phosphatidate generated by phospholipases C and D, respectively, have distinct fatty acid compositions and functions. Phospholipase D-derived diacylglycerol does not activate protein kinase C in porcine aortic endothelial cells. J Biol Chem 1997;272(28):17354-9.

123. Ichinose Y, Eguchi K, Migita K, Kawabe Y, Tsukada T, Koji T, Abe K, Aoyagi T, Nakamura H, Nagataki S. Apoptosis induction in synovial fibroblasts by ceramide: in vitro and in vivo effects. J Lab Clin Med 1998;131(5):410-6.

124. Sun HY, Hu KZ, Yin ZS. Inhibition of the p38-MAPK signaling pathway suppresses the apoptosis and expression of proinflammatory cytokines in human osteoarthritis chondrocytes. Cytokine 2017;90:135-43.

125. Hosseinzadeh A, Jafari D, Kamarul T, Bagheri A, Sharifi AM. Evaluating the Protective Effects and Mechanisms of Diallyl Disulfide on Interlukin-1beta-Induced Oxidative Stress and Mitochondrial Apoptotic Signaling Pathways in Cultured Chondrocytes. J Cell Biochem 2017.

126. Xu B, Li YY, Ma J, Pei FX. Roles of microRNA and signaling pathway in osteoarthritis pathogenesis. J Zhejiang Univ Sci B 2016;17(3):200-8.

127. Schlaak JF, Pfers I, Meyer Zum Buschenfelde KH, Marker-Hermann E. Different cytokine profiles in the synovial fluid of patients with osteoarthritis, rheumatoid arthritis and seronegative spondylarthropathies. Clin Exp Rheumatol 1996;14(2):155-62.

128. Liu Y, Hou R, Yin R, Yin W. Correlation of bone morphogenetic protein-2 levels in serum and synovial fluid with disease severity of knee osteoarthritis. Med Sci Monit 2015;21:363-70.

129. Schneiderman R, Rosenberg N, Hiss J, Lee P, Liu F, Hintz RL, Maroudas A. Concentration and size distribution of insulin-like growth factor-I in human normal and osteoarthritic synovial fluid and cartilage. Arch Biochem Biophys 1995;324(1):173-88.

130. Cuellar A, Reddi AH. Stimulation of Superficial Zone Protein/Lubricin/PRG4 by Transforming Growth Factor-beta in Superficial Zone Articular Chondrocytes and Modulation by Glycosaminoglycans. Tissue Eng Part A 2015;21(13-14):1973-81.

131. Khalafi A, Schmid TM, Neu C, Reddi AH. Increased accumulation of superficial zone protein (SZP) in articular cartilage in response to bone morphogenetic protein-7 and growth factors. J Orthop Res 2007;25(3):293-303.

132. Niikura T, Reddi AH. Differential regulation of lubricin/superficial zone protein by transforming growth factor beta/bone morphogenetic protein superfamily members in articular chondrocytes and synoviocytes. Arthritis Rheum 2007;56(7):2312-21.

133. Haubeck HD, Kock R, Fischer DC, Van de Leur E, Hoffmeister K, Greiling H. Transforming growth factor beta 1, a major stimulator of hyaluronan synthesis in human synovial lining cells. Arthritis Rheum 1995;38(5):669-77.

134. Recklies AD, White C, Melching L, Roughley PJ. Differential regulation and expression of hyaluronan synthases in human articular chondrocytes, synovial cells and osteosarcoma cells. Biochem J 2001;354(Pt 1):17-24.

135. Beers MF, Solarin KO, Guttentag SH, Rosenbloom J, Kormilli A, Gonzales LW, Ballard PL. TGF-beta1 inhibits surfactant component expression and epithelial cell maturation in cultured human fetal lung. Am J Physiol 1998;275(5 Pt 1):L950-60.

136. Cazzolli R, Shemon AN, Fang MQ, Hughes WE. Phospholipid signalling through phospholipase D and phosphatidic acid. IUBMB Life 2006;58(8):457-61.

137. Exton JH, Taylor SJ, Augert G, Bocckino SB. Cell signalling through phospholipid breakdown. Mol Cell Biochem 1991;104(1-2):81-6.

138. Sharma AR, Jagga S, Lee SS, Nam JS. Interplay between Cartilage and Subchondral Bone Contributing to Pathogenesis of Osteoarthritis. Int J Mol Sci; 2013. p. 19805-30.

139. Chakravarthy MV, Lodhi IJ, Yin L, Malapaka RR, Xu HE, Turk J, Semenkovich CF. Identification of a physiologically relevant endogenous ligand for PPARalpha in liver. Cell 2009;138(3):476-88.

140. Kersten S. Integrated physiology and systems biology of PPARalpha. Mol Metab 2014;3(4):354-71.

141. del Rincon I, Battafarano DF, Restrepo JF, Erikson JM, Escalante A. Glucocorticoid dose thresholds associated with all-cause and cardiovascular mortality in rheumatoid arthritis. Arthritis Rheumatol 2014;66(2):264-72.

142. Richardson DW, Dodge GR. Dose-dependent effects of corticosteroids on the expression of matrix-related genes in normal and cytokine-treated articular chondrocytes. Inflamm Res 2003;52(1):39-49.

143. Shimpo H, Sakai T, Kondo S, Mishima S, Yoda M, Hiraiwa H, Ishiguro N. Regulation of prostaglandin E(2) synthesis in cells derived from chondrocytes of patients with osteoarthritis. J Orthop Sci 2009;14(5):611-7.

144. Uddin MN, Siddiq A, Oettinger CW, D'Souza MJ. Potentiation of pro-inflammatory cytokine suppression and survival by microencapsulated dexamethasone in the treatment of experimental sepsis. J Drug Target 2011;19(9):752-60.

145. Huo Y, Rangarajan P, Ling EA, Dheen ST. Dexamethasone inhibits the Nox-dependent ROS production via suppression of MKP-1-dependent MAPK pathways in activated microglia. BMC Neurosci 2011;12:49.

146. Sullivan LC, Orgeig S. Dexamethasone and epinephrine stimulate surfactant secretion in type II cells of embryonic chickens. Am J Physiol Regul Integr Comp Physiol 2001;281(3):R770-7.

147. Hills BA, Ethell MT, Hodgson DR. Release of lubricating synovial surfactant by intra-articular steroid. Br J Rheumatol 1998;37(6):649-52.

148. John K, Marino JS, Sanchez ER, Hinds TD. The glucocorticoid receptor: cause of or cure for obesity? Am J Physiol Endocrinol Metab; 2016. p. E249-57.

149. Utomo L, van Osch GJ, Bayon Y, Verhaar JA, Bastiaansen-Jenniskens YM. Guiding synovial inflammation by macrophage phenotype modulation: an in vitro study towards a therapy for osteoarthritis. Osteoarthritis Cartilage 2016.

150. Gossye V, Elewaut D, Bougarne N, Bracke D, Van Calenbergh S, Haegeman G, De Bosscher K. Differential mechanism of NF-kappaB inhibition by two glucocorticoid receptor modulators in rheumatoid arthritis synovial fibroblasts. Arthritis Rheum 2009;60(11):3241-50.

151. Li Y, Wang Y, Chubinskaya S, Schoeberl B, Florine E, Kopesky P, Grodzinsky AJ. Effects of insulin-like growth factor-1 and dexamethasone on cytokine-challenged cartilage: relevance to post-traumatic osteoarthritis. Osteoarthritis Cartilage 2015;23(2):266-74.

152. Griese M, Gobran LI, Rooney SA. Ontogeny of surfactant secretion in type II pneumocytes from fetal, newborn, and adult rats. Am J Physiol 1992;262(3 Pt 1):L337-43.

153. Massaro D, Clerch L, Massaro GD. Surfactant secretion: evidence that cholinergic stimulation of secretion is indirect. Am J Physiol 1982;243(1):C39-45.

154. Oyarzun MJ, Clements JA, Baritussio A. Ventilation enhances pulmonary alveolar clearance of radioactive dipalmitoyl phosphatidylcholine in liposomes. Am Rev Respir Dis 1980;121(4):709-21.

155. Wood PG, Lopatko OV, Orgeig S, Joss JM, Smits AW, Daniels CB. Control of pulmonary surfactant secretion: an evolutionary perspective. Am J Physiol Regul Integr Comp Physiol 2000;278(3):R611-9.

156. Dennis EA, Cao J, Hsu YH, Magrioti V, Kokotos G. Phospholipase A2 enzymes: physical structure, biological function, disease implication, chemical inhibition, and therapeutic intervention. Chem Rev 2011;111(10):6130-85.

157. Guma M, Sanchez-Lopez E, Lodi A, Garcia-Carbonell R, Tiziani S, Karin M, Lacal JC, Firestein GS. Choline kinase inhibition in rheumatoid arthritis. Ann Rheum Dis 2015;74(7):1399-407.

158. Seki M, Kawai Y, Ishii C, Yamanaka T, Odawara M, Inazu M. Functional analysis of choline transporters in rheumatoid arthritis synovial fibroblasts. Mod Rheumatol 2017:1-9.

159. Dvir-Ginzberg M, Mobasheri A, Kumar A. The Role of Sirtuins in Cartilage Homeostasis and Osteoarthritis. Curr Rheumatol Rep 2016;18(7):43.

160. Niederer F, Ospelt C, Brentano F, Hottiger MO, Gay RE, Gay S, Detmar M, Kyburz D. SIRT1 overexpression in the rheumatoid arthritis synovium contributes to proinflammatory cytokine production and apoptosis resistance. Ann Rheum Dis 2011;70(10):1866-73.

161. Lomb DJ, Laurent G, Haigis MC. Sirtuins regulate key aspects of lipid metabolism. Biochim Biophys Acta 2010;1804(8):1652-7.

162. Schifferer R, Liebisch G, Bandulik S, Langmann T, Dada A, Schmitz G. ApoA-I induces a preferential efflux of monounsaturated phosphatidylcholine and medium chain sphingomyelin species from a cellular pool distinct from HDL(3) mediated phospholipid efflux. Biochim Biophys Acta 2007;1771(7):853-63.

163. Mendez AJ, Uint L. Apolipoprotein-mediated cellular cholesterol and phospholipid efflux depend on a functional Golgi apparatus. J Lipid Res 1996;37(12):2510-24.

164. Ecker J, Liebisch G. Application of stable isotopes to investigate the metabolism of fatty acids, glycerophospholipid and sphingolipid species. Prog Lipid Res 2014;54:14-31.

8. DECLARATION

"I declare that I have completed this dissertation single-handedly without the unauthorized help of a second party and only with the assistance acknowledged therein. I have appropriately acknowledged and referenced all text passages that are derived literally from or are based on the content of published or unpublished work of others, and all information that relates to verbal communications. I have abided by the principles of good scientific conduct laid down in the charter of the Justus Liebig University of Giessen in carrying out the investigations described in the dissertation."

Giessen, 17.05.2017 _____

Katarzyna Dominika Sluzalska

Der Lebenslauf wurde aus der elektronischen Version der Arbeit entfernt.

The curriculum vitae was removed from the electronic version of the paper.

[redacted]

[redacted]

[redacted]

Publications

- **K. D. Sluzalska**, G. Liebisch, G. Lochnit, B. Ishaque, H. Hackstein, G. Schmitz, M. Rickert, J. Steinmeyer. *Interleukin-1ß affects the phospholipid biosynthesis of fibroblast-like synoviocytes from human osteoarthritic knee joints.* (under revision in Osteoarthritis and Cartilage)

- **K. D. Sluzalska**, G. Liebisch, G. Lochnit, B. Ishaque, H. Hackstein, G. Schmitz, M. Rickert, J. Steinmeyer. *Growth factors regulate phospholipid biosynthesis of fibroblast-like synoviocytes from human osteoarthritic knee joints.* (in preparation)

- **K. D. Sluzalska**, G. Liebisch, G. Lochnit, B. Ishaque, H. Hackstein, G. Schmitz, M. Rickert, J. Steinmeyer. *Dexamethasone affects phospholipid metabolism of human osteoarthritic fibroblast-like synoviocytes.* (in preparation)

- Krząkała, **K. Służalska**, M. Widziołek, J. Szade, A. Winiarski, G. Dercz, A. Kazek, G. Tylko, J. Michalska, A. Iwaniak, A. M. Osyczka, W. Simka. *Formation of bioactive coatings on Ti-6Al-7Nb alloy by plasma electrolytic oxidation.* Electrochimica Acta, Volume 104, 1 August 2013, Pages 407-424.

- Krząkała, **K. Służalska**, G. Dercz, A. Maciej, A. Kazek, J. Szade, A. Winiarski, M. Dudek, J. Michalska, G. Tylko, A. M. Osyczka, W. Simka. *Characterisation of bioactive films on Ti–6Al–4V alloy.* Electrochimica Acta, Volume 104, 1 August 2013, Pages 425-438.

- D. Babilas, **K**. **Służalska**, A. Krząkała, A. Maciej, R. P. Socha, G. Dercz, G. Tylko, J. Michalska, A. M. Osyczka, W.Simka. *Plasma electrolytic oxidation of a Ti–15Mo alloy in silicate solutions.* Materials Letters, Volume 100, 1 June 2013, Pages 252-256.

Oral presentations

- **K. Sluzalska**, G. Liebisch, G. Lochnit, M. Rickert, B. Ishaque, G. Schmitz, J. Steinmeyer. *Biosynthesis of phospholipids by human osteoarthritic fibroblast-like synoviocytes.* 25-DKOU 2016, 28.10.2016, Berlin, Germany.

- **K. Sluzalska**, G. Tylko, A. M. Osyczka, W. Simka. *Enrichment of Ti-6Al-7Nb alloy oxide layer with calcium-phosphate enhances in vitro osteogenesis of human bone marrow-derived mesenchymal stem cells.* XXIII FECTS and ISMB Joint Meeting, 25-29.08.2012, Katowice, Poland.

Poster presentations

- **K. Sluzalska**, G. Liebisch, G. Lochnit, M. Rickert, G. Schmitz, J. Steinmeyer. *Development of an in vitro model to study biosynthesis of phospholipids by human fibroblast-like synoviocytes.* 8th Annual GGL Conference, 30.09-01.10 2015, Giessen, Germany.

- **K. Sluzalska**, G. Liebisch, G. Lochnit, M. Rickert, G. Schmitz, J. Steinmeyer. *Development of in vitro models to study biosynthesis and release of phospholipids from human fibroblast-like synoviocytes.* 7th Annual GGL Conference, 17-18.09.2014, Giessen, Germany.

- **K. Sluzalska**, G. Liebisch, G. Lochnit, M. Rickert, G. Schmitz, J. Steinmeyer. *Development of an in vitro model to study biosynthesis and efflux of phospholipids by human fibroblast-like synoviocytes – preliminary results.* 6th Annual GGL Conference, 11-12.09.2013, Giessen, Germany.

10. ACKNOWLEDGMENTS

In the last chapter of my thesis, I would like to take opportunity to thank and acknowledge all people who supported and encouraged me during the PhD studies period.

First of all, I would like to express my sincere gratitude to my supervisor Prof. Dr. rer. nat. Jürgen Steinmeyer for the opportunity to work in his research group. I am grateful for encouraging my research, his patience and advices. His professional guidance helped me in all the time of research and writing of this thesis.

I am grateful to Prof. Dr. med. Gerd Schmitz (Department of Clinical Chemistry and Laboratory Medicine, University Hospital Regensburg, Germany) for the opportunity of the cooperation in the lipidomic network.

I am deeply thankful to Dr. rer. nat. Gerhard Liebisch (Department of Clinical Chemistry and Laboratory Medicine, University Hospital Regensburg, Germany) for introducing me to the lipid analysis world. His precious comments and question expended my perspective.

My sincere acknowledgments go to the director of our Orthopaedics Clinic Prof. Dr. med. Markus Rickert. I would like to express my gratitude to the surgical team of our clinic for providing synovial tissue samples, especially to Dr. med. Bernd Ishaque, Dr. med. Gafar Ahmed, Dr. med. Dirk Stolz, Dr. med. Evangelos Rikas, Dr. med. Jan Gils and Dr. med. Oliver Bischel. I would also like to acknowledge all stuff members of the Orthopaedics Clinic, without their precious work it would not be possible to conduct this research.

I also owe my gratitude to Dr. rer. nat. Alexander Sigrüner (Department of Clinical Chemistry and Laboratory Medicine, University Hospital Regensburg, Germany) for providing me with LPDS.

My special thanks go to Dr. Jochen Wilhelm (ECCPS, Justus Liebig University Giessen) for consulting statistic and valuable advices.

I sincerely thank to Prof. Dr. rer. nat. Günter Lochnit (Protein Analytics, Department of Biochemistry, Justus Liebig University Giessen, Germany) for giving me an access to the equipment in his laboratory.

I am also grateful to Prof. Dr. Holger Hackstein (Institute for Clinical Immunology and Transfusion Medicine, Justus Liebig University Giessen, Germany) for an access to the FACS facility.

I also owe my gratitude to Prof. Dr. med. Michael Kracht (Institute of Pharmacology, Justus-Liebig-University of Giessen) for the access to the real-time PCR system.

I would like to thank Dr. Florian Veit (ECCPS, Justus Liebig University Giessen) for his help during the apoptosis measurement.

I owe my deep gratitude to the International PhD Programme of the Faculties of Veterinary Medicine and Medicine as well as Giessen Graduate Centre for the Life Sciences (GGL), especially to Prof. Dr. Eveline Baumgart-Vogt and Dr. Lorna Lück for the organization of excellent courses and training opportunities.

I would also like to thank Simone Duechtel and Doreen Mueller (Department of Clinical Chemistry and Laboratory Medicine, University Hospital Regensburg, Germany) for their excellent technical support.

Special thanks go to my beloved Christiane Hild for her precious help and friendship during last few years. Further, I would like to thank all my lab colleagues for creating a great work atmosphere.

I send my acknowledgment to my dear friends: Belit, Sylwia, Athanasios, Anja, Pawel, Paulina, Konrad and Joanna for being with me in good and bad times. You were the sun in the city of rain.

Finally, I would like to thank my Family: my Parents, my Sister Klaudia, my Brother Krystian and my beloved Nephew Bartosz for their endless love and constant support despite the distance. This thesis is dedicated to you!

Na koniec chciałabym podziękować mojej Rodzinie: moim Rodzicom, Siostrze Klaudii, Bratu Krystianowi i ukochanemu Siostrzeńcowi Bartoszowi za ich niekończącą się miłość i stałe wsparcie pomimo odległości. Ta praca jest dedykowana Wam!

édition scientifique
VVB LAUFERSWEILER VERLAG

VVB LAUFERSWEILER VERLAG
STAUFENBERGRING 15
D-35396 GIESSEN

Tel: 0641-5599888 Fax: -5599890
redaktion@doktorverlag.de
www.doktorverlag.de

ISBN: 978-3-8359-6621-5